

Relationships between Flow and the Physical Characteristics of Colorado Pikeminnow Backwater Nursery Habitats in the Middle Green River, Utah



Environmental Science Division
June 2017

About Argonne National Laboratory

Argonne is a U.S. Department of Energy laboratory managed by UChicago Argonne, LLC under contract DE-AC02-06CH11357. The Laboratory's main facility is outside Chicago, at 9700 South Cass Avenue, Argonne, Illinois 60439. For information about Argonne and its pioneering science and technology programs, see www.anl.gov.

DOCUMENT AVAILABILITY

Online Access: U.S. Department of Energy (DOE) reports produced after 1991 and a growing number of pre-1991 documents are available free via DOE's SciTech Connect (<http://www.osti.gov/scitech/>).

Reports not in digital format may be purchased by the public from the National Technical Information Service (NTIS):

U.S. Department of Commerce
National Technical Information Service
5301 Shawnee Road
Alexandria, VA 22312
www.ntis.gov
Phone: (800) 553-NTIS (6847) or (703) 605-6000
Fax: (703) 605-6900
Email: orders@ntis.gov

Reports not in digital format are available to DOE and DOE contractors from the Office of Scientific and Technical Information (OSTI):

U.S. Department of Energy
Office of Scientific and Technical Information
P.O. Box 62
Oak Ridge, TN 37831-0062
www.osti.gov
Phone: (865) 576-8401
Fax: (865) 576-5728
Email: reports@osti.gov

Disclaimer

This report was prepared as an account of work sponsored by an agency of the United States Government. Neither the United States Government nor any agency thereof, nor UChicago Argonne, LLC, nor any of their employees or officers, makes any warranty, express or implied, or assumes any legal liability or responsibility for the accuracy, completeness, or usefulness of any information, apparatus, product, or process disclosed, or represents that its use would not infringe privately owned rights. Reference herein to any specific commercial product, process, or service by trade name, trademark, manufacturer, or otherwise, does not necessarily constitute or imply its endorsement, recommendation, or favoring by the United States Government or any agency thereof. The views and opinions of document authors expressed herein do not necessarily state or reflect those of the United States Government or any agency thereof, Argonne National Laboratory, or UChicago Argonne, LLC.

Relationships between Flow and the Physical Characteristics of Colorado Pikeminnow Backwater Nursery Habitats in the Middle Green River, Utah

Prepared by

Mark Grippo, Kirk E. LaGory, David Waterman, John W. Hayse, Leroy J. Walston,
Cory C. Weber, A. Katarina Magnusson, and Xi Hui Jiang

Environmental Science Division
Argonne National Laboratory
Argonne, Illinois

Prepared for

Upper Colorado River Endangered Fish Recovery Program
Project FR BW-Synth

Final Report

June 2017

This page is intentionally left blank.

CONTENTS

EXECUTIVE SUMMARY	xvii
ACKNOWLEDGMENTS	xxiii
NOTATION	xxv
1 INTRODUCTION	1
2 METHODS	4
2.1 Site Description	4
2.2 Analysis of Aerial and Satellite Imagery	6
2.3 Backwater Habitat Surveys	7
2.4 Flow Data Analysis	7
2.5 Backwater Habitat Modeling	12
3 RESULTS AND DISCUSSION	16
3.1 Backwater Habitat Characteristics as Determined from Aerial and Satellite Imagery.....	16
3.2 Surveyed Backwater Topography and the Relationship between Backwater Topography and Flow	22
3.2.1 Representativeness of Surveyed Backwaters	23
3.2.2 Intraannual and Interannual Variability in the Relationships between Backwater Habitat Variables and Base Flows	25
3.2.3 Effects of Peak Flows on Backwater Characteristics.....	36
3.3 Natural and Dam-Related Changes in Flow and Backwater Characteristics	42
3.3.1 Influence of Dam Releases and Yampa River Flow on Base Flows in the Middle Green River	42
3.3.2 Influence of Dam Releases and Yampa River Flows during the Base- Flow Period on Backwater Characteristics in the Middle Green River.....	47
3.4 Colorado Pikeminnow Early Life Stages and Backwater Characteristics	55
3.4.1 Backwater Habitat Availability during the Colorado Pikeminnow Larval Drift Period.....	55
3.4.2 Relationships between Age-0 Colorado Pikeminnow Density and Backwater Magnitude	57
3.4.3 Relationship between Age-0 Colorado Pikeminnow Density and Base-Flow Characteristics	57
4 CONCLUSIONS.....	60
5 RECOMMENDATIONS	63
6 REFERENCES	64

CONTENTS (Cont.)

APPENDIX 1 Simulation of Flows in the Ouray Reach of the Green River from 2003 to 2008	67
A1.1 Problem Statement	69
A1.2 Empirical Wave Transformation of the Jensen Data and Correction for Water Extraction	73
A1.2.1 Analysis of Daily Variation of Q	73
A1.2.2 Accounting for Flow Extraction during the Summer Months	77
A1.2.3 Summary of the Wave Transformation Algorithm	79
A1.3 Time Lag Analysis	80
A1.3.1 Theoretical Considerations.....	82
A1.3.2 Empirical Analysis and Discussion.....	86
A1.3.3 Algorithm for Time Lagging the Unlagged Ouray Synthetic Daily Waves.....	88
A1.4 Backwater Stage-Discharge Relationships Prior to 2009	89
A1.5 References	92
APPENDIX 2 The Autonomous Backwater Identification System (ABIS): Modeling the Relationship between Green River Flows and Backwater Physical Characteristics 2003–2013	93
APPENDIX 3 Base-Flow Period Delineation	109
A3.1 Background	109
A3.2 Methods.....	109
A3.3 Reference.....	117
APPENDIX 4 Backwater Survey Locations, Relationships of Characteristics to Flow, and Changes in Characteristics during the Base-Flow Period	119
APPENDIX 5 Characteristics of the Base-Flow Period and Surveyed Backwaters from 2003 to 2013	171
APPENDIX 6 Characteristics of Surveyed Backwaters during the Colorado Pikeminnow Larval Drift Period (2003–2012)	185
A6.1 Reference.....	195

TABLES

1	Relationship between Base-Flow Characteristics, Geomorphic Parameters, and Riverine Habitats	2
2	Summer-Winter Base-Flow Recommendations for the Green River between the Confluences of the Yampa and White Rivers.....	2
3	Backwater Locations Surveyed in the ONWR Reach of the Middle Green River between 2003 and 2013	8
4	Water Elevation and Estimated Local Flow at the Time of Survey for Backwater Locations Surveyed between 2003 and 2013	11
5	Example Stage Table for BW03 Surveyed on October 8, 2008	15
6	Mean Surface Area of Surveyed Backwaters and the Surface Area of All Backwaters in the ONWR Reach and Jensen to Ouray Reach Reach as Determined from Aerial and Satellite Imagery	24
7	Mean Base Flows that Maximize Backwater Variables and the Peak Flow Characteristics That Were Tested as Independent Variables in Random Forest Regression Models.....	37
8	Total Explained Variation and Statistical Significance of Random Forest Models for the Flow That Maximized Backwater Surface Area, Volume, and Depth	38
9	Mean, Coefficient of Variation, and Minimum and Maximum Flow at the Greendale, Yampa River, and Ouray Gages during the Base-Flow Period.....	43
10	Mean and Mean Daily Variation in Surface Area, Volume, and Mean Depth of Surveyed Backwaters during the Base-Flow Period from 2003 to 2013.....	50
11	Characteristics of Surveyed Backwaters That Experienced Disconnection or Flow-Through Events during the Base-Flow Period from 2003 to 2013	51
A2-1	Reference Stage Characteristics for Backwater Locations Surveyed between 2003 and 2013.....	97
A2-2	Example Stage for BW10 Surveyed on June 27, 2012.....	99
A3-1	Start of the Base-Flow Period and Maximum Slope from 2003 to 2013	116
A5-1	Base-Flow Characteristics and Backwater Volume during the Base-Flow Period (2003-2013).....	174

TABLES (Cont.)

A5-2	Base-Flow Characteristics and Backwater Surface Area during the Base-Flow Period (2003-2013).....	176
A5-3	Base-Flow Characteristics and Backwater Mean Depth during the Base-Flow Period (2003-2013).....	178
A5-4	Base-Flow Characteristics and Backwater Maximum Depth during the Base-Flow Period (2003-2013).....	180

FIGURES

1	Overall Study Reach, Ouray National Wildlife Refuge Survey Area, and Backwater Survey Locations	5
2	Photos of Backwater Habitat Field Survey Activities	9
3	Development of the Elevation Grid Used as Input to ABIS.....	13
4	Relationship between Flow and Mean Backwater Surface Area, Number of Backwaters/RM, and Backwater Area/RM in the Jensen Reach Based on Imagery Collected in 1987, 1988, and 1989	17
5	Relationship between Flow and Mean Backwater Surface Area, Number of Backwaters/RM, and Backwater Area/RM in the Ouray Reach Based on Imagery Collected in 1987, 1988, and 1989	18
6	Mean Backwater Surface Area, Number of Backwaters/RM, and Backwater Area/RM in the Jensen and Ouray Reaches from 1987 to 2013.....	20
7	Comparison of Mean Backwater Area as Estimated Using Aerial and Satellite Imagery and ISMP Sampling.....	23
8	Relationships between Flow at the Ouray Gage and Backwater Surface Area, Volume, Mean Depth, and Maximum Depth in 2004	26
9	Relationships between Flow at the Ouray Gage and Backwater Surface Area, Volume, Mean Depth, and Maximum Depth in 2009	27
10	Relationships between Flow at the Ouray Gage and Backwater Surface Area, Volume, Mean Depth, and Maximum Depth in 2012	28

FIGURES (Cont.)

11	Backwater Surface Area in 2009—Relationship between Backwater Surface Area and Flow and Modeled Relationship between Surface Area and Hourly Flow during the Base-Flow Period	29
12	Visualization of BW02 in 2009 Showing the Significant Reductions in Backwater Surface Area Related to Variation in Flow at Ouray.....	31
13	Changes in BW02 Surface Area from 2003 to 2013—Relationship between Flow and Surface Area and Changes in Backwater Morphology.....	32
14	Changes in BW05 Surface Area from 2003 to 2012—Relationship between Flow and Surface Area and Changes in Backwater Morphology.....	33
15	Changes in BW07b Surface Area from 2009 to 2013—Relationship between Flow and Surface Area and Changes in Backwater Morphology.....	34
16	Changes in BW10 Surface Area from 2008 to 2013—Relationship between Flow and Surface Area and Changes in Backwater Morphology.....	35
17	Partial Dependence Plots of Flow That Maximizes Backwater Surface Area and Flow That Maximizes Backwater Volume with Respect to Peak Flow Magnitude, Peak Flow Magnitude in the Previous Year, and Peak Flow Duration	38
18	Peak Flow between 2003 and 2013 and the Corresponding Changes in Base Flows That Maximized Backwater Surface Area and Mean Depth	40
19	Relationship between Mean Height of Exposed Sandbars and Annual Peak Flow, Annual Peak Flow Duration, and Changes from 2003 to 2013.....	41
20	Mean Daily Flow at the Greendale, Yampa River, and Ouray Gages during the Base-Flow Periods of 2004, 2005, and 2010.....	45
21	Mean Daily Flow at the Greendale, Yampa River, and Ouray Gages in September 2003, October 2010, and August to October 2012	46
22	Mean Hourly Flow at the Greendale, Yampa River, and Ouray Gages in 2003, 2005, 2009, and 2010.....	47
23	Flow and Stage Variability during the Base-Flow Period from 2003 to 2013 as Reflected by Monthly Within-Day Flow Range at the Greendale and Ouray Gages and the Mean Daily Stage Change at the Ouray Gage	48
24	Example of Increasing Flow Creating a Flow-Through Condition That Eliminates a Large Portion of Backwater Habitat in BW05 in 2010.....	52

FIGURES (Cont.)

25	Changes in the Surface Area of BW05 in 2010—Relationship between Flow and Surface Area, and Changes in Surface Area as Related to Flow at Greendale, Yampa River, and Ouray in July, August, and October	53
26	Disconnection of BW13 from the Main Channel in 2013	54
27	Changes in the Surface Area of BW13 in 2013—Relationship between Flow and Surface Area and Repeated Disconnection Events in August 2013 Due to a Decrease in Flow at Ouray below 1,181 cfs	54
28	Mean Surface Area and Depth of Backwaters Surveyed in 2008 During the Colorado Pikeminnow Larval Drift Period.....	56
29	Relationships between the Density of Age-0 Colorado Pikeminnow and Mean Backwater Area, Number of Backwaters/RM, and Backwater Area/RM in the Jensen and Ouray Reaches.....	59
A1-1	Discharges Measured at the Jensen Gage Station and the Ouray Gage Station, Lagged by 32.0 hours	70
A1-2	Discharges Measured at the Jensen Gage Station and the Ouray Gage Station, Lagged by 38.5 hours	71
A1-3	Discharges Measured at the Jensen Gage Station and the Ouray Gage Station, Lagged by 33.5 hours	72
A1-4	Illustration of Flow Extraction between Jensen and Ouray Gage Stations	72
A1-5	Illustration of Instantaneous Deviations Relative to the 24-hour Moving Average....	74
A1-6	Instantaneous Deviations from the Mean Discharge throughout the Evaluation Period.....	75
A1-7	Comparisons of Wave Amplitudes at Jensen and Ouray Gage Stations	75
A1-8	Conceptual Illustration Determining whether Entire Waves Can Be Scaled with Amplitudes.....	76
A1-9	Comparison of the Dimensionless Waves; Each Curve Represents the Average of All 253 Daily Half-Waves Evaluated	76
A1-10	Flow That Was Extracted between Jensen and Ouray during the Base-Flow Seasons of 2009–2012	78
A1-11	Illustration of the Step Function Proposed for Flow Extraction.....	79

FIGURES (Cont.)

A1-12	Demonstration of the Algorithm Results Using 2012 Data.....	81
A1-13	Illustration of the Time Series Produced for Q_{Ouray} before the Gage Station Went into Operation	81
A1-14	Sketch of Variables Used to Describe the Daily Wave	83
A1-15	Data Used in Developing the Time Lag Function for Daily Waves.....	87
A1-16	USGS Rating Curves and Field Measurements at the Ouray Gage in the Low- Q Region.....	90
A1-17	USGS Rating Curves at the Jensen Gage in the Low- Q Region	90
A1-18	Jensen Rating Curves Based on a Dynamic Dataset at $Q = 1,360$ cfs, Stage = 1 ft; Ouray Rating Curve 3 Is Shown Based on the Same Dynamic Data	91
A2-1	Development of the Elevation Grid Used as Input for ABIS	100
A2-2	The Ouray Gage Station Site (USGS 09272400) on July 26, 2006.....	101
A2-3	USGS Discharge Measurements at the Ouray Gage Station (2009-2015).....	102
A2-4	Overlay of Spatial Extents of the Individual Surveys at BW02	105
A2-5	Mean Edge of Water Reference Elevation Surveyed at BW02 from 2004-2013.....	105
A2-6	Mean Edge of Water Reference Elevation Surveyed at BW10 from 2004-2013.....	106
A3-1	Jensen Gage Station Hydrograph in 2010	113
A3-2	Plot of $(\Delta Q/\Delta t)_{10}$ Versus t Illustrating the Method for Base-Flow Period Delineation in 2010.....	114
A3-3	Jensen Gage Station Hydrograph in 2011	114
A3-4	Plot of $(\Delta Q/\Delta t)_{10}$ Versus t Illustrating the Method for Base-Flow Period Delineation in 2011.....	115
A3-5	Jensen Gage Station Hydrograph in 2012	115
A3-6	Plot of $(\Delta Q/\Delta t)_{10}$ Versus t Illustrating the Method for Base-Flow Period Delineation in 2012.....	116
A4-1	Green River Backwater Areas BW01, BW02, BW03, BW04, BW05, and BW06 Surveyed and Modeled in 2003	121

FIGURES (Cont.)

A4-2	Surface Area of the Six Backwater Areas Surveyed in 2003 Modeled across Base Flows.....	122
A4-3	Surface Area of Each of the Six Backwater Areas Modeled during 2003	122
A4-4	Volume of the Six Backwater Areas Surveyed in 2003 Modeled across Base Flows.....	123
A4-5	Surface Area of Each of the Six Backwater Areas Modeled during 2003	123
A4-6	Maximum Depth of the Six Backwater Areas Surveyed in 2003 Modeled across Base Flows.....	124
A4-7	Maximum Depth of Each of the Six Backwater Areas Modeled during 2003	124
A4-8	Mean Depth of the Six Backwater Areas Surveyed in 2003 Modeled across Base Flows.....	125
A4-9	Mean Depth of Each of the Six Backwater Areas Modeled during 2003	125
A4-10	Green River Backwater Areas BW01, BW02, BW6, and BW07a Surveyed and Modeled in 2004.....	126
A4-11	Surface Area of the Six Backwater Areas Surveyed in 2004 Modeled across Base Flows.....	127
A4-12	Surface Area of Each of the Six Backwater Areas Modeled during 2004	127
A4-13	Volume of the Six Backwater Areas Surveyed in 2004 Modeled across Base Flows.....	128
A4-14	Volume of Each of the Six Backwater Areas Modeled during 2004	128
A4-15	Maximum Depth of the Six Backwater Areas Surveyed in 2004 Modeled across Base Flows.....	129
A4-16	Maximum Depth of Each of the Six Backwater Areas Modeled during 2004.....	129
A4-17	Mean Depth of the Six Backwater Areas Surveyed in 2004 Modeled across Base Flows.....	130
A4-18	Mean Depth of Each of the Six Backwater Areas Modeled during 2004	130
A4-19	Green River Backwater Areas BW02, BW05, BW07a, and BW08 Surveyed and Modeled in 2005	131

FIGURES (Cont.)

A4-20	Surface Area of the Four Backwater Areas Surveyed in 2005 Modeled across Base Flows.....	132
A4-21	Surface Area of Each of the Four Backwater Areas Modeled during 2005	132
A4-22	Volume of the Four Backwater Areas Surveyed in 2005 Modeled across Base Flows.....	133
A4-23	Volume of Each of the Four Backwater Areas Modeled during 2005	133
A4-24	Maximum Depth of the Four Backwater Areas Surveyed in 2005 Modeled across Base Flows.....	134
A4-25	Maximum Depth of Each of the Four Backwater Areas Modeled during 2005.....	134
A4-26	Mean Depth of the Four Backwater Areas Surveyed in 2005 Modeled across Base Flows.....	135
A4-27	Mean Depth of Each of the Four Backwater Areas Modeled during 2005	135
A4-28	Green River Backwater Areas BW02, BW06, BW07a, and BW13 Surveyed and Modeled in 2006.....	136
A4-29	Surface Area of the Four Backwater Areas Surveyed in 2006 Modeled across Base Flows.....	137
A4-30	Surface Area of Each of the Four Backwater Areas Modeled during 2006	137
A4-31	Volume of the Four Backwater Areas Surveyed in 2006 Modeled across Base Flows.....	138
A4-32	Volume of Each of the Four Backwater Areas Modeled during 2006	138
A4-33	Maximum Depth of the Four Backwater Areas Surveyed in 2006 Modeled across Base Flows.....	139
A4-34	Maximum Depth of Each of the Four Backwater Areas Modeled during 2006.....	139
A4-35	Mean Depth of the Four Backwater Areas Surveyed in 2006 Modeled across Base Flows.....	140
A4-36	Mean Depth of Each of the Four Backwater Areas Modeled during 2006	140
A4-37	Green River Backwater Areas BW02, BW03, BW07a, BW13, BW09, and BW10 Surveyed and Modeled in 2008	141

FIGURES (Cont.)

A4-38	Surface Area of the Six Backwater Areas Surveyed in 2008 Modeled across Base Flows.....	142
A4-39	Surface Area of Each of the Six Backwater Areas Modeled during 2008	142
A4-40	Volume of the Six Backwater Areas Surveyed in 2008 Modeled across Base Flows.....	143
A4-41	Volume of Each of the Six Backwater Areas Modeled during 2008	143
A4-42	Maximum Depth of the Six Backwater Areas Surveyed in 2008 Modeled across Base Flows.....	144
A4-43	Maximum Depth of Each of the Six Backwater Areas Modeled during 2008.....	144
A4-44	Mean Depth of the Six Backwater Areas Surveyed in 2008 Modeled across Base Flows.....	145
A4-45	Mean Depth of Each of the Six Backwater Areas Modeled during 2008	145
A4-46	Green River Backwater Areas BW02, BW06, BW07b, BW08, and BW10 Surveyed and Modeled in 2009	146
A4-47	Surface Area of the Five Backwater Areas Surveyed in 2009 Modeled across Base Flows.....	147
A4-48	Surface Area of Each of the Five Backwater Areas Modeled during 2009.....	147
A4-49	Volume of the Five Backwater Areas Surveyed in 2009 Modeled across Base Flows.....	148
A4-50	Volume of Each of the Five Backwater Areas Modeled during 2009.....	148
A4-51	Maximum Depth of the Five Backwater Areas Surveyed in 2009 Modeled across Base Flows.....	149
A4-52	Maximum Depth of Each of the Five Backwater Areas Modeled during 2009	149
A4-53	Mean Depth of the Five Backwater Areas Surveyed in 2009 Modeled across Base Flows.....	150
A4-54	Mean Depth of Each of the Five Backwater Areas Modeled during 2009.....	150
A4-55	Green River Backwater Areas BW02, BW05, BW06, BW07b, BW08, and BW10 Surveyed and Modeled in 2010	151

FIGURES (Cont.)

A4-56	Surface Area of the Six Backwater Areas Surveyed in 2010 Modeled across Base Flows.....	152
A4-57	Surface Area of Each of the Six Backwater Areas Modeled during 2010	152
A4-58	Volume of the Six Backwater Areas Surveyed in 2010 Modeled across Base Flows.....	153
A4-59	Volume of Each of the Six Backwater Areas Modeled during 2010	153
A4-60	Maximum Depth of the Six Backwater Areas Surveyed in 2010 Modeled across Base Flows.....	154
A4-61	Maximum Depth of Each of the Six Backwater Areas Modeled during 2010.....	154
A4-62	Mean Depth of the Six Backwater Areas Surveyed in 2010 Modeled across Base Flows.....	155
A4-63	Mean Depth of Each of the Six Backwater Areas Modeled during 2010	155
A4-64	Green River Backwater Areas BW02, BW05, BW07b, BW08, and BW10 Surveyed and Modeled in 2011	156
A4-65	Surface Area of the Five Backwater Areas Surveyed in 2011 Modeled across Base Flows.....	157
A4-66	Surface Area of Each of the Five Backwater Areas Modeled during 2011.....	157
A4-67	Volume of the Five Backwater Areas Surveyed in 2011 Modeled across Base Flows.....	158
A4-68	Volume of Each of the Five Backwater Areas Modeled during 2011.....	158
A4-69	Maximum Depth of the Five Backwater Areas Surveyed in 2011 Modeled across Base Flows.....	159
A4-70	Maximum Depth of Each of the Five Backwater Areas Modeled during 2011	159
A4-71	Mean Depth of the Five Backwater Areas Surveyed in 2011 Modeled across Base Flows.....	160
A4-72	Mean Depth of Each of the Five Backwater Areas Modeled during 2011.....	160
A4-73	Green River Backwater Areas BW02, BW05, BW07b, BW08, and BW10 Surveyed in 2012	161

FIGURES (Cont.)

A4-74	Surface Area of the Five Backwater Areas Surveyed in 2012 Modeled across Base Flows.....	162
A4-75	Surface Area of Each of the Five Backwater Areas Modeled during 2012.....	162
A4-76	Volume of the Five Backwater Areas Surveyed in 2012 Modeled across Base Flows.....	163
A4-77	Volume of Each of the Five Backwater Areas Modeled during 2012.....	163
A4-78	Maximum Depth of the Five Backwater Areas Surveyed in 2012 Modeled across Base Flows.....	164
A4-79	Maximum Depth of Each of the Five Backwater Areas Modeled during 2012	164
A4-80	Mean Depth of the Five Backwater Areas Surveyed in 2012 Modeled across Base Flows.....	165
A4-81	Mean Depth of Each of the Five Backwater Areas Modeled during 2012.....	165
A4-82	Green River Backwater Areas BW02, BW07b, BW10, BW13, and BW14 Surveyed in 2013	166
A4-83	Surface Area of the Five Backwater Areas Surveyed in 2013 Modeled across Base Flows.....	167
A4-84	Surface Area of Each of the Five Backwater Areas Modeled during 2013.....	167
A4-85	Volume of the Five Backwater Areas Surveyed in 2013 Modeled across Base Flows.....	168
A4-86	Volume of Each of the Five Backwater Areas Modeled during 2013.....	168
A4-87	Maximum Depth of the Five Backwater Areas Surveyed in 2013 Modeled across Base Flows.....	169
A4-88	Maximum Depth of Each of the Five Backwater Areas Modeled during 2013	169
A4-89	Mean Depth of the Five Backwater Areas Surveyed in 2013 Modeled across Base Flows.....	170
A4-90	Mean Depth of Each of the Five Backwater Areas Modeled during 2013.....	170
A6-1	Backwater Mean Surface Area and Mean Depth during the 2003 Colorado Pikeminnow Larval Drift Period	186

FIGURES (Cont.)

A6-2	Backwater Mean Surface Area and Mean Depth during the 2004 Colorado Pikeminnow Larval Drift Period	187
A6-3	Backwater Mean Surface Area and Mean Depth during the 2005 Colorado Pikeminnow Larval Drift Period	188
A6-4	Backwater Mean Surface Area and Mean Depth during the 2006 Colorado Pikeminnow Larval Drift Period	189
A6-5	Backwater Mean Surface Area and Mean Depth during the 2008 Colorado Pikeminnow Larval Drift Period	190
A6-6	Backwater Mean Surface Area and Mean Depth during the 2009 Colorado Pikeminnow Larval Drift Period	191
A6-7	Backwater Mean Surface Area and Mean Depth during the 2010 Colorado Pikeminnow Larval Drift Period	192
A6-8	Backwater Mean Surface Area and Mean Depth during the 2011 Colorado Pikeminnow Larval Drift Period	193
A6-9	Backwater Mean Surface Area and Mean Depth during the 2012 Colorado Pikeminnow Larval Drift Period	194

This page is intentionally left blank.

EXECUTIVE SUMMARY

Backwaters provide important nursery habitat for the endangered Colorado pikeminnow (*Ptychocheilus lucius*). Muth et al. (2000) described these habitats as “generally shallow area[s] within the river channel with little or no flow that is situated downstream of an obstruction, such as a sand or gravel bar, and that has some direct surface water connection with the river.” Bank-attached backwaters form as flows drop from the spring peak and one end of a side channel (usually the upstream end) becomes disconnected from the river flow, but the other end remains connected. This isolation from the flowing water of the river’s main channel allows water temperature in the backwater habitat to warm and produce conditions more conducive to growth of young fish.

Backwaters form during the base-flow period, which is the low-flow period after the annual snowmelt peak runoff that usually extends from early summer to the following spring. In their flow and temperature recommendations for endangered fishes in the Green River downstream of Flaming Gorge Dam, Muth et al. (2000) identified a set of recommendations for the baseflow period to provide suitable conditions in Colorado pikeminnow backwater nursery habitats. Our report provides a synthesis of physical data related to backwater habitats and river hydrology in the middle Green River in an effort to address uncertainties associated with these recommendations. Bestgen and Hill (2016) developed a related synthesis of biological information that evaluated long-term trends in reproduction, abundance, and recruitment of young Colorado pikeminnow in the Green and Yampa Rivers. The two synthesis reports are intended to provide input to the Upper Colorado River Endangered Fish Recovery Program’s (Program) ongoing evaluation of the Muth et al. (2000) flow recommendations.

The goal of the work presented in this report is to identify those physical factors that affect the availability and characteristics of backwater habitats, and, ultimately, the annual recruitment of Colorado pikeminnow. Factors evaluated included annual Flaming Gorge Dam operations, annual peak flow magnitude and duration, base-flow magnitude, and intraannual and within-day base-flow variability. Specific topics addressed in this report include:

- Changes in the size, number, and total area of backwater habitat in the middle Green River over time;
- The effects of base-flow magnitude on backwater habitat size, duration, and depth in the middle Green River;
- The effects of Flaming Gorge Dam releases and Yampa River flows on base flows and backwater characteristics in the middle Green River;
- The effect of peak-flow magnitude and duration on backwater characteristics during subsequent base flows in the middle Green River; and
- Relationships between Colorado pikeminnow early life stages and backwater characteristics.

To address these topics, we relied on previous studies (e.g., Pucherelli and Clark 1989 and 1990; Bell 1997; Rakowski and Schmidt 1999), reviews of remotely sensed imagery, and annual topographic surveys of backwaters and associated sandbars we conducted in the Ouray National Wildlife Refuge (ONWR).

The overall project study area was the approximately 68-mi (109-km) reach of the Green River between the Utah Route 149 bridge near Jensen, Utah (the location of the Jensen stream gage; U.S. Geological Survey [USGS] 09261000), and the Utah Route 88 bridge at Ouray, Utah (the location of the Ouray stream gage [USGS 09272400]) just upstream of the Duchesne River confluence. The project study area was located between approximately river mile (RM) 248.5 and 316.5 (river kilometer [RK] 400 and 509). This portion of the river flows through the Uinta Basin and represents most of the alluvial portions of Reach 2 where backwater nursery habitats occur. Much of the previously published work on backwaters was conducted in this reach.

From 2003 to 2013, we conducted ground surveys in the ONWR reach (RM 250.5 to 265.5 [RK 403 to 427] of the Green River to measure physical topographic features of backwater habitats during the base-flow period and quantify the relationships between base flows and backwater habitat. For survey, we selected downriver-facing backwaters associated with emergent sandbars, and with a surface area of at least 30 m² and maximum depth of at least 0.3 m. These size and depth characteristics correspond to criteria used by the Program for annual age-0 Colorado pikeminnow surveys. We surveyed selected backwaters once each year between July and October. Due to the temporal dynamics of sandbars and associated backwater habitats, individual backwater habitats could not be sampled in each year; it was common for previously surveyed backwaters to be absent in subsequent years and for new backwaters to form elsewhere.

Based on our analysis of aerial and satellite imagery from 1987 through 2013, the number of backwaters/RM declined over time in two reaches studied by Pucherelli and Clark (1989 and 1990) and Bell (1997)—the Jensen reach (RM 303 to 310 [RK 488 to 499]) and Ouray reach (RM 250.5 to 261.5 [RK 403 to 421])—while mean backwater area increased over the same period. These changes were most apparent between the earlier years of 1987 to 1989 (more, smaller backwaters) and the later years of 1993–2013 (fewer, larger backwaters). Although backwater area/RM varied among the years, especially in the Ouray reach, total area of backwater habitat/RM did not decrease or increase significantly between 1987 and 2013 in either reach.

One hypothesis that may explain these temporal changes is related to the effect of very large, potentially channel-widening flows. Lyons et al. (1992) reported that in the middle Green River, channel narrowing following construction of Flaming Gorge Dam ceased in 1974 producing a decrease mean width from 217 m to 204 m (6% reduction). They found that the large annual peak flows that occurred from 1983 to 1986 (21,000 to 40,000 cfs [594 to 1,132 m³/s]) reversed some of this narrowing and produced a mean channel width of 208 m (2% increase in width from 1974; 4% reduction from pre-dam width). We hypothesize that widening of the river channel may have increased the number of depositional sites and promoted formation of sandbars with associated backwaters. Subsequent years with lower peak flows (<14,500 cfs [410 m³/s] from 1987 to 1992) may have led to less sediment transport, less erosion of existing sediment deposits, and reduced scour of encroaching vegetation, resulting in gradual channel

narrowing as backwaters filled with sediment and were incorporated into the floodplain. Alternatively, reductions in daily fluctuations resulting from implementation of the 1992 Biological Opinion and Muth et al. (2000) recommendations may have resulted in the maintenance of larger backwaters during the base-flow period because higher fluctuations could result in the lower-elevation deposits on the downstream end of sandbars being reworked, shortening the length and size of backwaters over the base flow period. This hypothesis does not provide an explanation of the decrease in backwater numbers after 1992.

To assess the representativeness of our ground-surveyed backwaters, we compared the surface area of surveyed backwaters to the surface area of all backwaters in the ONWR reach and the Jensen to Ouray reach as determined from remotely sensed imagery. The analysis was limited to 2004, 2006, and 2013, which were the only survey years for which aerial or satellite imagery was available at base flows. In 2004, 2006, and 2013, we surveyed 12%, 14%, and 28%, respectively, of the backwaters in the ONWR reach. In all years, the mean surface area of surveyed backwaters was larger than the mean backwater surface area for the ONWR reach (>70th percentile) and Jensen to Ouray reach (>80th percentile).

We believe that our surveyed backwaters represent suitable nursery habitats for Colorado pikeminnow as defined by the maximum depth criterion of > 0.3 m used by the Program for backwater surveys. Mean depth of our surveyed backwaters averaged across the base-flow period was usually less than 1 m and often less than 0.5 m. Although mean backwater depth was less than 0.3 m for 25% of surveyed backwaters (13 of 51), mean maximum backwater depth was greater than 0.3 m in most years and backwaters. Many backwaters have large portions of their surface area with very shallow depth, while retaining areas with depths greater than 0.3 m. We included these very shallow depths in our calculation of mean depth.

Our topographic survey results indicated that within a single year, the characteristics of some backwaters changed significantly with flow during the base-flow period. For the 2003 to 2013 survey period, the base flows that produced the maximum volume, surface area, and depth were highly variable among backwaters. This variability resulted from the geomorphic complexity of most backwater habitats. In addition to variation between backwaters within a year, we observed significant interannual changes in geomorphology for most backwaters. The backwater survey results suggested there is large intraannual geomorphic variation between backwaters and large interannual geomorphic variation in individual backwaters. Therefore, our results support earlier findings that there is no narrow range of optimal base-flow conditions for maximizing backwater habitat in a single year or across multiple years.

Spring peak flows are considered the primary driver of interannual changes in backwater morphology. We tested this hypothesis using our survey data to examine the relationships between annual peak flow magnitude and duration and three dependent variables: base flows at maximum backwater surface area, base flows at maximum backwater volume, and base flows at maximum backwater depth. We used random forest regression to test models with instantaneous annual peak flow, instantaneous annual peak flow in the previous year, and peak flow duration (number of days in which flows were $\geq 75\%$ of the instantaneous annual peak flow) as independent variables. Annual peak flow and peak flow duration each contributed approximately equally to the model when other variables were held constant (48% and 52%, respectively) and

together explained 25.2% and 26.2%, of variation in the optimal base flow for backwater surface area and volume, respectively. Increases in both independent variables resulted in increases in the two dependent variables. Peak flow magnitude in the previous year was not important in any model. The model did not explain a significant percent of variation in the optimal base flow for backwater depth. Overall, our results support the hypothesis of Rakowski and Schmidt (1999) that there is a positive relationship between spring peak flows and the base flows that maximize backwater habitat, and that scaling the recommended yearly base flow to hydrologic condition is appropriate, with lower base flows provided in drier years and higher base flows provided in wetter years.

Given the complex non-linear relationships between flow and backwater characteristics, it is apparent that flow magnitude and variability can have important effects on backwater habitat characteristics between and within years. The mean daily variation in surface area ranged from 18.4 m² in 2008 to 620 m² in 2005, but most values were less than 250 m². Most daily changes in mean backwater depth were ≤ 0.02 m. Mean daily variation in volume ranged from 3.5 m³ in 2003 to 171.5 m³ in 2009 and were typically less than 75 m³.

Changes in dam releases produced relatively minor daily stage changes at Ouray of less than 0.06 m. Despite these relatively minor changes, some individual backwaters lost function either through a lowering of flow and disconnection from the river channel at the backwater mouth or through increasing flow and creation of a flow-through condition resulting from flows overtopping or cutting through the associated sandbar. These conditions occurred in 4 of the 10 years of our study in which at least one of the surveyed backwaters experienced flow-through or disconnection, usually the former condition resulting from an increase in flows.

Of the 51 backwaters ground-surveyed from 2003 through 2013, only 5 experienced flow-through or disconnection during the base-flow period. Affected backwaters tended to have lower surface area, lower maximum depth, and lower mean depth than other backwaters during the same year, but most, with the exception of BW04 in 2003, were comparable in size and depth to other backwaters.

Over the 10 years of survey, all or a portion of the Colorado pikeminnow larval drift period generally corresponded to the time when backwater depth and surface area were high. However, for the early portion of the drift period in most years, backwater surface area and depth were relatively lower than later in the drift period, because flows were still descending from the spring peak, and backwaters had not yet formed. This analysis supports the recommendation of Bestgen and Hill (2016) to time the onset of base-flow conditions with the first presence of Colorado pikeminnow larvae.

We used aerial and satellite imagery analysis to supplement the analyses of Bestgen and Hill (2016) and assess the relationships between age-0 Colorado pikeminnow density and reach-wide backwater habitat statistics within the Jensen and Ouray study reaches (RM 303 to 310 and RM 250.5 to 261.5). There were no statistically significant relationships between age-0 pikeminnow density and any of the backwater variables tested (i.e., mean backwater area,

backwater area/RM, and the number of backwaters/RM), but we note that data for both pikeminnow density and habitat characteristics were available in only 7 years, limiting the statistical power of our regressions.

Bestgen and Hill (2016) suggested that the amount of backwater habitat may not be limiting for Colorado pikeminnow in the middle Green River, and that habitat quality or other physical or biological factors drive population dynamics. Even if the amount of backwater habitat is not limiting, the number of pikeminnow larvae retained in the middle Green River may be higher when there is more habitat available because more habitat increases the potential for entraining drifting larvae and provides more habitat suitable for summer growth.

We recommend the following:

- Monitor channel narrowing in the middle Green River. Our analysis identified a decrease in the number of backwaters/RM and an increase in the mean area of individual backwaters since 1987. A possible explanation is related to channel narrowing and a decrease in channel complexity, which could have long-term repercussions on habitat quality and native fish production. We recommend periodic assessments of channel width, plant density, plant communities, and other habitat characteristics observable in aerial or satellite imagery to determine if the flow regime is adequate to prevent vegetation encroachment, channel narrowing, and simplification. An analysis of channel narrowing should include an assessment of channel response to very high flows (e.g., > 26,400 cfs, the recommended peak flow for wet years in Muth et al. [2000]) to determine the ability of high peak flow magnitudes and durations to reverse previous channel narrowing. High-resolution satellite imagery that is available at relatively low cost (about \$15,000 for the Jensen to Ouray reach) or aerial imagery (about \$50,000 for the reach) could be used to assess channel narrowing. U.S. Department of Agriculture's National Agriculture Imagery Program (NAIP) imagery is of lower, but potentially adequate, resolution and is available free of charge. LaGory et al. (2016) recommended a similar assessment.
- Monitor the mass balance of fine sediment (i.e., particles with grain sizes < 2 mm [i.e., sand, silt, and clay]) in the middle Green River. The formation and maintenance of backwater habitats are strongly dependent on fine sediment mass balance. To monitor the effect of flow regimes on fine sediment mass balance, we recommend installation of two gages: near the existing Jensen, Utah, stream gage (USGS 09261000) and near the existing Ouray, Utah, stream gage (USGS 09272400). These gages should be used to monitor suspended sediment flux in the middle Green River. LaGory et al. (2016) recommended similar monitoring.
- Continue an evaluation of long-term trends in backwater number and size in the middle Green River to build on the analysis presented in this report. Analyzing new imagery of the middle Green River (Jensen to Ouray) as it becomes available will enable monitoring trends in backwater habitat and determining relationships to age-0 Colorado pikeminnow captures. LaGory et al. (2016) recommended similar monitoring. Care should be taken to

use an approach that is consistent with earlier studies and to archive the imagery, polygons of digitized backwaters, and data on the area of individual backwaters. For the imagery analysis presented here, we provide such documentation in the supplement to this report (Hamada et al. 2017).

ACKNOWLEDGMENTS

We thank the numerous people who helped in the collection of field data, including staff of Argonne National Laboratory (Ben O'Connor, Adrienne Carr, and Scott Schlueter), Western Area Power Administration (WAPA; Judd Hopkins, Corey Diekman, and Jerry Wilhite), as well as the generous logistical support provided by the U.S. Fish and Wildlife Service Vernal Field Office staff especially Dave Beers, Tildon Jones, and Dave Irving. Reviews of earlier drafts of the report were provided by Kevin Bestgen (Colorado State University Larval Fish Laboratory), Tom Chart (Recovery Program), David Varyu (U.S. Bureau of Reclamation), Jerry Wilhite (WAPA), and Paul Grams (U.S. Geological Survey). The work presented in this report was funded by the Western Area Power Administration and the U.S. Bureau of Reclamation under Contract No. DE-AC02-06CH11357.

This page is intentionally left blank.

NOTATION

ABIS	autonomous backwater identification system
BW	backwater
cfs	cubic feet per second; 1 cfs = 0.028317 m ³ /s
cm	centimeter(s)
DEM	digital elevation model
ft	foot (feet)
ISMP	Interagency Standardized Monitoring Protocol
km	kilometer(s)
m	meter(s)
m ²	square meter(s)
m ³	cubic meter(s)
mi	mile(s)
NAIP	National Agriculture Imagery Program
ONWR	Ouray National Wildlife Refuge
Program	Upper Colorado River Endangered Fish Recovery Program
RK	river kilometer(s)
RM	river mile(s)
s	second(s)
USGS	U.S. Geological Survey

This page is intentionally left blank.

1 INTRODUCTION

Backwaters provide important nursery habitat for the endangered Colorado pikeminnow (*Ptychocheilus lucius*). Muth et al. (2000) described these habitats as “generally shallow area[s] within the river channel with little or no flow that is situated downstream of an obstruction, such as a sand or gravel bar, and that has some direct surface water connection with the river.” Bank-attached backwaters form as flows drop from the spring peak and one end of a side channel (usually the upstream end) becomes disconnected from the river flow, but the other end remains connected. This isolation from the flowing water of the river’s main channel allows water temperature in the backwater habitat to warm and produce conditions more conducive to growth of young fish.

Backwaters form during the base-flow period, which is the low-flow period after the annual snowmelt peak runoff that usually extends from early summer to the following spring. Important characteristics of base flows include magnitude, duration, timing, and variability. The general relationships of these base-flow characteristics to backwater and other riverine habitat availability are summarized in Table 1. Base-flow magnitude affects fine sediment (i.e., particles with grain sizes < 2 mm [sand, silt, and clay]) transport rates, bed composition, dimensions of in-channel habitats and groundwater-connected flooded bottomlands, types of in-channel habitats, amount of habitat in each reach, vegetation encroachment, velocity in spawning habitats, and shoreline complexity. Base-flow duration affects fine sediment transport, bed composition, and the availability of in-channel habitats and groundwater-connected flooded bottomland habitats. The timing of base flows affects the timing of in-channel habitat availability. Base-flow variability affects interannual availability of habitats, intraannual habitat stability, and within-day habitat stability.

In their flow and temperature recommendations for endangered fishes in the Green River downstream of Flaming Gorge Dam, Muth et al. (2000) identified a set of recommendations for the baseflow period to provide suitable conditions in Colorado pikeminnow backwater nursery habitats (Table 2). These recommendations focused on the middle Green River (Reach 2 of Muth et al. 2000), which flows from the confluence with the Yampa River through the Uinta Basin to the confluence of the White River. This was the focus of the recommendations because of the importance of the reach to the life history of the Colorado pikeminnow and the endangered razorback sucker (*Xyrauchen texanus*), and because Flaming Gorge Dam releases have an important influence on flows in this reach. Dam releases have less effect on flows in the lower Green River (Reach 3) because of additional tributary inputs and irrigation withdrawals (Muth et al. 2000). Recommendations for base flows in Reach 2 included:

- The magnitude of base flows should be scaled to annual hydrologic condition, with lower base flows in drier years and higher base flows in wetter years.
- Flow should gradually decline from peak flow to base flow, with the base flow reached by early to middle summer (depending on hydrologic conditions) and maintained through February.

TABLE 1 Relationship between Base-Flow Characteristics, Geomorphic Parameters, and Riverine Habitats Based on LaGory et al. (2003)

Parameter	Relationship to Riverine Habitat Characteristics
<i>Base-flow magnitude</i> : Overall flow level during the base-flow period	Affects fine sediment transport rates, bed composition, dimensions of in-channel habitats and groundwater-connected flooded bottomlands, types of in-channel habitats, amount of habitat in reach, vegetation encroachment, velocity in spawning habitats, and shoreline complexity.
<i>Base-flow duration</i> : Length of time between the onset of the base-flow period in early summer and the beginning of snow-melt runoff in the following spring	Affects fine sediment transport rates, bed composition, and the availability of in-channel habitats and groundwater-connected flooded bottomland habitats.
<i>Base-flow timing</i> : Date of the onset of the base-flow period	Affects the timing of in-channel habitat availability.
<i>Base-flow variability</i> : Variation in base-flow magnitude among years (interannual), within years (intraannual), and within days	Affects interannual availability of habitats, intraannual habitat stability, and within-day habitat stability.

TABLE 2 Summer-Winter Base-Flow Recommendations for the Green River between the Confluences of the Yampa and White Rivers (Muth et al. 2000)

	Hydrologic Condition				
	Wet (0 to 10% Exceedance)	Moderately Wet (10 to 30% Exceedance)	Average (30 to 70% Exceedance)	Moderately Dry (70 to 90% Exceedance)	Dry (90 to 100% Exceedance)
Mean base-flow magnitude	2,800 to 3,000 cfs (79 to 85 m ³ /s)	2,400 to 2,800 cfs (67 to 79 m ³ /s)	1,500 to 2,400 cfs (43 to 67 m ³ /s)	1,100 to 1,500 cfs (31 to 43 m ³ /s)	900 to 1,100 cfs (26 to 31 m ³ /s)
Rate of decline from peak flow to base flow ^a	Approximately 1,000 cfs (28 m ³ /s) per day	Approximately 1,000 cfs (28 m ³ /s) per day	Approximately 500 cfs (14 m ³ /s) per day	Approximately 350 cfs (10 m ³ /s) per day	Approximately 350 cfs (10 m ³ /s) per day
Base-flow period	About August 15 to March 1	About August 1 to March 1	About July 15 to March 1	About July 1 to March 1	About June 15 to March 1
Base-flow variability					
Within day	Flow variation resulting from hydropower generation at Flaming Gorge Dam should be limited to produce no more than a 0.1-m stage change within a day at the USGS gage near Jensen, Utah				
Between day	Differences due to reservoir operations in mean daily flows between consecutive days should not exceed 3%.				
Within season	Mean daily flows should be kept within \pm 40% of the annual mean base flow in summer–autumn (August through November) and within \pm 25% of the annual mean base flow in winter (December through February)				

- Within-day variability in base-flow magnitude caused by hydropower operations should be restricted to no more than 0.1 m.
- Between-day variability should not exceed 3%.
- Mean daily flows should be kept within $\pm 40\%$ of the annual mean base flow in summer–autumn (August through November) and within $\pm 25\%$ of the annual mean base flow in winter (December through February).

Because the Muth et al. (2000) recommendations were based on limited available information, there were a number of uncertainties associated with their implementation. The Green River Study Plan (Green River Study Plan Ad Hoc Committee 2007) identified monitoring and research to address these uncertainties, two of which were considered high-priority uncertainties related to backwater habitats in Reach 2:

- The effect of peak flows, sediment availability, and antecedent conditions on the relationship between base-flow level and backwater habitat availability, and
- The effect of base-flow variability (within-day, within-season, within-year, between years) on backwater habitat quality (e.g., temperature, productivity)

Our report provides a synthesis of physical data related to backwater habitats and river hydrology in an effort to address these uncertainties. Bestgen and Hill (2016) developed a related synthesis of biological information that evaluated long-term trends in reproduction, abundance, and recruitment of young Colorado pikeminnow in the Green and Yampa Rivers. The two synthesis reports are intended to provide important input to the Upper Colorado River Endangered Fish Recovery Program's ongoing evaluation of the Muth et al. (2000) flow recommendations.

The goal of the work presented in this report is to identify those physical factors that affect the availability and characteristics of backwater habitats, and, ultimately, the annual recruitment of Colorado pikeminnow. We focused our review on information for the middle Green River (Reach 2 of the flow recommendations), specifically between the Jensen and Ouray U.S. Geological Survey (USGS) stream gages where most information has been collected. Factors evaluated included annual Flaming Gorge Dam operations, annual peak flow magnitude and duration, base-flow magnitude, and intraannual and within-day base-flow variability. Specific topics addressed in this report include:

- Changes in the size, number, and total area of backwater habitat in the middle Green River over time;
- The effects of base-flow magnitude on backwater habitat size, duration, and depth in the middle Green River;

- The effects of Flaming Gorge Dam releases and Yampa River flows on base flows and backwater characteristics in the middle Green River;
- The effect of peak-flow magnitude and duration on backwater characteristics during subsequent base flows in the middle Green River; and
- Relationships between Colorado pikeminnow early life stages and backwater characteristics.

To address these topics, we relied on previous studies (e.g., Pucherelli and Clark 1990; Bell 1997; Rakowski and Schmidt 1999), analyses of remotely sensed imagery, and annual surveys of backwaters we conducted in the Ouray National Wildlife Refuge (ONWR).

2 METHODS

2.1 SITE DESCRIPTION

The overall project study area was the approximately 68-mi (109-km) reach of the Green River between the Utah Route 149 bridge near Jensen, Utah (the location of the Jensen stream gage [USGS 09261000]), and the Utah Route 88 bridge at Ouray, Utah (the location of Ouray stream gage [USGS 09272400]) just upstream of the Duchesne River confluence. The project study area was located between approximately river mile¹ (RM) 248.5 and 316.5 (river kilometer [RK] 400 and 509). This portion of the river flows through the Uinta Basin and represents most of the alluvial portions of Reach 2 where backwater nursery habitats occur. Much of the previously published work on backwaters was conducted in this reach.

The study area has a low gradient of 0.3 m/km, a substrate composed primarily of sand (particles with grain size of 0.062 mm to 2 mm), and a prevalence of backwater habitats. Restricted meanders are the primary geomorphic planform in this reach of the Green River (LaGory et al. 2003). Restricted meanders occur in relatively wide alluvial terraces in which only the outside bends of the river are in contact with bedrock. At various flow levels, these meanders permit the establishment of channel-margin habitats, such as backwaters, eddies, flooded tributary mouths, and side channels. Connected backwaters in restricted meanders are used more frequently by juvenile Colorado pikeminnow than backwaters in other planform types. The prevalence of connected backwaters along restricted meanders within the middle Green River is one reason why this reach is considered an important reach of the Green River subbasin for the recovery of the Colorado pikeminnow (Muth et al. 2000; LaGory et al. 2003).

The study area includes a 15-mi (24-km) reach of the Green River within ONWR between RM 250.5 and 265.5 (RK 403 and 427) (Figure 1) where we conducted annual ground

¹ River mile or river kilometer are measures of the distance along a river from its mouth. Values presented in this report are the distance from the Green River-Colorado River confluence.

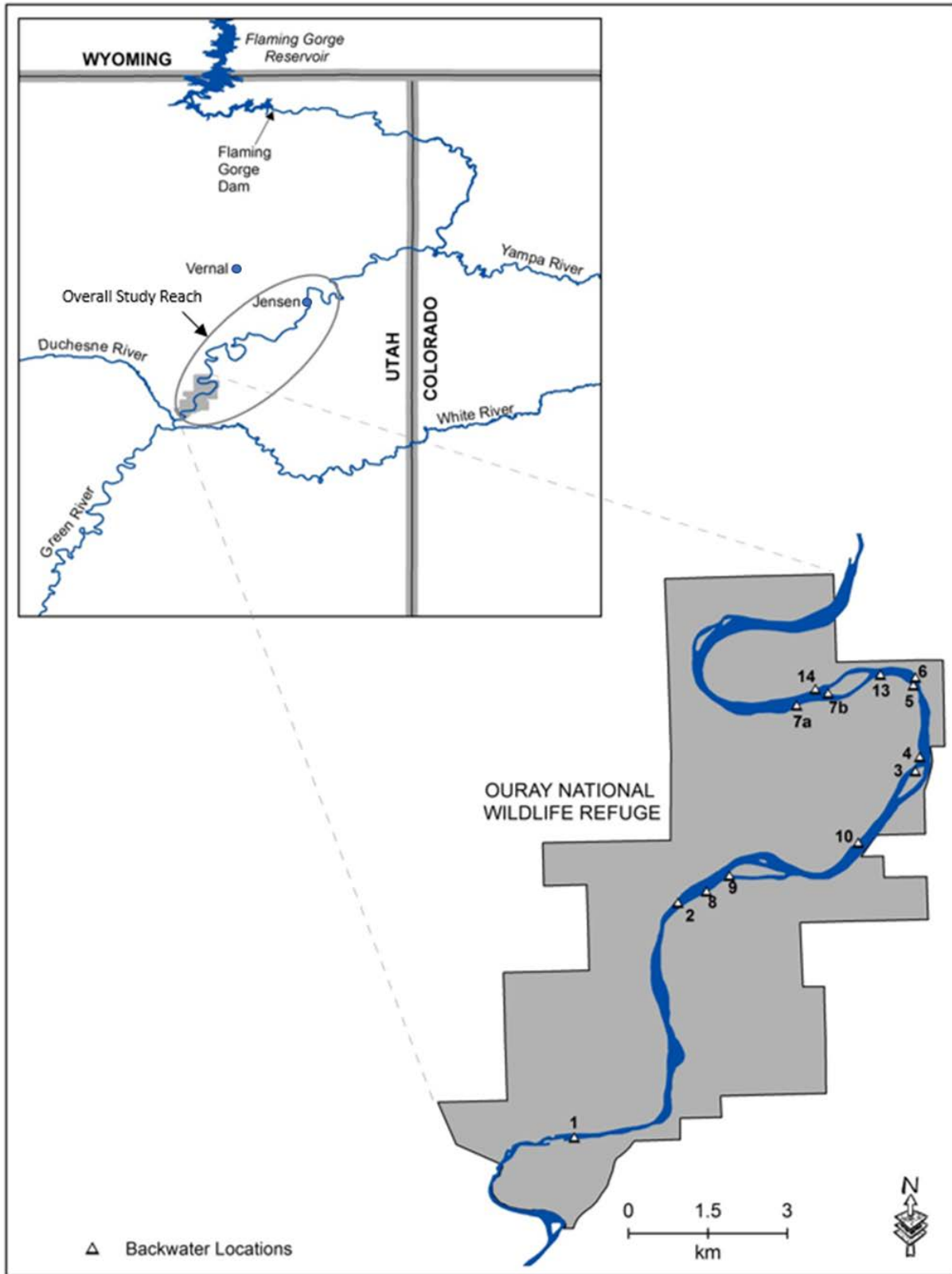


FIGURE 1 Overall Study Reach, Ouray National Wildlife Refuge Survey Area, and Backwater Survey Locations

surveys of selected backwater habitats from 2003 to 2013. This area is located approximately 240 km downstream of Flaming Gorge Dam. In addition, we considered two other subreaches for our aerial and satellite imagery analysis: Jensen (RM 303 to 310 [RK 488 to 499]) and Ouray (RM 250.5 to 261.5 [RK 403 to 421]). We chose these latter subreaches to match those evaluated by Pucherelli and Clark (1989 and 1990) and Bell (1997).

2.2 ANALYSIS OF AERIAL AND SATELLITE IMAGERY

Temporal changes in backwater habitat and the relationship between backwater habitat and flow were assessed using imagery analysis. Pucherelli and Clark (1989 and 1990) and Bell (1997) quantified the number and surface area of backwaters in aerial images from 1987 through 1996 in two reaches of the middle Green River—Jensen (RM 303 to 310 [RK 488 to 499]) and Ouray (RM 250.5 to 261.5 [RK 403 to 421]). We analyzed imagery from 2004, 2006, and 2013 in these same reaches to determine the more recent availability of backwater habitat in the middle Green River and determine if there had been changes in backwater number and surface area over time. We obtained aerial imagery from August 30, 2004, and July 14, 2006, from the U.S. Department of Agriculture's National Agriculture Imagery Program (NAIP); we obtained SPOT6 satellite imagery for September 18, 2013. Imagery of the river at base flows was not available for other years. Aerial photography was used by Pucherelli and Clark (1989 and 1990) in 1987 and 1988, and by Bell (1997) in 1993 and 1996. Pucherelli and Clark (1990) used aerial videography in 1989.

On the imagery, we identified as backwaters sandbar-associated aquatic habitats whose long axis was greater than the width of the mouth, and that had only upstream, downstream, or side connections to the mainstem, but not from more than one direction, which would indicate flow through the backwater. To maintain consistency with the methods of Pucherelli and Bell, we included all such backwaters including those with surface areas $<30 \text{ m}^2$. The depth of backwaters could not be determined from imagery.

A single analyst hand-digitized the area of individual backwaters to determine mean backwater size (i.e., the mean surface area of individual backwaters in each reach), total backwater area/RM, and the number of backwaters/RM. The second author of this report (LaGory) reviewed all digitized backwater polygons to ensure consistency and accuracy of interpretation. We used the 4-5 backwaters that we surveyed on the ground in the same years (see Section 2.3 for a description of those methods) to check the accuracy of our imagery interpretations. In all years used in our imagery analysis, all surveyed backwater features were clearly visible in the aerial imagery.

For the analysis of change through time, we included only backwaters from the 2004, 2006, and 2013 images that were located in the Jensen and Ouray study reaches of Pucherelli and Clark (1989 and 1990) as defined above. For other analyses, we included backwaters along the entire river between the Jensen and Ouray gages (RM 248.5 to 316.5 [RK 400 to RK 509]). Hamada et al. (2017) presents a description of our backwater identification approach, and provides the set of images analyzed (with delineated backwaters marked) and the statistics for

delineated backwaters. The Hamada et al. (2017) report was developed to document our approach and ensure that future efforts to identify and delineate backwaters are consistent.

2.3 BACKWATER HABITAT SURVEYS

From 2003 to 2013, we conducted ground surveys in the ONWR reach of the Green River to measure physical topographic features of backwater habitats during the base-flow period and quantify the relationships between base flows and backwater habitat. For survey, we selected downriver-facing backwaters associated with emergent sandbars, and with a surface area of at least 30 m² and maximum depth of at least 0.3 m. These size and depth characteristics correspond to criteria used by the Program to select backwaters for annual age-0 Colorado pikeminnow surveys. Most surveyed backwaters were secondary channels as defined by Day et al. (1999). We surveyed selected backwaters once each year between July and October. Due to the temporal dynamics of sandbars and associated backwater habitats, we could not sample the same individual backwater habitats each year; it was common for previously surveyed backwaters to be absent in subsequent years and for new backwaters to form elsewhere.

We surveyed 4–6 habitats per year for a total of 51 individual habitat surveys over the course of our study. These 51 surveys represent 13 different habitat locations, as shown in Figure 1. The backwaters surveyed, with the dates and times of each survey, are shown in Table 3. We collected field notes at each site to describe the surrounding habitat, illustrate the morphology of the backwater at the time of the survey, and record other ancillary information (e.g., presence of avian predator signs, visible fish in the backwater, etc.). At each backwater location, we conducted topographic (including bathymetric) surveys using standard surveying techniques and survey-grade equipment (e.g., Topcon GS GPS Unit; Leica TC805 Ultra Total Station) with ±1 cm horizontal and vertical accuracy. We used these surveys to characterize backwater bathymetry and the topography of the associated sandbar and upland areas, focusing on areas of noticeable elevation change such as shorelines, ridges within sandbars, and steeper elevation changes along the upland areas. In several years, sonar equipment (e.g., Hydrolite-TM; 200 kHz; 1-cm depth accuracy/0.1% of depth) was used to collect bathymetric data in deeper portions of backwaters. Photos of survey activities are shown in Figure 2.

2.4 FLOW DATA ANALYSIS

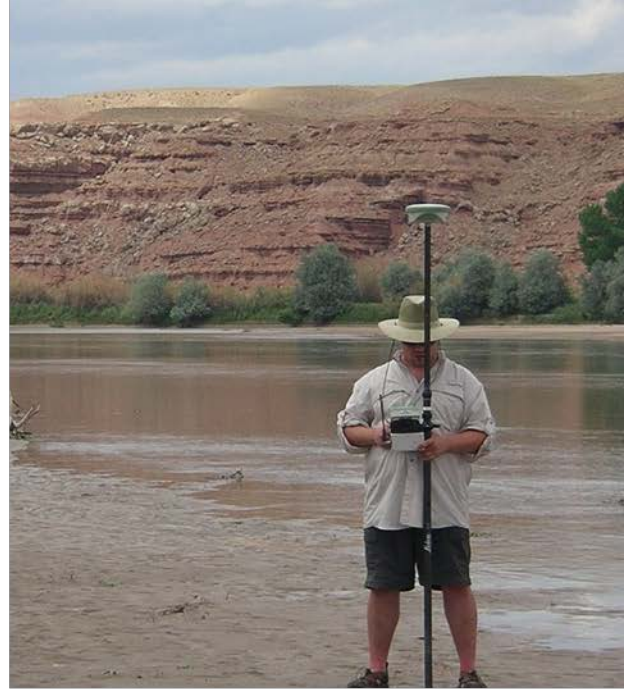
For 2009 to 2013, we estimated local flow at the time of our field survey using flow data from the Ouray gage, which was put into operation in May 2009, and was located just downstream of the project area. For the period 2003–2008, we estimated flow data in the study area using flow data from the upstream Jensen gage. The estimation technique included scaling the daily flow wave recorded at the Jensen gage to account for wave attenuation, followed by time lagging the scaled wave to account for the travel time between the two gages. For wave scaling, we developed an empirical relationship using available flow data when both gages were simultaneously in operation. The method involved decomposing both the Jensen and Ouray flow time series into their 24-hour moving averages and determining deviations from the 24-hour moving averages. We defined the amplitude as the maximum value of the deviation for each

TABLE 3 Backwater Locations Surveyed in the ONWR Reach of the Middle Green River between 2003 and 2013

Year	Date	Time	Backwater ID	Latitude (decimal degrees)	Longitude (decimal degrees)
2003	8/19/2003	15:00	BW01	40.10950	-109.64983
2003	8/20/2003	10:30	BW02	40.14950	-109.62283
2003	8/20/2003	15:00	BW03	40.17083	-109.57200
2003	8/20/2003	17:00	BW04	40.17317	-109.57067
2003	8/21/2003	10:00	BW05	40.18500	-109.57217
2003	8/21/2003	13:00	BW06	40.18617	-109.57150
2004	9/28/2004	10:00	BW01	40.10949	-109.64986
2004	9/28/2004	14:30	BW02	40.14926	-109.62291
2004	9/29/2004	14:00	BW06	40.18614	-109.57161
2004	9/30/2004	10:00	BW07a	40.18218	-109.59849
2005	9/27/2005	16:30	BW02	40.14958	-109.62342
2005	9/28/2005	13:30	BW05	40.18508	-109.57233
2005	9/28/2005	12:40	BW05	40.18613	-109.57162
2005	9/29/2005	13:00	BW07a	40.18257	-109.59330
2005	9/29/2005	15:30	BW08	40.14975	-109.61990
2006	9/26/2006	13:30	BW07a	40.18228	-109.59582
2006	9/27/2006	10:30	BW13	40.18674	-109.57789
2006	9/27/2006	13:00	BW06	40.18583	-109.57115
2006	9/28/2006	9:00	BW02	40.15019	-109.62249
2008	10/7/2008	11:00	BW07a	40.18262	-109.59008
2008	10/7/2008	15:30	BW02	40.14749	-109.62730
2008	10/8/2008	10:30	BW13	40.18671	-109.57771
2008	10/8/2008	15:00	BW03	40.17079	-109.57141
2008	10/9/2008	9:30	BW09	40.15359	-109.61356
2008	10/9/2008	12:00	BW10	40.15879	-109.58461
2009	10/13/2009	14:15	BW02	40.14923	-109.62333
2009	10/14/2009	15:30	BW06	40.18591	-109.57122
2009	10/15/2009	10:30	BW07b	40.18489	-109.58863
2009	10/14/2009	10:30	BW09	40.15273	-109.61517
2009	10/14/2009	13:00	BW10	40.15785	-109.58564
2010	7/20/2010	11:30	BW02	40.14965	-109.62289
2010	7/21/2010	13:45	BW05	40.18493	-109.57191
2010	7/21/2010	12:45	BW06	40.18618	-109.57143
2010	7/22/2010	10:30	BW07b	40.18610	-109.58724
2010	7/20/2010	14:30	BW08	40.15227	-109.61600
2010	7/21/2010	10:00	BW10	40.15808	-109.58569
2011	9/7/2011	10:15	BW02	40.14906	-109.62360
2011	9/8/2011	9:30	BW10	40.15528	-109.58837
2011	9/7/2011	14:45	BW08	40.15208	-109.61604
2011	9/8/2011	13:45	BW05	40.18618	-109.57448
2011	9/9/2011	9:30	BW07b	40.18539	-109.58784
2012	6/26/2012	11:00	BW02	40.14916	-109.62306
2012	6/28/2012	15:30	BW05	40.18499	-109.57193
2012	6/28/2012	11:00	BW07b	40.18571	-109.58764
2012	6/26/2012	14:30	BW08	40.15055	-109.61832
2012	6/27/2012	12:00	BW10	40.15359	-109.59090
2013	9/10/2013	10:30	BW02	40.14758	-109.62703
2013	9/11/2013	10:00	BW07b	40.18544	-109.58794
2013	9/10/2013	14:45	BW10	40.15544	-109.58844
2013	9/12/2013	13:45	BW13	40.18701	-109.58033
2013	9/11/2013	10:00	BW14	40.18469	-109.59349



A. Collecting topographic information using total station equipment.



B. Collecting topographic information using a GPS rover.



C. Collecting bathymetric information using total station equipment in shallow water.



D. Collecting bathymetric information using sonar with a GPS rover in deep water.

FIGURE 2 Photos of Backwater Habitat Field Survey Activities

daily wave, and made direct comparisons of the amplitudes of individual waves that traveled between the gages to develop an empirical relationship. We determined that the scaling of the entire wave with the amplitude relationship was valid using a non-dimensionalization of the daily wave data. Based on the analysis, we could decompose any flow time series recorded at Jensen in the same manner and implement the scaling relationship to generate the unlagged Ouray flow time series. We then implemented the time lag using an empirical relationship between the peak flow of the daily wave and the travel time of observed daily waves between the gages. These methods are more fully described in Appendix 1.

Table 4 presents the water elevation and estimated local flow for each backwater location surveyed from 2003 to 2013. We calculated water elevation at the time of survey (referred to here as reference stage) by averaging all of the water edge topographic measurements.

To relate water elevation to local flows at the survey locations, we developed a local stage-flow rating for each survey site; for any site that we surveyed over multiple years, we developed a new rating each year it was surveyed. The method for developing the local rating consisted of three steps. First, we determined the water surface elevation at the time of the survey by averaging the measured edge of water elevations obtained at the survey site. This elevation is referred to as the reference stage ($S_{ref,i}$), where the subscript i indicates that the value is valid for site i . Second, we estimated the instantaneous flow at the time the reference stage was surveyed, and referred to this flow as the reference flow, $Q_{ref,i}$. The pair forms the point $(Q_{ref,i}, S_{ref,i})$ on the local rating curve. To obtain $Q_{ref,i}$, we determined the flow value for the time of the survey as described earlier in this section. Third, we used the rating curve developed by the USGS for the Ouray gage station to predict relative changes in stage for flows different than $Q_{ref,i}$, under the assumption that the hydraulic characteristics of the river at the survey sites was approximately the same as at the Ouray gage station. This involved a simple translation of the stages from the Ouray rating curve to represent elevations valid at the survey site; i.e., the flow values are unchanged but the elevations are shifted. Using the value $Q_{ref,i}$ determined above, we found the reference stage at Ouray from the Ouray rating curve as the point $(Q_{ref,i}, S_{ref,Ouray})$. We then added the value $\Delta S_i = (S_{ref,i} - S_{ref,Ouray})$ to each point that comprised the Ouray rating curve to complete the translation and establish the local rating curve.

As described in Section 2.5, we then used the relationship between flow and stage for each backwater to determine changes in surveyed backwater characteristics in response to the flows recorded during the base-flow period. We determined the onset of the base-flow period for each year analytically using the methods described in Appendix 3.

We used a qualitative approach to determine the relative effect of dam releases and Yampa River flow on variation in mean daily flow and hourly flow in the middle Green River by examining patterns in the recorded Greendale flows, Yampa River flows, and Ouray flow. In this case, we did not consider a statistical analysis of the flow data to be practical because of the temporally variable travel time lag between the Yampa River and Ouray, and between Greendale and Ouray. It would have been very difficult to determine these relationships at the temporal resolution need for a statistical analysis.

TABLE 4 Water Elevation and Estimated Local Flow at the Time of Survey for Backwater Locations Surveyed in the ONWR Reach of the Middle Green River between 2003 and 2013

Year	Date	Time	Backwater	Water Elevation (m) ^a	Estimated Local Flow (cfs) ^b
2003	8/19/2003	15:00	BW01	1,416.19	868
2003	8/20/2003	10:30	BW02	1,424.79	872
2003	8/20/2003	15:00	BW03	1,424.59	869
2003	8/20/2003	17:00	BW04	1,422.52	868
2003	8/21/2003	10:00	BW05	1,426.59	865
2003	8/21/2003	13:00	BW06	1,424.31	865
2004	9/28/2004	10:00	BW01	1,419.40	1,789
2004	9/28/2004	14:30	BW02	1,420.01	1,789
2004	9/29/2004	14:00	BW06	1,421.35	1,729
2004	9/30/2004	10:00	BW07a	1,422.26	1,689
2005	9/27/2005	16:30	BW02	1,419.76	1,879
2005	9/28/2005	10:00	BW05	1,421.65	1,839
2005	9/29/2005	13:00	BW07a	1,422.21	1,919
2005	9/29/2005	15:30	BW08	1,420.11	1,869
2006	9/28/2006	9:00	BW02	1,419.88	1,659
2006	9/27/2006	13:00	BW06	1,421.49	1,639
2006	9/26/2006	13:30	BW07a	1,422.16	1,519
2006	9/27/2006	10:30	BW13	1,421.49	1,639
2008	10/7/2008	15:30	BW02	1,420.00	1,959
2008	10/8/2008	15:00	BW03	1,421.20	1,909
2008	10/7/2008	11:00	BW07a	1,422.28	1,969
2008	10/9/2008	9:30	BW09	1,420.18	1,839
2008	10/9/2008	12:00	BW10	1,420.82	1,840
2008	10/8/2008	10:30	BW13	1,421.80	1,919
2009	10/13/2009	14:15	BW02	1,420.18	2,209
2009	10/14/2009	15:30	BW06	1,421.73	2,199
2009	10/15/2009	10:30	BW07b	1,422.23	2,139
2009	10/14/2009	10:30	BW08	1,420.37	2,169
2009	10/14/2009	13:00	BW10	1,421.00	2,209
2010	7/20/2010	11:30	BW02	1,420.09	2,578
2010	7/21/2010	13:45	BW05	1,421.68	2,468
2010	7/21/2010	12:45	BW06	1,421.75	2,478
2010	7/22/2010	10:30	BW07b	1,422.20	2,468
2010	7/20/2010	14:30	BW08	1,420.18	2,529
2010	7/21/2010	10:00	BW10	1,421.13	2,468
2011	9/7/2011	10:15	BW02	1,420.31	3,328
2011	9/8/2011	13:45	BW05	1,421.96	3,288
2011	9/9/2011	9:30	BW07b	1,422.38	3,338
2011	9/7/2011	14:45	BW08	1,420.41	3,298
2011	9/8/2011	9:30	BW10	1,421.20	3,358
2012	6/26/2012	11:00	BW02	1,419.80	1,459
2012	6/28/2012	15:30	BW05	1,421.61	1,419
2012	6/28/2012	11:00	BW07b	1,421.97	1,369

TABLE 4 (Cont.)

Year	Date	Time	Backwater	Water Elevation (m) ^a	Estimated Local Flow (cfs) ^b
2012	6/26/2012	14:30	BW08	1,420.08	1,509
2012	6/27/2012	12:00	BW10	1,420.69	1,399
2013	9/10/2013	10:30	BW02	1,419.84	1,439
2013	9/11/2013	10:00	BW07b	1,421.98	1,419
2013	9/10/2013	14:45	BW10	1,420.68	1,349
2013	9/12/2013	13:45	BW13	1,421.75	1,369
2013	9/11/2013	10:00	BW14	1,422.15	1,399

^a Water elevation was estimated as the average elevation of all shoreline measurements.

^b Local flow was estimated as the simulated (2003–2008) or actual (2009–2013) flow at the Ouray gage. Note that 1 cfs = 0.028317 m³/s.

2.5 BACKWATER HABITAT MODELING

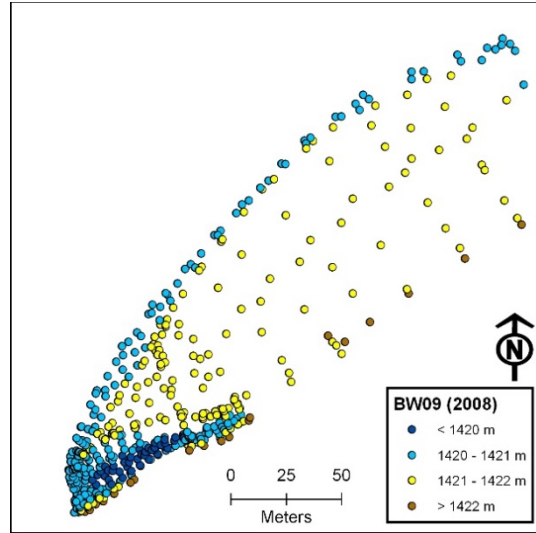
We used the field survey of backwater habitats and associated sandbars to develop a digital elevation model (DEM) of each backwater-sandbar complex. We used survey data to interpolate estimated elevations across each surveyed area using the ESRI Spatial Analyst tool for ArcGIS 9.x (McCoy and Johnston 2001). Interpolated elevation grids were represented as floating point (continuous) grids. As described below, we used this DEM as the basis for our determinations of the surface area, volume, and depth of backwaters under different flows.

We developed a computerized system, which we referred to as the Autonomous Backwater Identification System (ABIS), to facilitate the modeling of physical backwater characteristics under various flow conditions. (A detailed description of the ABIS method is provided in Appendix 2.) ABIS was programmed in C++ and runs under Microsoft Windows[®]. Implementation of ABIS started with creation of a grid with 1-m² cells for each surveyed area with cell values that consisted of 8-bit integers ranging from 0 to 255. These values represented relative elevation of each cell compared to the full range of surveyed elevation values; the lowest elevation surveyed was assigned a value of 0 and the highest elevation was assigned a value of 255. Because each habitat had a different elevation range, each habitat also had a different relationship between 8-bit value and elevation; among surveyed backwaters, increments between 8-bit values ranged from 4 to 23 mm.

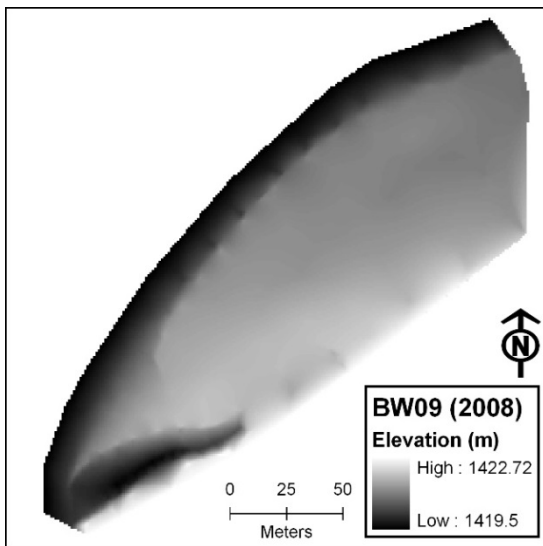
ABIS incorporated an image-processing algorithm to determine surface area, volume, and depth of backwaters at different flows for each surveyed backwater location. The 8-bit integer grid was exported as a bitmap (.bmp) image for model implementation. Figure 3 illustrates the development of the required elevation grids.



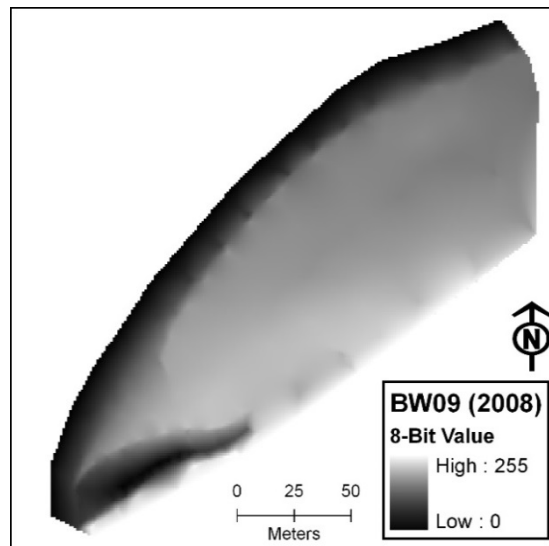
a) Photo of Backwater 9 in 2008. View is looking downstream with the main channel to the right.



b) Topographic survey points collected at Backwater 9 in 2008. Flow is from upper right to lower left with main channel on the left.



c) Continuous elevation grid for Backwater 9.



d) 8-bit integer grid for Backwater 9.

FIGURE 3 Development of the Elevation Grid Used as Input to ABIS. For (a) any backwater area, (b) topographic survey measurements were obtained throughout the backwater and sandbar areas, (c) the survey measurements were then interpolated to represent continuous estimated elevation values across the scene, and (d) the elevation grid was exported as an 8-bit integer grid for direct input into ABIS.

Using the 8-bit grid, and for each 8-bit value between 0 and 255, ABIS sequentially connected contiguous shoreline points (defined for each stage as points just above the waterline), ultimately forming a polygon. ABIS identified a polygon as a backwater when the area inside the backwater polygon was greater than:

$$((d_{mouth}/2)^2 \times \pi)/2$$

where d_{mouth} is the diameter of the mouth of the polygon. This operational definition of a backwater was used to identify habitats whose surface area was greater than a semicircle with a diameter that was the width of the mouth; thus, ABIS identified habitats that were longer than the width of their mouths as backwaters. The minimum width of connection between the backwater and the main channel was 1 m, which is the minimum cell size used in the ABIS calculations. Note that, as described above, the polygons identified by ABIS for consideration as backwaters are for areas with contiguous shoreline points, and therefore any habitat that has a break in the shoreline (e.g., is receiving flow through an upstream channel) was not considered backwater habitat.

Using this automated algorithm, the stage tables generated by ABIS show predicted backwater surface area (m^2), volume (m^3), maximum depth (m), and mean depth (m) at each incremental ABIS stage. We calculated backwater parameters at each flow as follows:

$$\text{Surface area } (A) = N_{pixels} \times 1 \text{ m}^2 \text{ (the size of each pixel)}$$

$$\text{Depth } (D) \text{ for each pixel } i = (\text{mean } (Bit_{s,water\ edge}) - Bit_{s,i}) \times \text{Scale}_{bit}$$

$$\text{Volume } (V) = \sum D_i \times A$$

where

- N_{pixels} = number of pixels in the backwater
- $\text{mean } (Bit_{s,water\ edge})$ = mean 8-bit integer value for pixels along the water edge
- $Bit_{s,i}$ = 8-bit integer value for pixel i
- Scale_{bit} = the actual (continuous) stage change corresponding to an incremental stage change in the 8-bit grid;
- D_i = depth of pixel i

As shown in Table 5, predictions at each ABIS stage (bit-value) were then associated with measurable stage changes and local flow conditions.

The ABIS method makes certain assumptions regarding the temporal and spatial stability of local stage discharge relationships, the stability of backwater topography during the baseflow period, and the importance of hydraulic gradients. First, ABIS assumes that the shape of the

TABLE 5 Example Stage Table for BW03 Surveyed on October 8, 2008

Backwater Parameter Values at Elevation ^a								
Water Elevation (m)	Relative Stage (m)	Flow-Related Stage at Ouray (m) ^b	Flow (cfs) ^c	Bit	Inundated Surface Area (m ²)	Water Volume (m ³)	Max Depth (m)	Mean Depth (m)
1,420.90	-0.30	4.51	761	72	361	233.46	1.30	0.65
1,420.91	-0.29	4.52	822	73	368	240.91	1.31	0.65
1,420.93	-0.27	4.54	884	74	375	248.11	1.33	0.66
1,420.95	-0.25	4.56	940	75	402	259.81	1.35	0.65
1,420.97	-0.23	4.58	1,000	76	399	262.94	1.37	0.66
1,420.99	-0.21	4.59	1,070	77	433	278.39	1.39	0.64
1,421.00	-0.20	4.61	1,130	78	391	273.26	1.40	0.70
1,421.02	-0.18	4.63	1,200	79	406	277.60	1.42	0.68
1,421.04	-0.16	4.65	1,270	80	425	288.00	1.44	0.68
1,421.06	-0.14	4.67	1,330	81	412	287.60	1.46	0.70
1,421.07	-0.13	4.68	1,390	82	417	295.76	1.48	0.71
1,421.09	-0.11	4.70	1,460	83	415	306.34	1.49	0.74
1,421.11	-0.09	4.72	1,530	84	439	318.17	1.51	0.72
1,421.13	-0.07	4.74	1,610	85	439	318.06	1.53	0.72
1,421.15	-0.05	4.76	1,680	86	587	343.08	1.55	0.58
1,421.16	-0.04	4.77	1,760	87	705	364.01	1.57	0.52

^a Determined from DEM using ABIS

^b Determined from USGS stage-flow relationship.

^c 1 cfs = 0.028317 m³/s.

USGS rating curve at the Ouray gage station was valid for each of the backwater survey sites within a single baseflow period and across survey years. Part of the reason for making this assumption is the inability to obtain a more accurate estimate of local ratings in the absence of establishing a stage gage at each backwater site. In addition, as discussed in Appendix 2, data obtained from the Ouray gage station qualitatively suggests that the temporal and spatial variability of the Ouray rating curve is not substantial enough to invalidate the assumption that the shape of the rating curve was relatively static within the study reach over the period of survey.

The ABIS model does not account for site-specific hydraulic conditions. When the water level in the backwater is well below any potential sandbar breach locations, ABIS provides an accurate hydrodynamic description. However, when the water level in the backwater approaches the elevation of a potential breach location, particularly those further upstream, hydrodynamic considerations potentially become important. In these cases, the water level on the river side may exceed the breach elevation slightly before ABIS predicts it will, because ABIS does not take into account the energy gradient across the breach point. However, the energy gradient of the river in the study area was very modest and shallow flow over the backwater breach would

experience high-energy losses with increasing velocity that would rapidly satisfy the modest energy gradient that exists between the river side of the bar and the backwater side of the bar.

The backwater-flow relationships developed with ABIS for each survey year were based on backwater surveys conducted only once per year during the baseflow period. Our analysis assumed that there was no significant change in backwater topography following the start of the baseflow period and therefore backwater-flow relationships were constant during the baseflow period. There may be some change in sandbar topography within the baseflow period each year, especially in response to large increases in flow resulting from storms or changes in operations, as noted by Pucherelli (1987), but any such changes would be modest compared to the reworking that occurs in response to the annual peak flow. We consider our topographic surveys to be representative of the range of conditions that occurred each year within our study reach and the response of backwater habitats to changes in hourly and daily flows.

3 RESULTS AND DISCUSSION

In this section, we present the results of our evaluation of inter- and intraannual variability in backwater characteristics and discuss their implications for age-0 Colorado pikeminnow habitat availability. Included is (1) an evaluation of temporal variability in backwater abundance, size, and distribution as determined from aerial and satellite imagery, (2) characteristics of backwaters surveyed from 2003 to 2013, and (3) potential relationships between early life stages of Colorado pikeminnow and these backwater conditions. For the second topic, we look at interannual variability and the implications of this variability on the effects of dam operations and changes in tributary flows during the base-flow period. We also explore the role of peak flow on the size of sandbars and associated backwaters.

3.1 BACKWATER HABITAT CHARACTERISTICS AS DETERMINED FROM AERIAL AND SATELLITE IMAGERY

We used interpretations of aerial and satellite imagery collected in the Jensen and Ouray reaches by Pucherelli and Clark (1989 and 1990), Bell (1997), and Argonne to evaluate three backwater variables: (1) mean surface area of individual backwaters, (2) the number of backwaters/RM, and (3) total backwater surface area/RM. This evaluation included a comparison of the relationships between base flow and backwater variables and changes in values of the variables through time.

Pucherelli and Clark (1989 and 1990) used aerial photography and video in 1987 and 1989 to assess the number of backwaters and backwater size (surface area) at multiple flows in each year, which permitted an analysis of backwater habitat at different flows. In 1987, there was a decrease in the mean backwater area, the number of backwaters/RM, and backwater area/RM as flows increased in both the Jensen and Ouray study reaches (Figures 4 and 5). In the Jensen reach, the decreases in the number of backwaters/RM and the total backwater area/RM were statistically significant; in the Ouray reach, only the decrease in the number of

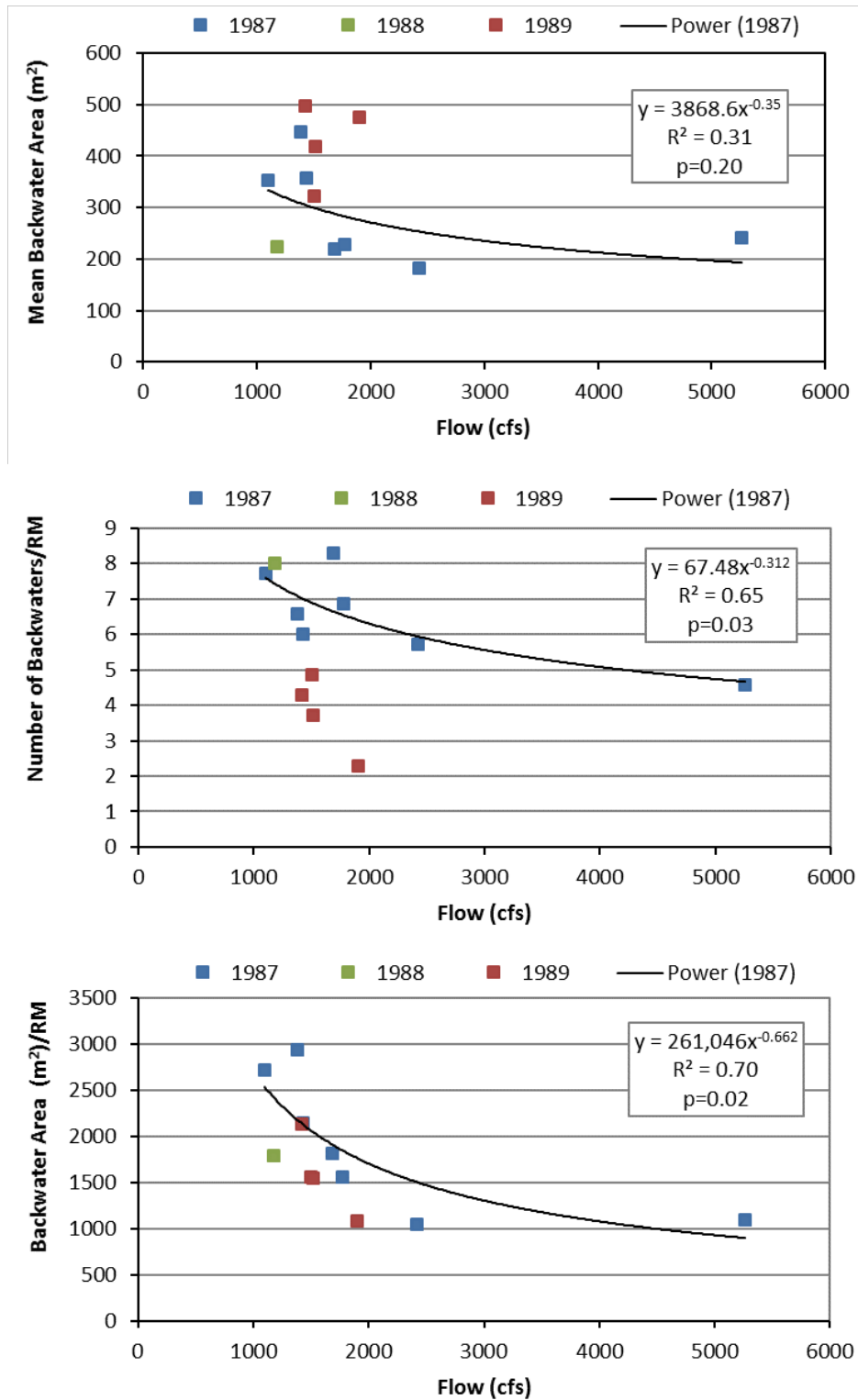


FIGURE 4 Relationship between Flow and Mean Backwater Surface Area, Number of Backwaters/RM, and Backwater Area/RM in the Jensen Reach (RM 303-310) Based on Imagery Collected in 1987, 1988, and 1989 by Pucherelli and Clark (1989 and 1990). Regressions for 1987 data are shown.

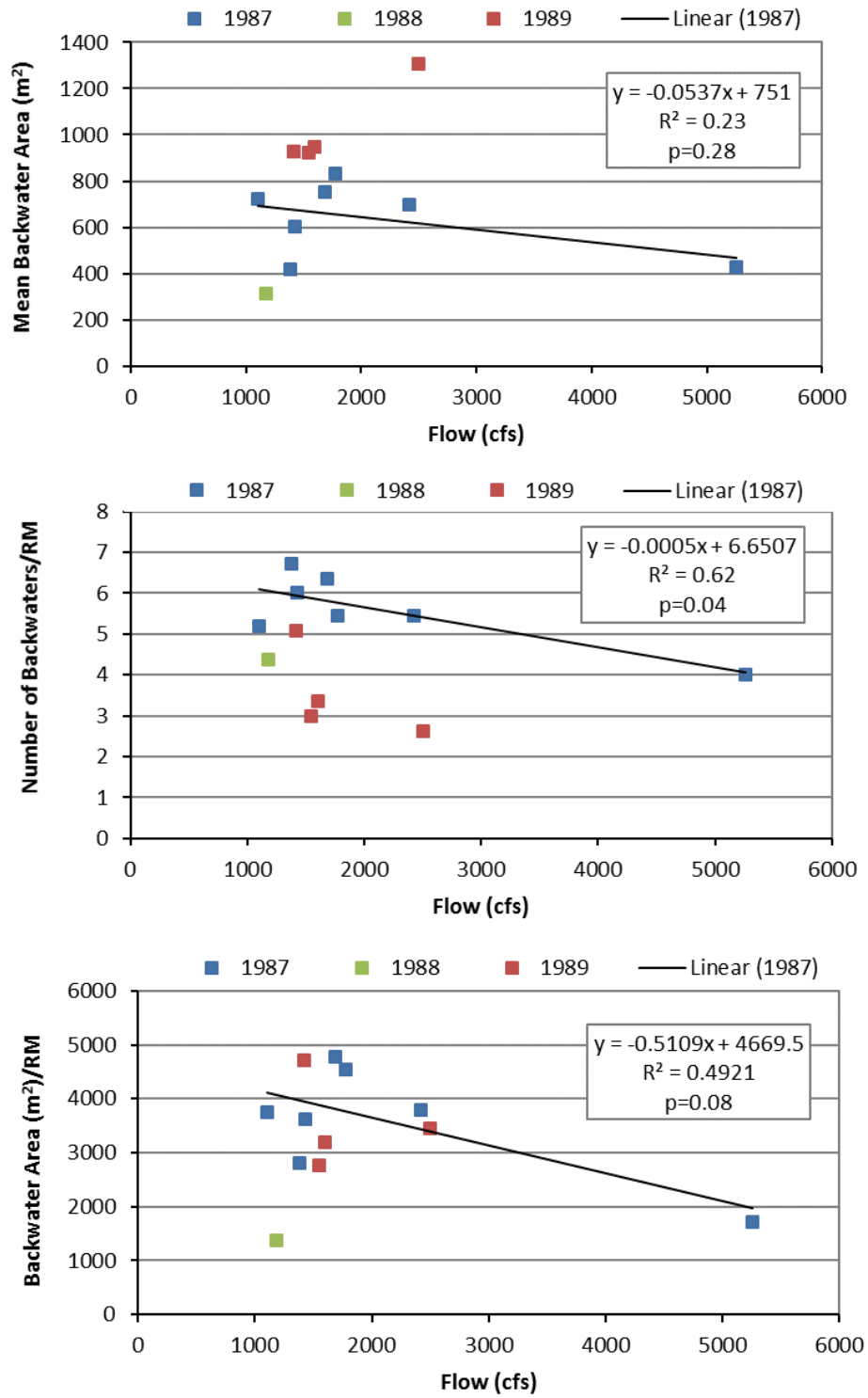


FIGURE 5 Relationship between Flow and Mean Backwater Surface Area, Number of Backwaters/RM, and Backwater Area/RM in the Ouray Reach (RM 130.5-261.6) Based on Imagery Collected in 1987, 1988, and 1989 by Pucherelli and Clark (1989 and 1990). Regressions for 1987 data are shown.

backwaters/RM was significant. The 1989 data showed a similar pattern to 1987 data in both study reaches, but, compared to 1987, the mean backwater area was higher, the number of backwaters/RM was lower, and the total backwater area/RM) was about the same.

We analyzed aerial images obtained at single low flows (ranging from 1,180-2,090 cfs [$33.4 \text{ m}^3/\text{s}$ - $59.2 \text{ m}^3/\text{s}$]) in 1988, 1993, 1996, 2004, 2006, and 2013 to determine if changes had occurred in the mean size, number, or total amount of backwater habitat through time. For years with multiple flows (1987 and 1989), we included the mean for these variables at flows between 1,000-2,500 cfs in the trend analysis. Figure 6 presents the values for backwater variables over the 26-year period in each of the 8 years studied. The mean surface area of individual backwaters showed a significant increase over time at Jensen and Ouray, while the number of backwaters/RM significantly decreased over this period. Backwater area/RM was quite variable over this same period, and did not show a significant increasing or decreasing trend. This suggests that total backwater habitat area over the 26-year period was not decreasing despite the apparent decrease in the number of backwaters, and that the decrease in number was offset by an increase in the average size of the backwaters.

Bell (1997) compared his data from 1993 and 1996 to the 1987 data of Pucherelli and Clark (1989 and 1990), and noted the same trend of increased size and decreased number of backwaters. He speculated that the very low peak flow in 1987 (10,900 cfs [$309 \text{ m}^3/\text{s}$]) compared to the higher peaks in 1993 and 1996 of 20,400 cfs ($578 \text{ m}^3/\text{s}$) and 22,400 ($634 \text{ m}^3/\text{s}$), respectively, may have resulted in these differences. Peak flows in 2003, 2006, and 2013 were 19,400 cfs ($549 \text{ m}^3/\text{s}$), 19,200 cfs ($544 \text{ m}^3/\text{s}$), and 10,400 cfs ($294 \text{ m}^3/\text{s}$), respectively, suggesting that there may be a more complex relationship.

In the following paragraphs, we discuss three hypotheses that could explain the changes in backwater number and size over time: (1) channel narrowing; (2) reduction in fluctuations; and (3) differences in approach or analysts among the three studies.

Lyons et al. (1992) reported that in the middle Green River, channel narrowing following construction of Flaming Gorge Dam ceased in 1974, producing a decrease in mean width from 217 m to 204 m (6% reduction). They found that the large annual peak flows that occurred from 1983 to 1986 (21,000 to 40,000 cfs [594 to $1,132 \text{ m}^3/\text{s}$]) reversed some of this narrowing and produced a mean channel width of 208 m (2% increase in width from 1974; 4% reduction from pre-dam width). We hypothesize that widening of the river channel may have increased the number of depositional sites that promoted formation of sandbars with associated backwaters. Subsequent years with lower peak flows ($<14,500$ cfs [$410 \text{ m}^3/\text{s}$] from 1987 to 1992) may have led to less sediment transport, less erosion of existing sediment deposits, and reduced scour of encroaching vegetation, resulting in gradual channel narrowing. Although no imagery is available immediately following the high peak flow in 2011 (32,200 cfs [$912 \text{ m}^3/\text{s}$]), the first available imagery (2013) does not indicate that the number of backwaters increased. This does not necessarily disprove our hypothesis, because long periods without high flows could reduce the effect of channel widening during a subsequent high flow. Contributing to channel narrowing is vegetation encroachment, particularly by invasive tamarisk (*Tamarix* spp.) and Russian olive (*Elaeagnus angustifolia*). Vegetation encroachment can occur during extended low-flow periods during which high flows do not occur frequently enough to remove new vegetation and the low

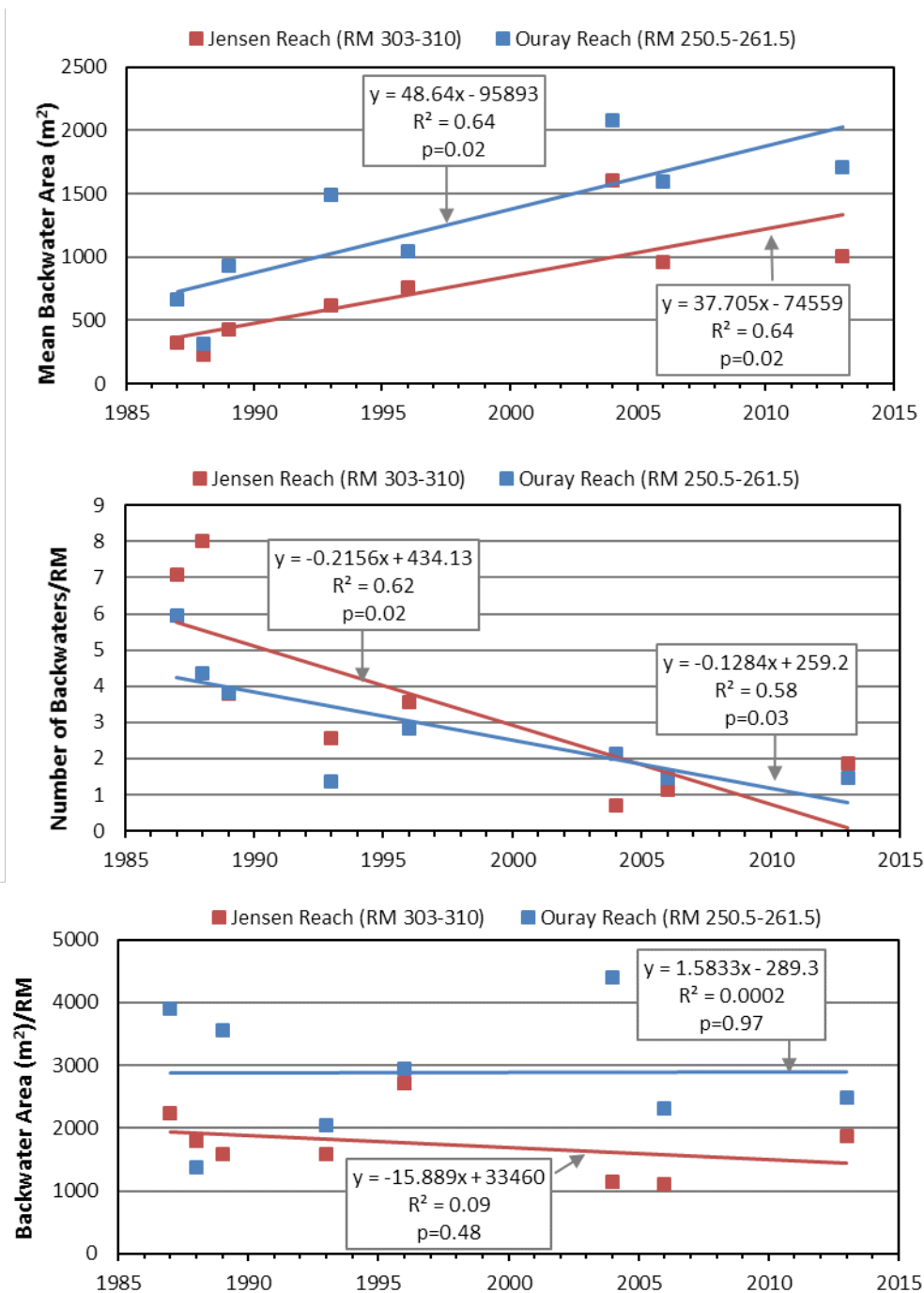


FIGURE 6 Mean Backwater Surface Area, Number of Backwaters/RM, and Backwater Area/RM in the Jensen and Ouray Reaches from 1987 to 2013. For years with multiple flows (1987 and 1989), the mean for flows between 1,000 and 2,500 cfs was used. Data from 1987 to 1989 are from Pucherelli and Clark (1989 and 1990); data from 1993 and 1996 are from Bell (1997); other data were newly analyzed for this study.

flows maintain soil moisture for the vegetation. Vegetation encroachment tends to promote deposition of sediment along channel margins, further reducing channel width. Pucherelli et al. (1987) suggested that vegetation-related channel narrowing in the Green River may result from a reduction in the frequency of high-magnitude peak flows.

A contributing factor, or an alternative to the channel-narrowing hypothesis, may be related to the magnitude of fluctuations during the base-flow period. The increase in backwater size between 1987 and 2013 may be a result of the reduction in daily base-flow variation following the implementation of the 1992 Biological Opinion (FWS 1992). The Biological Opinion identified a target range of base flows between 1,100–1,800 cfs (31–51 m³/s) in the summer with daily fluctuations restricted to 25% or less of the mean daily flow. The 2006 Biological Opinion (FWS 2006) modified the base-flow restriction to be no more than a 0.1 m change in water surface elevation within a day. We compared hourly dam releases from three periods: 1989 through 1991, 1992 through 2000, and 2001 through 2006. Within-day variability from July through September, as measured by the coefficient of variation in hourly flow, averaged 20.2, 13.8, and 10.5, respectively, demonstrating the reduction in flow variability over this period. Relatively high fluctuations could result in the lower-elevation deposits on the downstream end of sandbars being reworked, shortening the length and size of backwaters. Under the 1992 Biological Opinion flows and current operations, much less reworking of the lower elevation portions of the sandbars might occur because daily variations in flow at Ouray are relatively small. Thus, the topography that exists at the end of the spring high flow would be more likely to be preserved for a longer period (i.e., would have little reduction in size) during the base-flow period. This hypothesis does not provide an explanation of the decrease in backwater numbers after 1992. The results of a study conducted by Pucherelli and Clark (1990) in 1989 to determine the effects of fluctuating flows on backwaters in the middle Green River demonstrated that flows that fluctuated between 1,600 and 2,900 cfs affected backwater number and area, but the response was different between the Jensen and Ouray study reaches. In the Jensen reach, backwater number increased and total backwater area was stable (indicating individual backwater area was decreased) in response to fluctuating flows; in the Ouray reach, backwater number did not change, but backwater area decreased (again indicating that individual backwater area decreased) in response to fluctuating flows.

A reviewer of our draft report expressed concern that the temporal trends identified in Figure 6 could be related to differences in approach or analyst bias among the studies. For any comparison of new results to published results, there is the potential for interpretations to be affected by such differences. For example, smaller backwaters are more difficult to detect in aerial and satellite imagery and differences between analysts' ability to discern them is a potential source of bias. It is possible that there were more backwaters with a smaller mean surface area recorded in 1987, 1988, and 1989 simply because Pucherelli and Clark were better at identifying them than Bell or we were.

Although we acknowledge the potential for such an effect, there are several reasons why we think that our analysis is robust. The 1987, 1988, and 1989 imagery analyses of Pucherelli and Clark (1989 and 1990) were conducted by the same analysts using the same delineation approach. Bell (1997) worked in Pucherelli's group and conducted his analysis for the express purpose of determining backwater conditions in 1993 and 1996 and comparing his values to

those of Pucherelli and Clark. Bell's report is a memorandum to Pucherelli. His report identified the decline in number and increase in area of backwaters, as noted above, and our analysis produced values consistent with his that showed the trend had continued into the 2000s.

We took precautions to ensure internal consistency in our results by using a single analyst, single reviewer, and comparing the backwater areas we identified from imagery with those studied during ground surveys in the same year. To evaluate the potential effect of detectability of small backwaters, we eliminated small backwaters from the Pucherelli and Clark (1990) report and our analyses and reexamined the pattern in number and area through time. (Note that Bell did not present the number of backwaters in different size categories, and Pucherelli and Clark binned their small backwaters differently in 1987 and 1989 as $< 20 \text{ m}^2$ and $< 50 \text{ m}^2$, respectively). Since there were relatively few backwaters identified in these categories in any study, the original pattern of a decrease in the number of backwaters/RM was still apparent after eliminating small backwaters (Jensen reach in 1987, 1989, 2004, 2006, 2013: 6.3, 3.0, 0.7, 1.1, 1.9, respectively; Ouray reach in the same years: 5.5, 3.6, 2.1, 1.5, 1.5, respectively). Small backwaters contribute little to the average size or total area of backwaters, because there are relatively few of them, but we could not calculate the effect of eliminating them on area because area for different size classes was not presented in Pucherelli and Clark (1990).

Finally, the mean size of backwaters sampled for age-0 Colorado pikeminnow during ISMP sampling (presented in Table 4 of Bestgen and Hill 2016) are consistent with imagery estimates, and show a similar increase in backwater surface area from 1986–2012 (Figure 7). It should be noted that the mean annual backwater size for ISMP sampling is likely to be higher than the mean size of all backwaters in the middle Green River because the smallest backwaters are not sampled during ISMP (sampled backwaters must have a maximum depth of at least 0.3 m and surface area of at least 30 m^2). It seems unlikely, however, that the apparent increase in size through time shown in Figure 7 is a reflection of this sampling bias.

3.2 SURVEYED BACKWATER TOPOGRAPHY AND THE RELATIONSHIP BETWEEN BACKWATER TOPOGRAPHY AND FLOW

This section describes surveyed backwater habitat conditions and the relationship between backwater habitat and flow conditions in the middle Green River. We describe intra- and interannual variation in backwater characteristics during the base-flow period and changes in the relationship between flow and backwater morphology. We also discuss whether there are optimal base flows for maximizing backwater habitat and whether interannual changes in the optimal base flows can be explained by interannual variation in antecedent spring flows.

As described in Section 2.3, we annually surveyed the topography of selected backwater habitats and associated sandbars from 2003 to 2013. We used this information to develop a DEM of each surveyed backwater-sandbar complex and the relationships among flow and backwater characteristics for each of the surveyed habitats (see Section 2.4). Appendix 4 contains figures illustrating the relationships among backwater physical characteristics (volume, surface area, maximum depth, and mean depth) and local flow conditions in the Ouray study area during the

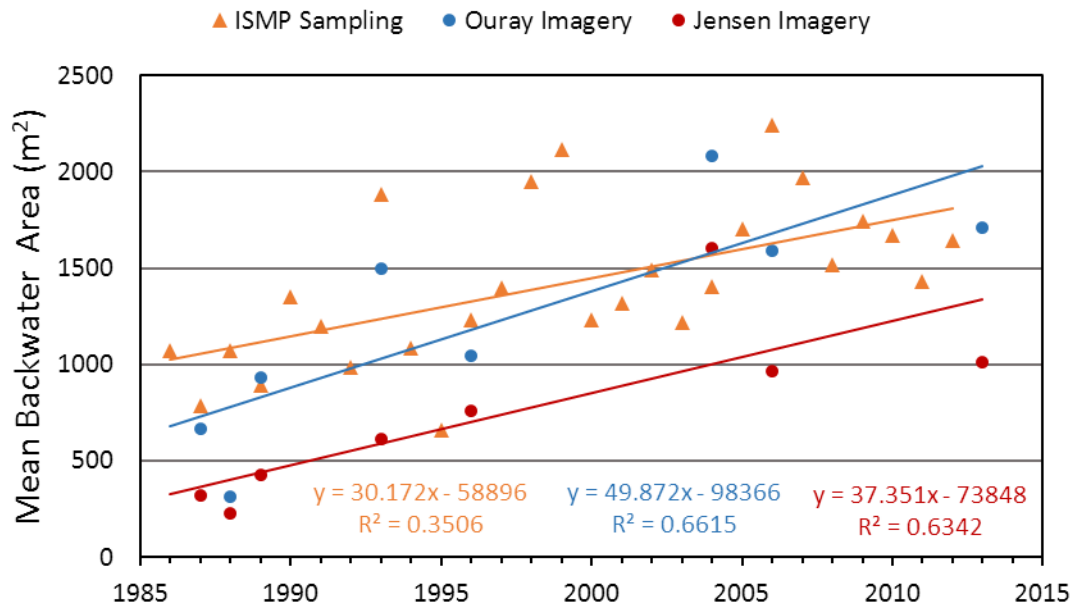


FIGURE 7 Comparison of Mean Backwater Area as Estimated Using Aerial and Satellite Imagery and ISMP Sampling

base-flow period of each survey year. Simulated backwater physical characteristics (surface area, volume, and mean depth) across the range of typical base flows (800–4,000 cfs [23–113 m³/s]) for each backwater and survey year are presented in tabular form in Appendix 5.

3.2.1 Representativeness of Surveyed Backwaters

Detailed topographic information was needed to develop models of backwater characteristics under different flow conditions. However, because of time and budget constraints, we could only survey 4 to 6 backwaters each year, and these represent a small percentage of the total number of backwaters that occur in the 15-mi (24-km) ONWR study reach and the overall 68-mi (109-km) reach between the Jensen and Ouray gages. Our imagery analysis indicated that the ONWR reach and Jensen to Ouray reach had comparable numbers of backwaters/RM and mean surface area of backwaters (Table 6).

To assess the representativeness of our surveyed backwaters, we compared the surface area of surveyed backwaters to the surface area of all backwaters in the ONWR reach and the Jensen to Ouray reach as determined from remotely sensed imagery (Table 6). The analysis was limited to 2004, 2006, and 2013, which were the only survey years for which aerial or satellite imagery was available at base flows.

TABLE 6 Mean Surface Area of Surveyed Backwaters and the Surface Area of All Backwaters in the ONWR Reach and Jensen to Ouray Reach as Determined from Aerial and Satellite Imagery

Variable	Year		
	2004	2006	2013
Imagery Analysis			
Date of imagery collection	8/30	7/14, 7/15	9/18, 11/2
Jensen gage flow(cfs) at time of imagery acquisition	1,220	2,090; 1,950	1,800; 1,660
<i>ONWR Reach: RM 250.5 to 265.5</i>			
Number of backwaters	33	28	18
Number of backwaters/RM	2.6 ^a	1.9	1.2
Mean surface area (m ²)	1,515	1,287	1,618
<i>Jensen to Ouray Reach: RM 248.5 to 316.5</i>			
Number of backwaters	109	156	88
Number of backwaters/RM	2.2 ^b	2.3	1.3
Mean surface area (m ²)	1,143	1,176	1,352
Backwater Survey in ONWR Reach			
Date of survey	9/28-30	9/26-28	9/10-12
Ouray flow (cfs) at time of survey	1,689-1,789	1,519-1,659	1,349-1,439
Number of backwaters surveyed	4	4	5
Percent of total backwaters in ONWR reach	12.1	14.3	27.8
Mean surface area (m ²)	1,793	2,703	2,882
Percentile rank relative to all ONWR backwater surface area values	73	88	84
Percentile rank relative to all Jensen-Ouray backwater surface area values	81	88	83

^a Imagery was available for a total of 12.5 mi of river in the ONWR reach in 2004 (imagery not available for RM 250.5 to 253.0).

^b Imagery was available for a total of 50 mi of river in the Jensen to Ouray reach in 2004 (imagery not available for RM 248.5 to 253.0, RM 272 to 281, and RM 283.5 to 288).

From this analysis, we determined that we surveyed 12%, 14%, and 28%, respectively, of the backwaters in the ONWR reach in 2004, 2006, and 2013 (Table 6). In all years, the mean surface area of surveyed backwaters was larger than the mean backwater surface area for the ONWR reach and Jensen to Ouray reach. The percentile ranks of surveyed backwaters were 73, 88, and 84 relative to all ONWR surface area values in 2004, 2006, and 2013, respectively, and 81, 88, and 83 relative to all survey values in the Jensen to Ouray reach in the same years (Table 6). Flow conditions at the time the imagery and survey data were obtained were within 500 cfs (Table 6), which suggests that the observed differences between our surveyed backwaters and those in the entire reach were not a result of differences in flow. We selected backwaters to

survey based on depth and size, intentionally selecting backwaters that met the Recovery Program's Interagency Standardized Monitoring Program (ISMP) minimum criteria for suitable Colorado pikeminnow habitat of 30 m² in area and 0.3 m in depth. This introduced a bias in our selection process that resulted in the selection of larger backwaters.

Given the small sample size of surveyed backwaters relative to the total number of backwaters, and the observed variability in sandbar topography, it is not surprising that the backwater morphological characteristics derived from survey results differ from those that can be obtained from aerial or satellite imagery. Despite the identified differences, we believe these data and the models built on these data provide valuable insight into the likely effects of flow variation on backwater habitats used by Colorado pikeminnow.

In addition, we believe that our surveyed backwaters represent suitable nursery habitats for Colorado pikeminnow as defined by the maximum depth criterion of ≥ 0.3 m used by the Program for backwater surveys. Mean depth of our surveyed backwaters averaged across the base-flow period was usually less than 1 m and often less than 0.5 m (Appendix 5). Although mean backwater depth was less than 0.3 m for 25% of surveyed backwaters (13 of 51), mean *maximum* backwater depth was greater than 0.3 m in all years and backwaters, except for BW06 in 2010, which had a mean maximum depth of 0.2 m (Appendix 5). Many backwaters have large portions of their surface area with very shallow depth, while retaining areas with depths greater than 0.3 m. We included these very shallow depths in our calculation of mean depth. Day et al. (1999) captured age-0 pikeminnow in backwaters as shallow as 0.04 m.

3.2.2 Intraannual and Interannual Variability in the Relationships between Backwater Habitat Variables and Base Flows

The relationships between backwater variables (surface area, volume, mean depth, and maximum depth) and base flows for all surveyed backwaters in all survey years are presented in Appendix 4. Mean values of these variables for all surveyed backwaters during the base-flow period are presented in Appendix 5. Our survey results indicate that these relationships were highly variable among backwaters both within and between years. For example, based on ABIS simulations, maximum backwater surface area and volume in 2004 would be achieved at a base flow of approximately 3,500 cfs (99 m³/s) at BW07a, while maximum surface area and volume at BW02 would occur at approximately 2,500 cfs (71 m³/s) (Figure 8). In 2009, surface area, volume, and depth of BW02 would be maximized at approximately 2,000 to 2,300 cfs (57 to 65 m³/s), which is much lower than the >3,000 cfs (85 m³/s) flow that would maximize these values for BW06, BW07b, and BW10 (Figure 9). Similarly, in 2012, surface area and volume for BW07b and BW02 would be maximized at much higher flows than BW10 and BW08 (Figure 10). Backwater depth in 2004 and 2009 was also maximized at a wide range of flows for different backwaters in the same year.

Simulations indicate that backwater characteristics change significantly over the range of base flows experienced in most years. For example, in 2009, the surface area of BW02 varied between 1,000 and >7,000 m² within the base-flow range of 2,000 to 3,500 cfs (57 to 99 m³/s) (Figure 11a). Maximum backwater surface area at BW02 occurred at approximately 2,100 cfs

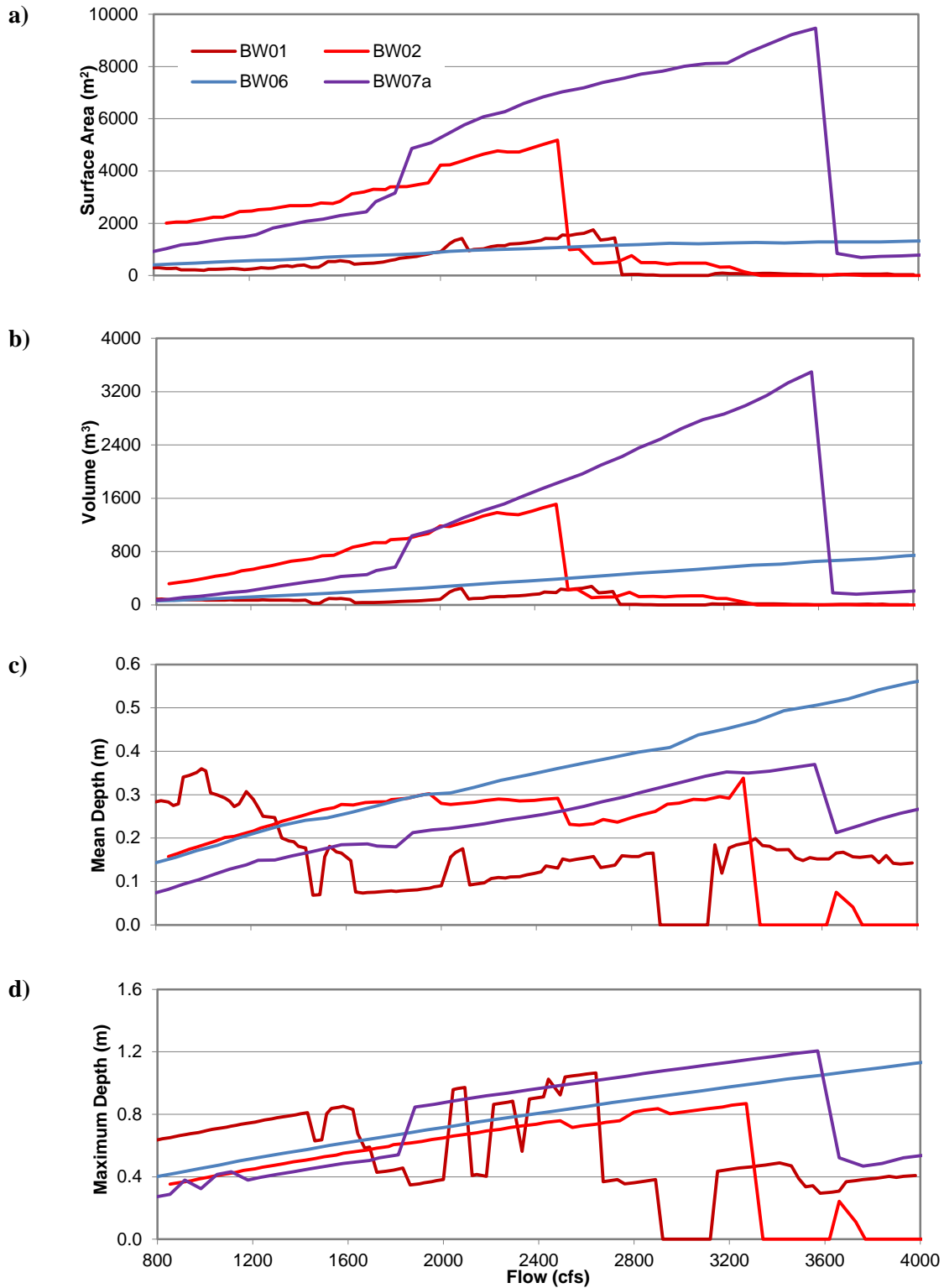


FIGURE 8 Relationships between Flow at the Ouray Gage and Backwater (a) Surface Area, (b) Volume, (c) Mean Depth, and (d) Maximum Depth in 2004

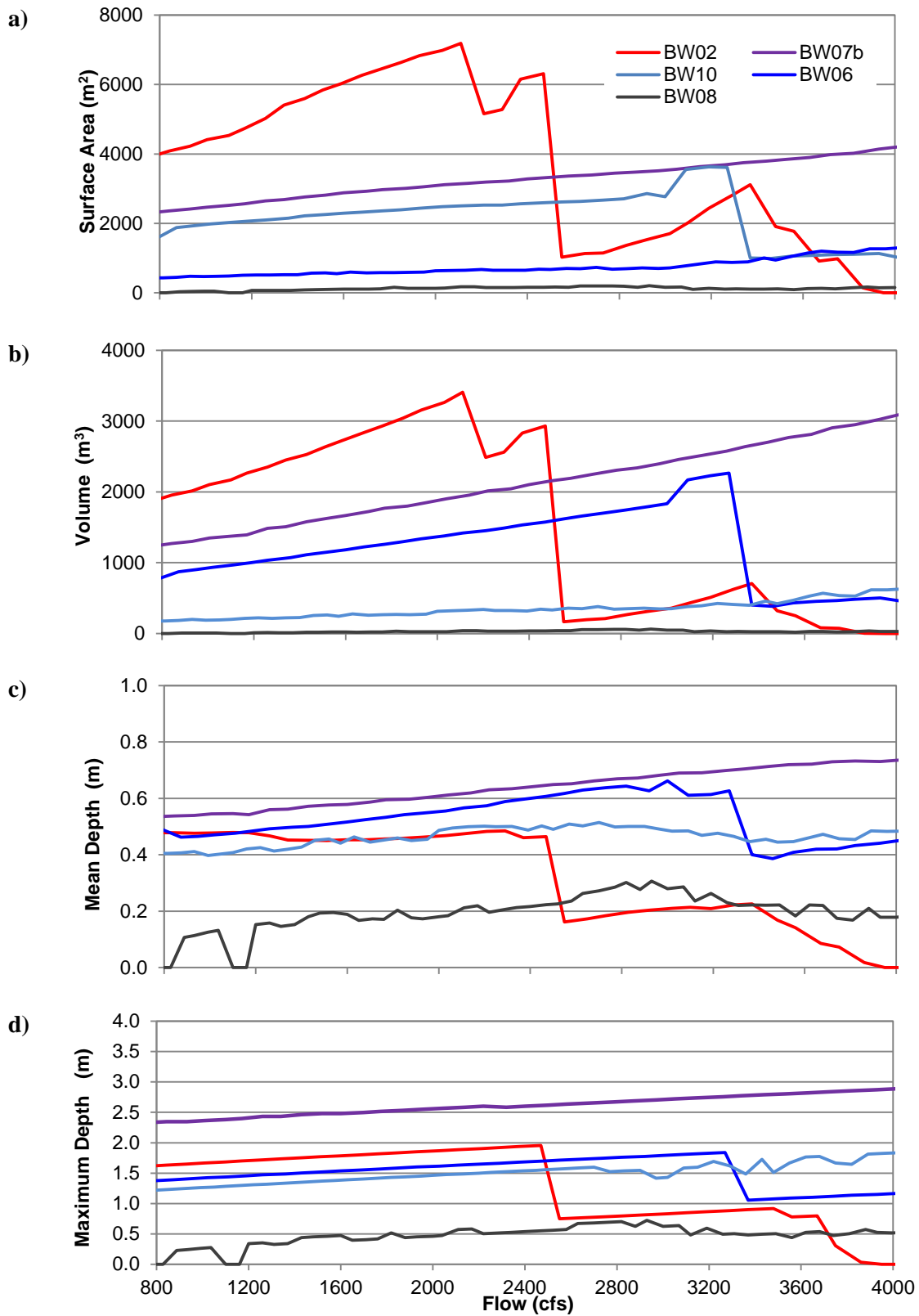


FIGURE 9 Relationships between Flow at the Ouray Gage and Backwater (a) Surface Area, (b) Volume, (c) Mean Depth, and (d) Maximum Depth in 2009

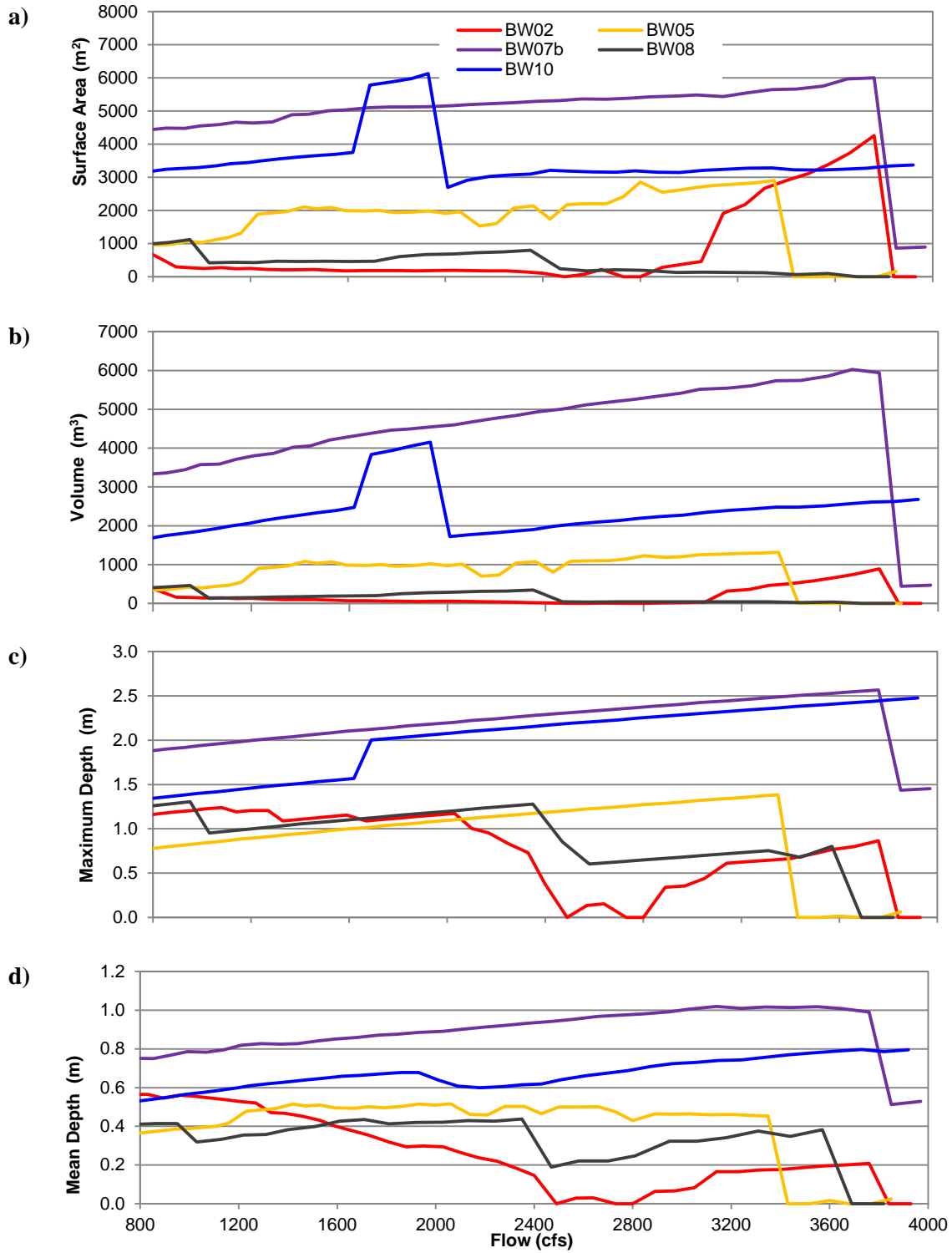


FIGURE 10 Relationships between Flow at the Ouray Gage and Backwater (a) Surface Area, (b) Volume, (c) Mean Depth, and (d) Maximum Depth in 2012

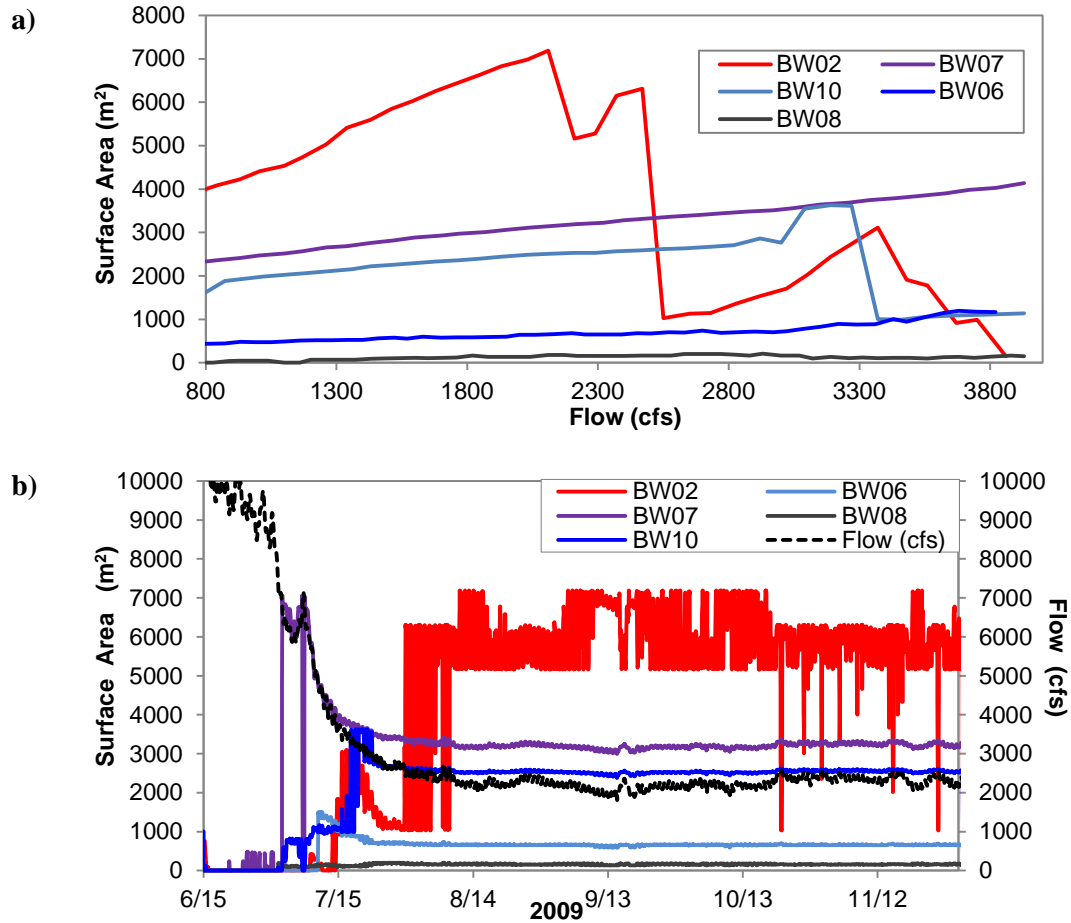


FIGURE 11 Backwater Surface Area in 2009—(a) Relationship between Backwater Surface Area and Flow and (b) Modeled Relationship between Surface Area and Hourly Flow during the Base-Flow Period

(59 m³/s), but exhibited a steep reduction in surface area at flows greater than 2,100 cfs (59 m³/s), as higher flows resulted in water flowing through various cross channels through the sandbar (see Figure 12 and associated discussion below). Thereafter, backwater surface area increased between flows of 2,210 cfs and 2,470 cfs (62 and 70 m³/s), but then decreased significantly at higher flows before increasing again between 2,830 and 3,370 cfs (80 and 95 m³/s). Consequently, fluctuations in flow during the base-flow period resulted in significant temporal variation in backwater surface area at BW02 from August to December 2009 (Figure 11b). We discuss this temporal variation in backwater characteristics and the roles of dam releases and tributary inflows in Section 3.3.

The variable relationship between backwater characteristics and flow during the base-flow period resulted from the geomorphic complexity of most backwater habitats. We observed several types or styles of backwaters during our surveys, each with characteristic responses to changes in flows:

1. Backwaters with relatively simple geometry consisting of a high sandbar and deep backwater trough that decreases gradually in depth from downstream mouth to upstream end, increase in volume and depth as flow increases and provide relatively stable habitat over the course of a base-flow period (e.g., BW07b in Figure 9).
2. Backwaters similar to type 1 except the downstream tail of the bar extends underwater across most or all of the mouth of the backwater creating a shallow ridge that blocks flow into the backwater at lower flows. This type of backwater becomes disconnected at flows that drop below the elevation of the mouth bar.
3. Backwaters similar to type 1 in terms of characteristics of the backwater trough, but which have lower elevation portions of the bar surface that convey river flows across the bar surface at higher flow, and decrease the length of the backwater trough at these higher flows. This type of backwater increases gradually in size as flows increase, but then experiences a sharp decrease in surface area, volume, and depth as flow connections through the bar occur at higher flows (e.g., BW02 in Figure 9 and Figure 12).
4. Backwaters similar to types 2 and 3 with both a mouth ridge and one or more cross-sandbar channels. This type of backwater experiences disconnection from the main channel at lower flows and flow-through at higher flows.

Based on our survey results for BW02 in 2009, flows greater than approximately 2,110 cfs (60 m³/s) result in the loss of a significant amount of BW02 due to the formation of a second flow connection through the sandbar between the main channel and the backwater (Figure 12). At higher flows (2,250 cfs [64 m³/s]), additional connections result in further loss of backwater habitat. Our simulations suggest that significant changes in backwater area can occur over relatively small changes in flow, 400 cfs (11 m³/s) in this example.

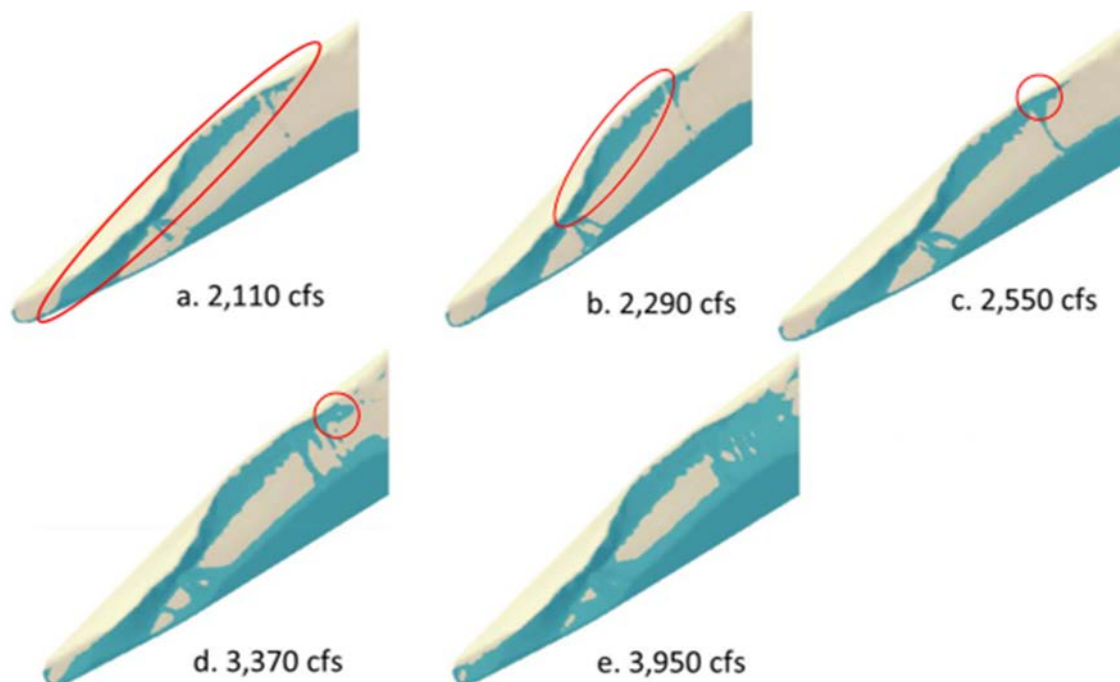


FIGURE 12 Visualization of BW02 in 2009 Showing the Significant Reductions in Backwater Surface Area Related to Variation in Flow at Ouray. Areas considered backwater habitat at each flow are circled in red. Rising flows form a cross-bar connection, resulting in a significant reduction in backwater area. Backwater habitat loss continues as increasing flow at Ouray results in a second cross-bar connection. The direction of river flow is from upper right to lower left in the figure.

In addition to variation among backwaters within a year, we observed significant interannual changes in topography for most backwaters. For example, Figure 13 to Figure 16 illustrate the morphology of BW02, BW05, BW07, and BW10 across survey years. Due to these changes in topography, there were also significant changes in the flow-surface area relationships. These results reflect the significant reworking of the sandbars during the peak flow period (Rakowski and Schmidt 1999), even during years with relatively low peak flow. For example, the surface area-flow curves in 2004, 2012, and 2013 (all years with peak flows less than 12,000 cfs [340 m³/s]) were very different from those in the year immediately preceding (Figures 12 to 15). Because of these changes in topography, the characteristics of individual backwaters varied dramatically between years. For example, the mean volume of BW02 during the base-flow period ranged from 169 m³ in 2005 to 6,354 m³ in 2013. BW07a, BW07b, and BW10 showed similar variation in volume between 2003 and 2013 (Appendix 5).

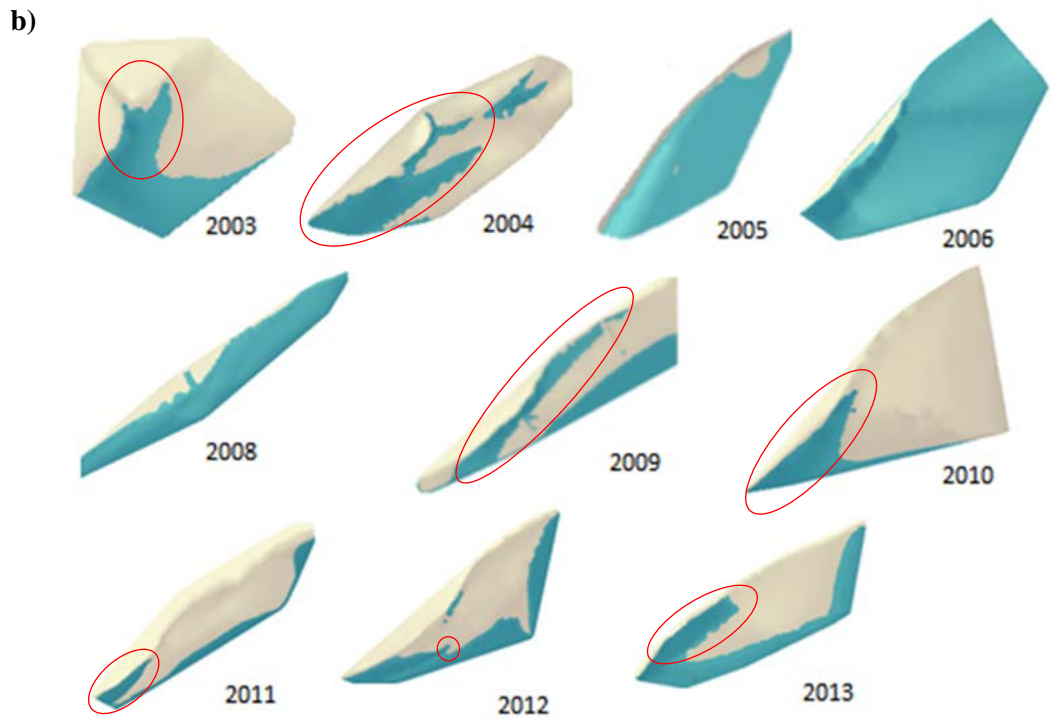
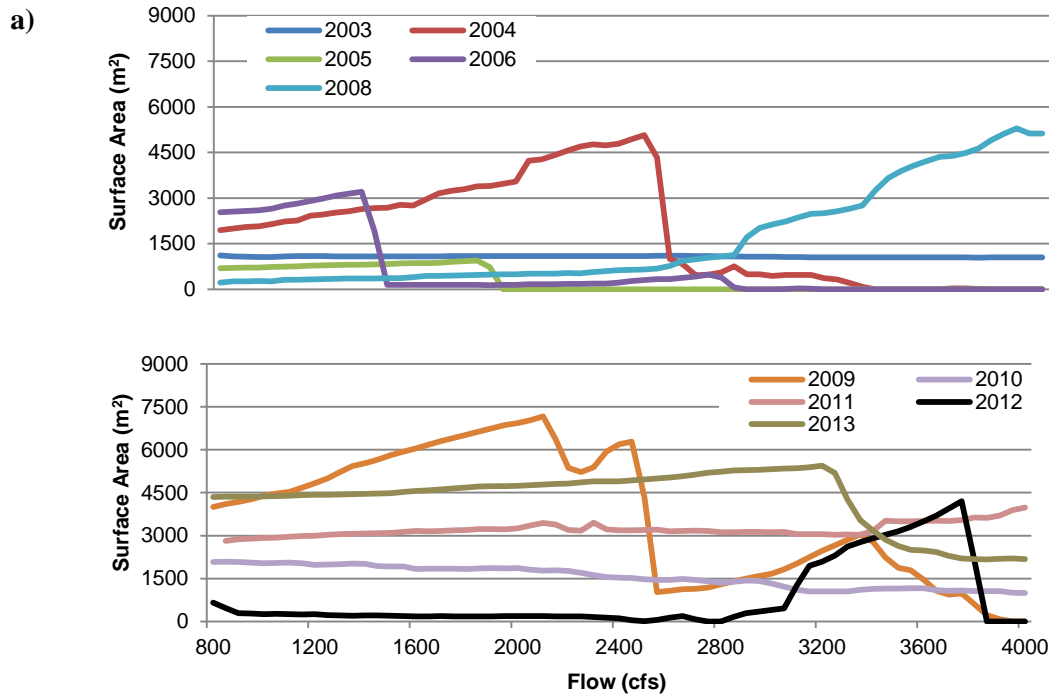


FIGURE 13 Changes in BW02 Surface Area from 2003 to 2013—(a) Relationship between Flow and Surface Area and (b) Changes in Backwater Morphology at 2,000 cfs (57 m³/s). Areas considered backwater habitat at each flow are circled in red. The direction of river flow is from upper right to lower left in the figure.

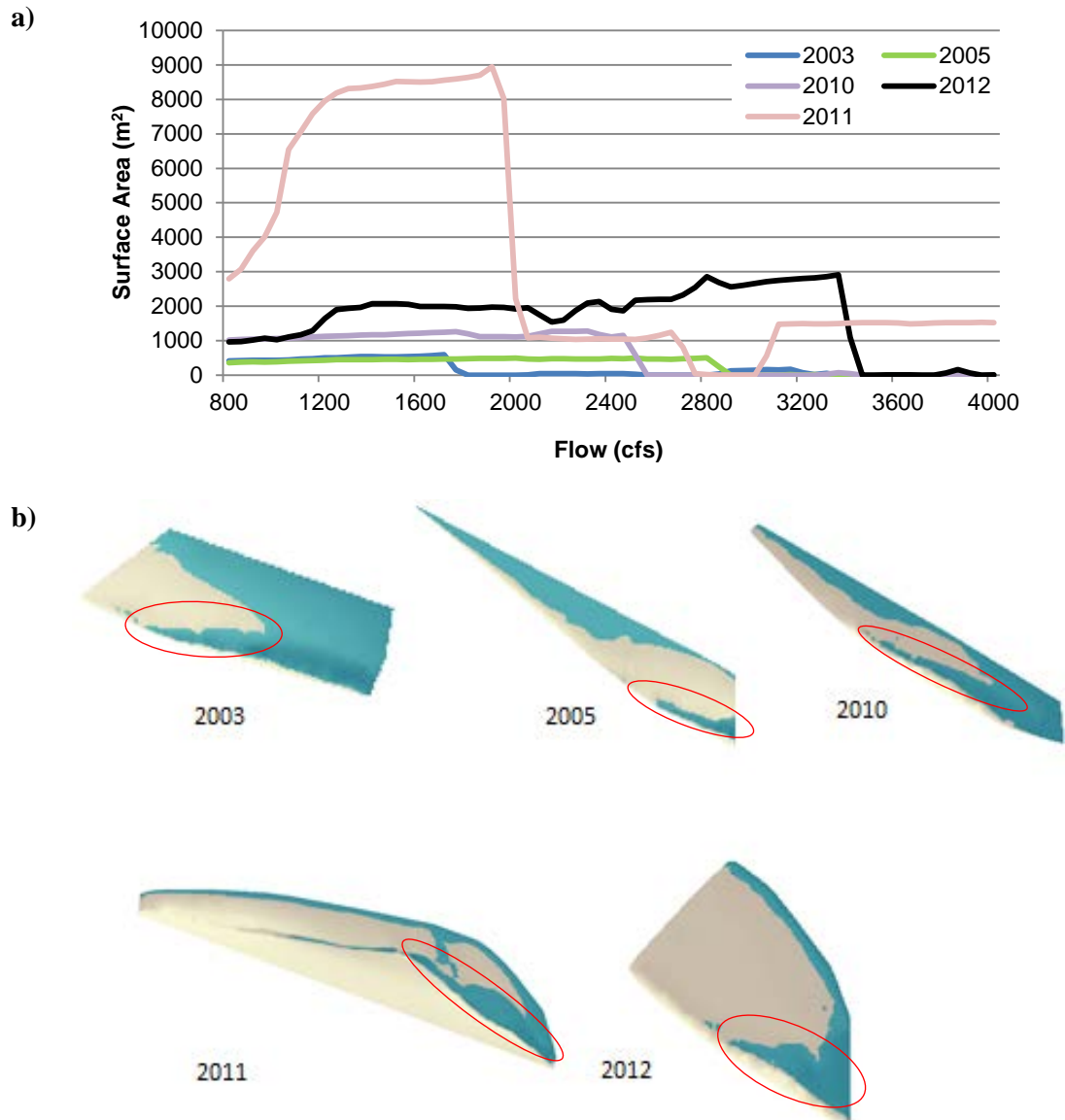


FIGURE 14 Changes in BW05 Surface Area from 2003 to 2012—(a) Relationship between Flow and Surface Area and (b) Changes in Backwater Morphology at 2,000 cfs ($57 \text{ m}^3/\text{s}$). Areas considered backwater habitat at each flow are circled in red. The direction of river flow is from upper left to lower right in the figure.

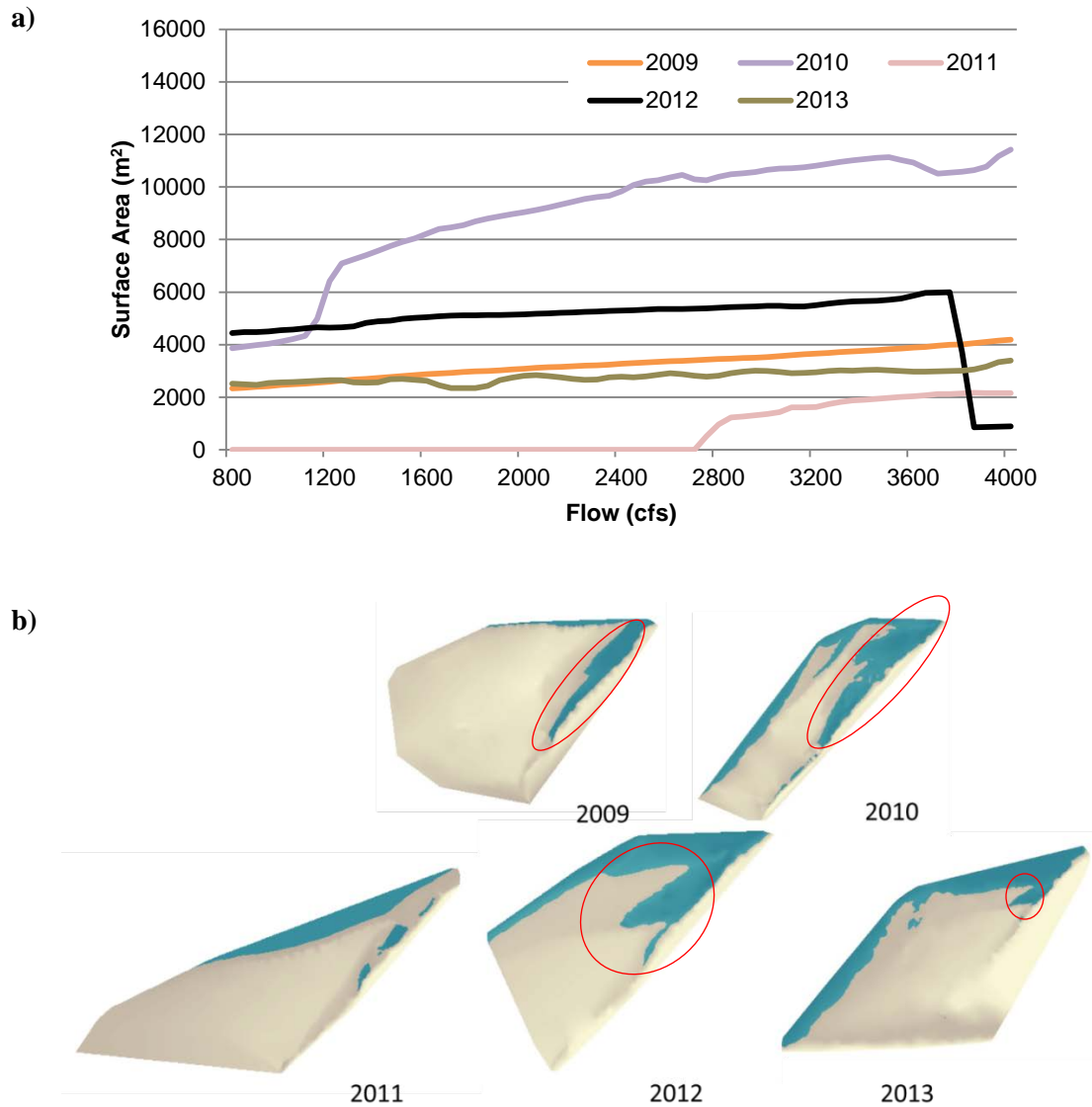


FIGURE 15 Changes in BW07b Surface Area from 2009 to 2013—(a) Relationship between Flow and Surface Area and (b) Changes in Backwater Morphology at 2,000 cfs ($57 \text{ m}^3/\text{s}$). Areas considered backwater habitat at each flow are circled in red. The direction of river flow is from lower left to upper right in the figure.

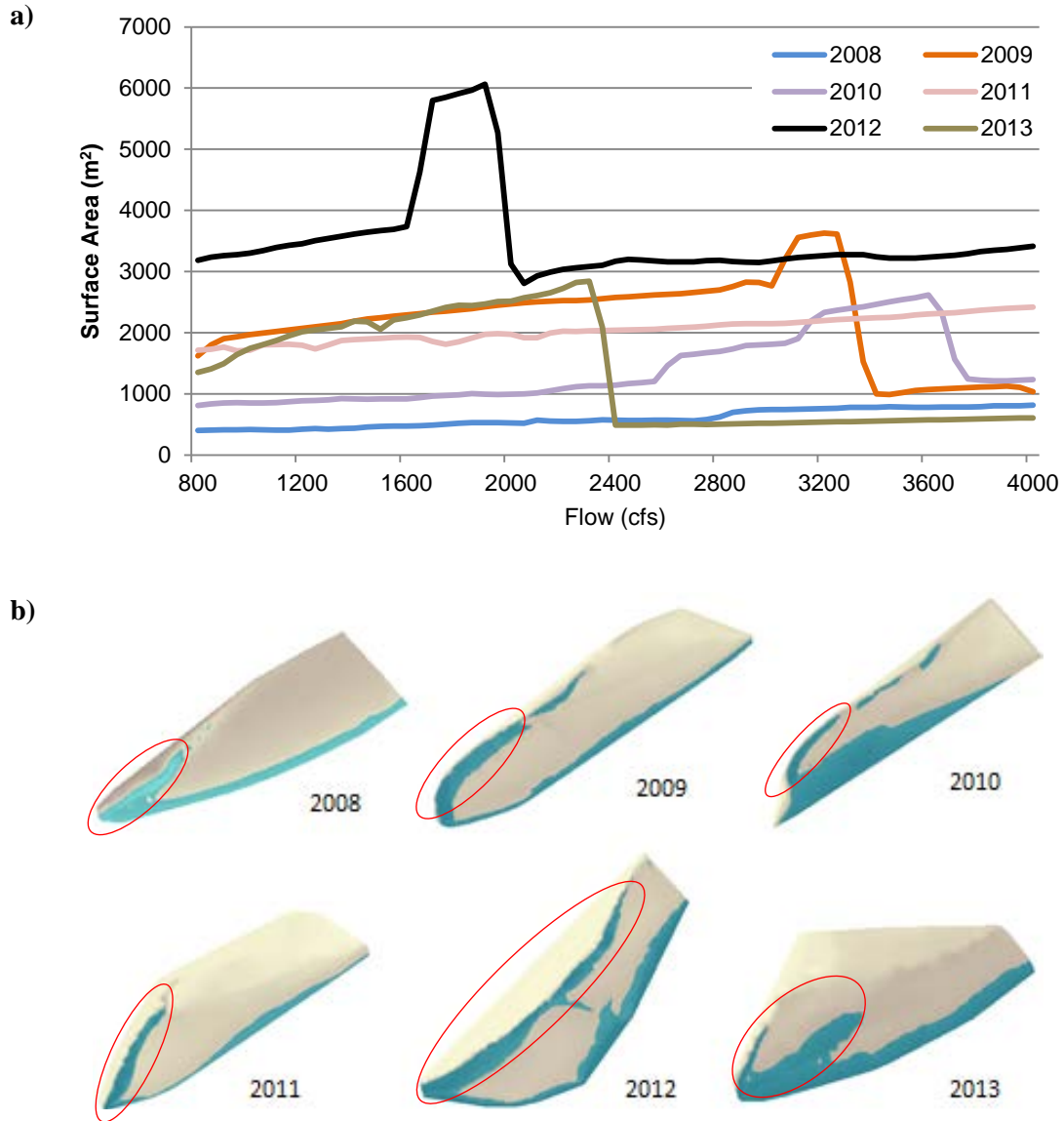


FIGURE 16 Changes in BW10 Surface Area from 2008 to 2013—(a) Relationship between Flow and Surface Area and (b) Changes in Backwater Morphology at 2,000 cfs ($57 \text{ m}^3/\text{s}$). Areas considered backwater habitat at each flow are circled in red. The direction of river flow is from upper right to lower left in the figure.

In summary, our backwater survey results demonstrate that there was large intraannual geomorphic variation among backwaters and large interannual variation in individual backwaters. Therefore, our results support the hypothesis that there is not a consistent range of flow conditions that maximizes backwater habitat among habitats in a single year or across several years. This is not a surprising finding given the variability in peak flows among years and the resultant dynamics of sediment erosion, transport, and deposition.

3.2.3 Effects of Peak Flows on Backwater Characteristics

Spring peak flows are considered the primary driver of interannual changes in backwater morphology. Rakowski and Schmidt (1999) found that higher peak flows built up sandbars by depositing sediments at higher elevation. Conversely, lower peak flows were found to erode sandbars and fill in the bed of backwaters. Based on these findings, they hypothesized that higher base flows were necessary to maximize backwater habitat in years with high spring peak flow. We tested this hypothesis using our survey data to examine the relationships among annual peak flow magnitude and duration and three dependent variables—flows at maximum backwater surface area, flows at maximum backwater volume, and flows at maximum backwater depth. Backwater bathymetry and topography of the associated sandbar determine the flows that maximized the values of these dependent variables. Note that the flows that maximized the values of backwater variables were not necessarily realized with the base flows that occurred in the year of the survey.

We used random forest regression to test models with instantaneous annual peak flow, instantaneous annual peak flow in the previous year, and peak flow duration (number of days in which flows were $\geq 75\%$ of the instantaneous annual peak flow)² as independent variables. Random forest regression is a non-parametric statistical technique that analyzes the relative importance of a set of predictor variables that have complex interactions. Random forest regression first randomly partitions the data into a training sample for model building and then tests samples to validate model performance. Regression trees, each estimating the dependent variable given the predictor variables, are created by repeatedly resampling the training data, with replacement. Regression trees are then averaged to provide an estimate of the dependent variable and to identify the variables that contribute most to predicting the dependent variable. We examined relationships among the dependent and independent variables using the random forest regression procedure in R (package “randomForest,” version 4.6.7; Breiman and Cutler 2013). We tested statistical significance of each model using a permutation test (Murphy et al. 2010; Evans et al. 2011). No significant relationships were found using the individual values for each backwater. Because of the high intraannual variability among backwaters, models were run using annual means of each dependent variable (Table 7).

² During the runoff period, instantaneous flow often varies considerably as a result of changes in weather and freeze-thaw cycles. The 75% threshold was chosen to represent duration of the peak flow runoff period. Other threshold values could be used, but they are likely to be strongly correlated, and it seems unlikely a different threshold would result in substantially different analytical results.

TABLE 7. Mean Base Flows that Maximize Backwater Variables and the Peak Flow Characteristics That Were Tested as Independent Variables in Random Forest Regression Models

Year	N	Mean Base Flow That Maximizes Backwater Variable			Peak Flow Characteristics		
		Surface Area (m ²)	Volume (m ³)	Mean Depth (m)	Magnitude (cfs)	Magnitude in Previous Year (cfs)	Duration (days)
2003	6	1,485	2,072	6,496	19,400	7,570	13
2004	4	3,590	3,590	3,816	11,500	19,400	6
2005	4	3,350	3,333	2,883	19,900	11,500	18
2006	4	2,215	2,215	4,226	19,200	19,900	11
2008	6	6,391	6,863	7,723	24,000	19,200	16
2009	5	3,968	3,938	4,520	19,600	24,000	20
2010	6	5,130	5,130	5,113	20,500	19,600	18
2011	5	4,682	4,912	7,820	32,200	20,500	27
2012	4	2,833	1,960	1,440	10,600	32,200	5
2013	5	4,241	4,241	4,616	11,000	10,600	24
Mean		3,789	3,825	4,865	18,790	18,447	16

Annual peak flow magnitude and peak flow duration each contributed approximately equally to the model when other independent variables were held constant (48% and 52%, respectively; Figure 17) and together explained 25.2% and 26.2%, respectively, of the variation in the base flow that maximized backwater surface area and volume (Table 8). Increases in both independent variables resulted in increases in the two dependent variables. Peak flow magnitude in the previous year was not important in any model (Figure 17). Flows that maximized backwater area and volume were highly correlated (Spearman rank correlation; $r=0.96$, $P<0.001$), and thus resulted in very similar model statistics (Table 8) and partial dependence plots (Figure 17). The model did not explain a significant percent of variation in the base flow that maximized backwater depth (Table 8; Figure 17).

Another way to examine the relationship between peak flows and flows that maximize the values of backwater variables is to examine the temporal changes in annual peak flow and base flows that maximize backwater habitat, with the assumption that the two should follow similar patterns of change over time. For example, based on Rakowski and Schmidt (1999), if annual peak flow were to increase significantly compared to the previous year, the flow that maximizes backwater surface area should increase as well. For this reason, we examined the temporal correspondence between changes in peak flow and optimal base flows rather than their absolute magnitude in a given year.

TABLE 8 Total Explained Variation (R^2) and Statistical Significance (P) of Random Forest Models for the Flow that Maximized Backwater Surface Area, Volume, and Depth^a

Dependent Variable	R^2 %	P
Flow that maximized backwater surface area	25.2	0.015
Flow that maximized backwater volume	26.2	0.006
Flow that maximized backwater depth	0	0.21

^a For each of the three backwater variables, the mean annual value of all surveyed backwaters was used in the analysis.

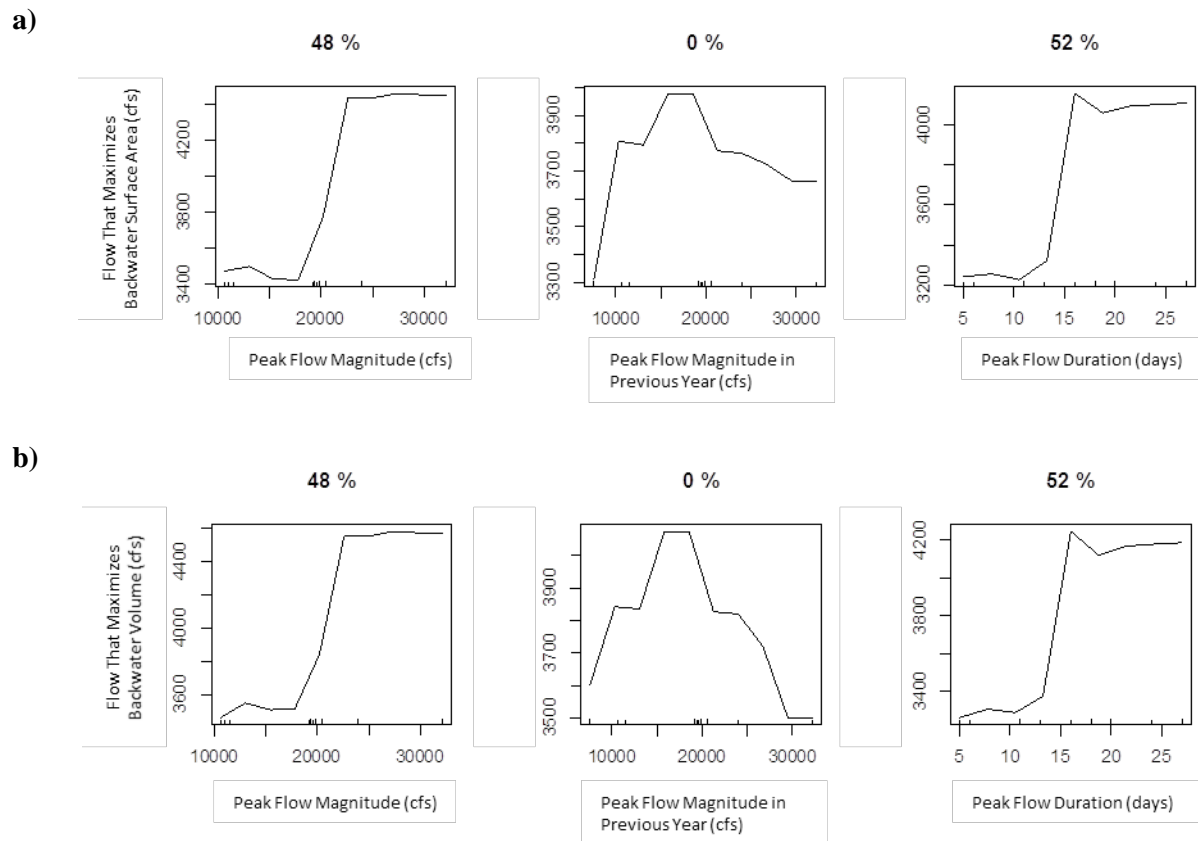


FIGURE 17 Partial Dependence Plots of (a) Flow That Maximizes Backwater Surface Area and (b) Flow That Maximizes Backwater Volume with Respect to Peak Flow Magnitude, Peak Flow Magnitude in the Previous Year, and Peak Flow Duration. Partial dependence plots show marginal effect on the dependent variable with other variables already accounted for; values shown above each plot are the relative contribution of each independent variable to the model.

We did not find a consistent correspondence between peak flow magnitude and the base flow that maximized backwater surface area or backwater volume (note that volume data are not shown, but were correlated to surface area). Peak flow magnitude and the base flow for maximizing backwater surface area followed opposite trends in several years (Figure 18a). For example, peak flow increased significantly between 2004 and 2005 and between 2010 and 2011, while the base flow that maximized surface area decreased during the same periods. However, peak flow magnitude and flow that maximized surface area did track in other years (i.e., 2008–2010 and 2011–2012). In contrast, the base flow that maximized backwater depth tracked annual changes in peak flow in most years (Figure 18b). To convert the temporal changes into statistically testable data, we regressed the annual changes in maximizing flow between consecutive years against the annual change in peak flow magnitude. We found a significant positive relationship between the two variables ($R^2=0.638$; $P=0.017$; Figure 18c).

As described above, Rakowski and Schmidt (1999) found that higher peak flows increased sandbar elevation, while low peak flows increased backwater bed elevation by depositing sediments scoured from higher elevations. Using our backwater survey data, we assessed the relationships among annual peak flow magnitude, annual peak flow duration, exposed sandbar elevation at 2,000 cfs ($57 \text{ m}^3/\text{s}$), mean backwater depth at 2,000 cfs ($57 \text{ m}^3/\text{s}$), and the sum of the exposed sandbar elevation and mean backwater depth, which represented the vertical distance from the top of the sandbar to the bed of the associated backwater. We determined the mean elevation of the exposed sandbar and backwater bed using the DEM generated by the backwater survey data. We calculated mean exposed sandbar elevation for a flow of 2,000 cfs ($57 \text{ m}^3/\text{s}$) to normalize sandbar elevation across the survey period. The shoreline elevation at 2,000 cfs ($57 \text{ m}^3/\text{s}$) was subtracted from the exposed bar surface elevations to eliminate the differences in the sandbar elevation among backwaters due to upstream to downstream elevation changes. We tested the relationship between these variables using linear regression.

We found a significant relationship between annual peak flow and mean height of exposed sandbars ($R^2=0.22$; $P=0.002$) (Figure 19a). We also found a significant relationship between mean sandbar height and average number of days $\geq 75\%$ of peak flow ($R^2=0.26$; $P=0.001$) (Figure 19). Annual peak flow and sandbar elevation showed some consistency in temporal trends, but this varied in strength among years (Figure 19c). There was no significant relationship between annual peak flow magnitude or duration and backwater mean depth or exposed sandbar elevation + mean depth, suggesting that bed elevation increased with sandbar elevation with higher, longer peak flows. An increase in bed elevation and increase in sandbar height with higher, longer peak flows would produce the type of relationship between peak flow and the flow that maximized backwater depth shown in Figure 18, because a higher bed would require higher flows to maximize depth.

Overall, our results support the hypothesis of Rakowski and Schmidt (1999) that there is a positive relationship between spring peak flows and the base flows that would maximize backwater habitat. Different lines of evidence identified peak flow magnitude and duration as important driving forces for changes in base flows that maximized either backwater surface area, volume, or mean depth. Random forest regressions identified peak flow magnitude and duration as important variables determining the base flow that maximized surface area and volume, while

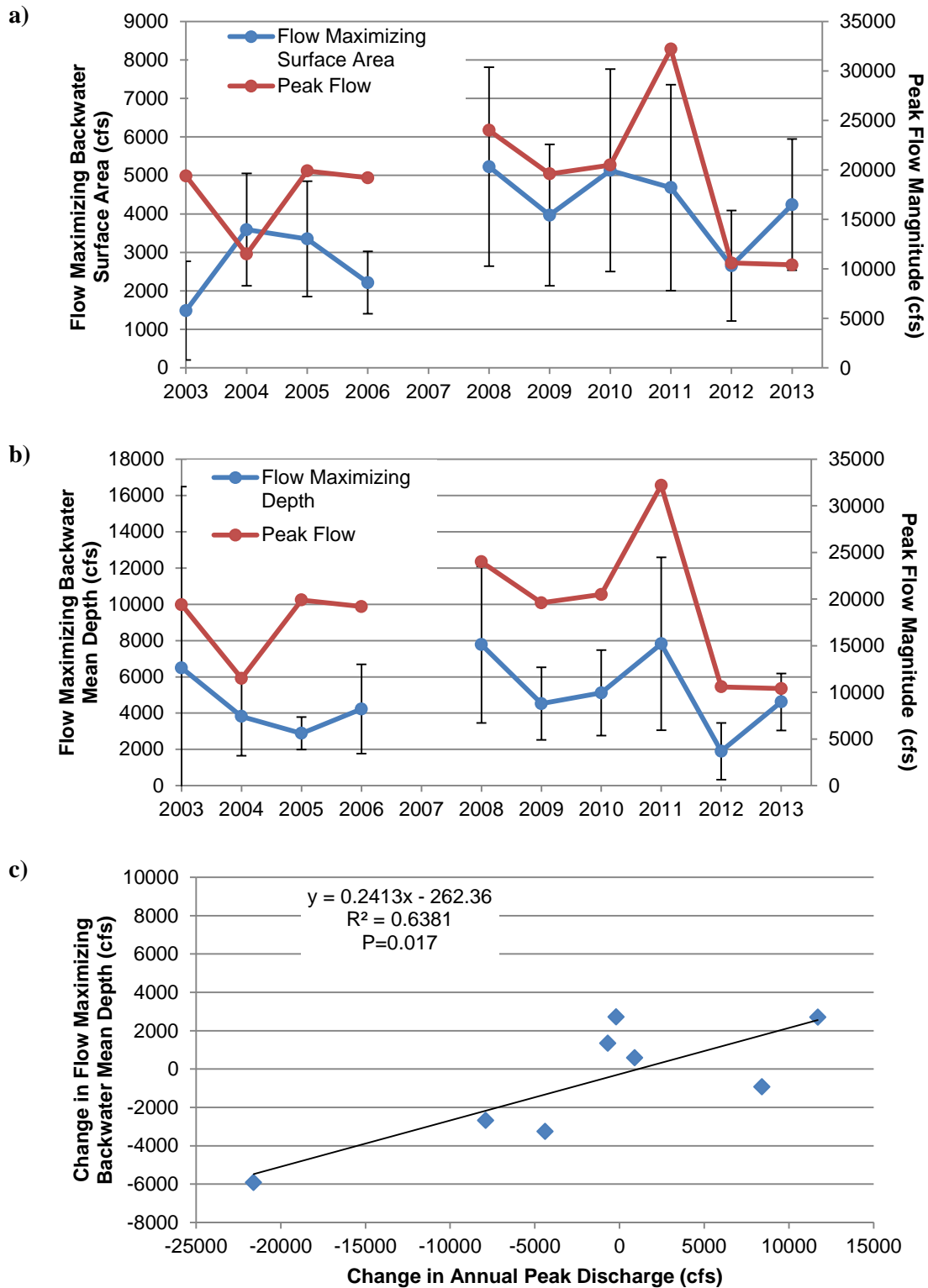


FIGURE 18 Peak Flow between 2003 and 2013 and the Corresponding Changes in Base Flows (mean ±SD) That Maximized Backwater (a) Surface Area and (b) Mean Depth. Figure 20c Shows the Relationship between Yearly Change in Annual Peak Flow and the Yearly Change in Flow That Maximized Backwater Depth.

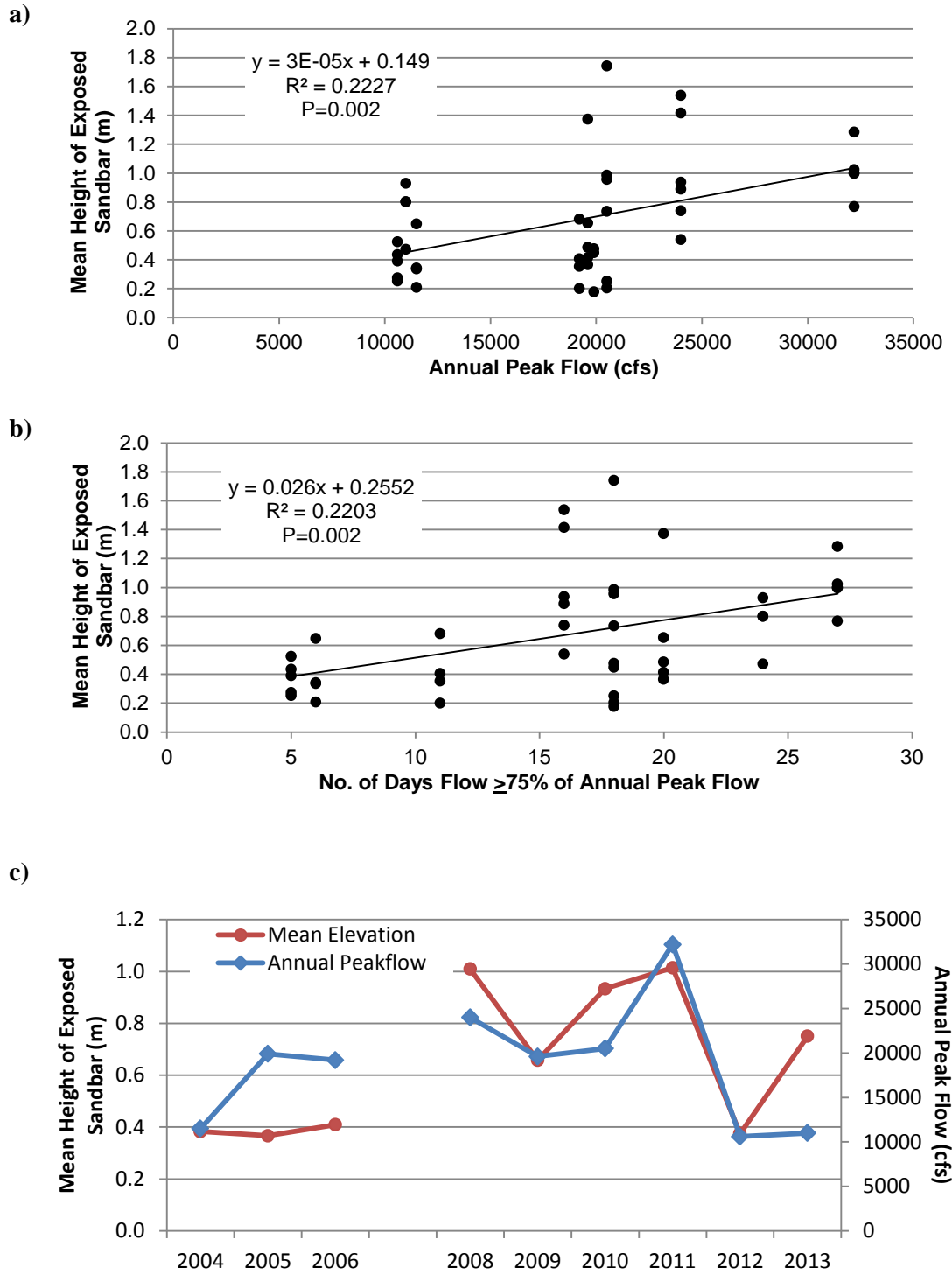


FIGURE 19 Relationship between Mean Height of Exposed Sandbars and (a) Annual Peak Flow, (b) Annual Peak Flow Duration, and (c) Changes from 2003 to 2013. Mean sandbar height is based on the height of the bar surface above 2,000 cfs (57 m³/s).

the change analysis indicated that flows that maximize mean backwater depth appeared to track most closely with changes in spring peak flow magnitude. As a mechanism to explain this relationship between antecedent flow and maximizing backwater flows, Rakowski and Schmidt (1999) proposed that high spring peak flows increased sandbar elevation. We found a significant relationship between mean sandbar height and annual peak flow and peak flow duration, and the variables did appear to track one another over time, which provided support for this hypothesis. Backwater bed elevation also appears to increase in tandem with the bar building associated with high peak flows. These results indicate that scaling the recommended yearly base flow to hydrologic condition is appropriate, with lower base flows provided in drier years and higher base flows provided in wetter years.

Our analysis is limited by the number of backwaters and associated sandbars we were able to survey each year. Given the amount of variability we saw in backwater characteristics within a year, a larger sample size would be needed (e.g., 20 per year) to be representative of the middle Green River reach as a whole. Advances in surveying techniques (e.g., autonomous surveying platforms) or more sophisticated remote sensing techniques capable of determining surface area and depth would be needed to accomplish these larger sample sizes.

3.3 NATURAL AND DAM-RELATED CHANGES IN FLOW AND BACKWATER CHARACTERISTICS

3.3.1 Influence of Dam Releases and Yampa River Flow on Base Flows in the Middle Green River

Releases from Flaming Gorge Dam and flow inputs from the Yampa River are the dominant contributors to flow in the middle Green River. Each contributes approximately 50% of the total annual volume that flows through the middle Green River (Muth et al. 2000). Daily, monthly, and seasonal patterns of flow are quite different among years, and result from dam operations that reflect the multiple purposes of Flaming Gorge Dam and the unregulated nature of Yampa River flows. During the spring runoff period, the Yampa River contribution to flow in the middle Green River is substantially higher than that of the upper Green River (Muth et al. 2000). However, during the base-flow period, dam releases are generally the greatest contributor to middle Green River flows (Muth et al. 2000).

Mean daily flow at the Greendale gage (USGS 09234500), located immediately downstream of Flaming Gorge Dam, was relatively consistent across the early and middle base-flow period compared to flow in the Yampa River (Table 9). Therefore, changes in flow at Ouray during the base-flow period often reflected changes in flow in the Yampa River. The critical role of the Yampa River in supporting the magnitude and duration of spring peak flows in the Green River has long been recognized (Holden 1980), but it is clear that the magnitude and variation in Yampa River flow during the base-flow period also plays a critical role in flow magnitude and variability at Ouray. For example, a visual comparison of multi-year flow data between June and November illustrates the strong correspondence between flow recorded at the Ouray gage and flow in the Yampa River (estimated as the sum of flows at the Maybell [USGS 09251000] and

TABLE 9 Mean, Coefficient of Variation (CV), and Minimum and Maximum Mean Daily Flows at the Greendale, Yampa River, and Ouray Gages during the Base-Flow Period (from the onset of base flows through November 30)

Year	Mean Daily Flow (cfs)			
	Mean ^a	CV	Maximum	Minimum
2003				
Greendale	882	0.06	1,220	774
Yampa	194	0.47	380	43
Ouray	1,131	0.14	1,426	837
2004				
Greendale	996	0.14	1,440	838
Yampa	471	0.54	1,107	31
Ouray	1,511	0.22	2,232	975
2005				
Greendale	1,433	0.03	1,540	1,220
Yampa	382	0.39	750	113
Ouray	2,011	0.10	2,362	1,651
2006				
Greendale	929	0.15	1,250	821
Yampa	514	0.57	1,424	104
Ouray	1,448	0.29	2,248	852
2008				
Greendale	1,379	0.16	1,670	1,100
Yampa	407	0.31	246	874
Ouray	2,023	0.17	3,105	1,612
2009				
Greendale	1,859	0.07	2,010	1,650
Yampa	368	0.35	689	138
Ouray	2,277	0.07	2,720	1,950
2010				
Greendale	1,351	0.24	1,780	955
Yampa	443	0.40	1,086	144
Ouray	2,039	0.11	2,620	1,430
2011				
Greendale	2,083	0.19	2,520	1,520
Yampa	693	0.40	2,105	387
Ouray	2,966	0.18	4,650	1,960
2012				
Greendale	1,138	0.20	1,460	816
Yampa	153	0.62	350	37
Ouray	1,319	0.09	1,700	1,040
2013				
Greendale	1,000	0.14	1,195	806
Yampa	387	0.61	848	78
Ouray	1,553	0.16	1,991	1,131

^a 1 cfs = 0.028317 m³/s.

Lily [USGS 09260000] gages) (Figure 20). Variability in Yampa River flows during the base-flow period typically resulted from storms in the Yampa River basin, and sometimes resulted in significant short-term increases in flow in the middle Green River that lasted for a few days to several weeks (Figure 20 and October 25-30 in Figure 21b).

Changes in dam operations during the base-flow period also produced flow variation at Ouray (Figure 21). The influence of dam releases (represented by flows at the Greendale gage) was most obvious during the late base-flow period (September and November) when flow in the Yampa River was lower than at the Greendale gage. For example, in September 2003, an increase in flow recorded at the Greendale gage was followed by a similar increase in flow at Ouray (Figure 21a), and, in October 2010 and 2012, a decrease in flow at Greendale corresponded to a reduction in flow at Ouray (Figures 20b and 20c).

The effects of dam operations were also evident in the variation in within-day flow at Ouray (Figure 22). The within-day flow fluctuations common to Greendale and Ouray were mostly a function of variation in water releases at Flaming Gorge Dam, because within-day flow variation was generally minimal in the Yampa River (Muth et al. 2000) (Figure 22b, 22c, and 22d). During the base-flow periods of 2003-2013, within-day flow variation at the Greendale gage was generally less than 1,000 cfs (28 m³/s). The within-day flow variation at Ouray was less than 300 cfs (9 m³/s) in July and less than 150 cfs (4 m³/s) from August to November (Figure 23a). The <300 cfs (9 m³/s) mean within-day flow variation at Ouray was significantly less than the within-day flow variation recorded at Greendale, reflecting substantial flow fluctuation attenuation over the intervening distance between gages. These changes in flow at the Greendale gage produced relatively minor mean daily stage changes at Ouray of 0.06 m or less (Figure 23b). The observed small within-day flow variations at the Ouray gage are expected because the dam was operated during this period to produce no more than a 0.1-m change in stage at the Jensen gage, and additional attenuation in flow variation occurred by the time flows reached the Ouray gage.

In summary, although the Yampa River affected the overall magnitude of base flows, most flow variability (especially within-day variability) resulted from changes in dam operations. The exception to this is the effect of runoff from storms in the Yampa River and other tributaries; these events frequently affected flows in the middle Green River for a few days to several weeks.

3.3.2 Influence of Dam Releases and Yampa River Flows during the Base-Flow Period on Backwater Characteristics in the Middle Green River

Given the complex non-linear relationships between flow and backwater characteristics discussed in Section 3.2.2, it is apparent that flow magnitude and variability can have important effects on backwater habitat characteristics between and within years. As described in Section 3.3.1, our modeling indicates that releases from Flaming Gorge Dam created relatively minor within-day stage changes at Ouray; the mean modeled within-day stage change was less than 0.06 m. Recorded Ouray gage flow data from 2009 to 2013 and simulated Ouray flows from 2003 to 2008 were used with DEMs of backwaters and their associated sandbars to estimate the effect of stage changes on backwater characteristics during the base-flow period of these years.

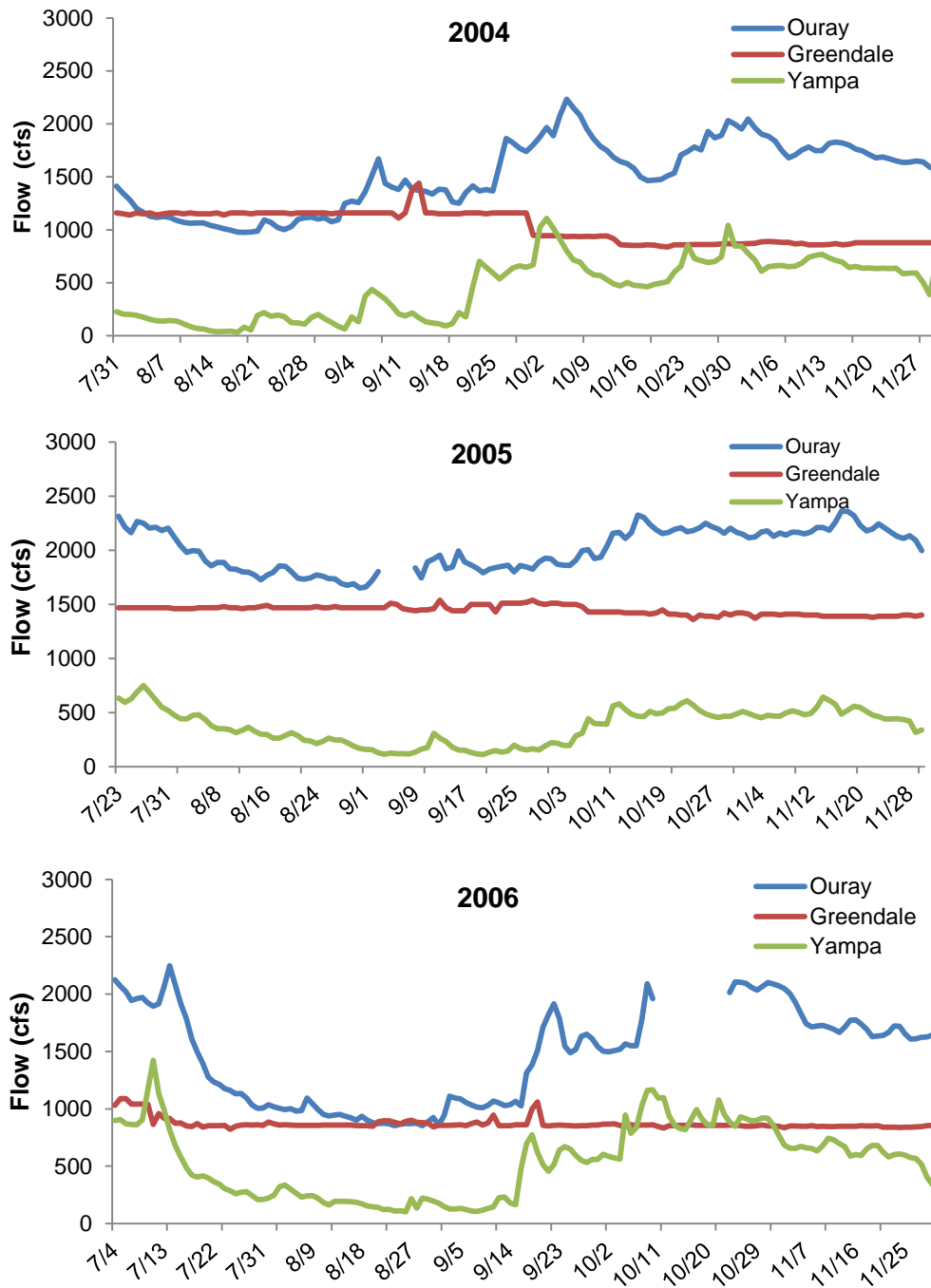


FIGURE 20 Mean Daily Flow at the Greendale, Yampa River, and Ouray Gages during the Base-Flow Periods of 2004, 2005, and 2006

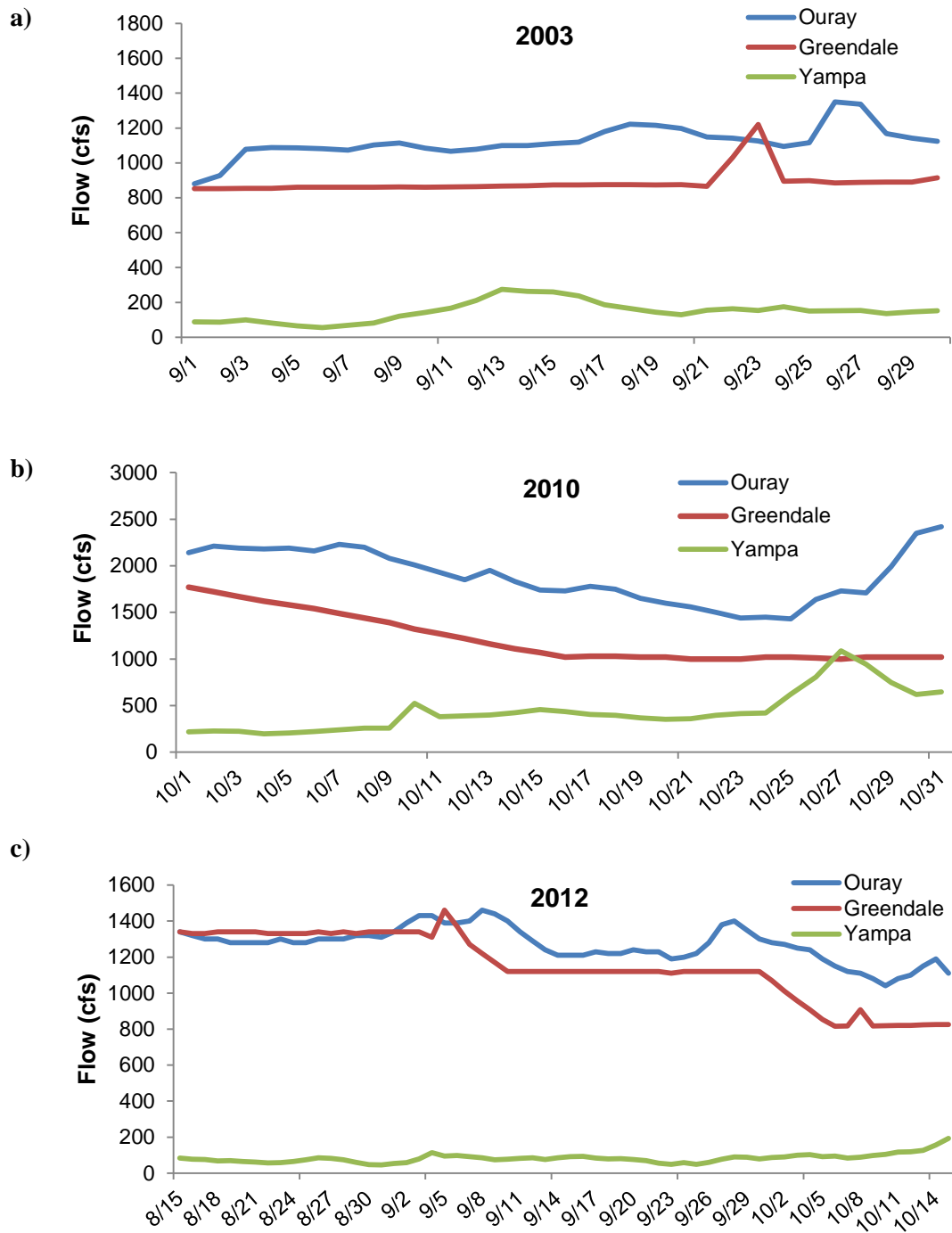


FIGURE 21 Mean Daily Flow at the Greendale, Yampa River, and Ouray Gages in (a) September 2003, (b) October 2010, and (c) August to October 2012, Illustrating the Effect of Dam Operations and Yampa River Flow on Ouray Flow during the Base-Flow Period

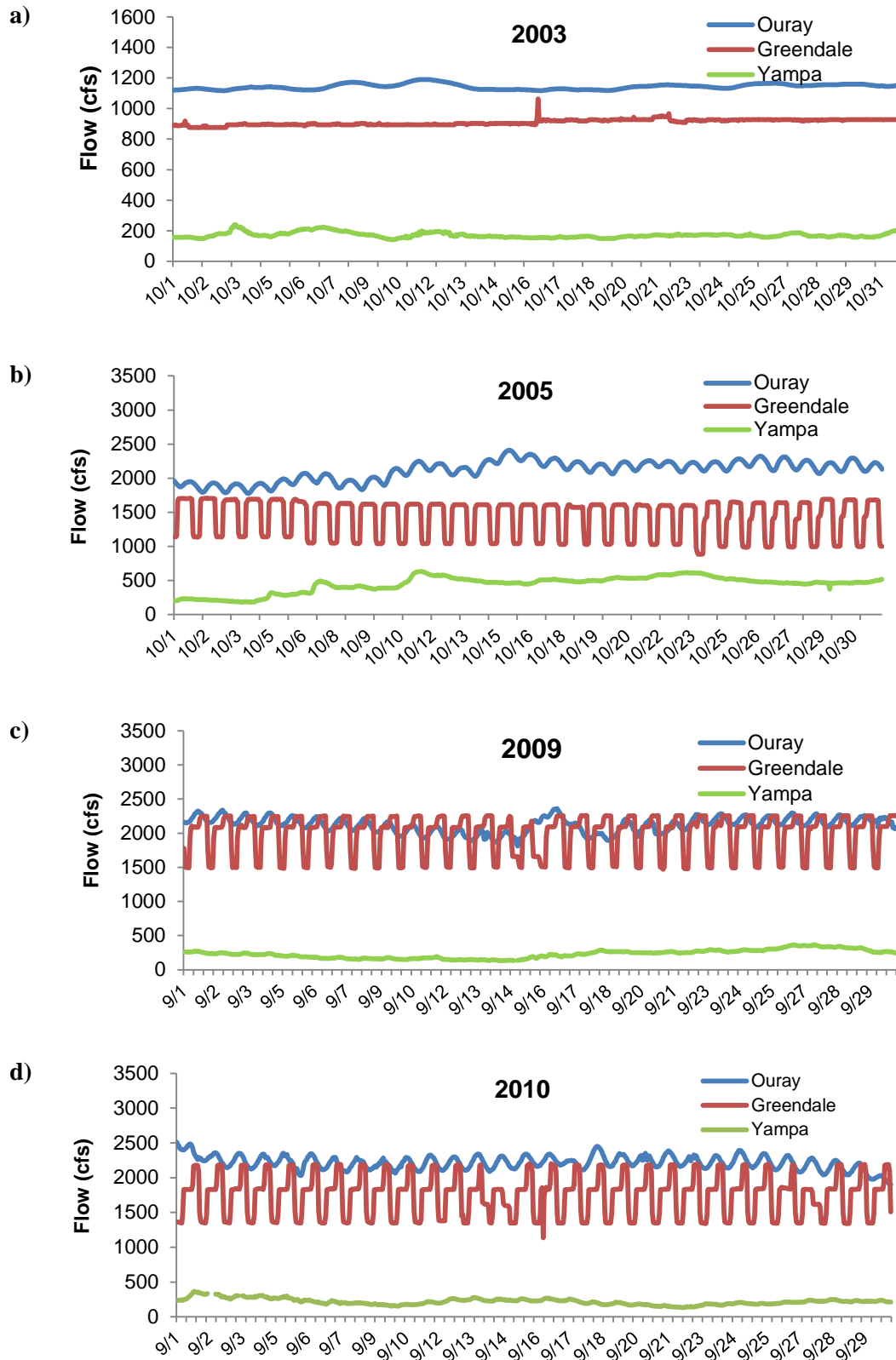


FIGURE 22 Mean Hourly Flow at the Greendale, Yampa River, and Ouray Gages in (a) 2003, (b) 2005, (c) 2009, and (d) 2010

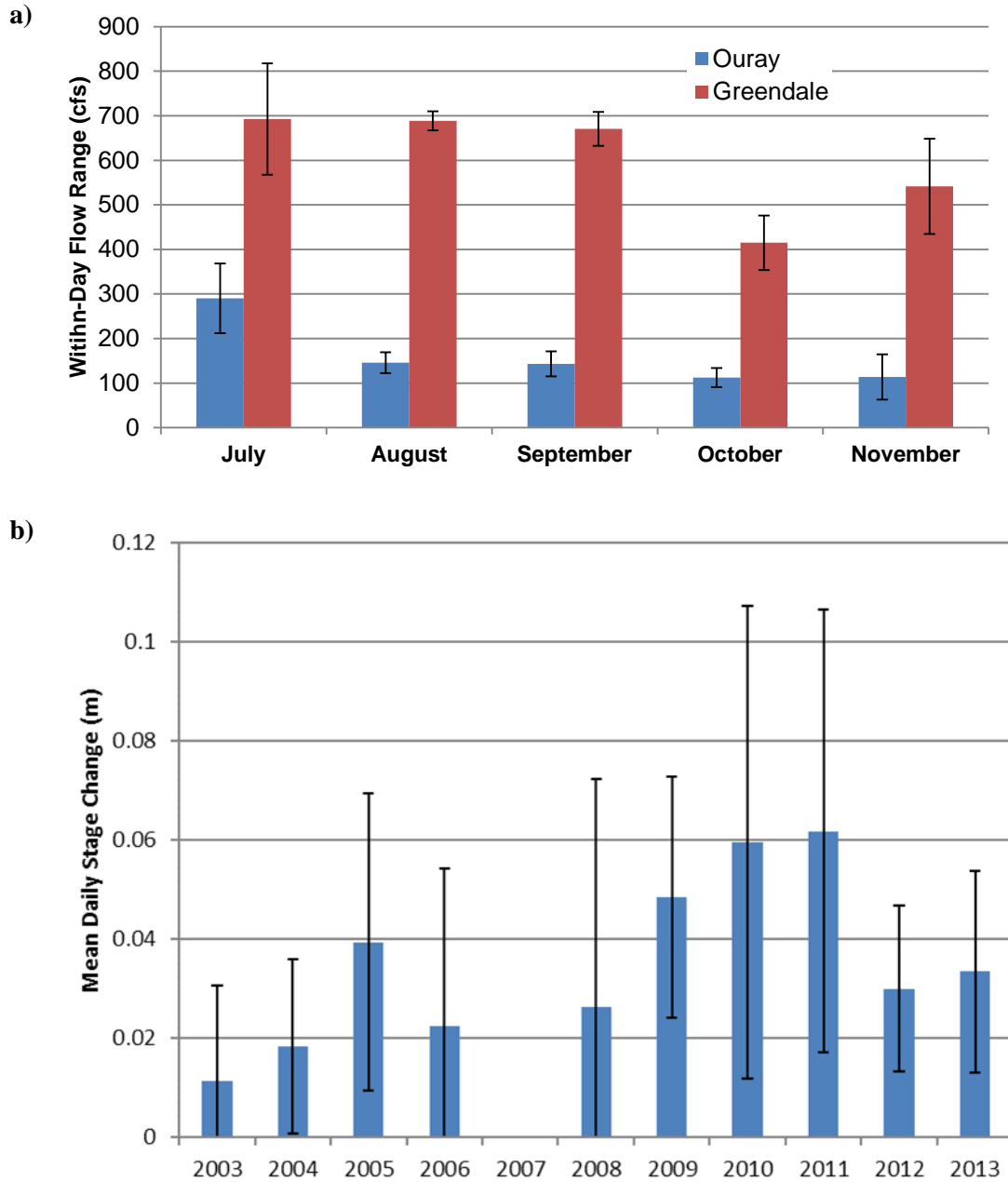


FIGURE 23 Flow and Stage Variability during the Base-Flow Period from 2003 to 2013 as Reflected by (a) Monthly Within-Day Flow Range ($Flow_{max}-Flow_{min}$) at the Greendale and Ouray Gages and (b) the Mean Daily Stage Change at the Ouray Gage. Error bars represent ± 1 standard deviation. Ouray gage values were simulated for 2003 to 2008.

We defined variation as the difference between the maximum and minimum values of surface area, volume, and mean depth in a single day. The mean daily variation in surface area ranged from 18.4 m² in 2008 to 620 m² in 2005, but most values were less than 250 m² (Table 10). Most daily changes in mean backwater depth were ≤ 0.02 m (Table 10). Mean daily variation in volume ranged from 3.5 m³ in 2003 to 171.5 m³ in 2009 and were typically less than 75 m³ (Table 10).

Relatively small changes in depth can produce relatively large changes in area or volume under certain conditions. The magnitude of the changes were a function of the complexity of sandbar topography. Some changes were a consequence of inundation of relatively flat portions of sandbars, but most of the short-term variation resulted from connection or disconnection of portions of the sandbar/backwater complex that resulted in either a flow-through condition or elimination of connection at the mouth of the backwater. Repeated disconnection and reconnection over small depth changes sometimes resulted in high temporal variation in mean backwater area. Some degree of backwater function would likely persist following these types of events. For example, a pool that temporarily disconnected from the main channel or a backwater that developed a second connection to the river mainstem would likely retain the habitat characteristics of a backwater for some time after these events occurred especially if the flow-through connection through the bar was shallow or the backwater was relatively deep.

On the basis of the relationships discussed above, we evaluated the frequency with which surveyed backwater habitats would become disconnected from the main channel or would experience a flow-through condition. In addition, we examined the relative influence of dam operations and Yampa River flows on producing these changes.

Our modeling predicted relatively few instances of flow-through or disconnection during the base-flow period over our survey period as flows increased or decreased (Table 11). These conditions occurred in 4 of the 10 years of our study (Table 11), over the range of flows that occurred during the base-flow period of each year (Appendix 5). Of the 51 backwaters surveyed from 2003 through 2013, we predicted that only 5 experienced either flow-through or disconnection. The cumulative number of hours of these conditions ranged from 191 to 1,746 hours (Table 11). The average duration of contiguous hours of these conditions was less than 100 hours in most instances (Table 11), although conditions that lasted longer than 100 hours were predicted to occur in 2003 and 2011. Backwaters that experienced flow-through or disconnection tended to have lower surface area, lower maximum depth, and lower mean depth than other backwaters during the same year (Appendix 5), but most, with the exception of BW04 in 2003, were comparable in size and depth to other backwaters (Table 11).

Our modeling indicated that loss of backwater characteristics was most commonly the result of an increase in flows that resulted in flow-through conditions (Table 11). An example of the loss of backwater characteristics due to rising water was BW05 in 2010 in which flow-through occurred periodically from July to November due to flow fluctuations between 2,470 and 2,530 cfs (70 and 72 m³/s) (Figure 24 and Figure 25). BW05 formed in late July as Yampa River flows decreased. A short-term loss of BW05 in early August 2010 resulted from an increase in Yampa River flow and creation of a flow-through channel through the sandbar at the upstream end of the backwater (Figure 24 and Figure 25). A similar event occurred in late

TABLE 10 Mean and Mean Daily Variation (Maximum–Minimum) in Surface Area, Volume, and Mean Depth of Surveyed Backwaters during the Base-Flow Period from 2003 to 2013

Year	No. Backwaters Surveyed	Mean Surface Area (m ²)	Mean Daily Variation in Surface Area \pm SD (m ²)	Mean Volume (m ³)	Mean Daily Variation in Volume \pm SD (m ³)	Mean Depth (m)	Mean Daily Variation in Depth \pm SD (m)
2003	6	690	5.1 \pm 7.3	324	3.5 \pm 4.1	0.36	0.01 \pm 0.01
2004	4	1,670	142.5 \pm 176.5	368	40.8 \pm 48.4	0.21	0.01 \pm 0.01
2005	5	578	620.2 \pm 108.2	411	53.1 \pm 57.5	0.50	0.06 \pm 0.06
2006	4	2,301	371.0 \pm 751.0	712	74.6 \pm 140.9	0.36	0.01 \pm 0.01
2008	6	513	18.4 \pm 32.6	214	8.0 \pm 11.9	0.40	0.01 \pm 0.01
2009	5	2,438	367.7 \pm 238.2	1,302	171.5 \pm 123.9	0.47	0.02 \pm 0.01
2010	6	2,379	113.5 \pm 102.4	1,087	85.5 \pm 73.1	0.39	0.02 \pm 0.02
2011	5	1,637	153.6 \pm 121.6	1,364	96.85 \pm 66.3	0.64	0.04 \pm 0.04
2012	5	2,176	89.6 \pm 74.9	1,463	66.9 \pm 51.1	0.56	0.01 \pm 0.00
2013	5	3,226	214.9 \pm 119.7	2,141	74.7 \pm 58.5	0.55	0.02 \pm 0.01

August, but was related to an increase in water release from Flaming Gorge Dam, rather than increased Yampa River flow. Backwater habitat loss also occurred in late October due to a spike in Yampa River flows (Figure 25). Within-day changes in dam releases typically caused only small within-day fluctuations in backwater surface area rather than backwater loss.

Other examples of loss of backwater characteristics include BW04 in 2003, in which rising water was predicted to temporarily breach the sandbar, creating a second connection to the river. This flow-through condition was predicted to occur multiple times during September and October 2003. Flow-through conditions were caused by increased flows from the Yampa River and from fluctuations at Greendale related to dam operations. BW04 may have been particularly sensitive to small fluctuations in flow due to its small size (78 m² surface area) and shallow mean depth (0.1 m; Table 11). Fluctuations in flow between 2,700 and 3,100 cfs (76 and 88 m³/s) were predicted to cause multiple reconnections and disconnections of BW05 from the main channel during August through November 2011, and small fluctuations in flow between approximately 2,700 and 2,800 cfs (76 and 79 m³/s) were predicted to result in disconnection of BW07 in 2011. BW07 was predicted to repeatedly disconnect from the main channel in October and November when flow at Ouray fell below 2,770 cfs (78 m³/s).

Disconnection of BW13 was predicted in 2013, when Ouray flow fluctuated between 1,100 and 1,400 cfs (31 and 40 m³/s), resulting in multiple instances in August and September (Figure 26 and Figure 27). BW13 was predicted to convert to a pool after it disconnected from the main channel at flows below 1,181 cfs (33 m³/s) (Figure 26). The fluctuation in flow at Ouray appeared to result from within-day variation in dam releases (Figure 27). Although BW13 had a maximum depth of >0.6 m, its mean depth was shallow (0.1 m).

TABLE 11 Characteristics of Surveyed Backwaters That Were Predicted to Experience Disconnection or Flow-Through Events during the Base-Flow Period from 2003 to 2013^a

Year ^b	BW ID	Mean Surface Area \pm SD (m ²)	Maximum Depth \pm SD (m)	Mean Depth \pm SD (m)	Date Range for Events	Total Duration of Events (hr) ^c	Mean Duration of Events \pm SD (hr)	Flow at Which Event Occurred (cfs) ^d	Type and Cause of Loss
2003	BW04	78 \pm 93	0.3 \pm 0.3	0.1 \pm 0.1	7/18–11/30	1,746	194.3 \pm 306	>1,130	Flow through caused by increases in Yampa River flows and dam releases.
2010	BW05	1,120 \pm 299	0.9 \pm 0.2	0.4 \pm 0.1	7/19–11/30	191	21.1 \pm 35	>2,470	Flow through caused by increases in Yampa River flows and dam releases.
2011	BW05	1,090 \pm 534	1.7 \pm 0.8	0.5 \pm 0.2	8/18–11/2	259	10.4 \pm 8	2,800–3,000	Flow through and disconnect caused by increases and decreases in Yampa River flows.
2011	BW07b	1,148 \pm 787	0.9 \pm 0.6	0.2 \pm 0.2	10/3–11/30	748	68 \pm 182	<2,700	Disconnection cause uncertain.
2013	BW13	2,306 \pm 1,383	0.6 \pm 0.3	0.1 \pm 0.1	8/7–9/8	246	10 \pm 7	<1,181	Disconnection caused by increases and decreases in Yampa River flows.

^a Disconnection and flow-through conditions were modeled with ABIS using the recorded hourly flows at Ouray over the base-flow period and the DEM of surveyed backwaters and their associated sandbars.

^b None of the surveyed backwaters experienced disconnection or flow-through during the base-flow periods of 2004, 2005, 2006, 2008, 2009, or 2012. No backwaters were surveyed in 2007.

^c Sum of hours of disconnection or flow-through during the base-flow period. Hours are not necessarily sequential.

^d 1 cfs = 0.028317 m³/s.

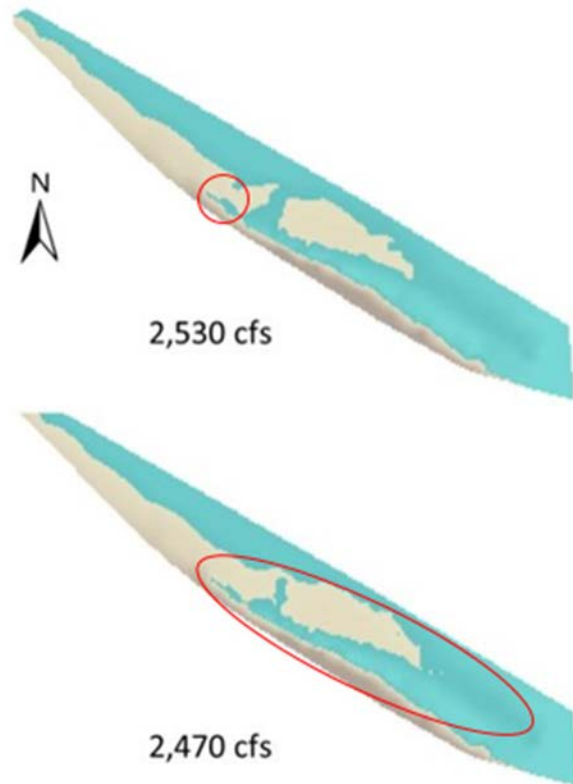


FIGURE 24 Example of Increasing Flow Creating a Flow-Through Condition That Eliminates a Large Portion of Backwater Habitat in BW05 in 2010. Areas considered backwater habitat at each flow are circled in red. Flow-through occurs between flows of 2,470 cfs and 2,530 cfs (70 and 72 m³/s). Direction of river flow is from upper left to lower right in figure.

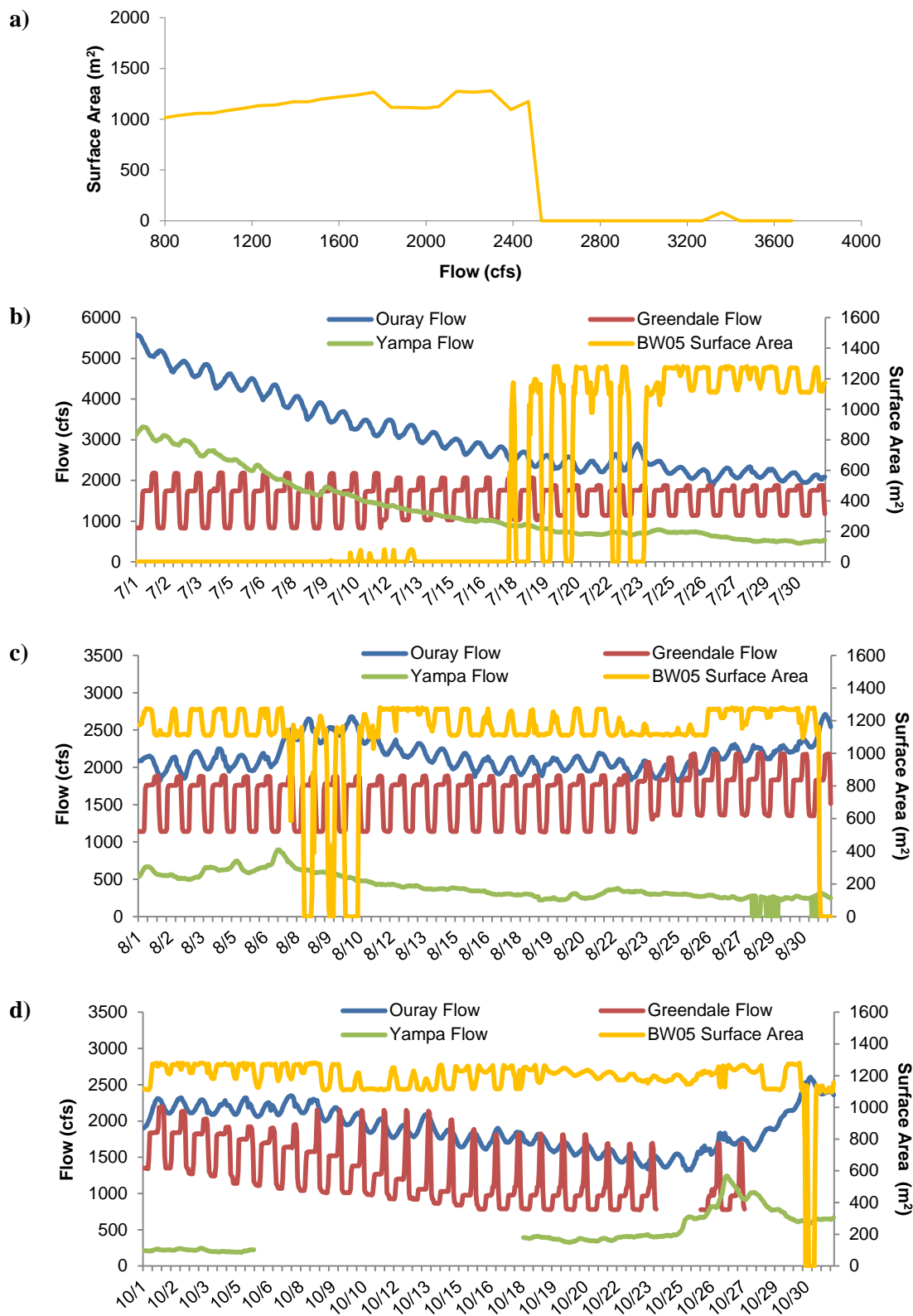


FIGURE 25 Changes in the Surface Area of BW05 in 2010—(a) Relationship between Flow and Surface Area, and Changes in Surface Area as Related to Flow at Greendale, Yampa River, and Ouray in (b) July, (c) August, and (d) October

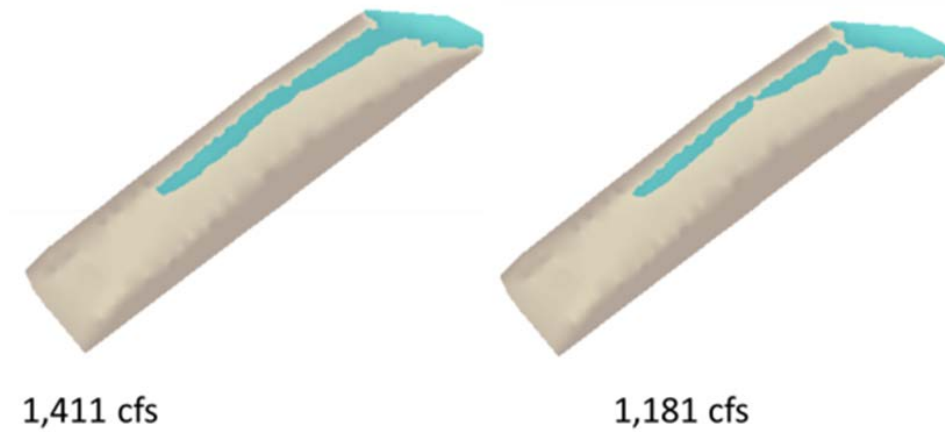


FIGURE 26 Disconnection of BW13 from the Main Channel in 2013. Direction of river flow is from lower left to upper right in figure.

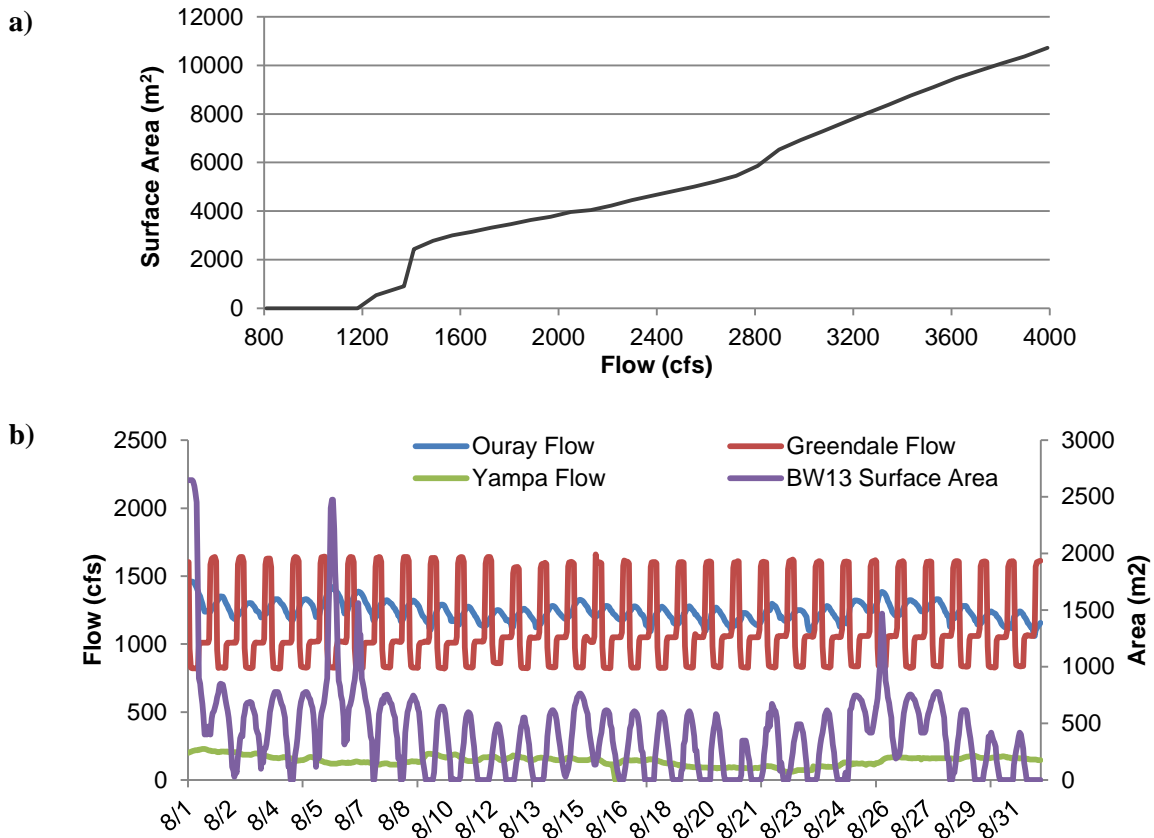


FIGURE 27 Changes in the Surface Area of BW13 in 2013—(a) Relationship between Flow and Surface Area and (b) Repeated Disconnection Events in August 2013 Due to a Decrease in Flow at Ouray below 1,181 cfs (33 m³/s)

In summary, occasional disconnection or flow-through of backwater habitats during the 2003–2013 survey period was predicted to result from natural fluctuations in flow in the Yampa River, changes in Flaming Gorge Dam operations, or both. A visual inspection of flow data indicated that broad monthly trends in backwater habitat availability at Ouray were primarily determined by flow trends in the Yampa River, especially in the early base-flow period as these flows had a strong effect on the overall magnitude of base flows. However, monthly or seasonal changes in water releases from Flaming Gorge Dam also influenced flow and backwater habitat at Ouray and, in some cases, caused temporary loss of backwater habitat in surveyed backwaters. Typically, short-term, within-day fluctuations in flow related to dam releases resulted only in small changes in backwater habitat surface and volume. However, the size and depth of some backwaters were observed to change significantly over a relatively small range of Ouray flows (<500 cfs [$14 \text{ m}^3/\text{s}$]). Therefore, given the small size of some backwaters and their sensitivity to flow, there were instances of backwater loss related to daily water releases from Flaming Gorge Dam.

3.4 COLORADO PIKEMINNOW EARLY LIFE STAGES AND BACKWATER CHARACTERISTICS

Bestgen and Hill (2016) provided a synthesis of information related to abundance and recruitment of age-0 Colorado pikeminnow in the Green and Yampa Rivers. In this section, we use information on backwater habitats that we gathered and analyzed to supplement their analysis where possible. Included is an evaluation of the availability of backwater habitat during the Colorado pikeminnow larval drift period and relationships between age-0 pikeminnow density, backwater characteristics, and flow.

3.4.1 Backwater Habitat Availability during the Colorado Pikeminnow Larval Drift Period

Bestgen and Hill (2016) defined the drift period as the period in which pikeminnow larvae were detected in drift net captures at Echo Park at the confluence of the Green and Yampa Rivers. Over the 9 years examined by Bestgen and Hill (2016) that overlap our survey period (i.e., 2003-2006 and 2008-2012), our survey data indicate that all or a portion of the larval drift period generally corresponded to the time when backwater depth and surface area were high (Appendix 6). For example, in 2008, the drift period lasted from late June to mid-August, during which time backwater surface area and depth were high relative to the non-drift period (Figure 28). However, for the early portion of the drift period in most years, backwater surface area and depth were lower than later in the drift period, because flows were still descending from the spring peak, and backwaters had not yet formed (Appendix 6). This analysis supports the Bestgen and Hill (2016) recommendation that the onset of base-flow conditions should be timed to coincide with first presence of Colorado pikeminnow larvae to ensure adequate backwater conditions throughout the reproductive period and provide longer growing seasons for age-0 Colorado pikeminnow.

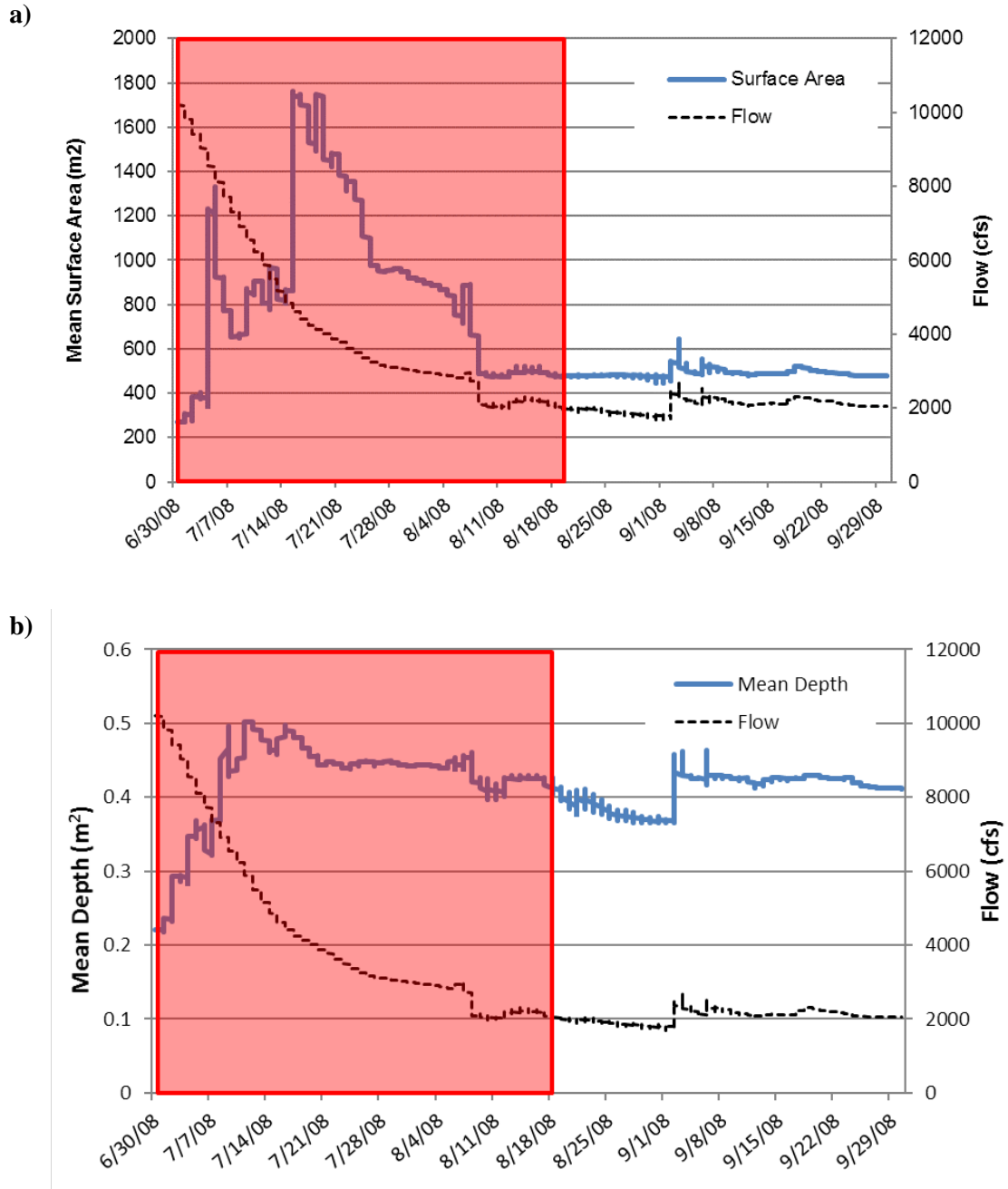


FIGURE 28 Mean Surface Area (a) and Depth (b) of Backwaters Surveyed in 2008 During the Colorado Pikeminnow Larval Drift Period. The red box corresponds to the larval drift period as reported in Bestgen and Hill (2016).

3.4.2 Relationship between Age-0 Colorado Pikeminnow Density and Base-Flow Magnitude

Bestgen and Hill (2016) examined the relationship between age-0 Colorado pikeminnow density (pikeminnow/10 m²) and August-September base flow using data from 1979 through 2012, and concluded that pikeminnow density in the middle Green River was more often above the mean density (0.5/10 m²) in years with moderate base flows (1,700 cfs-3,000 cfs [48 m³/s-85 m³/s). They hypothesized that, in years with lower base flows, the low density of age-0 Colorado pikeminnow might be due to suboptimal habitat conditions or lack of sufficient larvae transported to nursery areas to produce a strong year class. They speculated that, in years when base flows were higher than 3,000 cfs (85 m³/s) in the middle Green River, abundance of age-0 Colorado pikeminnow in autumn may have been low because few backwaters developed in such years or larvae never colonized those backwaters. They acknowledged that the underlying factors that produced their observed relationship between age-0 Colorado pikeminnow density and base-flow magnitude were complex and poorly understood.

We used our ground-survey data from 2003 through 2013 and aerial and satellite imagery analysis to determine if backwater characteristics (number, surface area, volume, and depth) might explain the pattern in pikeminnow density that Bestgen and Hill (2016) reported. Based on our analysis of ground-survey data, flows that would maximize backwater habitat availability varied greatly from year to year, but was most often (7 out of 10 years) highest at flows above 3,000 cfs (85 m³/s; Table 7). The mean base flow that would maximize backwater surface area of our surveyed backwaters ranged from 1,485 cfs (42 m³/s) in 2003 to 6,391 cfs (181 m³/s) in 2008 with a mean of 3,789 cfs (107 m³/s; Table 7). For the aerial imagery analysis, there was only one year (1987) when backwater habitat availability was assessed over a wide range of flows in the middle Green River (Pucherelli and Clark 1990). In this year, the number of backwaters/RM was highest at 1,687 cfs (48 m³/s) in the Jensen reach (8.3 backwaters), and at 1,381 cfs (39 m³/s) in the Ouray reach (6.7 backwaters); at both sites, there was a statistically significant decrease in number of backwaters as flows increased (Figures 4 and 5). Backwater area/RM was highest at 1,381 cfs (39 m³/s) in the Jensen reach (2,938 m²/RM) and at 1,687 cfs (48 m³/s) in the Ouray reach (4,783 m²/RM). These analyses demonstrate that there is large annual variability in the flow to habitat relationship, and suggest that, consistent with Bestgen and Hill's (2016) conclusions, habitat availability alone may not explain their hypothesized relationship between pikeminnow density and base-flow magnitude.

3.4.3 Relationships between Age-0 Colorado Pikeminnow Density and Backwater Characteristics

From 1979 to 2012, age-0 Colorado pikeminnow were sampled in autumn by seining backwaters of the middle and lower Green River (Bestgen and Hill 2016). Age-0 pikeminnow were moderately abundant in the middle Green River through 1993, but after 1994 had very low abundance (except during 2009 and 2010). The proportion of backwaters where age-0 Colorado pikeminnow were detected also declined with time in both the middle Green River and the lower Green River. Bestgen and Hill (2016) evaluated potential relationships between age-0 Colorado

pikeminnow density and backwater habitat characteristics to better understand the role, if any, that habitat characteristics play in determining pikeminnow density.

Bestgen and Hill (2016) reported a weak negative correlation in the middle Green River ($r = -0.28$) between age-0 Colorado pikeminnow density (number of fish per area swept by seine) and the mean surface area of the backwaters (as estimated at the time of survey) in which the pikeminnow were seined. This observation suggests that the distribution of larvae among backwaters was independent of the size of backwaters resulting in approximately the same number of fish in all backwaters and consequently lower densities in larger backwaters. Bestgen and Hill (2016) also found that density of age-0 Colorado pikeminnow was higher in the lower than the middle Green River, and that there were fewer and smaller backwaters in the lower than the middle Green River. They hypothesized that higher densities in the lower Green River was a consequence of having less available habitat; thus, the number of larvae produced in or transported to the lower Green River had fewer habitats to occupy, resulting in higher densities within backwaters.

We used the results of our aerial and satellite imagery analysis (described in Section 3.1) to evaluate these same relationships between age-0 Colorado pikeminnow density and reach-wide backwater habitat statistics within the Jensen and Ouray study reaches (RM 303 to 310 and RM 250.5 to 261.5). Of the years considered in Bestgen and Hill (2016), imagery was available for 1987, 1988, 1989, 1993, 1996, 2004, and 2006.

Linear regression was used to test the significance of the association between the density of age-0 pikeminnow and mean backwater area, number of backwaters/RM, and backwater area/RM. Although there appeared to be a negative relationship between age-0 pikeminnow density and mean backwater area and backwater area/RM (Figure 29a and c) as reported in Bestgen and Hill (2016), neither relationship was statistically significant ($R^2=0.414$, $P=0.119$ and $R^2=0.404$, $P=0.125$, respectively). The relationship between age-0 pikeminnow density and the number of backwaters/RM appeared to be positive, but also was not statistically significant ($R^2=0.389$; $P=0.135$; Figure 29b). All three relationships were strongly influenced by a single high pikeminnow density value (2.3 pikeminnow/m² in 1988). It should be noted that the statistical power of our regressions was limited because data for both pikeminnow density and habitat characteristics were available for only 7 years.

On the basis of their analysis described above, Bestgen and Hill (2016) stated that backwater habitat quantity or quality was not necessarily limiting for age-0 Colorado pikeminnow during their study period (1979-2012) except in the highest base flow years. However, even if the amount of habitat is not limiting, the number of pikeminnow larvae retained in the middle and lower Green River may be higher when there is more habitat available because more habitat increases the potential for entraining drifting larvae and provides more habitat areas suitable for summer growth. Although habitat may not be limiting now, Bestgen and Hill (2016) acknowledge that channel narrowing and simplification may limit distribution and number of backwaters in the future with potential adverse effects on recruitment.

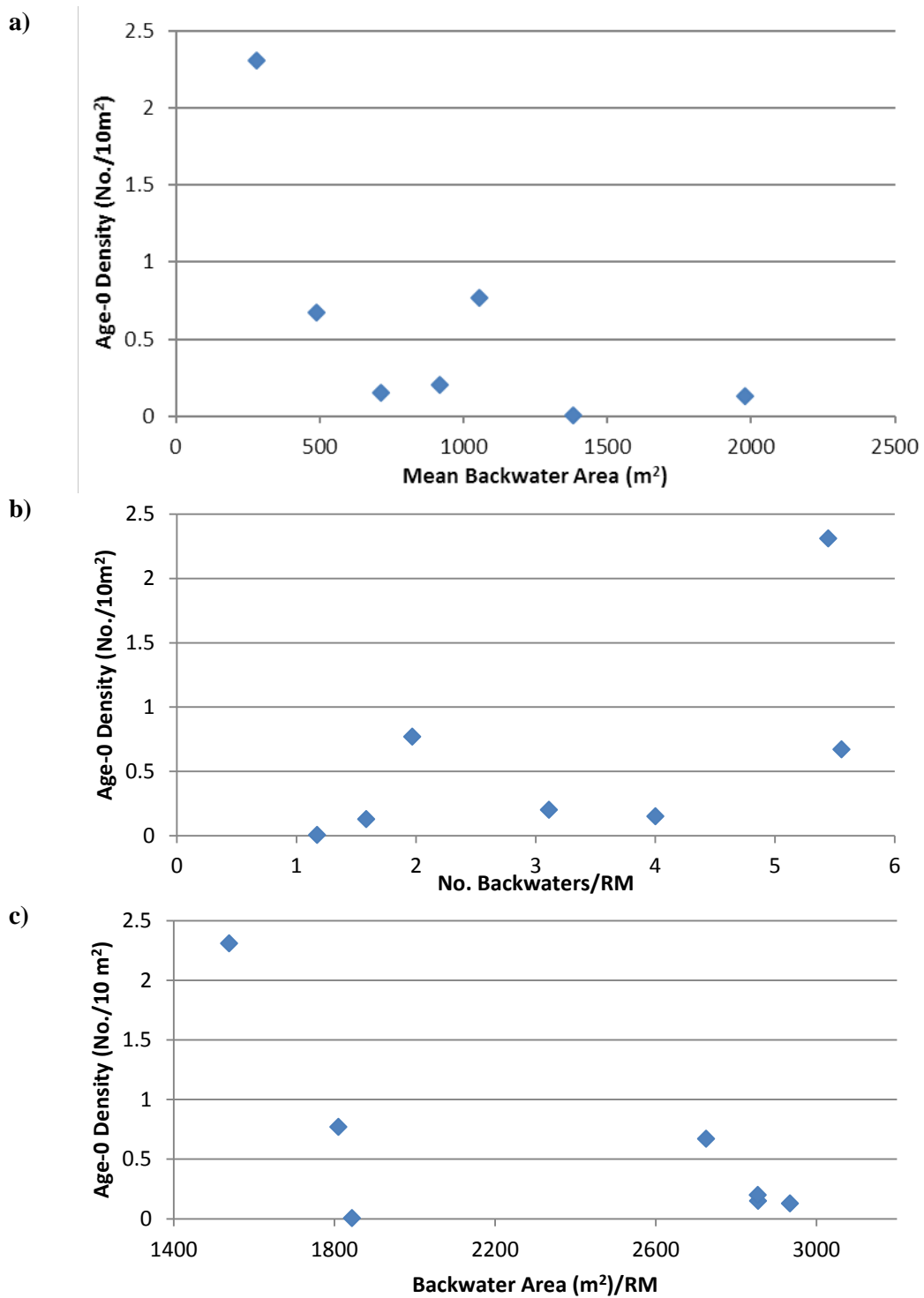


FIGURE 29 Relationships between the Density of Age-0 Colorado Pikeminnow and (a) Mean Backwater Area; (b) Number of Backwaters/RM, and (c) Backwater Area/RM in the Jensen and Ouray Reaches. Densities of Colorado pikeminnow are from Bestgen and Hill (2016).

As discussed in Section 3.1, our imagery analysis indicated that there was a decrease in the number of backwaters, an increase in the mean size of backwaters, but no change in the total amount of backwater habitat available between 1987 and 2013. These backwater changes coincide with the observed decrease in the abundance of age-0 Colorado River pikeminnow, but we do not know if these changes contributed to the observed decrease in recruitment.

Bell (1997) questioned what the effect was on fish in the middle Green River of the shift from more, smaller backwaters to fewer, larger backwaters. If other things were equal, more numerous backwaters could benefit the Colorado pikeminnow population by decreasing the significance of individual backwater losses (from flow-through or disconnection) on recruitment in any given year; however, as our analysis showed, larger backwaters were less likely to be affected by changes in flow during the base-flow period. Larger, and presumably deeper, backwaters are also less likely to suffer catastrophic losses from aquatic and terrestrial predators. Day et al. (1999) found that the mean size of occupied backwaters in the middle Green River was 992 m² compared to 404 m² for unoccupied backwaters, potentially reflecting a preference for larger backwaters, a higher probability of entrainment in larger backwaters, or a higher survivorship in larger backwaters. Given our finding of the greater stability of larger backwaters, and the Day et al. (1999) finding of preference for larger backwaters, we might have expected that conditions for age-0 Colorado pikeminnow have improved since 1987 rather than declined because mean backwater size increased over this period.

At this time, there is insufficient information to determine if there was an effect on age-0 Colorado pikeminnow from the shift to fewer larger backwaters in the middle Green River. There are other factors that have changed over the same time and that could contribute to the decline in Colorado pikeminnow recruitment. Since 1979, there has been (1) great variability in hydrology including several wet periods (e.g., mid-80s, late 90s) and periods of extended drought, (2) changes in hydropower operations, and (3) increases in the abundance and diversity of nonnative fish. It is most likely that declines in recruitment are the result of multiple factors that are interdependent and affect recruitment in complex ways.

Uncertainties related to potential causes of the pikeminnow density decline point out the need for additional work to resolve these uncertainties; the Program is currently working towards this objective. Experimental increases in August-September base flow, as recommended in Bestgen and Hill (2016), together with additional studies of the effects on backwater habitat of flow, sediment, and channel morphology that are suggested by the analyses presented in this report could lead to a better understanding of the factors affecting pikeminnow recruitment.

4 CONCLUSIONS

The aerial and satellite imagery analysis and ground-survey results described in this report quantify interannual, intraannual (seasonal), and within-day variation in backwater characteristics, their relationship to flow conditions in the middle Green River (Reach 2 of Muth et al. 2000), and how these changes in backwater habitat are related to natural and dam-related variation in flow conditions. We draw the following conclusions from our results:

- Based on our analysis of aerial and satellite imagery from 1987 to 2013, the number of backwaters/RM and mean surface area of individual backwaters appear to have decreased and increased, respectively, while total area of backwater habitat appears to have remained the same. We hypothesize that large annual peak flows in the early and middle 1980s, which resulted in some widening of the channel, may have created additional sandbar depositional sites that favored the formation of more backwaters in the late 1980s. Subsequent years with lower annual peak flows may have contributed to a resumption of channel narrowing, the simplification of in-channel habitats, and reduction in the number of sandbar deposition sites and backwaters. In addition, vegetation encroachment, particularly tamarisk and Russian olive, could have increased the rate of channel narrowing and backwater loss. Alternatively, reductions in fluctuations resulting from implementation of the 1992 Biological Opinion and Muth et al. (2000) recommendations may have resulted in the maintenance of larger backwaters through the base-flow period.
- We conducted annual topographic surveys from 2003 through 2013 on 12% to 28% of the backwaters in the ONWR reach. In all years, the mean surface area of surveyed backwaters was larger than the mean backwater surface area for the ONWR reach and Jensen to Ouray reach. We selected backwaters for survey based on depth and size, intentionally selecting backwaters that met the Recovery Program's ISMP criteria for suitable Colorado pikeminnow habitat (at least 30 m² in area and with a maximum depth of at least 0.3 m). This resulted in the selection of larger backwaters (>70th percentile).
- Based on our topographic surveys, mean backwater depth averaged across the base-flow period was usually less than 1 m and often less than 0.5 m. Although mean backwater depth was less than 0.3 m for 25% of surveyed backwaters (13 of 51), mean *maximum* backwater depth was greater than 0.3 m in most years and backwaters. Many backwaters have large portions of their surface area with very shallow depth, while still retaining habitat with depths greater than 0.3 m.
- There was considerable variation in the topography of backwaters and their associated sandbars both within and between years. Consequently, the relationship between flow and backwater characteristics varied considerably among individual backwaters during the base-flow period. Similarly, for an individual backwater site, the same flow conditions produced significantly different backwater characteristics in different years, due to interannual changes in sandbar geomorphology. As a result, there was no consistent base flow that maximized backwater habitat availability among years.
- Overall, our results supported the hypothesis of Rakowski and Schmidt (1999) that there is a positive relationship between the base flows that maximize backwater habitat and the magnitude and duration of spring peak flows. Different lines of evidence identified peak flow magnitude and duration as important driving forces for changes in base flows that maximized backwater surface area, volume, or mean depth. We found a significant relationship between mean sandbar height and annual peak flow and peak-flow duration, and the variables appeared to track each other over time. Backwater bed elevation also

appeared to increase in tandem with the bar building associated with high peak flows. These results indicated that scaling the recommended yearly base flow to hydrologic condition is appropriate, with lower base flows provided in drier years and higher base flows provided in wetter years.

- During the base-flow period, flow conditions in the middle Green River were affected by both natural and dam-related flow variation. Since flows at Ouray are the sum of upstream flows, including dam releases and Yampa River flows, the relative influence of the two sources depends on their relative contribution at any one time. During the spring peak flow, the Yampa River flow is high relative to dam releases, and the Yampa River's contribution dwarfs the contribution of dam releases. During the base-flow period, releases from Flaming Gorge Dam were frequently higher than flows from the Yampa River, resulting in a stronger influence of dam releases on base-flow magnitude and variability. Almost all within-day variability in flow in the middle Green River resulted from fluctuations in dam releases. The exception to this was the strong contribution of sudden increases in Yampa River flows that result from storms in the Yampa River basin. These storms can contribute to changes in flows at Ouray that generally last for a few days.
- Given the complex non-linear relationships between flow and backwater characteristics, it is apparent that flow magnitude and variability can have important effects on backwater habitat characteristics between and within years. The mean daily variation in surface area ranged from 18.4 m² in 2008 to 620 m² in 2005, but most values were less than 250 m². Most daily changes in mean backwater depth were ≤ 0.02 m. Mean daily variation in volume ranged from 3.5 m³ in 2003 to 171.5 m³ in 2009 and were typically less than 75 m³. Changes in dam releases produced relatively minor daily stage changes at Ouray of less than 0.06 m. Despite these relatively minor changes, for some individual habitats, backwater characteristics were lost either through a lowering of flow and disconnection from the river channel at the backwater mouth or through increasing flow and creation of a flow-through condition resulting from flows overtopping or cutting through the associated sandbar. These conditions occurred in 4 of the 10 years of our study in which at least one of the surveyed backwaters experienced such an event, usually from increasing flows.
- Of the 51 backwaters ground-surveyed from 2003 through 2013, only 5 experienced flow-through or disconnection during the base-flow period. Affected backwaters tended to have lower surface area, lower maximum depth, and lower mean depth than other backwaters during the same year, but most, with the exception of BW04 in 2003, were comparable in size and depth to other backwaters.
- Over the 10 years of ground survey, all or a portion of the larval drift period generally corresponded to the time when backwater depth and surface area were high. However, for the early portion of the drift period in most years, backwater surface area and depth were relatively lower than later in the drift period, because flows were still descending from the spring peak, and backwaters had not yet formed. This analysis supports the

recommendation of Bestgen and Hill (2016) to time the onset of base-flow conditions with the first presence of Colorado pikeminnow larvae.

- There were no statistically significant relationships between age-0 pikeminnow density and any of the backwater variables tested (i.e., mean backwater area, backwater area/RM, and the number of backwaters/RM), but we note that data for both pikeminnow density and habitat characteristics were available in only 7 years, limiting the statistical power of our regressions.
- Bestgen and Hill (2016) suggested that the amount of backwater habitat may not be limiting for Colorado pikeminnow in the middle Green River, and that habitat quality or other physical or biological factors drive population dynamics. Even if the amount of backwater habitat is not limiting, the number of pikeminnow larvae retained in the middle Green River may be higher when there is more habitat available because more habitat increases the potential for entraining drifting larvae and provides more habitat suitable for summer growth.

5. RECOMMENDATIONS

- Monitor channel narrowing in the middle Green River. Our analysis identified a decrease in the number of backwaters/RM and an increase in the mean size of backwaters since 1987. A possible explanation is related to channel narrowing and a decrease in channel complexity, which could have long-term repercussions on habitat quality and native fish production. We recommend periodic assessments of channel width, plant density, plant communities, and other habitat characteristics observable in aerial or satellite imagery to determine if the flow regime is adequate to prevent vegetation encroachment, channel narrowing, and simplification. An analysis of channel narrowing should include an assessment of channel response to very high flows (e.g., > 26,400 cfs, the recommended peak flow for wet years in Muth et al. [2000]) to determine the ability of high peak flow magnitudes and durations to reverse previous channel narrowing. High-resolution satellite imagery that is available at relatively low cost (about \$15,000 for the middle Green River reach) or aerial imagery (about \$50,000 for the reach) could be used to assess channel narrowing. U.S. Department of Agriculture's National Agriculture Imagery Program (NAIP) imagery is of lower, but potentially adequate, resolution and is available free of charge. LaGory et al. (2016) recommended a similar assessment.
- Monitor the mass balance of fine sediment (i.e., particles with grain sizes < 2 mm [i.e., sand, silt, and clay]) in the middle Green River. The formation and maintenance of backwater habitats are strongly dependent on fine sediment mass balance. To monitor the effect of flow regimes on fine sediment mass balance, we recommend installation of two gages: near the existing Jensen, Utah, stream gage (USGS 09261000) and near the existing Ouray, Utah, stream gage (USGS 09272400). These two gages should be used to

monitor suspended sediment flux in the middle Green River. LaGory et al. (2016) recommended similar monitoring.

- Continue an evaluation of long-term trends in backwater number and size in the middle Green River to build on the analysis presented in this report. Analyzing new imagery of the middle Green River (Jensen to Ouray) as it becomes available will enable monitoring trends in backwater habitat and determining relationships to age-0 Colorado pikeminnow captures. LaGory et al. (2016) recommended similar monitoring. Care should be taken to use an approach that is consistent with earlier studies and to archive the imagery, polygons of digitized backwaters, and data on the area of individual backwaters. For the imagery analysis presented here, we provide such documentation in the supplement to this report (Hamada et al. 2017).

6 REFERENCES

Bell, A., 1997, "Green River Flooded Bottomlands and Backwater Habitat Mapping," Technical Memorandum No. 8260-97-01, U.S. Bureau of Reclamation, Technical Service Center, Denver, Colo.

Bestgen, K.R., and A.A. Hill, 2016, *Reproduction, Abundance, and Recruitment Dynamics of Young Colorado Pikeminnow in the Green and Yampa Rivers, Utah and Colorado, 1979-2012*. Final report to the Upper Colorado River Endangered Fish Recovery Program, Project FW BW-Synth. Larval Fish Laboratory, Department of Fish, Wildlife, and Conservation Biology, Colorado State University, Fort Collins, Contribution 183.

Breiman, L, and A. Cutler, 2013, "Breiman and Cutler's Random Forests." Available at <http://stat-www.berkeley.edu/users/breiman/RandomForests>. Accessed February 4, 2015.

Day, K.S., K.D. Christopherson, and C. Crosby, 1999, *An Assessment of Young of the Year Colorado Pikeminnow (Ptychocheilus lucius) Use of Backwater Habitats in the Green River, Utah*. Final report to the Recovery Implementation Program for the Endangered Fish Species in the Upper Colorado River Basin, Project FG-33. Utah Division of Wildlife Resources, Vernal, Utah.

Evans, J.S., M.A. Murphy, Z.A. Holden, and S.A. Cushman, 2011, "Modeling Species Distribution and Change Using Random Forests," Chapter 8 in: *Predictive Species and Habitat Modeling in Landscape Ecology*, C.A. Drew, Y.F. Wiersma, and F. Heuttmann (eds.).

FWS (U.S. Fish and Wildlife Service), 1992, *Final Biological Opinion on Operation of Flaming Gorge Dam*, Fish and Wildlife Service, Mountain Prairie Region, Denver, Colorado.

FWS, 2006, *Final Biological Opinion on the Operation of Flaming Gorge Dam*, Fish and Wildlife Service, Utah Field Office, West Valley City, Utah.

Green River Study Plan Ad Hoc Committee, 2007, *Study Plan for the Implementation and Evaluation of Flow and Temperature Recommendations for Endangered Fishes in the Green River Downstream of Flaming Gorge Dam*, Final Report, Upper Colorado River Endangered Fish Recovery Program, Denver, Colo.

Hamada, Y., K.E. LaGory, and X.H. Jiang, 2017, *Identification of Backwater Nursery Habitats of Colorado Pikeminnow Using High Resolution Remotely Sensed Imagery*. Final report to the Upper Colorado River Endangered Fish Recovery Program, Project FW BW-Synth. Environmental Science Division, Argonne National Laboratory, Argonne, Illinois.

Holden, P.B., 1980, *The Relationship between Flows in the Yampa River and Success of Rare Fish Populations in the Green River System*, final report of BIO/WEST, Inc., to National Park Service, Denver, Colorado.

LaGory, K.E., J.W. Hayse, and D. Tomasko, 2003, *Recommended Priorities for Geomorphology Research in Endangered Fish Habitats of the Upper Colorado River Basin*, Final report to Upper Colorado River Endangered Fish Recovery Program, Denver, Colorado, U.S. Fish and Wildlife Services, Denver, Colorado.

LaGory, K.E., T. Chart, and J. Mohrman, 2016, *A Strategy to Evaluate Peak Flow Recommendations for Sediment Transport and Habitat Maintenance in the Upper Colorado River Basin—A Technical Supplement to the Green River and Aspinall Study Plans*. Final report to Upper Colorado River Endangered Fish Recovery Program, Denver, Colorado, U.S. Fish and Wildlife Services, Denver, Colorado.

Lyons, J.K., M.J. Pucherelli, and R.C. Clark, 1992, “Sediment Transport and Channel Characteristics of a Sand-Bed Portion of the Green River below Flaming Gorge Dam, Utah, USA,” *Regulated Rivers: Research and Management* 7:219–232.

McCoy, J., and K. Johnston, 2001, *Using ArcGIS Spatial Analyst*. Environmental Systems Research Institute, Inc., Redlands, California.

Murphy, M.A., J.S. Evans, and A.S. Storfer, 2010, “Quantify *Bufo boreas* Connectivity in Yellowstone National Park with Landscape Genetics,” *Ecology* 91:252–261.

Muth, R.T., L.W. Crist, K.E. LaGory, J.W. Hayse, K.R. Bestgen, J.K. Lyons, T.P. Ryan, and R.A. Valdez, 2000, *Flow Recommendations for Endangered Fishes in the Green River Downstream of Flaming Gorge Dam*, final report to Upper Colorado River Endangered Fish Recovery Program, Denver, Colorado, U.S. Fish and Wildlife Service, Denver, Colorado.

Pucherelli, M.J., 1987, “A Summary of Methods and Results for the Green River Backwater Pilot Study Using Remote Sensing and GIS (Geographic Information Systems),” *Applied Sciences Referral Memorandum* No. AP-87-4-2.

Pucherelli, M.J., and R.C. Clark, 1989, “Comprehensive Report (1986-1988) on the Effects of Green River Flows on Backwater Habitat Availability as Determined by Remote Sensing Techniques (Remote Sensing),” *Applied Sciences Referral Memorandum* No. AP-89-4-5.

Pucherelli, M.J., and R.C. Clark, 1990, “Green River Backwater Habitat Mapping; Fluctuating Flow Test, Utilizing Airborne Videography Techniques,” (Endangered Fish) *Applied Sciences Referral Memorandum* No. 90-4-4.

Pucherelli, M.J., J.N. Halls, and R.C. Clark, 1987, “Green River Channel Mapping Study,” *Applied Sciences Referral Memorandum* No. AP-88-4-1.

Rakowski, C. L., and J. C. Schmidt, 1999, “The Geomorphic Basis of Colorado Pikeminnow Nursery Habitat in the Green River near Ouray, Utah,” Report A in *Flaming Gorge Studies: Assessment of Colorado Pikeminnow Nursery Habitat in the Green River*. Final report of Utah Division of Wildlife Resources to Upper Colorado River Endangered Fish Recovery Program, Denver, Colorado.

Trammell, M. A., and T. E. Chart. 1999. “Colorado Pikeminnow Young-of-the Year Habitat Use, Green River, Utah, 1992–1996.” Report C in *Flaming Gorge Studies: Assessment of Colorado pikeminnow nursery habitat in the Green River*. Final Report of Utah Division of Wildlife Resources to Upper Colorado River Endangered Fish Recovery Program, Denver, Colorado.

APPENDIX 1

**SIMULATION OF FLOWS IN THE OURAY REACH
OF THE GREEN RIVER FROM 2003 TO 2008**

This page is intentionally left blank.

APPENDIX 1

SIMULATION OF FLOWS IN THE OURAY REACH OF THE GREEN RIVER FROM 2003 TO 2008

This appendix describes the methods for simulating flows at the Ouray reach for the backwater survey years (2003–2008) before the Ouray gage station was installed in 2009.

A1.1 PROBLEM STATEMENT

Analysis of the relations between flow and backwater physical characteristics requires accurate knowledge of topography/bathymetry, discharge, and local stage-discharge relationships. The most accurate discharge records are obtained from nearby U.S. Geological Survey (USGS) gage stations; the nearest upstream gage station is at Jensen (09261000) and the nearest downstream gage station is at Ouray (09272400). The Ouray gage station can be used to represent discharges and relative stage-discharge relationships at the backwater sites, due to the proximity and similarity in geomorphic setting of the Ouray gage station relative to the backwater sites. However, that gage station has only been operational since 2009. Prior to 2009, the nearest gage station was at Jensen, which is approximately 54 river miles upstream of the backwater sites. The simplest approach for estimating flows in the study reach prior to 2009 would be to use the Jensen discharge time series. However, based on physical principles, the daily waves are known to attenuate as they propagate downstream along the Green River; furthermore, flows may be input and extracted between the Jensen gage station and the study reach. Based on these considerations, the first issue addressed in this appendix is to quantify to what extent the discharge time series differs between the Jensen gage station and the Ouray gage station (after properly accounting for travel time between the two sites) and, based on the findings, to indicate whether additional treatment is warranted to achieve a discharge time series that is more representative of the backwater sites than that obtained using the Jensen data prior to 2009.

As an example of the wave transformation between Jensen and Ouray, Figure A1-1 shows 14 days of winter discharge data from a period when both the Ouray and the Jensen gage stations were in operation. A 32-hour time lag was used on the Ouray record. Figure A1-1 illustrates a fairly classic wave transformation as the daily wave propagates downstream. The peak is reduced; the trough is increased as the waves spread and become superimposed; and the peak is shifted a little toward earlier time, because the peak travels downstream faster than the trailing trough.

Figure A1-2 shows another example at a lower summer discharge, where the Ouray data is lagged by 38.5 hours. During the summer months, the total flow conveyed past the Ouray gage is less than the flow conveyed past the Jensen gage upstream (Figure A1-2). The wave overlay does not follow the typical pattern shown in Figure A1-1; the troughs are roughly equal, but the peaks are considerably different. This could be a result of two factors (or a combination of these

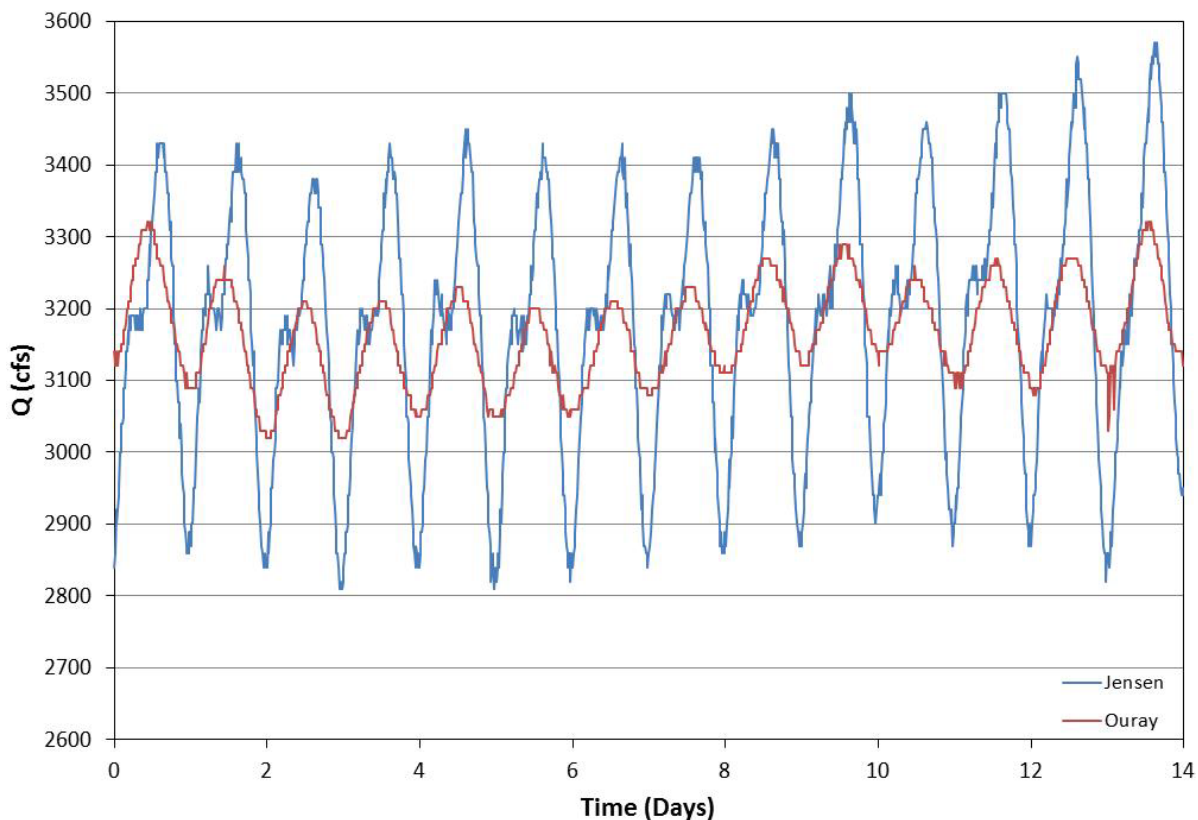


FIGURE A1-1 Discharges Measured at the Jensen Gage Station and the Ouray Gage Station, Lagged by 32.0 hours (Time 0 is 02/05/12, 10:00 am at the Jensen gage; Time 0 is 02/06/12, 18:00 at the Ouray gage)

two factors). The first potential explanation is that the rating curve at the Ouray station is inaccurate at the low end of the curve. The second potential explanation is that considerable flow is being extracted from Green River between Jensen and Ouray for irrigation, hatchery operations, and other purposes; for example, if about 150 cfs was added to the Ouray discharge record, then the overlay would look very similar to the classic transformation pattern shown in Figure A1-1. Given that this data period is during the summer, the flow extraction explanation likely has some validity.

In Figure A1-3, the discharge recorded at the Ouray gage is within a fairly narrow range; therefore, inaccuracy in the rating curve does not explain why the first 8 days experience lower than expected discharge, while the last 6 days experiences expected discharge. The data illustrated in Figure A1-3 isolates the issue of gage station inaccuracy and excludes it as the primary cause of the discharge discrepancies. Flow extraction during the first 8 days of this record thus appears to be the most likely explanation.

Another illustration of apparent flow extraction is shown in Figure A1-4.

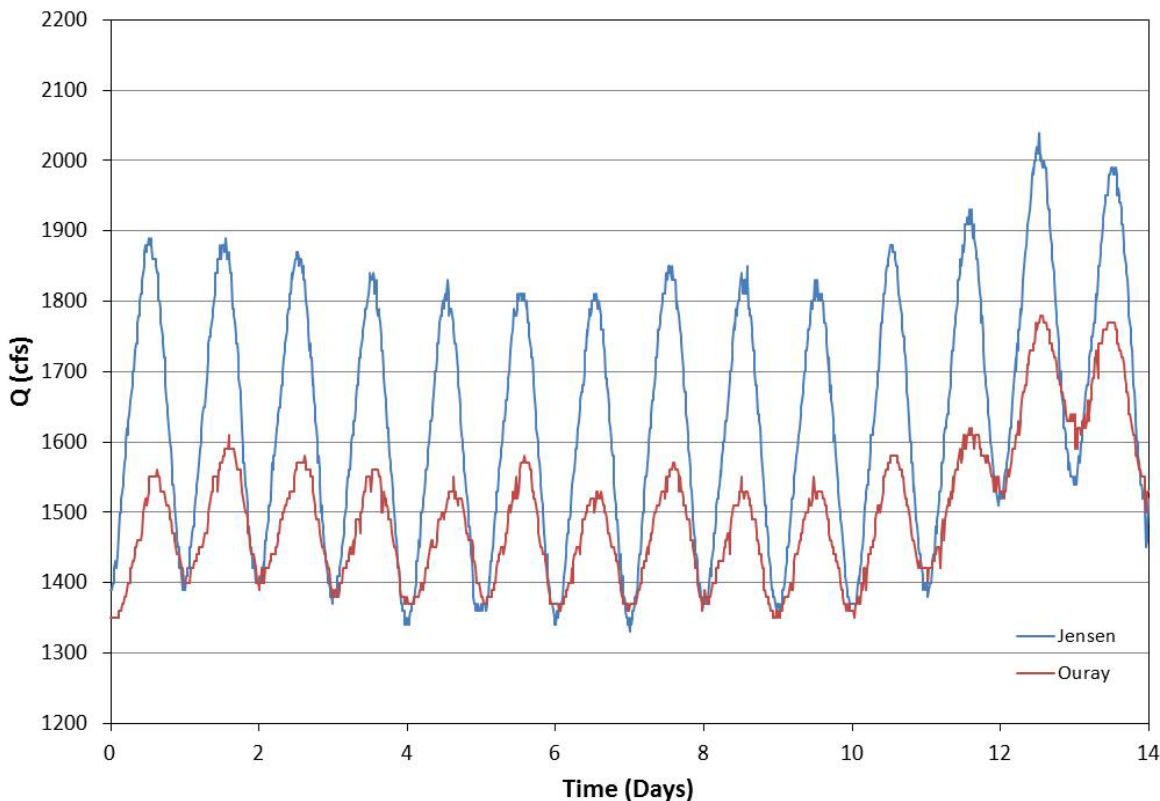


FIGURE A1-2 Discharges Measured at the Jensen Gage Station and the Ouray Gage Station, Lagged by 38.5 hours (Time 0 is 06/30/12, 18:00 at the Jensen gage; Time 0 is 07/02/12, 08:30 at the Ouray gage)

The evidence presented in Figures A1-1 through A1-4 suggests that, even when accounting for the time lag, significant differences in discharge exist between the Jensen gage and the Ouray gage. The more important question is whether the difference is important with respect to the evaluation of habitat area/volume curves. The greatest sensitivity in stage change occurs at the low end of the rating curve, where the curve is steepest; therefore a low Q is most appropriate for estimating maximum error. Considering the case illustrated in Figure 2, Q_{Jensen} varies from 1340 cfs to 1840 cfs on Day 4; applying this discharge record to the backwater sites yields a stage that varies by 0.41 ft. (based on the Ouray rating curve). In comparison, Q_{Ouray} on Day 4 varies from 1370 cfs to 1560 cfs; this yields a stage that varies by only 0.16 ft (based on the Ouray rating curve). As expected, using untransformed Q_{Jensen} values overestimates the daily fluctuations in stage at the backwater sites. Given the sensitivity of the habitat/area volume curves to small changes in stage, it was decided that effort was warranted to provide a more accurate estimate of discharges than using the Jensen gage station data directly.

In summary, (a) the daily waves as measured at Jensen have greater daily variation in Q than at Ouray, due to downstream wave transformation (500 cfs daily variation at Jensen translates to about 200 cfs daily variation at Ouray) and (b) there also appeared to be a considerable amount of flow extraction during the summer between these two locations. The methods used to correct for both issues are addressed in Section A1.2.

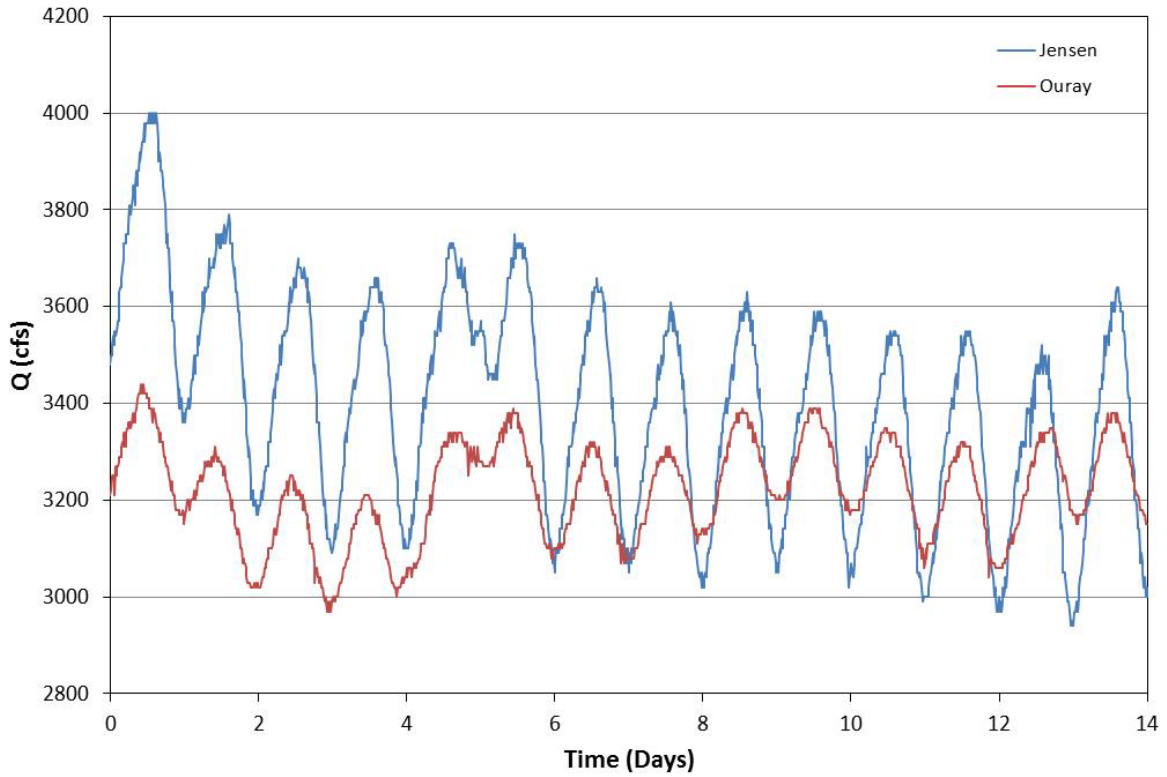


FIGURE A1-3 Discharges Measured at the Jensen Gage Station and the Ouray Gage Station, Lagged by 33.5 hours (Time 0 is 08/24/11, 10:15am at the Jensen gage; Time 0 is 08/25/11, 19:45 at the Ouray gage.)

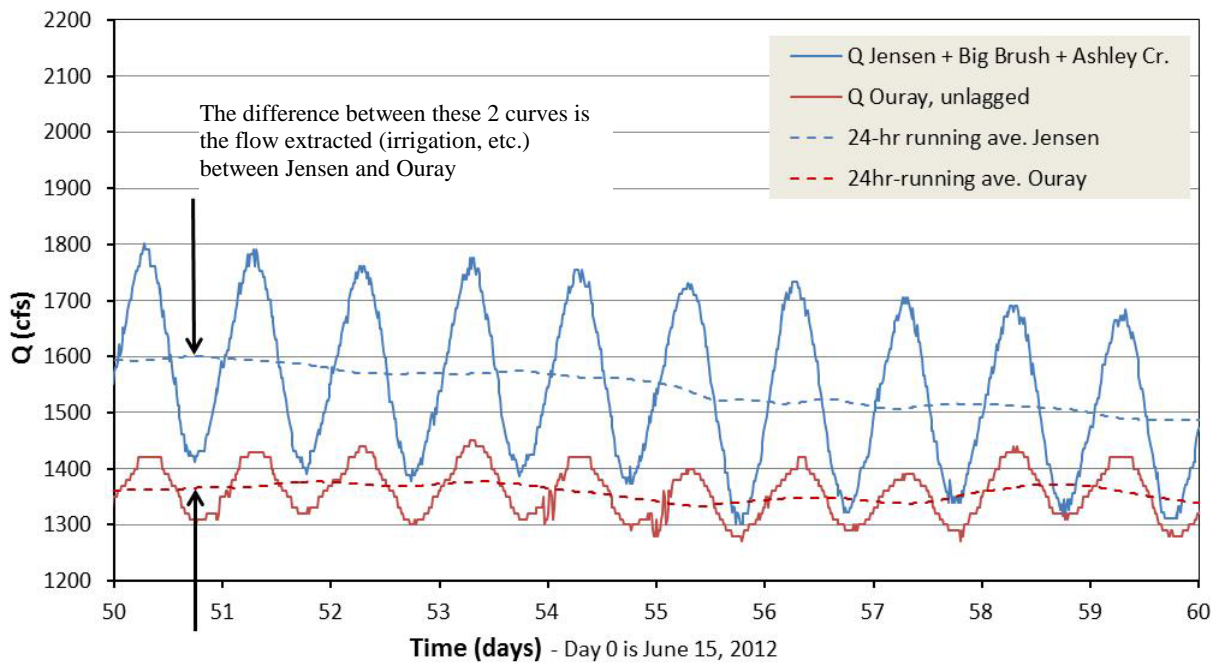


FIGURE A1-4 Illustration of Flow Extraction between Jensen and Ouray Gage Stations

A1.2 EMPIRICAL WAVE TRANSFORMATION OF THE JENSEN DATA AND CORRECTION FOR WATER EXTRACTION

A1.2.1 Analysis of Daily Variation of Q

In this analysis, evaluating the daily variation in Q is performed by calculating instantaneous deviations from the 24-hour moving average. The instantaneous deviation is referred to as Q' and is calculated as follows:

$$Q'(t) = Q(t) - Q_{ave,24hr}(t), \quad (1)$$

where $Q_{ave,24hr}$ is the 24-hour moving average as illustrated in the dashed lines of Figure A1-4. The 24-hour period is the proper time scale for averaging, because it generally encompasses the full wave and thus eliminates oscillations in the mean associated with averaging. Using instantaneous deviations from the 24-hour moving average eliminates complications associated with periods of rising or falling discharge over multi-day time scales. An illustration of the physical meaning of Q' is provided as Figure A1-5.

The analysis is provided for the daily waves in the time period from 06/01/12 to 10/07/12 because it contains well-defined daily waves with a broad range of daily variations and the 2012 Ouray rating curve is the most recent (as of the time of this analysis in February 2013) and therefore provides the best estimates of Q_{Ouray} . This time period yields a population of 127 daily

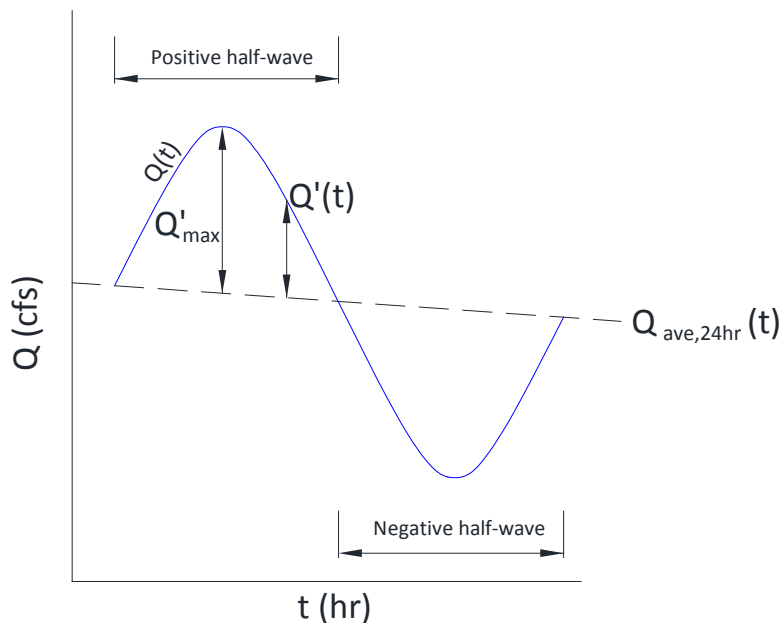


FIGURE A1-5 Illustration of Instantaneous Deviations Relative to the 24-hour Moving Average

waves, each having a half-wave with positive Q' and a half-wave with negative Q' , as illustrated in Figure A1-5. After adjusting for time lag such that the wave measured at Jensen directly overlays the wave measured at Ouray (as shown in Figures A1-1 through A1-4), the discharge record is decomposed into a record of Q'_{Jensen} and Q'_{Ouray} , as shown in Figure A1-6.

The next step is to compare the corresponding amplitudes of each daily wave; the amplitude was defined as the greatest deviation from the mean: $|Q'_{max}|$ (as illustrated in Figure A1-5). The absolute value of each half-wave was considered for this analysis; in other words, the negative Q' values were evaluated on the same basis as the positive values. This yields a population of 253 points, of the form $(|Q'_{max,Jensen}|, |Q'_{max,Ouray}|)$, that are plotted as shown on Figure A1-7.

The data points in Figure A1-7 were fit to a linear curve, a power-law curve, and a second-order polynomial curve. The best fit to the data according to the maximum R^2 was the second-order polynomial. The equation is:

$$|Q'_{max,Ouray}| = 0.0005902(|Q'_{max,Jensen}|)^2 + 0.2427|Q'_{max,Jensen}|. \quad (2)$$

Defining a new variable K_{wave} , and using Equation (2) yields the following:

$$K_{wave} \equiv \frac{|Q'_{max,Ouray}|}{|Q'_{max,Jensen}|} = 0.0005902|Q'_{max,Jensen}| + 0.2427, \quad (3)$$

where K_{wave} represents the scaling factor between the amplitudes of the Ouray wave and the Jensen wave. The next issue to be addressed was whether the entire wave could be scaled according to the scaling of the amplitudes in Equation (3). The concepts are illustrated in Figure A1-8.

In Figure A1-8, $f(t)$ represents the decomposed Jensen wave, $g(t)$ represents the decomposed Ouray wave, and the ratio (b/a) represents the scaling factor K_{wave} . The goal of the current analysis was to be able to estimate $g(t)$ using the Jensen gage data decomposed into $f(t)$ for the years 2003 to 2008, when data to allow decomposition of $g(t)$ does not exist. To facilitate the effort, the following dimensionless variables are introduced:

$$Q'^* = \frac{|Q'(t)|}{|Q'_{max}|}, \text{ and} \quad (4a)$$

$$t^* = \frac{t}{T}, \quad (4b)$$

where Q'^* is dimensionless Q' ; t^* is dimensionless time; $|Q'_{max}|$ is the maximum deviation for the daily wave under consideration; T is the duration of the half-wave, which in all cases is in the vicinity of 12 hours. Each of the daily waves were non-dimensionalized in this manner to generate curves of Q'^* versus t^* . Each curve was discretized into 51 points with $\Delta t^* = 0.02$. All 253 Jensen curves were then overlaid and an average Q'^* was calculated for each discretized interval of Δt^* . The same procedure was then repeated for the Ouray curves. The averages thus calculated are shown in Figure A1-9.

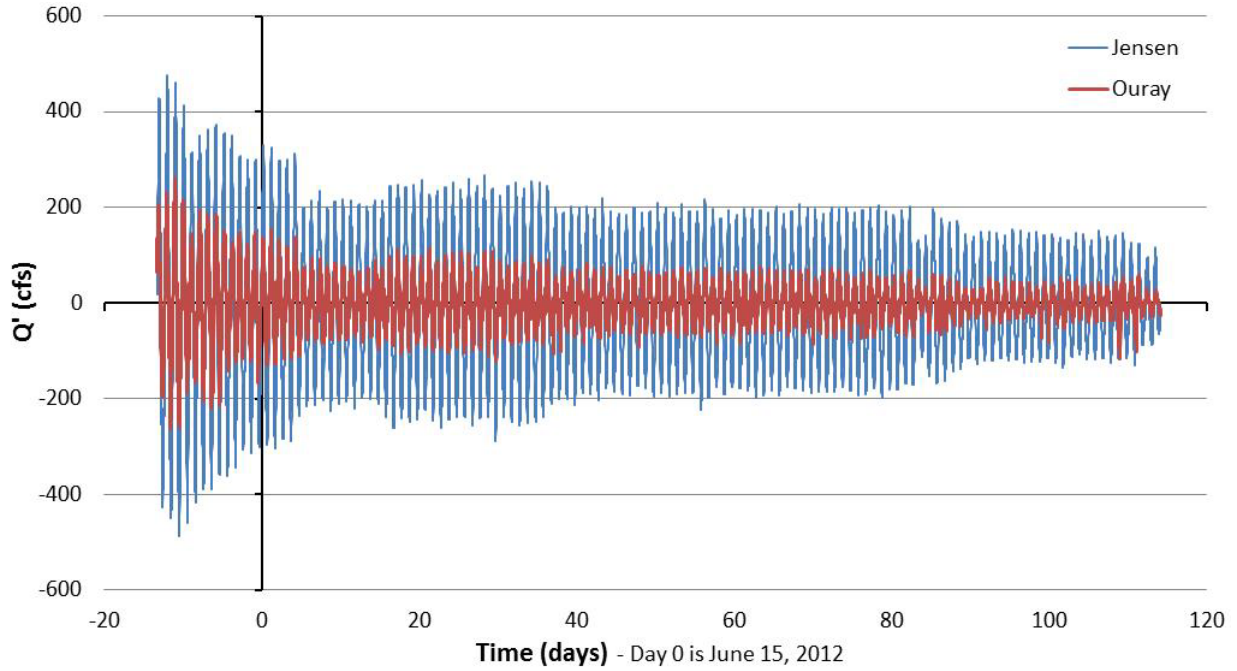


FIGURE A1-6 Instantaneous Deviations from the Mean Discharge throughout the Evaluation Period

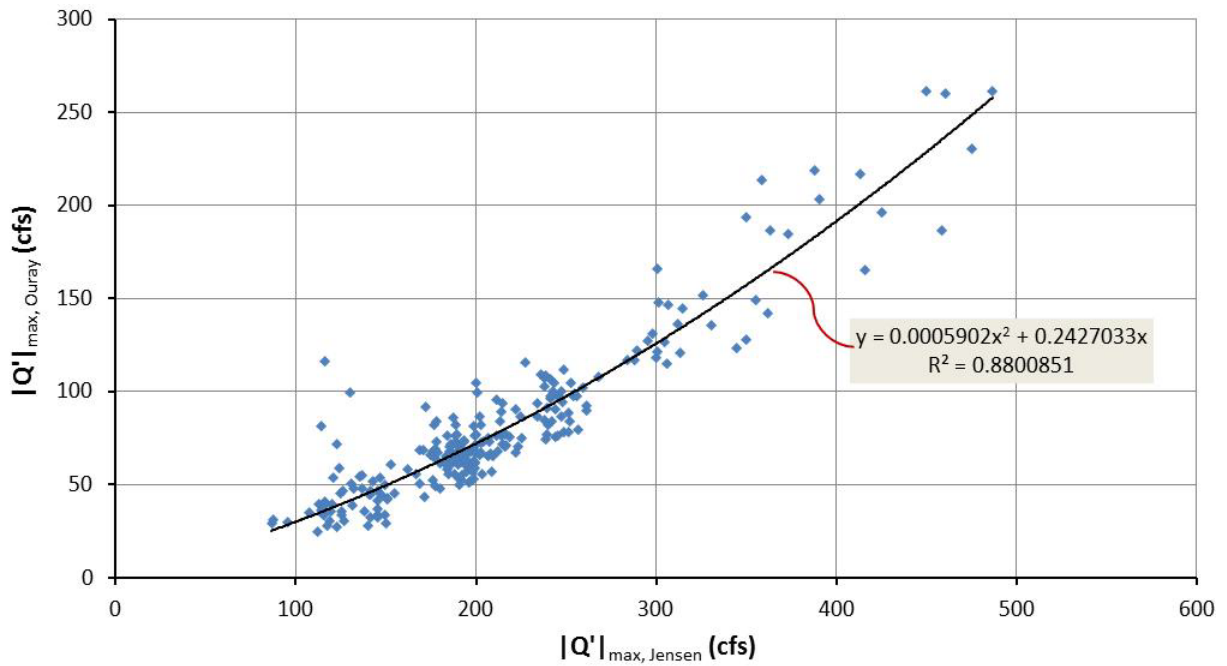


FIGURE A1-7 Comparisons of Wave Amplitudes at Jensen and Ouray Gage Stations

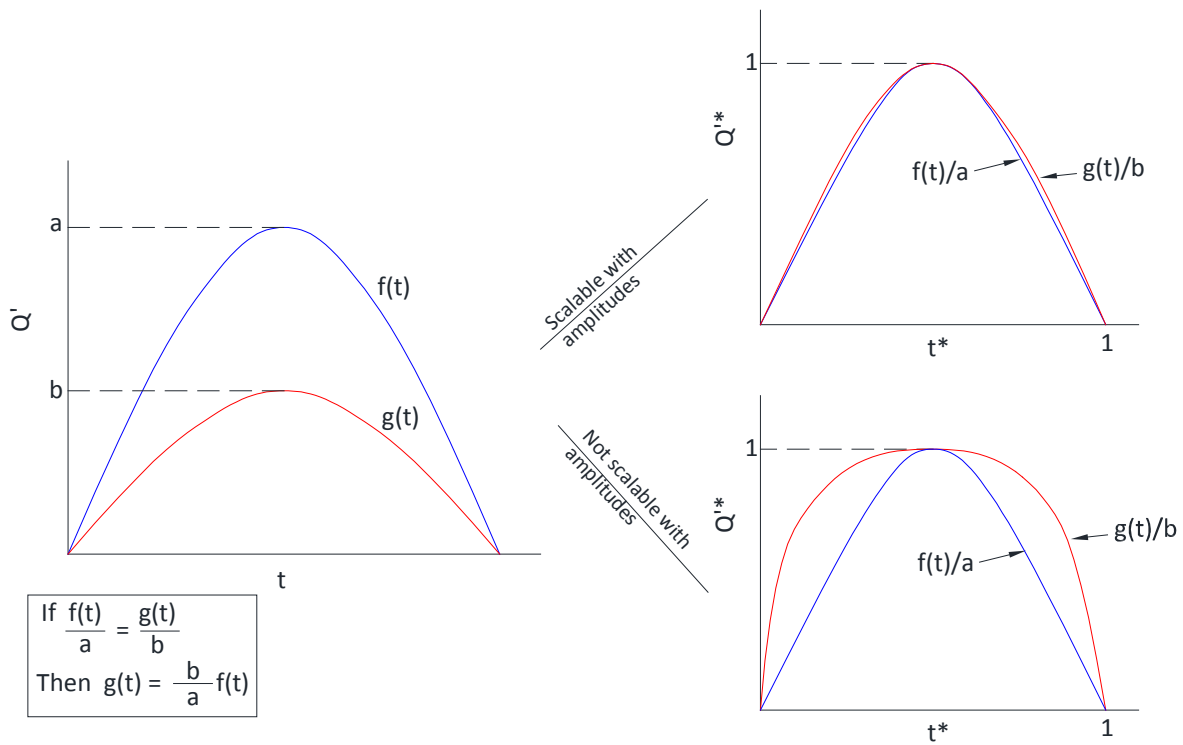


FIGURE A1-8 Conceptual Illustration Determining whether Entire Waves Can Be Scaled with Amplitudes (See Eq. [4] for definition of dimensionless variables.)

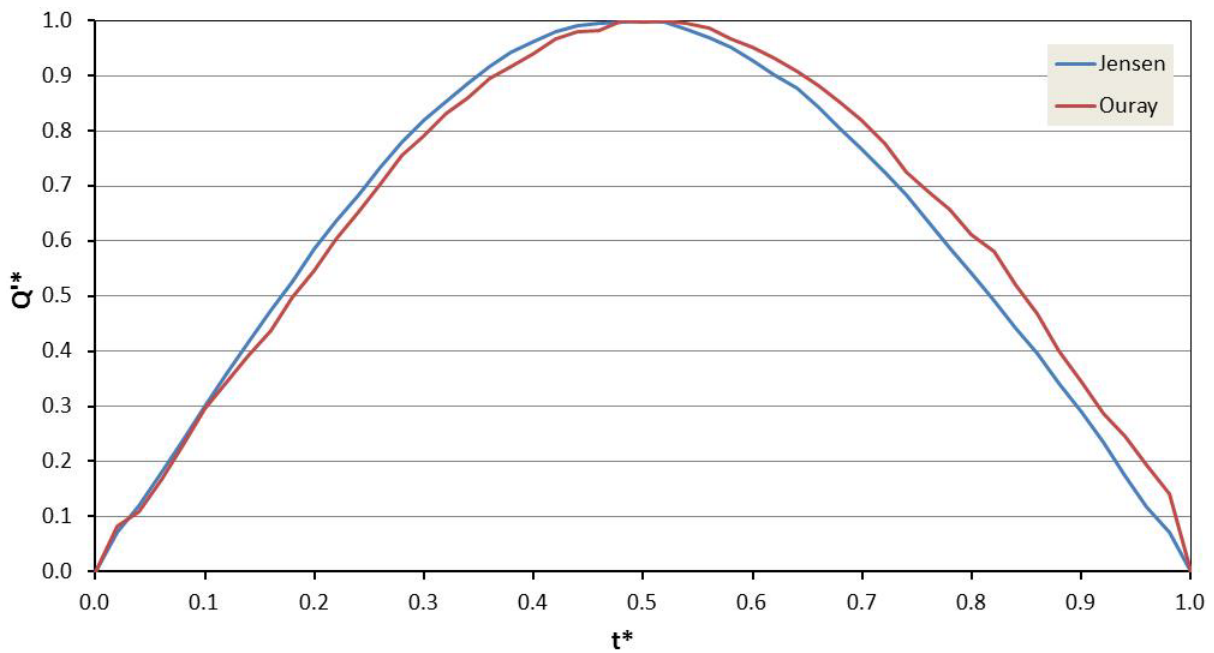


FIGURE A1-9 Comparison of the Dimensionless Waves; Each Curve Represents the Average of All 253 Daily Half-Waves Evaluated

As shown in Figure A1-9, the shape of the Ouray curve appears to be reasonably well represented by the shape of the Jensen curve. The maximum error is 8.9%, which is acceptable error; as such, the entire wave can be scaled with the scaling of the amplitudes per Equation (3).

Therefore, for the years 2003 to 2008, the Jensen waves were decomposed as shown in Figure A1-6 to yield a time series of Q'_{Jensen} versus t ; the amplitude of each daily half-wave can be identified; the scaling factor K_{wave} for the half-wave can then be calculated per Equation (3); and finally, by multiplying each value of Q'_{Jensen} by K_{wave} , we achieve a time series of Q'_{Ouray} . The only task remaining is to determine an appropriate estimate of the 24-hour moving average at Ouray, to which Q'_{Ouray} will be added.

A1.2.2 Accounting for Flow Extraction during the Summer Months

When daily waves are overlaid by implementing the proper time lag, mass conservation with no inflows or outflows between the Jensen gage station and the Ouray gage station requires that the 24-hour moving averages be equal at the two gage stations. Any difference between the 24-hour moving averages represents the net flows input or extracted between the Jensen gage station and the Ouray gage station (this difference is illustrated in Figure A1-4). We know that some flow inputs exist between Jensen and Ouray, in particular Ashley Creek and Big Brush Creek, which are gaged streams that enter Green River near Vernal, Utah. However, despite the known flow inputs, less flow is observed at Ouray than at Jensen, as shown in Figure A1-4, which suggests that flow is being extracted.

For this analysis, the time series of flow at the Big Brush Creek and Ashley Creek gage stations was added to the time series of flow at the Jensen gage station. Such an addition assumes that the flows recorded at an instant in time from the three gage stations simultaneously converge at a point in the Green River. Because such an assumption has not been verified, and because transformations of the Big Brush Creek and Ashley Creek hydrographs occur between the gage stations and the mouths of the streams, a 24-hour moving average is used for the Big Brush Creek and Ashley Creek time series. This minimizes potential errors associated with time lags and hydrograph transformations from the two tributaries. The instantaneous difference in the 24-hour moving averages (as illustrated in Figure A1-7) is referred to as $Q_{extract}$, where a positive value represents net flow extraction and a negative value represents net flow addition between the gage stations:

$$Q_{extract}(t) = \langle Q_{Jensen}(t) + Q_{BigBrush,24}(t) + Q_{Ashley,24}(t) \rangle_{ave,24hr} - \langle Q_{Ouray}(t) \rangle_{ave,24hr} \quad (5)$$

where $Q_{BigBrush}$ and Q_{Ashley} are filtered using their 24-hour moving averages (denoted by the subscript “24”) before being added to Q_{Jensen} . The results of the analysis are shown in Figure A1-10.

As is evident from Figure A1-10, there was considerable variability between years. The variability can partly be explained by the inherent error associated with the rating curves, particularly at the Ouray gage, where the rating curve is based on limited discharge measurements and is still being refined with additional measurements. The year 2011 exhibited

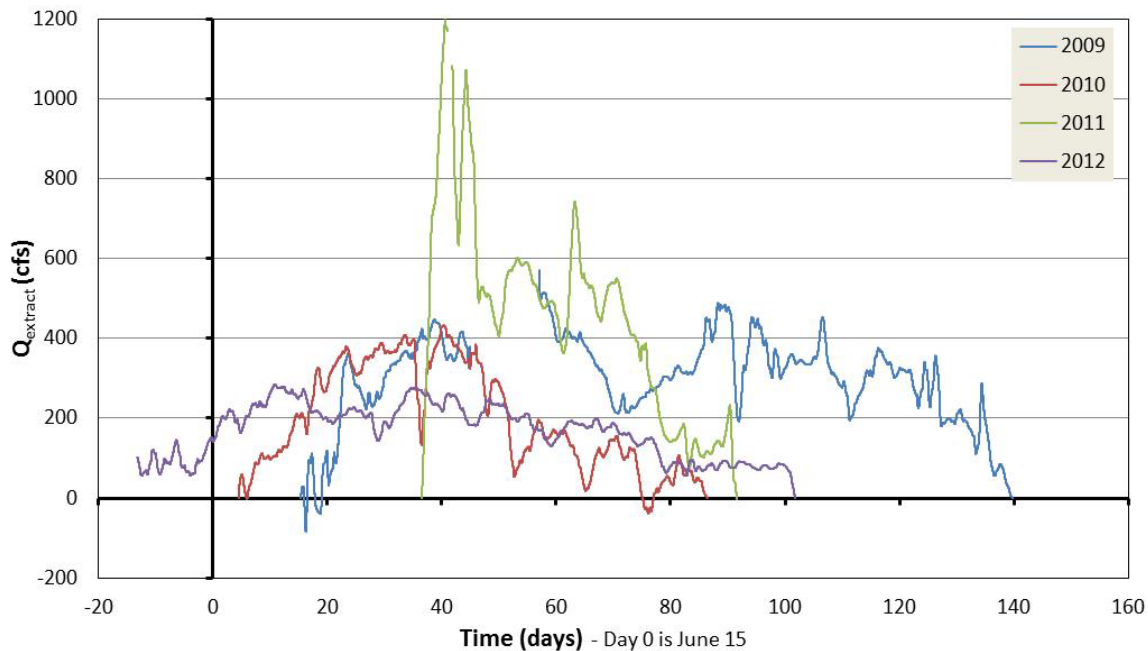


FIGURE A1-10 Flow That Was Extracted between Jensen and Ouray during the Base-Flow Seasons of 2009–2012

very high flow, with flows $>10,000$ cfs persisting into late July. At these high flows, the estimated discharge is very sensitive to small changes in stage; furthermore, the error associated with the discharge measurements on which the rating curve is based is usually estimated to be 5 to 8% (good to fair discharge measurement quality code). At high discharge, an error of a few percentage points translates into hundreds of cubic feet per second, which means that the very high estimated $Q_{extract}$ for 2011 is highly suspect. The year 2012 appears to be the most reliable dataset for several reasons: (1) the discharge is based on the most accurate rating curve fit to the greatest number of measurements; (2) it is the lowest discharge year, with discharge dropping below 5000 cfs per month earlier than the remainder of the years – the lower discharge suggests less absolute error when the relevant scale of measurement is on the order of hundreds of cubic feet per second; (3) it yielded the lowest volume of flow extracted, such that use of this data represents the most conservative estimate when attempting to project into the past.

Because of the variation in Figure A1-10, and the small population of only four samples, general trends can be distinguished qualitatively, but no statistical analysis was even attempted. The general trends were as follows: (1) during June or July, net flow begins to be extracted from the Green River; (2) the amount of flow extracted is on the order of hundreds of cubic feet per second; (3) sometime between early September and late October, flow stops being extracted.

Averaging $Q_{extract}$ over the entire 2012 period, where $Q_{extract} > 100$ cfs (06/13/12 through 09/01/12) yields a mean $Q_{extract} = 205$ cfs. Qualitatively representing the flow extracted as a constant 200 cfs for the period between June 15 and August 31 was chosen as a reasonable, conservative approximation of flow extraction until more data is obtained in the future. The 200 cfs flow extraction is illustrated relative to the 2012 data in Figure A1-11.

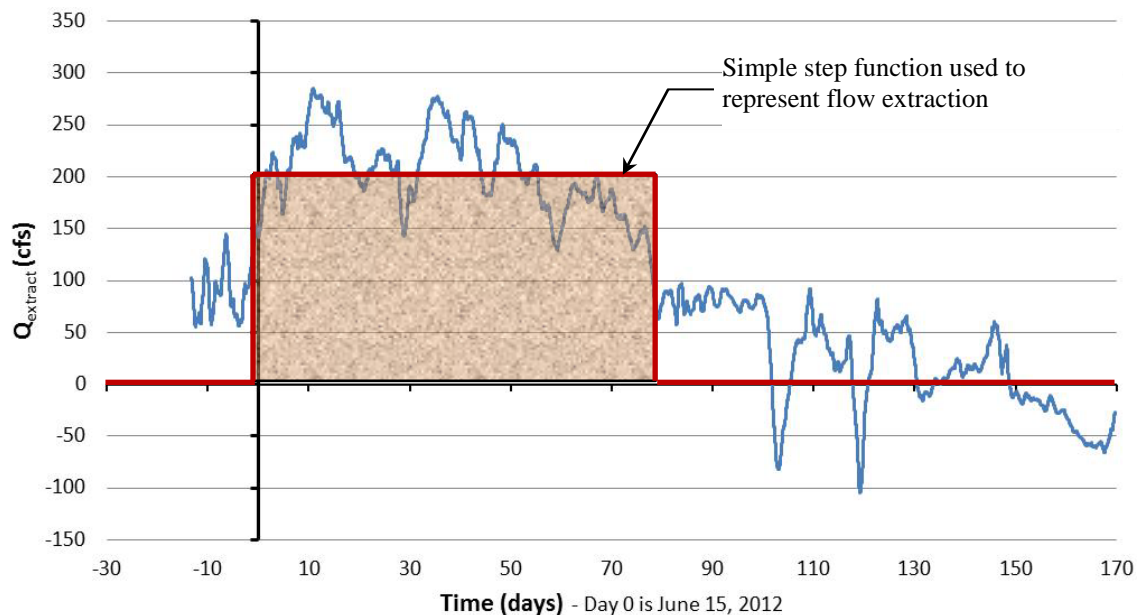


FIGURE A1-11 Illustration of the Step Function Proposed for Flow Extraction (It is a simplified representation of the 2012 flow extraction data, which is represented by the blue curve.)

A1.2.3 Summary of the Wave Transformation Algorithm

The following is a step-by-step description of the algorithm for un-lagged synthetic hydrograph generation:

1. Tabulate the Jensen gage station discharge time series (15-minute time intervals): $Q_{Jensen}(t)$.
2. Tabulate the Ashley Creek gage station discharge time series (15-minute time intervals): $Q_{Ashley}(t)$.
3. Tabulate the Big Brush Creek gage station discharge time series (15-minute time intervals): $Q_{BigBrush}(t)$.
4. Generate a 15-minute time series of the 24-hour moving average of the Ashley Creek and Big Brush Creek flow data: $Q_{Ashley,24}(t)$ and $Q_{BigBrush,24}(t)$.
5. Perform the sum: $Q_{Sum,upper}(t) = Q_{Jensen}(t) + Q_{Ashley,24}(t) + Q_{BigBrush,24}(t)$. This generates a time series of discharge from the upper end of the reach under consideration. That is the solid blue curve shown in Figure A1-2.
6. Generate a 15-minute time series of the 24-hour moving average of that sum: $Q_{Sum,upper,24}(t)$. That is the dashed blue curve shown in Figure A1-2.

7. Generate a 15-minute time series of instantaneous deviations from the 24-hour moving average, calculated as $Q'_{Jensen}(t) = Q_{Sum,upper}(t) - Q_{Sum,upper,24}(t)$. (This is the blue curve shown in Figure A1-4).
8. Identify all the locations in the time series where $Q'_{Jensen}(t)$ changes sign from negative to positive or positive to negative. These are known as the crossover positions, and define the limits of each half-wave shown in Figure A1-3.
9. Identify $|Q'_{max,Jensen}|$ between each of the crossover positions.
10. Calculate the scaling factor K_{wave} for each half-wave according to Equation (3).
11. Generate a 15-minute time series of $Q'_{Ouray}(t) = K_{wave} Q'_{Jensen}(t)$.
12. Determine the 24-hour moving average of discharge for the Ouray gage station:
 - a. If the time associated with the Jensen wave is between June 15 and August 31, then $Q_{Ouray,24}(t) = Q_{Sum,upper,24}(t) - 200$ cfs.
 - b. If the time associated with the Jensen wave is between September 1 and the end of the year, then $Q_{Ouray,24}(t) = Q_{Sum,upper,24}(t)$.
13. Finally, calculate the time series of flow at Ouray: $Q_{Ouray}(t) = Q_{Ouray,24}(t) + Q'_{Ouray}(t)$.

Examples of the results of the procedure are shown in Figures A1-12 and A1-13. Figure A1-12 shows an Ouray discharge time series calculated using 2012 Jensen data; it provides direct comparison with actual Ouray gage station data to ensure expected results of the algorithm. Figure A1-13 shows the results for a time series in 2005, when Ouray gage station data does not exist.

A1.3 TIME LAG ANALYSIS

The goal of the wave transformation effort was to be able to generate a synthetic discharge record for the Ouray gaging station during the time period before it went into operation. To calibrate the wave scaling, the Ouray daily waves were directly overlain onto the Jensen daily waves during the period when both gaging stations were in operation (May 2009 to present). Putting the waves on the same time datum for the direct overlay required the Ouray waves be “unlagged,” or shifted backwards in time.

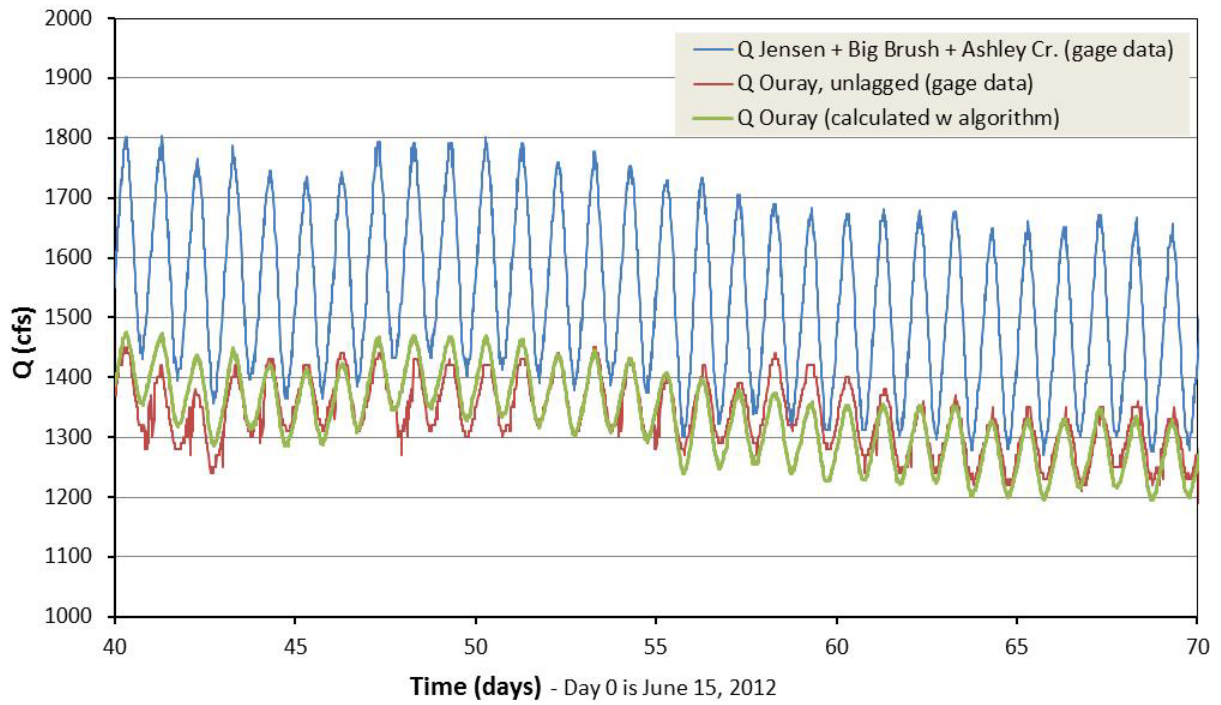


FIGURE A1-12 Demonstration of the Algorithm Results Using 2012 Data

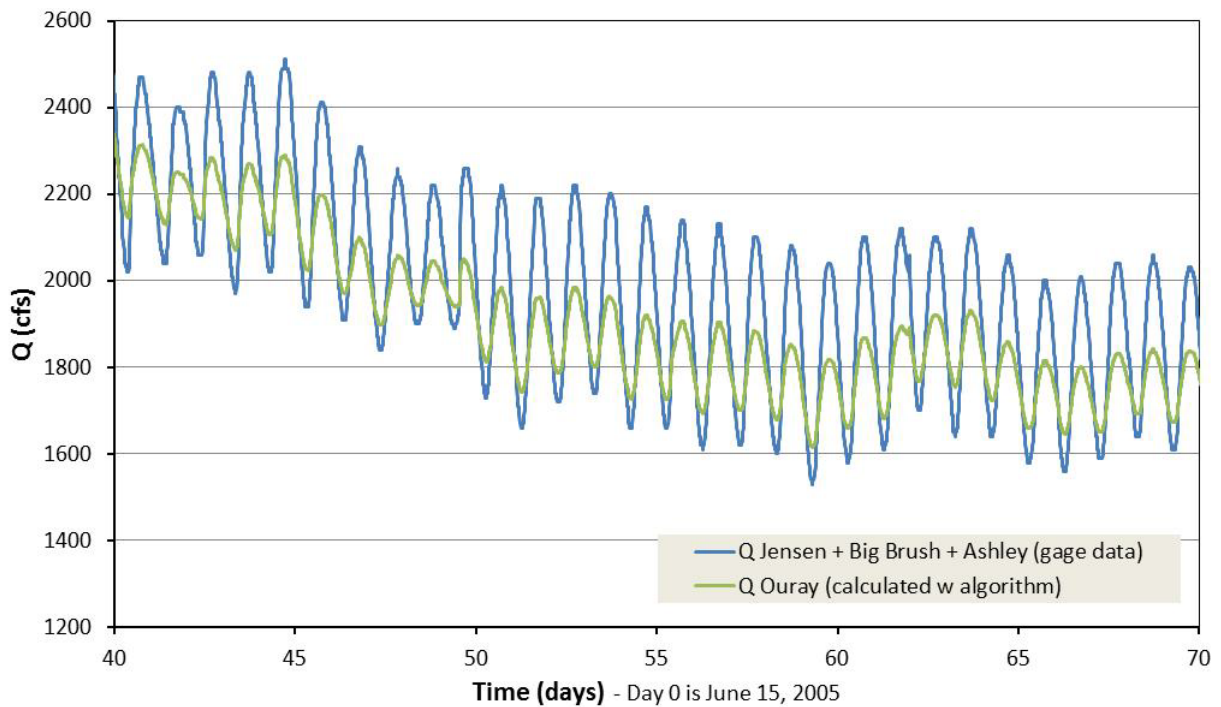


FIGURE A1-13 Illustration of the Time Series Produced for Q_{Ouray} before the Gage Station Went into Operation

The algorithm developed for wave scaling (Section A1.1.2) generated an unlagged synthetic Ouray discharge record on the same time datum as the Jensen discharge record. Therefore, the final step in generating a synthetic discharge record for the Ouray gage station is to properly “lag” the synthetic Ouray waves, or shift them forward in time to account for the wave travel time between the two gage stations. This section describes the method that was used for the time lag.

A1.3.1 Theoretical Considerations

The time lag between Jensen and Ouray in its simplest conceptual form is the distance between the two stations divided by the mean velocity of wave propagation (known as the “wave celerity”). The distance between the two stations is known, and so the relevant variable in the analysis is the wave celerity (c). The time lag is intended to be determined empirically, but the best empirical correlations can be expected by using variables that theoretically determine c .

Kinematic waves are gradually varying waves typical of natural flood events where the gradient of the stream is the primary driving force in the momentum equation; in other words, the gravitational force is much larger than the pressure gradient that is caused by the different water depths that exist in the longitudinal direction within the wave. A kinematic wave in a uniform channel deforms as it propagates downstream; the peak shifts forward, but the magnitude of the peak does not change downstream and the wave does not appreciably lengthen. In the Green River between Jensen and Ouray, it has been demonstrated that the wave peak does subside considerably and the wave lengthens as it propagates downstream, and therefore the daily wave cannot be considered a kinematic wave in the strictest sense. Whether the observed wave deformation is dominated by modification of the water surface slope due to the wave form or by the nonuniformity of the channel geometry creating local backwater effects has not yet been determined. However, conceptually, the kinematic wave approach provides a reasonable basis for selecting variables for the proposed empirical correlation.

The peak is the portion of the kinematic wave that travels downstream the fastest, which is why the peak tends to shift downstream relative to the rest of the wave as it propagates. This makes Q_{max} the most important instantaneous discharge on the kinematic wave, and as such, the variable Q_{max} provides the best variable for correlation. Of secondary importance is the variable ΔQ , the maximum daily variation in discharge. Both variables are illustrated in Figure A1-14.

The secondary importance of the variable ΔQ in altering the water surface slope can be demonstrated using approximations of geometry, stage-discharge relationships, and typical discharge characteristics of the Green River in the study reach. The net channel gradient between the Jensen gage station and the Ouray gage station from the profile in Rakowski (1997) is approximately 0.00028. This slope generates the primary gravitational driving force; under the approximation of locally uniform flow, the water surface slope is approximately equal to the net channel gradient. A deviation from the locally uniform flow slope is associated with the form of the wave front (along with any local backwater effects associated with non-uniform geometry). The steepest configuration of a wave front of fixed period occurs when velocity is low. Assuming a low mean velocity of 1 foot per second and a 12-hour time span between peak and

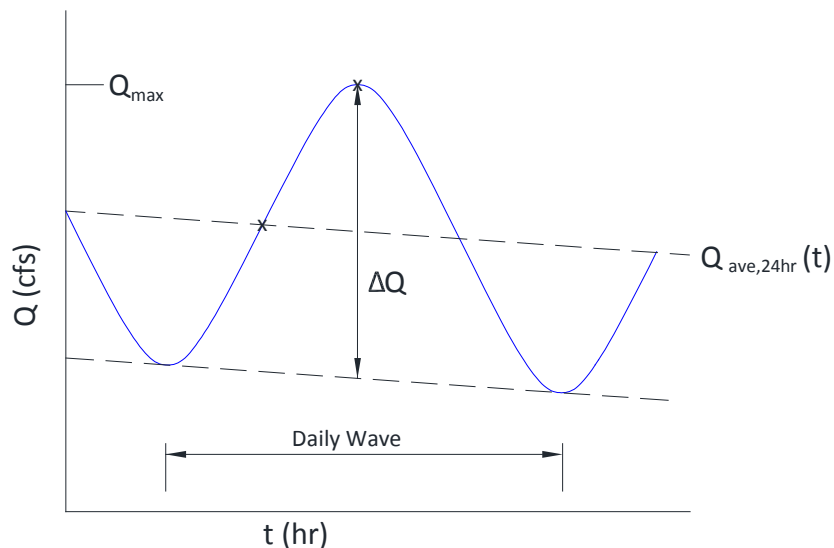


FIGURE A1-14 Sketch of Variables Used to Describe the Daily Wave

trough, the distance of the trough downstream of the peak is 43,200 feet. The elevation difference associated with the mean bed slope over the 43,200 feet is approximately 12.1 feet. For the wave-form-induced slope to double the water surface slope relative to the locally uniform condition, the flow stage associated with the peak discharge would need to be 12.1 feet higher than the flow stage associated with the trough discharge; for the wave-form induced slope to add even 10% to the water surface slope would require a stage difference of 1.2 feet between peak and trough. Under normal dam operating procedures, the daily stage differences associated with peaks and troughs observed at Jensen are considerably less than 1 foot, so ΔQ is clearly of secondary importance in terms of altering water surface slope downstream of Jensen; this provides some justification for using a kinematic wave approach.

The term ΔQ also alters the propagation velocity (celerity) of a kinematic wave even in the absence of significant effects on water surface slope. Based on derivations using only a mass conservation equation, the celerity of the wave will always exceed the steady uniform flow velocity calculated from Q_{max} . In a wave that does not deform as it propagates down a channel of uniform width, the celerity is proportional to $\Delta Q/\Delta H$ where ΔH is the change in stage associated with the peak and trough. However, assuming that the wave can deform, the celerity of any given discharge on the wave is equal to the local value:

$$c_k = \frac{1}{B} \frac{dQ}{dH}, \quad (6)$$

where c_k is the celerity of any discharge on the kinematic wave; the subscript k indicates that this form is valid only for a kinematic wave. The full derivation of Equation (6) can be found in Henderson (1966) and Chow et al. (1988). The relationship dQ/dh can be readily obtained from a stage-discharge relationship, but it is known that dQ/dh always increases with stage in a natural channel. Therefore the maximum value of c_k will be at the peak of the wave.

Despite complicating factors such as wave celerity that exceeds the calculated steady uniform flow velocity of the peak discharge and Q_{max} that subsides in the downstream direction, an interesting result is found in the results of Belarde (2012). A relationship between the Jensen to Ouray time lag (t_{lag}) and Q_{max} as measured at Jensen was found to take the following form:

$$t_{lag} = AQ^{-0.323}, \quad (7)$$

where A is an empirical coefficient that depends on the units of Q . (Note that Q in Equation [7] was not explicitly stated to be Q_{max} , but it appears to be the variable used in the correlation to calculate the time lags.) This result is interesting because a form almost identical to Equation (7) can be arrived at on theoretical grounds based on the assumption of steady uniform flow (i.e., a flat hydrograph with no wave form). The derivation is as follows. The momentum balance for locally uniform flow in a wide shallow rectangular channel yields:

$$U^2 = \frac{gHS}{C_f}, \quad (8)$$

where U is the cross-sectional average mean flow velocity, g is the gravitational acceleration constant, H is the flow depth, S is the water surface slope (equal to the bed slope), and C_f is a dimensionless friction coefficient. Equation (8) is of the same form as the commonly used Chezy formula for open channel flow. If a constant net channel gradient and a flow depth-invariant friction coefficient are assumed, then Equation (8) can be re-expressed as follows:

$$U^2 = K_1 H, \quad (9)$$

where K_1 is a constant obtained from a multiplication of the other constants (i.e., $K_1 = gS/C_f$). In the simple case of the wide shallow rectangular channel considered,

$$Q = UBH, \quad (10)$$

where B is the channel width, assumed to be a constant in the downstream direction. Combining Equations (9) and (10) yields the following:

$$U^2 = K_1 \frac{Q}{UB} = K_2 \frac{Q}{U}, \quad (11)$$

where K_2 is a constant equal to K_1/B . Therefore, from Equation (11):

$$U^3 = K_2 Q, \quad (12)$$

$$U = K_3 Q^{1/3}, \quad (13)$$

where K_3 is a constant that is equal to K_2 to the power 1/3. The travel time between two points can be expressed as follows:

$$t_{lag} = \frac{L}{U}, \quad (14)$$

where L is the longitudinal distance between Jensen and Ouray, which is a constant. Combining Equations (13) and (14) yields the following:

$$t_{lag} = \frac{L}{K_3 Q^{1/3}} = K_4 Q^{-1/3}, \quad (15)$$

where K_4 is a constant equal to L/K_3 . Note that this is almost precisely the form of Equation (7) from Belarde (2012), which was determined empirically. Such a formulation is well suited to a steady uniform flow, but it is not immediately evident that it should apply to the case of wave propagation. The two primary complicating factors in the wave propagation problem are: (1) the wave celerity is known to be greater than the value of U calculated based on an assumption of locally uniform flow from Equation (7); and (2) the value of Q used in the analysis (Q_{max} at Jensen) is known to decrease in the downstream direction such that the wave celerity c_k also continually varies in the downstream direction. Regarding issue 1, Equation (6) can be used to show that c_k is directly proportional to U calculated from the assumption of locally uniform flow:

$$c_k = \frac{1}{B} \frac{dQ}{dH} = \frac{1}{B} \frac{d}{dH} (UBH) = \frac{B}{B} \frac{d}{dH} (UH) = \frac{d}{dH} \left(\sqrt{\frac{gHS}{c_f}} H \right) = \sqrt{\frac{gS}{c_f}} \frac{d}{dH} (H^{3/2}) = \frac{3}{2} \sqrt{\frac{gHS}{c_f}} = \frac{3}{2} U. \quad (16)$$

Substituting Equation (13):

$$c_k = \frac{3}{2} K_3 Q^{1/3} = K_5 Q^{1/3}, \quad (17)$$

where K_5 is a new coefficient equal to $3/2 K_3$. The wave celerity c_k is the relevant velocity to use in Equation (14):

$$t_{lag} = \frac{L}{K_5 Q^{1/3}} = K_6 Q^{-1/3}. \quad (18)$$

Therefore, assuming that the wave celerity calculated from Q_{max} at Jensen remains constant in the downstream direction, we again get the form of Belarde (2012), just with a different constant. Now let us consider issue 2 regarding the variation of Q_{max} (and thus c_k) in the downstream direction. It is difficult to specify a functional form for the variation of Q_{max} in the downstream direction based solely on the mathematics of the dynamic wave equations. (Note that the dynamic wave equations take into account the backwater effects neglected in the kinematic wave approach.) As a first-order approximation, we may consider an exponential decay of Q_{max} :

$$\frac{dQ}{dx} = k_d Q, \quad (19)$$

where k_d is a decay rate that is negative. It is convenient to assume the decay rate is constant regardless of the magnitude of the daily wave peak discharge observed at Jensen. It was shown in Figure A1-10 that the decay rate is actually dependent on the daily variation in discharge ΔQ ; however, an analysis of the dependence on Q_{max} has not been performed. The simplified

assumption of constant decay rate is appropriate for the first-order approach herein. The solution of Equation (19) is as follows:

$$Q(x) = Q_{Jen} e^{k_d x}, \quad (20)$$

where Q_{Jen} is the peak of the daily wave measured at Jensen. The mean velocity (celerity) between Jensen and Ouray is obtained by integrating the varying c_k over the entire length:

$$c_{k,Ave} = \frac{1}{L} \int_{x_{Jensen}}^{x_{Ouray}} c_k(x) dx, \quad (21)$$

where $c_{k,Ave}$ represents the reach-averaged wave celerity; x_{Jensen} represents a downstream distance from some arbitrary reference point to Jensen, and x_{Ouray} represents a downstream distance from the same reference point to Ouray. For convenience, the longitudinal reference point will be considered to be the Jensen gage station such that $x_{Jensen} = 0$ and $x_{Ouray} = L$. Therefore:

$$c_{k,Ave} = \frac{1}{L} \int_0^L (K_5 Q(x)^{1/3}) dx = \frac{K_5}{L} \int_0^L (Q_{Jen} e^{k_d x})^{1/3} dx = \frac{3}{k_d} \frac{K_5}{L} Q_{Jen}^{1/3} [e^{k_d x/3}]_0^L. \quad (22)$$

The term in brackets is simply a constant that can be calculated and then lumped by multiplication with the other constant terms in front of $Q_{Jen}^{1/3}$ as follows:

$$c_{k,Ave} = K_7 Q_{Jen}^{1/3}. \quad (23)$$

Therefore, using the reach-averaged $c_{k,Ave}$ that takes into account the continual reduction in Q_{max} in the downstream direction as the relevant velocity term in Equation (14):

$$t_{lag} = \frac{L}{K_7 Q_{Jen}^{1/3}} = K_8 Q_{Jen}^{-1/3}. \quad (24)$$

Therefore, the basic form obtained by Belarde (2012) would appear to have a theoretical basis even in the case of a daily wave whose peak subsides in the downstream direction. It should be noted that many assumptions were made in this analysis, most importantly that the daily wave propagates as a kinematic wave. Strictly speaking, this is not true because local backwater effects associated with variable channel cross geometry cause the wave peak to subside and cause the wave to significantly broaden in the downstream direction.

A1.3.2 Empirical Analysis and Discussion

The time lags were calculated using the actual discharge records from the Jensen and Ouray gage stations; in other words, the synthetic hydrographs were not used in the time lag determination. Time lags were calculated using the wave “crossover” position illustrated with an “x” in Figure A1-14; the crossover is where the instantaneous discharge crosses the 24-hour moving average ($Q_{ave,24hr}$) on the rising limb of the hydrograph. The reason the crossover position was used rather than the peak or trough location was that the high instantaneous rate of

change of discharge in this part of the daily wave allows a discrete position to be clearly identified; at the peak and trough where the instantaneous rates of change are low, a discrete point is much less distinct and therefore introduces the potential for additional error. Because the wave shape at Jensen scales nearly exactly with the wave shape at Ouray, the specific portion of the wave selected for identification is not important; it is only important that the same position can be clearly identified on both waves. The time lag (t_{lag}) is calculated as the crossover time identified on the Ouray daily wave subtracted from the crossover time on the corresponding Jensen wave.

Data was used during the period containing a record from both gage stations (May 2009 to December 2012); discharges from all times of the year were used, provided that well-defined daily waves existed. Data points for each wave were compiled in the form (Q_{max}, t_{lag}) , where Q_{max} is the peak of the daily wave as measured at Jensen. The plot of all the data points is shown in Figure A1-15.

The best fit shown in Figure A1-15 is a power law, expressed as Equation (19A):

$$t_{lag} = 292.42Q_{max}^{-0.2674}, \quad (25)$$

where t_{lag} is in hours and Q_{max} is in cubic feet per second. The r^2 value of the best-fit curve shown in Figure A1-16 is 0.824. The differences between Equation (25) here and Equation (2) from Belarde (2012) are minor; evaluating the curves in the range of Q_{max} between 1000 and

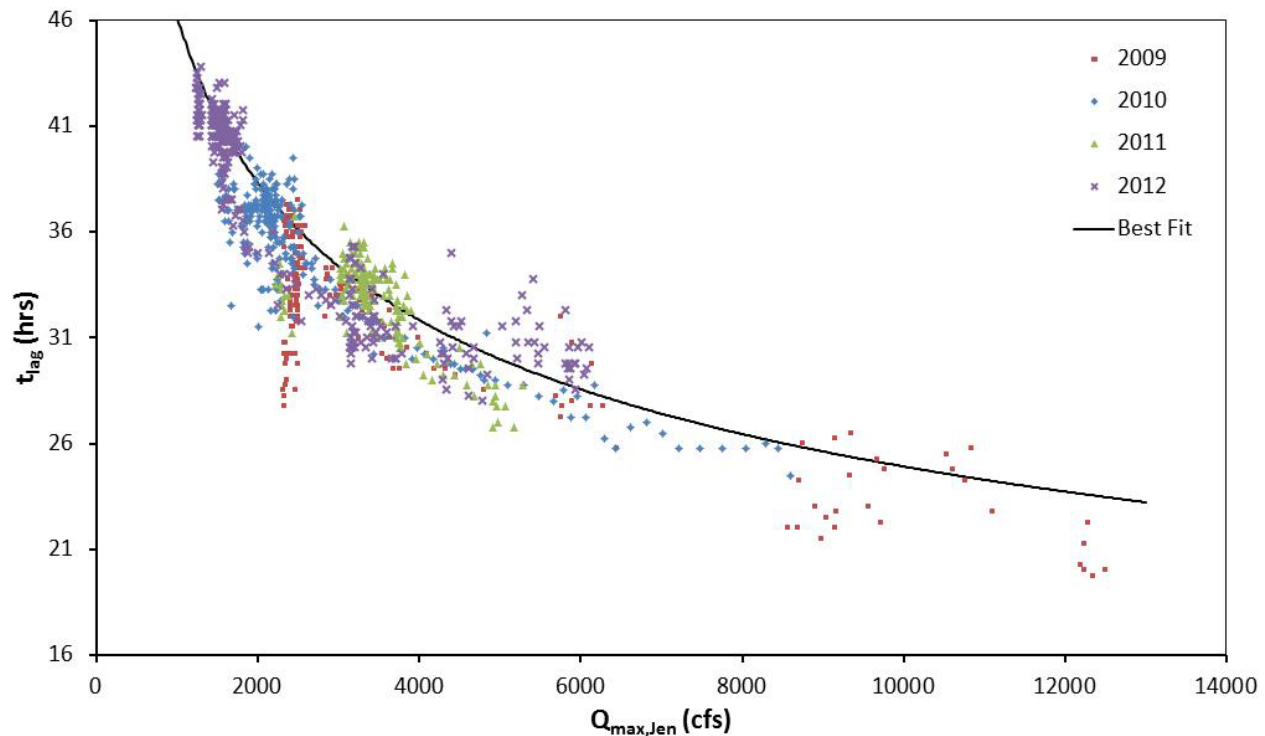


FIGURE A1-15 Data Used in Developing the Time Lag Function for Daily Waves

12,000 cfs, the maximum deviation in the predicted time lag from the two formulations is 2.3 hours.

The substantial scatter of the data points in Figure A1-15 is somewhat troublesome; at any given magnitude of discharge for which there is a large number of data points, the time lag commonly varies by 8 hours or more. The scatter is probably not a result of an insufficient dataset whose quality will improve with time. The scatter may be explained on the basis of a number of physical factors. One potential cause is that t_{lag} is primarily related to Q_{max} , but is secondarily influenced by ΔQ , as described previously in this document. An effort was made to stratify the data points on Figure A-15 according to ΔQ , but no clear trend was evident. Another potential cause of scatter is the varying magnitude of flow extraction between Jensen and Ouray throughout the year; because only Q_{max} recorded at Jensen is used in the correlation, any flow extraction effects are not included. The mean wave celerity between Jensen and Ouray determined by integration in Equation (22) will certainly be affected by significant flow extraction. The primary factor causing the scatter is probably the geometric changes in the dynamic sand bed throughout the year. During the spring high flow season, constrictions tend to scour and the thalweg of the river tends to change its configuration (see the cross-sections in Rakowski 1997). During the tail of the spring high flow hydrograph and extending into the base-flow season, the areas that originally scoured will tend to infill. The high flow season also leaves behind large dunes scaled to the depth of the high discharge that gradually become reworked to the scale of the shallower flow depth. The thalweg may also readjust during this time period. The varying configuration of the bed influences cross-sectional areas that dictate the local backwater effects present in any non-uniform channel; it also significantly influences the roughness experienced by the flow (high roughness equates to lower mean velocities). Because of these somewhat continual changes in the dynamic sand bed, the scatter will likely continue to be observed as the discharge record for comparison gets longer.

A1.3.3 Algorithm for Time Lagging the Unlagged Ouray Synthetic Daily Waves

The time-lag algorithm is fairly simple. The synthetic Ouray daily waves as illustrated in Figures A1-12 and A1-13 are treated individually; each daily wave is defined to extend from trough to trough. The peak discharge of the corresponding Jensen daily wave (Q_{max}) is identified; using that Q_{max} value, the time lag (t_{lag}) is calculated from Equation (25). The entire synthetic Ouray daily wave is then moved forward in time by that amount.

The only moderately complicating factor occurs when consecutive daily waves have considerably different values of t_{lag} . This results in either a gap between consecutive waves or an overlap between consecutive waves on the lagged timeline. The case of a gap is resolved by linearly interpolating between the end points bounding the gap in the timeline. The case of the overlap is resolved by finding the location of the intersection between the two wave tails on the lagged timeline, and truncating the tails beyond the intersection. This approach for dealing with gaps and overlaps is only a rough approximation, because filling in a gap effectively adds flow volume and truncating the tails eliminates flow volume (i.e., mass conservation is not achieved). The gaps and overlaps were generally of limited extent, so the simplified methods introduce minimal error.

A1.4 BACKWATER STAGE-DISCHARGE RELATIONSHIPS PRIOR TO 2009

With the synthetic hydrographs (time series of discharge) generated for the backwater reach described in Section A1.1.2 and A1.1.3, the final relationship needed for the backwater analysis is a stage-discharge relationship at the backwater sites. A stage-discharge relationship determined for a cross section is commonly referred to as a rating curve. Such relationships require field measurements of a range of discharges and the associated stages; even if a hydraulic model is used, such data is necessary for model calibration. Typically, such field data only exists at USGS gage stations. The hydraulics at a gage station generally cannot be considered exactly representative of an entire river reach. Site-specific factors such as the downstream hydraulic control, the position within a pool-riffle sequence, and the position with respect to natural channel width variations may result in different hydraulic behavior at the gage station site than at other nearby sections of the river. However, in the absence of site-specific measurement data, using the relationship obtained from a gage station is the soundest alternative. The gage station selected should be the one that most accurately represents the channel geometry (width, depth, longitudinal slope, hydraulic control, etc.) in the reach of concern. The two closest gage stations to the backwater sites are the Ouray gage station (09272400) and the Jensen gage station (09261000). The Ouray gage station is in a geomorphic setting more similar to the backwater sites than the Jensen gage station. However, the Ouray gage station was not present prior to 2009. The issue addressed in this section is whether the Ouray rating curves or Jensen rating curves should be used to represent local rating curves at the backwater sites in the years prior to 2009.

The Ouray gage station (09272400) is new. It began operation in May 2009, and its rating curve is being refined as more field measurements are obtained by the USGS. The rating curves are based on a total of 33 field measurements by the USGS between May 26, 2009, and the date the rating curve analysis was completed (January 2013). Three rating curves were used at the Ouray gage station. Modified rating curve shapes appear to be based more on an improved dataset than on changing channel hydraulics. For example, at the low end of Q , the curve is expected to be at its steepest, and then to become less steep with increasing Q . The flatness of rating curve 1 (see Figure A1-16) at low Q appears to be an artifact of the curve fit based on limited data points; the actual field measurements from that time period suggest a steeper configuration in the region between 1000 and 3000 cfs than rating curve 1 suggests.

Based on the limited period of operation and continued refinement of the Ouray rating curves, the most recent rating curve (rating curve 3) appears to be the most accurate representation of the shape of the stage-discharge relationship in the vicinity of the Ouray gage station.

The Jensen gage station (09261000) is located approximately 61 river miles upstream from the Ouray gage; it has been in operation since 1946. The USGS reports 400 field measurements between 1958 and the present. Changes in the rating curve at this station in recent years are more likely to be the result of changes in hydraulic conditions rather than an artifact of curve-fitting. Four rating curve equations have been generated by the USGS since the first backwater survey in 2002. The curves are shown in Figure A1-17.

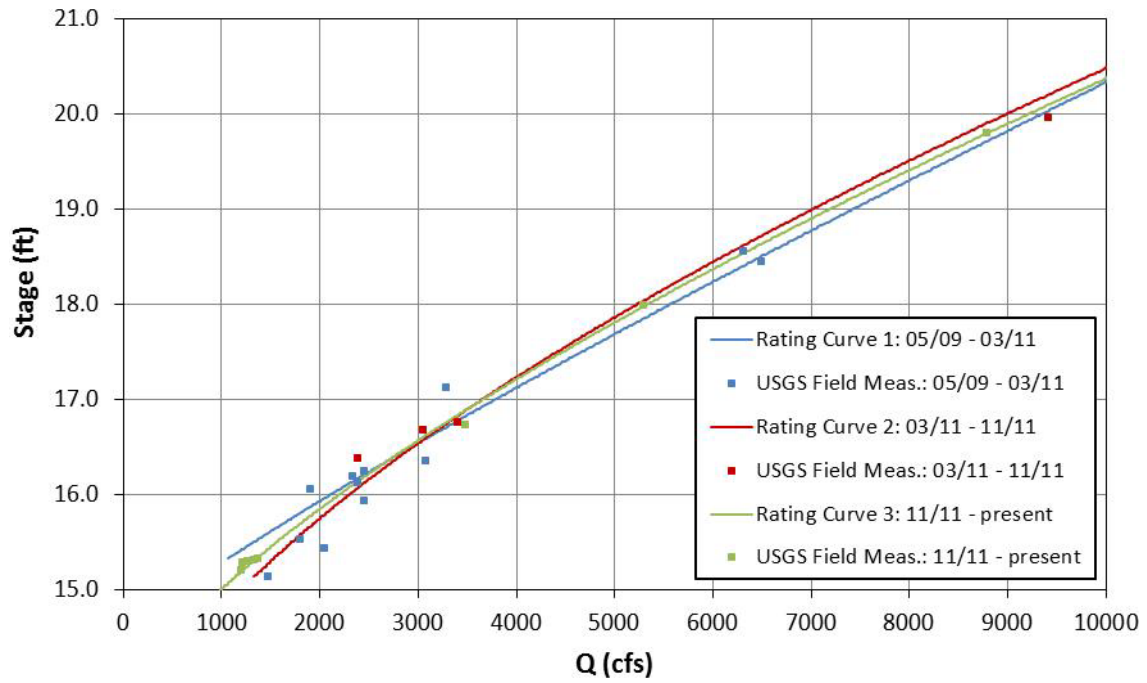


FIGURE A1-16 USGS Rating Curves and Field Measurements at the Ouray Gage in the Low-*Q* Region

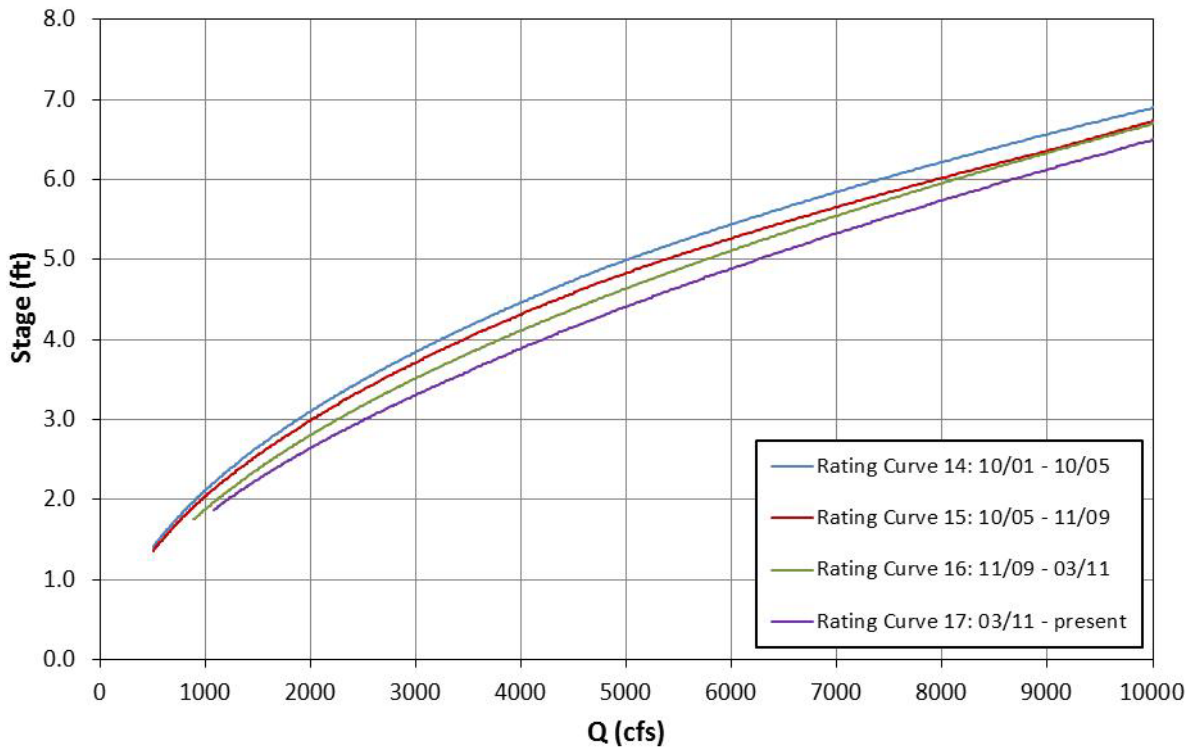


FIGURE A1-17 USGS Rating Curves at the Jensen Gage in the Low-*Q* Region

As is evident in Figure A1-17, there has been a systematic decrease in stage at this gage station since 2001. The reason for this is unknown. What is important to the question at hand is the shape of the rating curves rather than the actual values, because a dynamic datum rather than an absolute datum is used at the backwater sites to set the reference stage and discharge. If we set the stage at $Q = 1360$ cfs equal to 1 ft as a dynamic datum, then the shapes of the curves can be more directly compared. ($Q = 1360$ cfs is chosen because it is the lowest value of Q with a discrete value on each of the Jensen and Ouray rating curves being evaluated.) Collapsing the data in this manner allows isolation of the curves' shapes. The curves relative to the dynamic datum are illustrated in Figure A1-18. The Ouray stage-discharge relationship is then readily compared to the Jensen curves using the same dynamic datum; the most recent curve (rating curve 3) for the Ouray gage was determined to be the most accurate, so it is overlaid on the Jensen curves for comparison.

Figure A1-18 illustrates that the slope of the Ouray rating curve does not decrease with increasing Q as rapidly as the rating curve at the Jensen gage. Nevertheless, in the region below $Q = 5000$ cfs, the Ouray curve lies within the scatter of the various Jensen curves. If we assumed that both the Jensen curves and the Ouray curve are 100% accurate (which actually they are not), then at $Q = 5000$ cfs there is a maximum error of 0.19 ft, or about only 8% error (the estimated value of $\Delta Stage = 2.29$ ft relative to the stage at $Q = 1360$ cfs from Jensen rating curve 17), which is within acceptable limits. If we were to use the Ouray rating curve back into the pre-2009 period rather than a Jensen rating curve, this would assume that the current Ouray rating curve represents past conditions to within 8% error.

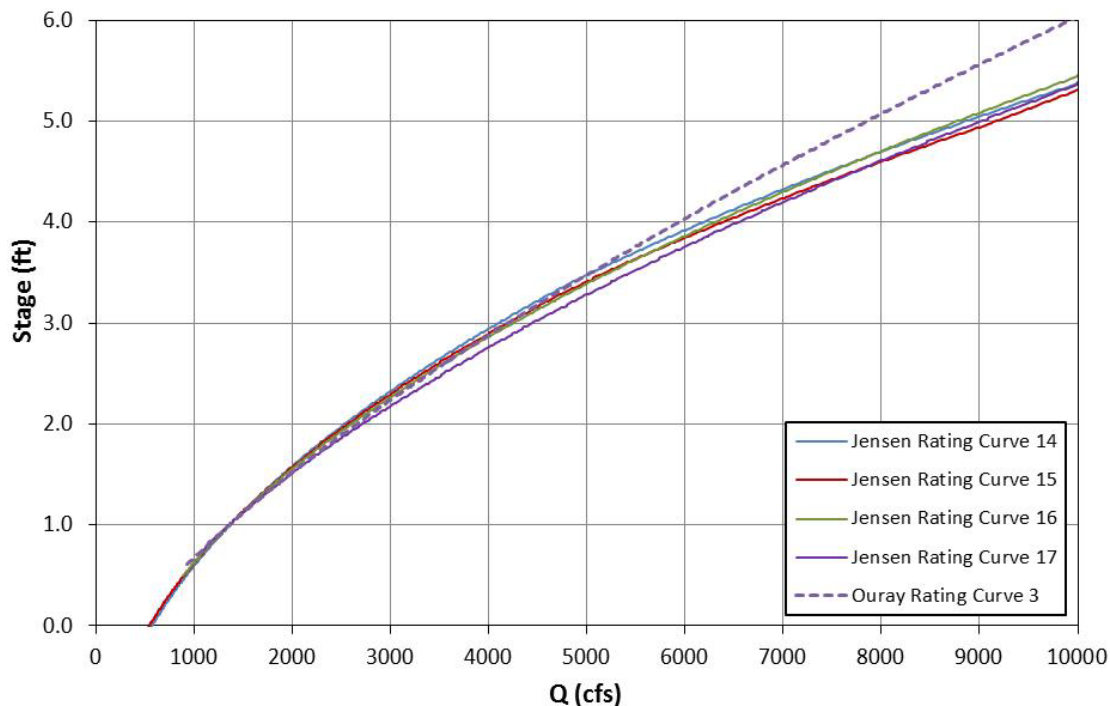


FIGURE A1-18 Jensen Rating Curves Based on a Dynamic Dataset at $Q = 1,360$ cfs, Stage = 1 ft; Ouray Rating Curve 3 Is Shown Based on the Same Dynamic Data

In general, below $Q = 5000$ cfs, the Jensen and Ouray rating curves are very similar (Figure A1-17). Thus, using either the most recent Ouray rating curve or an older Jensen rating curve would represent hydraulics within the backwater reach reasonably well, even during the period prior to 2009. Above $Q = 5000$ cfs, the Jensen curves deviate far enough from the Ouray curves that a more recent Ouray rating curve appears to be a more suitable choice than using an older Jensen rating curve to represent the hydraulics of the Ouray reach prior to 2009.

A1.5 REFERENCES

- Belarde, T.A., 2012, *Evaluating Cumulative Effects of Within-Day Flow Fluctuations and Presence of Non-native Species on Age-0 Colorado Pikeminnow (*Ptychocheilus lucius*) in Nursery Habitats of the Green River (Utah)*. Master's thesis, Humboldt State University, Arcata, California.
- Chow, V.T., Maidment, D.R., and Mays, L.W., 1988, *Applied Hydrology*. McGraw-Hill, Inc., New York, New York.
- Henderson, F.M., 1966, *Open Channel Flow*. The MacMillan Company, New York, New York.
- Rakowski, C.L., 1997, *The Geomorphic Basis of Colorado Squawfish Nursery Habitat in the Green River near Ouray, Utah*. Master's thesis, Utah State University, Logan, Utah.

APPENDIX 2

**THE AUTONOMOUS BACKWATER IDENTIFICATION SYSTEM (ABIS):
MODELING THE RELATIONSHIP BETWEEN GREEN RIVER FLOWS AND
BACKWATER PHYSICAL CHARACTERISTICS FROM 2003–2013**

This page is intentionally left blank.

APPENDIX 2

THE AUTONOMOUS BACKWATER IDENTIFICATION SYSTEM (ABIS): MODELING THE RELATIONSHIP BETWEEN GREEN RIVER FLOWS AND BACKWATER PHYSICAL CHARACTERISTICS FROM 2003–2013

The Autonomous Backwater Identification System (ABIS) determines the effect of flow on backwater habitat characteristics by evaluating the effects of incremental stage changes on these characteristics. Within the 8-bit integer grid, stage changes correspond to incremental changes in integer pixel values (scale: 0–255). To utilize the 8-bit integer grid for modeling the effects of stage change on backwater habitat availability, a relationship needed to be established between the scales of the continuous and 8-bit grids. This relationship between grid scales was established using the following equation:

$$\text{Scale}_{bit} = (\text{FloatGrid}_{max} - \text{FloatGrid}_{min})/256 \quad (1)$$

where

- Scale_{bit} , expressed in the measured elevation units (e.g., meters), represents the actual (continuous) stage change corresponding to an incremental stage change in the 8-bit grid;
- FloatGrid_{max} represents the maximum estimated elevation from the floating point elevation grid; and
- FloatGrid_{min} represents the minimum estimated elevation from the floating point elevation grid.

The difference between $\text{FloatGrid}_{max} - \text{FloatGrid}_{min}$ is then divided by the range of possible 8-bit integer values to calculate the incremental stage change for each increment in 8-bit value. For example, a Scale_{bit} value of 0.05 m means that each 8-bit value corresponds to a 0.05 m (5 cm) stage. To relate 1-m² pixel values in the continuous elevation grid to those in the 8-bit integer grid, the Scale_{bit} value is used to establish a linear relationship between the two grids:

$$\text{Bit}_s = (\text{Elevation}_s - \text{FloatGrid}_{min})/\text{Scale}_{bit} \quad (2)$$

where

- Bit_s is the pixel value (rounded to the nearest integer) of the 8-bit integer grid at the relative water elevation stage s ;
- Elevation_s is the measurable elevation (e.g. meters) at water elevation stage s ;
- FloatGrid_{min} is the minimum elevation estimated in the continuous elevation grid; and

- $Scale_{bit}$ represents the actual (continuous) stage change corresponding to an incremental stage change in the 8-bit integer grid (see Equation 1).

Stage s refers to a standardized measurable stage (e.g., meters) of the water surface relative to the stage at the time of survey ($s = 0.00$ at this reference stage). At the reference stage, Bit_s is calculated using the average of shoreline elevation measurements as the $Elevation_s$ value. The $Scale_{bit}$ value and Bit_s value that correspond to the reference stage are shown in Table A2-1.

Incremental relative stage changes are $\pm 1 Scale_{bit}$ above and below the reference stage. Therefore, after the correct bit-value has been determined for the reference stage, incremental bit values may be assigned to determine relative stages above and below the reference stage. Similarly, given the appropriate bit-value for the reference stage, the entire range of water elevations ($Elevation_s$) at each stage (s) for the entire 8-bit scale (0–255) were calculated by incrementally adding or subtracting the $Scale_{bit}$ value from the water elevation at the reference stage.

Table A2-2 provides an example of the stage characteristics (including flows) for the reference stage and three incremental stages above and below the reference stage. Predicted backwater physical characteristics, as output from ABIS, were associated with stage measurements and local flow estimates to complete the stage tables. As described below, the stage tables were then used to create graphical illustrations to understand the relationship between flow and predicted backwater physical characteristics (Figure A2-1).

Using the DEM, for each stage between 0 and 255, ABIS sequentially connected contiguous shoreline points (defined for each stage as points just above the waterline), ultimately forming a polygon. The polygon was mathematically defined as being a backwater when the area inside the backwater polygon was greater than:

$$((d_{mouth}/2)^2 \times \pi)/2 \quad (3)$$

where d_{mouth} is the diameter of the mouth of the polygon. The minimum connection size threshold between the backwater and the main channel was 1 m, which is the minimum cell size used in the ABIS calculations. Using this automated algorithm, the stage tables generated by ABIS show predicted backwater surface area (m^2), volume (m^3), maximum depth (m), and mean depth (m) at each incremental ABIS stage. As shown in Table 5 in the main body of this report, predictions at each ABIS stage (bit-value) were then associated with measurable stage changes and local flow conditions.

There were certain assumptions associated with applying ABIS to the study reach. First, the most important assumption used in the development of local rating curves at each backwater survey site for use in ABIS is that the shape of the rating curve at the Ouray gage station is also valid for each of the survey sites and across survey years. Part of the reason for assuming the rating curve to be valid throughout years and throughout the river is the inability to obtain a more accurate estimate of local ratings in the absence of establishing a makeshift stage gage at each backwater site, along with collecting and analyzing data obtained throughout the base-flow

TABLE A2-1 Reference Stage Characteristics for Backwater Locations Surveyed between 2003 and 2013

Year	Date	Backwater	Water Elevation (m) ^a	Estimated Local Flow (cfs) ^b	Scale _{bit} (m) ^c	8-Bit Pixel Value (Bit) _s ^d
2003	8/19/2003	BW01	1416.19	867	0.013	88
2003	8/20/2003	BW02	1424.68	872	0.012	117
2003	8/20/2003	BW03	1424.59	869	0.005	93
2003	8/20/2003	BW04	1422.52	868	0.007	107
2003	8/21/2003	BW05	1426.59	865	0.007	107
2003	8/21/2003	BW06	1424.31	865	0.016	154
2004	9/28/2004	BW01	1419.40	1789	0.007	134
2004	9/28/2004	BW02	1420.01	1789	0.011	55
2004	9/29/2004	BW06	1421.35	1729	0.025	26
2004	9/30/2004	BW07	1422.26	1689	0.018	44
2005	9/27/2005	BW02	1419.76	1879	0.016	104
2005	9/28/2005	BW05	1421.65	1839	0.004	131
2005	9/29/2005	BW07	1422.21	1919	0.008	105
2005	9/29/2005	BW08	1420.11	1869	0.008	145
2006	9/28/2006	BW02	1419.88	1659	0.018	125
2006	9/27/2006	BW06	1421.49	1639	0.012	127
2006	9/26/2006	BW07	1422.16	1519	0.011	99
2006	9/27/2006	BW13	1421.49	1639	0.010	91
2008	10/7/2008	BW02	1420.00	1959	0.015	86
2008	10/8/2008	BW03	1421.20	1909	0.018	89
2008	10/7/2008	BW07	1422.28	1969	0.008	75
2008	10/9/2008	BW09	1420.18	1839	0.013	60
2008	10/9/2008	BW10	1420.82	1839	0.015	80
2008	10/8/2008	BW13	1421.80	1919	0.010	80
2009	10/13/2009	BW02	1420.18	2209	0.017	112
2009	10/14/2009	BW06	1421.73	2199	0.012	125
2009	10/15/2009	BW07	1422.23	2139	0.017	153
2009	10/14/2009	BW08	1420.37	2169	0.011	53
2009	10/14/2009	BW10	1421.00	2209	0.016	103
2010	7/20/2010	BW02	1438.21	2578	0.013	93
2010	7/21/2010	BW05	1439.80	2468	0.015	69
2010	7/21/2010	BW06	1439.87	2478	0.010	87
2010	7/22/2010	BW07	1440.32	2468	0.017	91
2010	7/20/2010	BW08	1438.29	2529	0.014	105
2010	7/21/2010	BW10	1439.30	2468	0.016	98
2011	9/7/2011	BW02	1420.31	3328	0.015	112
2011	9/8/2011	BW05	1421.96	3288	0.020	113
2011	9/9/2011	BW07	1422.38	3338	0.016	85
2011	9/7/2011	BW08	1420.41	3298	0.013	65
2011	9/8/2011	BW10	1421.20	3358	0.023	151
2012	6/26/2012	BW02	1419.80	1459	0.017	86
2012	6/28/2012	BW05	1421.61	1419	0.016	59
2012	6/28/2012	BW07	1421.97	1369	0.020	101
2012	6/26/2012	BW08	1420.08	1509	0.025	150

TABLE A2-1 (Cont.)

Year	Date	Backwater	Water Elevation (m) ^a	Estimated Local Flow (cfs) ^b	Scale _{bit} (m) ^c	8-Bit Pixel Value (Bit _s) ^d
2012	6/27/2012	BW10	1420.69	1399	0.019	102
2013	9/10/2013	BW02	1419.84	1439	0.020	123
2013	9/11/2013	BW07	1421.98	1419	0.017	75
2013	9/10/2013	BW10	1420.68	1349	0.143	53
2013	9/12/2013	BW13	1421.75	1369	0.018	78
2013	9/11/2013	BW99	1422.15	1399	0.020	99

^a Water elevation was estimated as the average elevation of all shoreline measurements.

^b Local flow was estimated as the simulated (2003–2006, 2008) or actual (2009–2013) flow at the Ouray gage.

^c Scale_{bit} refers to the measured stage change (m) corresponding with a single incremental change in the 8-bit pixel value (see Equation 1).

^d The 8-bit pixel value at the reference stage, rounded to the nearest integer (see Equation 2).

TABLE A2-2 Example Stage Table for BW10 Surveyed on June 27, 2012^a

Elevation	Scale _{bit} (m) ^b	Relative Stage <i>s</i> (m) ^c	8-Bit Pixel Value (Bit _{<i>s</i>}) ^d	Flow- Related Stage (m) ^e	Estimated Local Flow (m ³ • s ⁻¹) ^f
1,420.635	0.019	-0.0567	99	4.628	1,189
1,420.654	0.019	-0.0378	100	4.647	1,249
1,420.673	0.019	-0.0189	101	4.666	1,319
1,420.692	0.019	0.0000	102	4.685	1,399
1,420.711	0.019	0.0189	103	4.704	1,469
1,420.730	0.019	0.0378	104	4.723	1,549
1,420.749	0.019	0.0567	105	4.741	1,619

^a The reference stage is highlighted and ± 3 stage increments are shown.

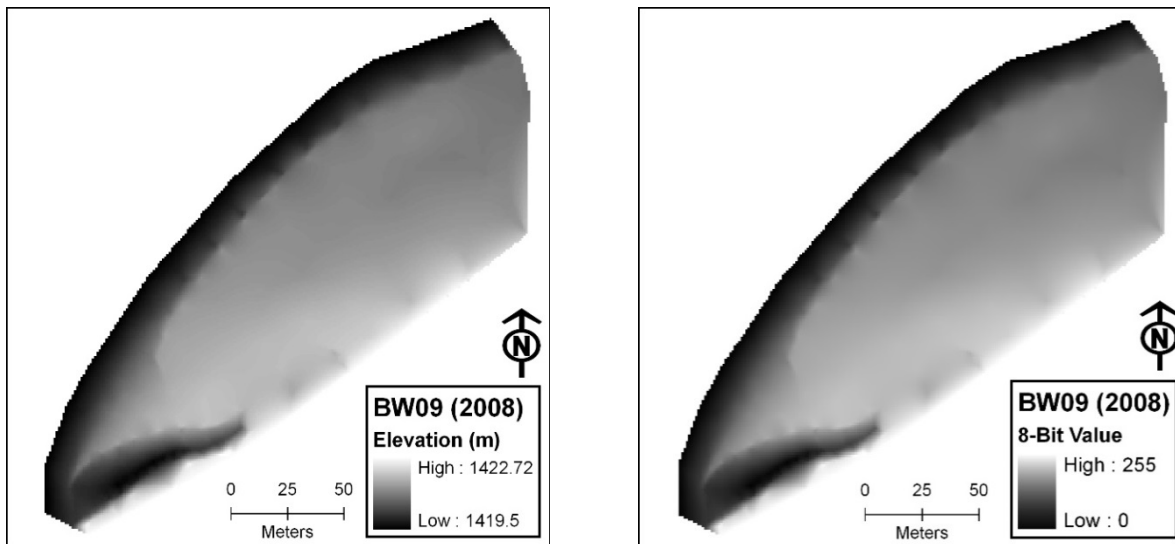
^b Scale_{bit} refers to the measured stage change (m) corresponding with a single incremental change in the 8-bit pixel value (Equation 1).

^c Relative stage (*s*) is the elevation of each stage change relative to the reference stage. At the reference stage, *s* = 0.00. Incremental relative stage changes are ± 1 Scale_{bit} above and below the reference stage.

^d Bit_{*s*} is the pixel value of the 8-bit grid, rounded to the nearest integer, at relative stage *s*. The 8-bit value increases and decreases incrementally from the reference stage by 1 bit value. At the reference stage, Bit_{*s*} is calculated according to Equation 2.

^e The flow-related stage (FRS), expressed in elevation units (e.g., meters), at the relative stage *s*. At the reference stage, FRS is the stage corresponding to the flow at the time of the survey based on stage-flow data collected at the Ouray gauge. The FRS for all other stages is offset incrementally by the Scale_{bit} value.

^f At the reference stage and all other stages above/below the reference stage, local flow values are the actual values at the Ouray gauge.



a) Continuous elevation grid for Backwater 9.

b) 8-bit integer grid for Backwater 9.

FIGURE A2-1 Development of the Elevation Grid Used as Input for ABIS. For (a) the survey measurements are interpolated to represent continuous estimated elevation values across the scene, and (b) the elevation grid is exported as an 8-bit integer grid for direct input into ABIS.

season. We recognize that this assumption can only be considered approximate; however, we also provide some justification below that, in an approximate sense, the assumption is valid.

During moderate and low flows, the dominant morphological feature that influences hydrodynamics in the river is a repeated sequence of transverse bars (diagonal bars), which yield a water surface profile best described as subdued pools and riffles. The “pools” are generated upstream of the transverse bar crests and the “riffles” are where the flow passes over the crest of the transverse bars. The backwater sites are generally at the upstream end of each pool where the transverse bars are attached to the banks. The transverse bars are formed and modified during the passage of the spring snowmelt flow event. Starting early in the base-flow season, the flow finds paths of least resistance and incises through submerged transverse bar crests and as the incision progresses with time, submerged bar crests are gradually reduced in elevation. Large dunes that are developed during high flows, especially in the pool areas, are also gradually planed down to smaller dimensions as they adjust to the lower base-flow magnitudes. Therefore, it is reasonable to expect a time-dependent stage-discharge relationship, particularly early in the season.

Despite these physical characteristics that can be expected to generate temporal variability in stage-discharge relationships, data obtained from the Ouray gage station do not indicate anomalies that are readily interpreted as signatures of time-dependence. Note that the Ouray gage station is positioned in a similar geomorphic setting as the remainder of the Ouray reach, where transverse bars are expected to be the dominant physical features that control stage-discharge relationships during low and moderate flows. Figure A2-2 shows the location of the Ouray gage station. This aerial photograph was captured at a low enough stage and with clear enough water that the diagonal bars downstream are clearly evident.

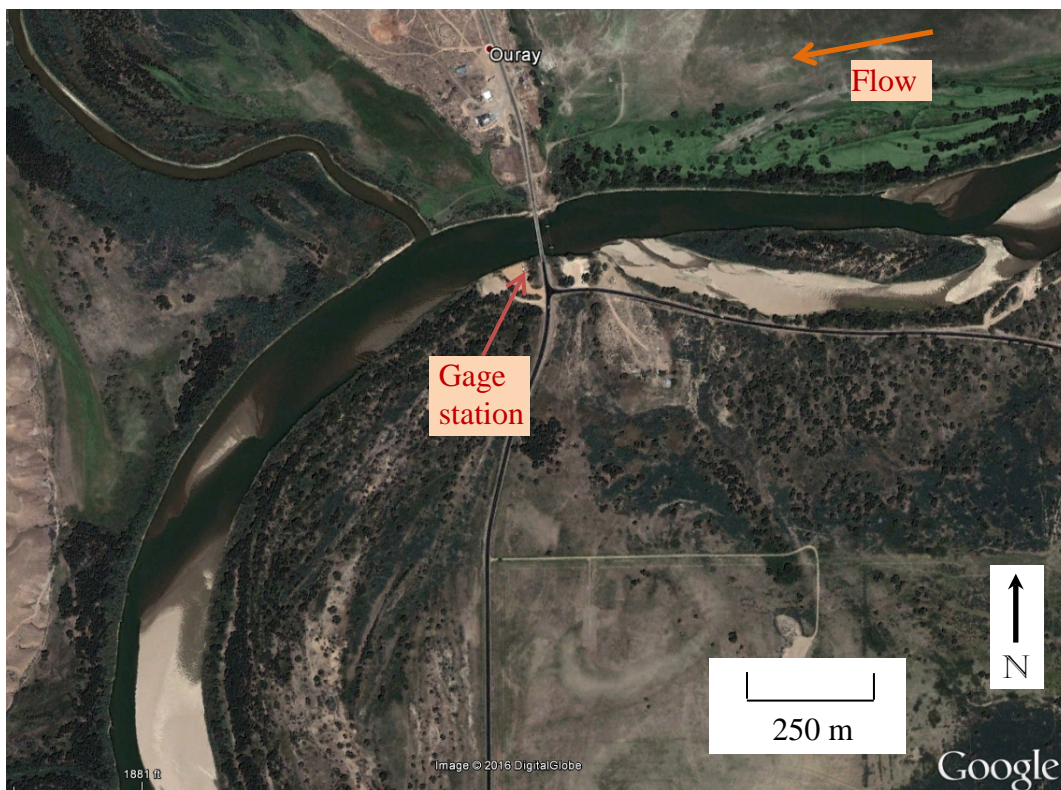


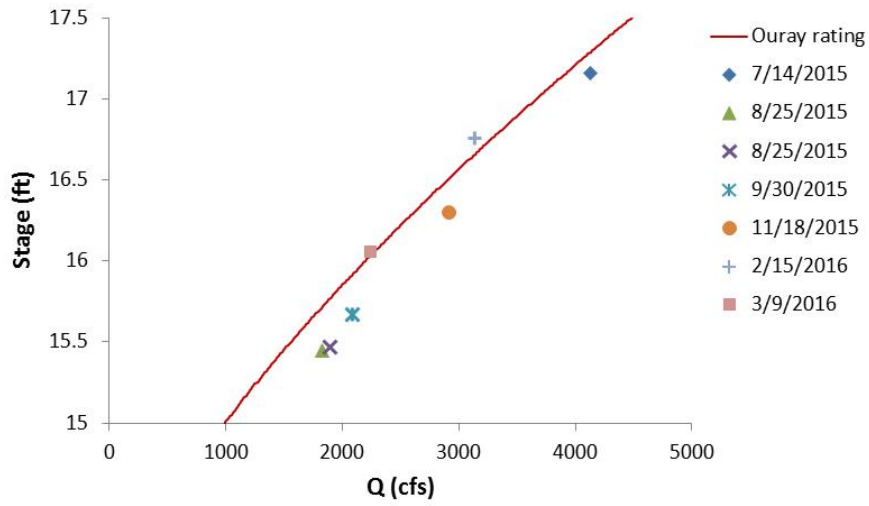
FIGURE A2-2 The Ouray Gage Station Site (USGS 09272400) on July 26, 2006 (flow is approximately 1,250 cfs)

The gage has only been in operation since 2009. Base-flow discharge measurements have been performed by the USGS approximately monthly. The measurements taken with $Q < 5,000$ cfs during each year are illustrated in Figure A2-3. The measurement points are illustrated on a year-by-year basis to clearly show annual variability. Of particular interest are measurements taken months apart at approximately the same discharge. Note that the Ouray rating curve is the same in each figure, and it is the one used in the ABIS analysis.

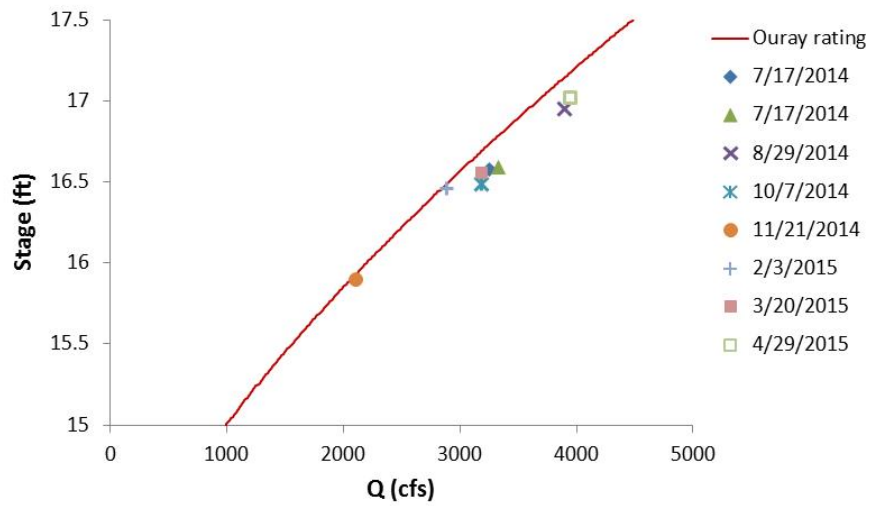
The data points illustrated in Figure A2-3 do not fall exactly on the rating curve at all times; but, in general, the scatter about the rating curve is limited, and it is important to remember that the discharge measurements have inherent error. The data qualitatively suggest that the temporal variability of the rating curve during the baseflow season (at least at the Ouray gage) is not substantial enough to invalidate the assumption that the shape of the rating curve is static in time.

Next, we consider spatial variability in the shape of the stage-discharge rating curve due to non-uniform channel geometry. The most effective way to perform such a comparison would be to have a number of measurements during a single base-flow season at several backwater sites that would be directly comparable to the graphs in Figure A2-3. Because such data do not exist, the only data available for comparison are the $(Q_{ref,i}, \zeta_{ref,i})$ pairs from the survey data at a single site over a number of years. We would expect considerably more scatter in such a

a) 2015



b) 2014



c) 2013

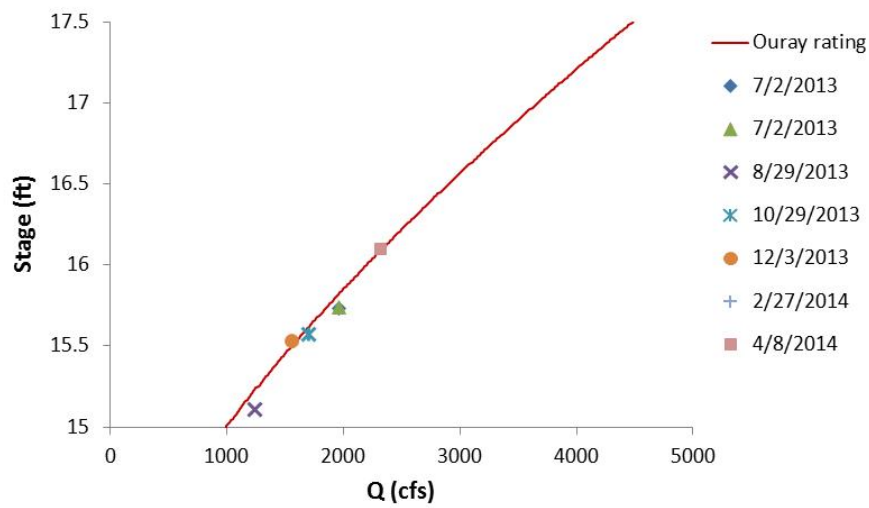
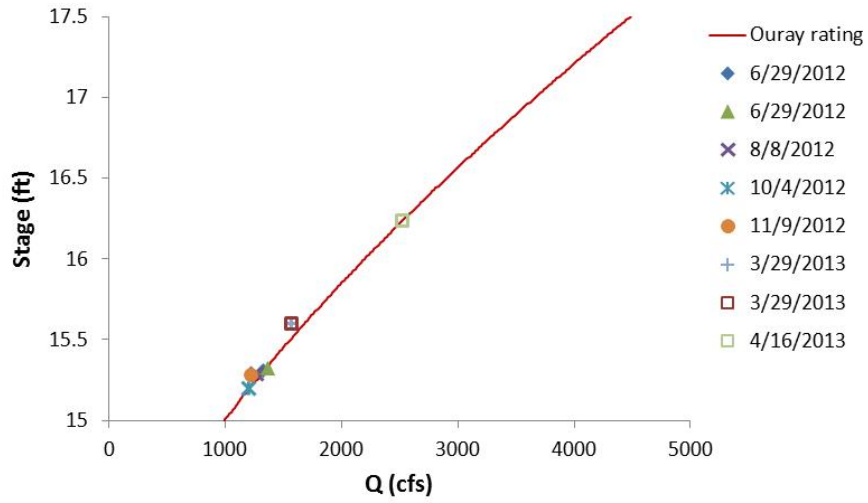
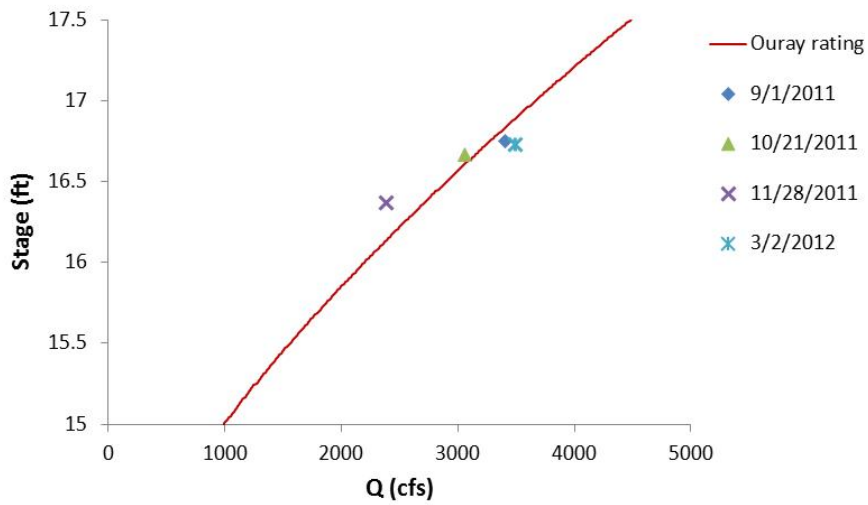


FIGURE A2-3 USGS Discharge Measurements at the Ouray Gage Station (2009-2015)

d) 2012



e) 2011



f) 2010

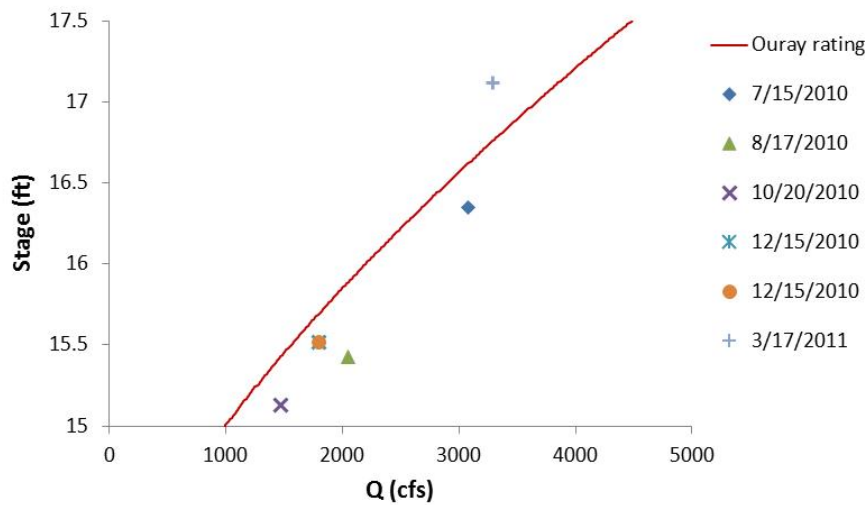


FIGURE A2-3 (Cont.)

g) 2009

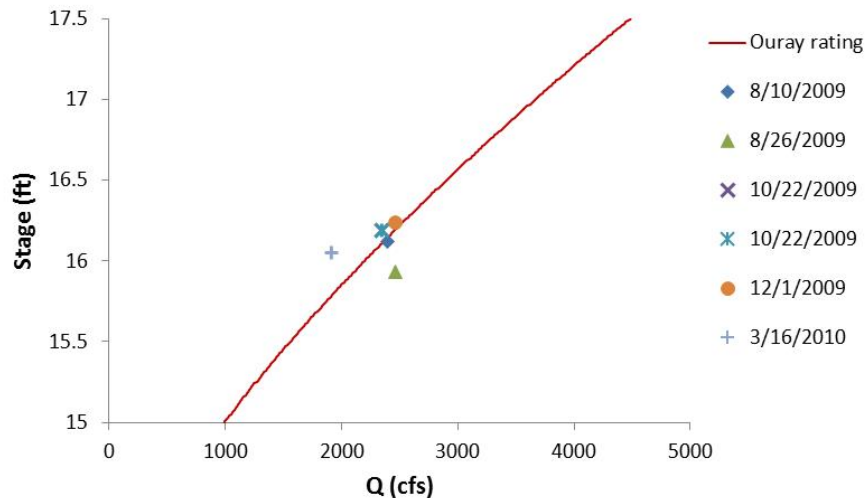


FIGURE A2-3 (Cont.)

relationship because changes in the local hydraulic controls between years will compound the variability. The greatest number of surveys at individual backwater sites was from BW02 and BW10. The position of BW02 is more variable from year to year than BW10. The variable spatial position of BW02 is shown in Figure A2-4. Considering that the mean water surface slope of the river is approximately 0.00027 ft/ft, then a shift in the centroid of the survey area by 1,000 feet would be expected to yield approximately 0.3 ft elevation difference for a given discharge. No attempt is made to correct for this potential modification in elevations for a given discharge due to the exact position of the backwater; the issue is raised only to highlight a potential source of scatter in the data.

Taking the reference elevations and discharge ($Q_{\text{ref},i}$, $\zeta_{\text{ref},i}$) for each year of the BW02 survey and assembling them onto one graph yields Figure A2-5. (Note that the 2003 data point was not shown, as there was an issue with the vertical datum that year, which does not allow a direct comparison with the data from other years.)

The Ouray rating curve shown on Figure A2-5 was simply translated upwards such that the stage values relate to elevations at the backwater survey site. Note that the two points that are furthest off the curve are 2005 and 2009. These are the years when BW02 was furthest downstream and furthest upstream, respectively. That the 2005 point should lie below the curve due to its position furthest downstream and that the 2009 point should lie above the curve due to its position upstream is exactly as expected. The shape of the rating curve appears to match well the surveyed elevations, despite the expected increase in variability due to year-to-year changes in local hydraulic controls. No inferences can be made for discharges greater than 3,328 cfs.

The position of BW10 is much more strongly fixed in position. The reference elevations and discharges surveyed for the six years of the survey are shown in Figure A2-6. As was the case with BW02, the points do not fall exactly on the rating curve, but the general agreement seems satisfactory given the many sources that may yield variability.

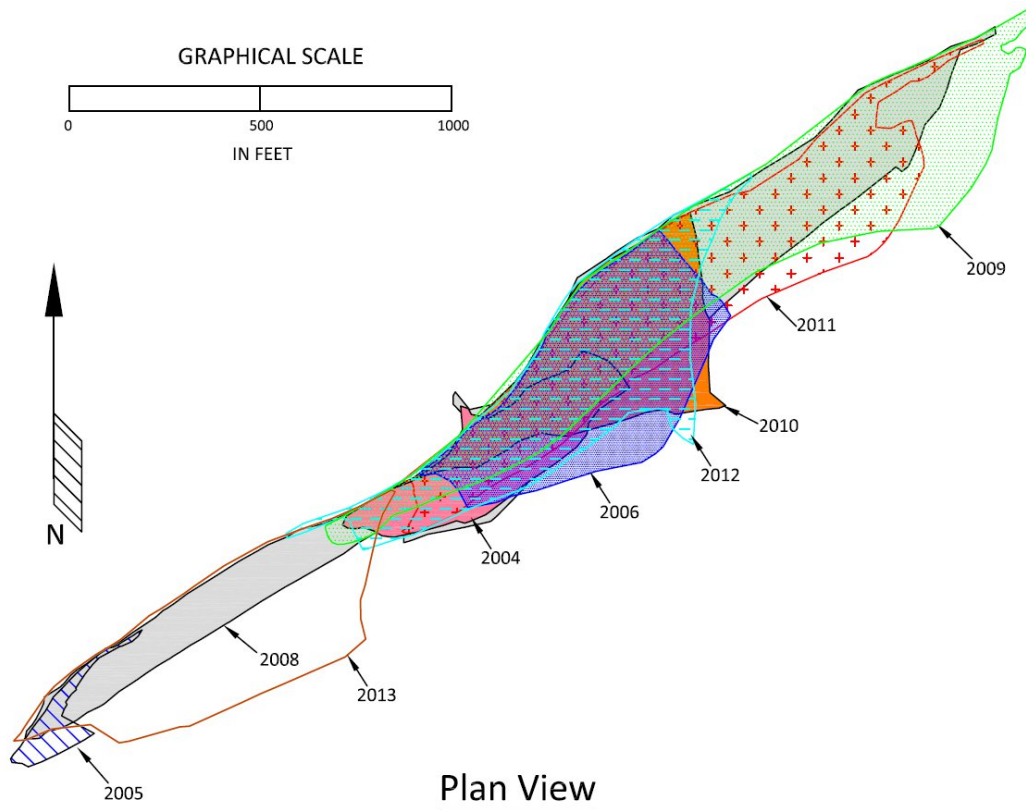


FIGURE A2-4 Overlay of Spatial Extents of the Individual Surveys at BW02

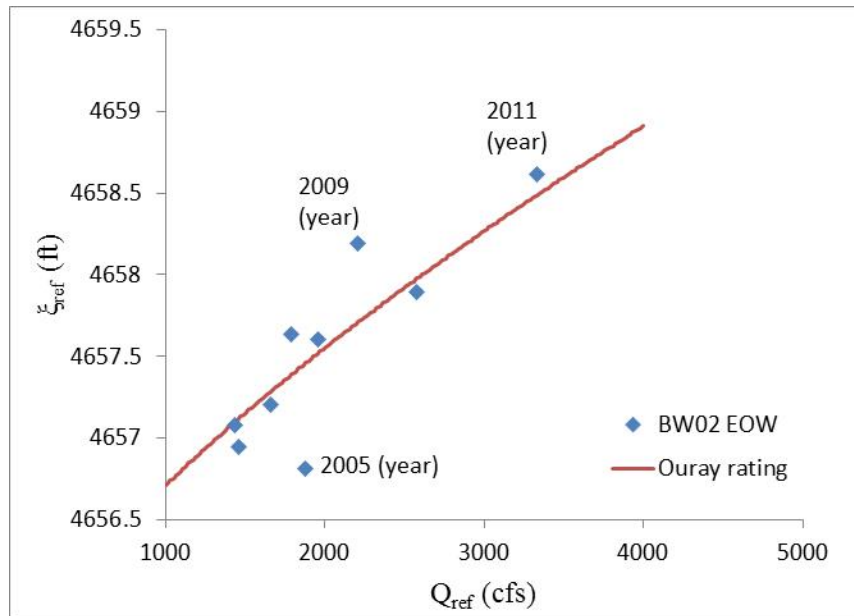


FIGURE A2-5 Mean Edge of Water Reference Elevation Surveyed at BW02 from 2004-2013

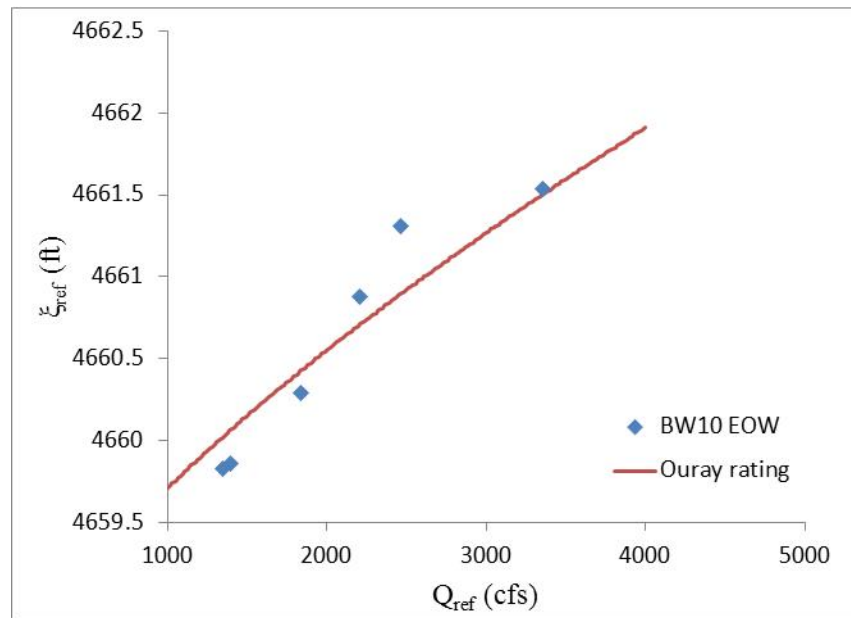


FIGURE A2-6 Mean Edge of Water Reference Elevation Surveyed at BW10 from 2004-2013

It should also be noted that the ABIS model does not account for hydraulics. Under certain circumstances such an approach is accurate from a hydrodynamic point of view; in some other cases it is an assumption that we feel is a reasonable approximation for the purposes of the analysis. For example, in instances where the water level in the backwater is well below any potential sandbar breach locations (i.e., where the water level would exceed the elevation of the sandbar crest), then ABIS provides an accurate hydrodynamic description. Water will enter the backwater from the down-river end of the bar. A gradually varied flow calculation under the steady state condition in which no flow is leaving or entering the backwater ($Q = 0$) is that the mean velocity is 0 and the water surface slope is 0. Thus, ABIS accurately represents a steady-state condition in which there is only connection from the downstream end of the bar.

In circumstances when the water level in the backwater approaches very close to a potential breach location, then hydrodynamic considerations potentially become important. Near the time of breaching, the water level on the river side will generally be slightly higher than on the backwater side because the backwater connection is at the down-river end of the bar and the water surface slope within the backwater is 0. ABIS does not take into account this energy gradient across the breach point, and the water level on the river side may exceed the breach elevation slightly before ABIS predicts it will. However, the energy gradient of the river is very modest; water surface slopes have been measured as approximately 0.00027 ft/ft. Assuming a potential breach is located 500 ft. up-river from the downstream backwater connection, this represents an elevation difference of 0.135 feet. This is a typical height of small sand ripples on the surface and represents a level of detail that generally is not obtained with our topographic surveying. The further upstream a potential breach is located, the greater is the potential that the water level on the river side will exceed the breach before ABIS predicts it will. In cases where the water level on the backwater side exceeds the breach elevation, then there is a near certainty that flow will enter the backwater for the same energy gradient reason described above.

However, the magnitude of the flow entering may be very modest, as shallow flows over the breach are expected to yield high energy losses with increasing velocity that would rapidly satisfy the modest energy gradient that exists between the river side of the bar and the backwater side of the bar.

Finally, even if a hydrodynamic calculation was made that would indicate the magnitude of discharge into the backwater, to our knowledge there is no criteria regarding mean velocity or temperature difference between the backwater and the river that would serve as a suitable criteria to indicate when backwater functionality is lost. Once the water level at the downriver connection well exceeds the breach elevation, then there is certainty that flow will be conveyed into and through the backwater. Thus, it is only at water levels very close to breaching that the assumption made by ABIS would be in doubt. In the absence of criteria to establish a flow threshold that would separate functional backwater habitat from non-functional backwater habitat, any hydrodynamic treatment would be of little use.

This page is intentionally left blank.

APPENDIX 3
BASE-FLOW PERIOD DELINEATION

This page is intentionally left blank.

APPENDIX 3

BASE-FLOW PERIOD DELINEATION

A3.1 BACKGROUND

In a natural catchment, “base flow” is the portion of flow in the stream that is not the direct result of a runoff event (e.g., the spring melt-off or an individual precipitation event). A “base-flow period” will be defined herein as a continuous period of time when the stream contains only base flow. The base flow is often conceptually considered as the outflow from the catchment’s reservoir of groundwater. If the outflow rate from the groundwater reservoir is linearly proportional to the storage volume in the groundwater reservoir, then the base-flow hydrograph (flow rate Q on the y-axis versus time t on the x-axis) will be characterized by an exponential curve whose slope continually decreases with time. When such a hydrograph is plotted as a semi-log plot of $\text{Log}(Q)$ on the y-axis versus t on the x-axis, the base-flow period will be indicated by a constant slope region bounded by clear inflection points (e.g., Chow et al. 1988). Delimiting the period when the stream contains only base flow is commonly considered a straightforward issue, and the key issue in the literature on base-flow separation is how to estimate the base-flow contribution during the runoff hydrograph (i.e., when a portion of the flow is contributed by the groundwater reservoir and a portion of the flow is contributed by the source of the runoff event).

In a river with large catchment and substantial flow regulation, delineating the base-flow period is not a trivial problem. On the Green River downstream of the Jensen gage station, plots of $\text{Log}(Q)$ versus t do not yield obvious constant-slope regions in the summer that are bounded by obvious inflection points that indicate when the spring snowmelt hydrographs ended. This is largely due to the river flow being regulated, which confounds the signal associated with the natural processes.

A3.2 METHODS

The summer base-flow period is considered to be a prolonged period of time with nearly constant or slightly declining flows. Inflows from runoff associated with summer precipitation events in the basin downstream of the Flaming Gorge Dam (particularly from Yampa River) will superimpose time-localized increases and decreases in flow. The most accurate method of analysis would be to perform base-flow separation to eliminate the contributions of summer runoff events from the flow record; however, this would take substantial effort, and the techniques for base-flow separation are not precise. The proposed alternative approach is to consider drawdown on a time scale that is long enough to reduce the contribution of summer runoff relative to the overall signal associated with base-flow drawdown.

The base-flow period will be considered herein to be a period characterized by a limited range of slopes ($\Delta Q/\Delta t$) on the hydrograph, when the slope is evaluated over a substantially long

time period. To reiterate, an instantaneous slope (dQ/dt) calculated on the falling limb of a summer daily wave will have a large negative slope that may be larger than the instantaneous slopes during the falling limb of the spring snowmelt hydrograph; increasing the time scale, when the slope is calculated by linear regression over a 12-hour period, the slope will oscillate between large positive and negative slopes; when the slope is calculated by linear regression over a 24-hour period, the daily oscillations are largely eliminated from the signal and the trend in daily flow changes become evident. However, the range of calculated slopes will be dominated by the contributions from superimposed runoff hydrographs associated with summer precipitation events; when the slope is calculated over time periods longer than the duration of superimposed runoff hydrographs, then more general trends in the base-flow drawdown will be dominant.

For the current analysis, 15-minute time series of flows were evaluated during the period March 1 through December 31 (or the last recording before measurements were no longer taken due to ice cover). The Jensen gage station is used for the analysis. The years 2010, 2011, and 2012 are used to illustrate the technique; these constitute a relatively normal year, a very wet year, and a very dry year, respectively. For each data point on the hydrograph, a linear regression is calculated that spans a 10-day time window encompassing 5 days previous to and 5 days after the measurement. This yields a continuous record of $(\Delta Q/\Delta t)_{10}$, which is the nomenclature for the slope of the 10-day linear regressions.

The falling limb of the spring snowmelt hydrograph is characterized by large negative slopes; the base-flow period is characterized by small slopes. The conceptual basis for separating the runoff period from the base-flow period is that a maximum negative value of $(\Delta Q/\Delta t)_{10}$ defines the maximum rate of drawdown during the base-flow period; a value of $(\Delta Q/\Delta t)_{10}$ that is more negative indicates a drawdown during the runoff period. The steps used to determine base flow are as follows:

- (a) Start from the most negative point on the $(\Delta Q/\Delta t)_{10}$ versus t curve, which represents the steepest part of the spring snowmelt runoff hydrograph drawdown.
- (b) Identify all the maxima and minima on the curve that exist in the time after the most negative point on the curve (the maxima and minima are where the second derivative of the curve is equal to 0); this indicates a period where the drawdown rate has become constant over a 10-day time window.
- (c) Find the first maximum, and evaluate whether it is within the range of all following maxima and minima; if it is more negative, then it is outside the base-flow range; proceed until a maximum is found that is within the range of all the maxima and minima that follow. This is the first maximum that is within the base-flow period; it is referred to as “Point A.”
- (d) Starting from Point A, find the most negative minimum within the remainder of the season; this defines the maximum negative value of $(\Delta Q/\Delta t)_{10}$ that can be considered to represent base-flow drawdown; the value is referred to as $(\Delta Q/\Delta t)_{10,\text{bfmax}}$.

- (e) Starting from Point A, proceed backwards in time until $(\Delta Q/\Delta t)_{10}$ is more negative than $(\Delta Q/\Delta t)_{10, \text{bfmax}}$. This is referred to as “Point B”; it defines the beginning of the base-flow period. The entire drawdown period before Point B associated with the spring snowmelt hydrograph has $(\Delta Q/\Delta t)_{10}$ that is more negative; thus these high drawdown rates cannot be considered representative of base-flow drawdown.

Examples of the base-flow period delineation using these steps are illustrated in Figures A3-1 through A3-6.

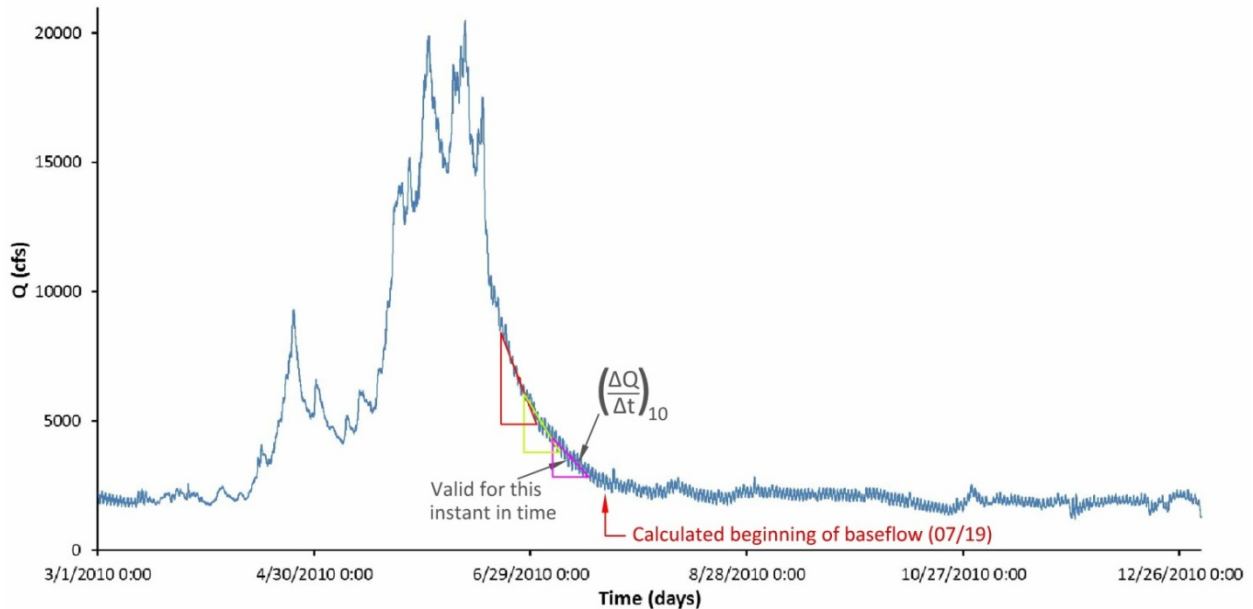


FIGURE A3-1 Jensen Gage Station Hydrograph in 2010 (Triangles represent 10-day drawdown slopes to illustrate the meaning of the term $(\Delta Q/\Delta t)_{10}$. Beginning of the base-flow period is shown for reference, but is based on the analysis provided in Figure A3-2.)

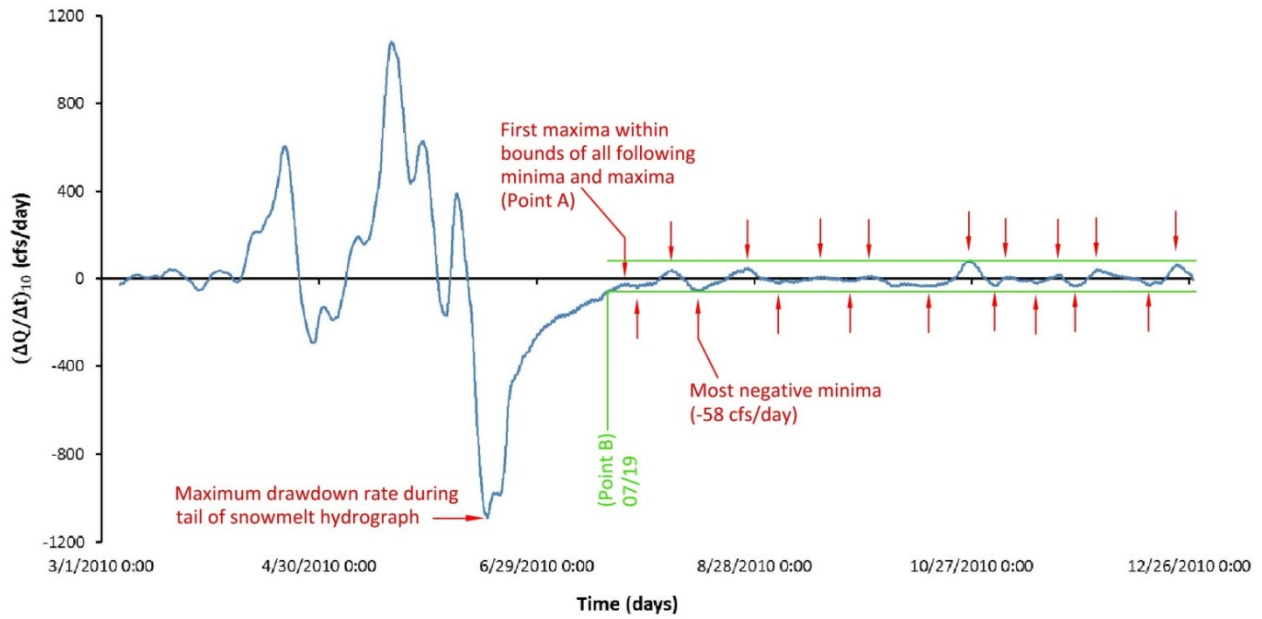


FIGURE A3-2 Plot of $(\Delta Q/\Delta t)_{10}$ Versus t Illustrating the Method for Base-Flow Period Delineation in 2010 (Maxima and minima are indicated with red arrows. 2010 base flow defined in this way starts on July 19, 2010.)

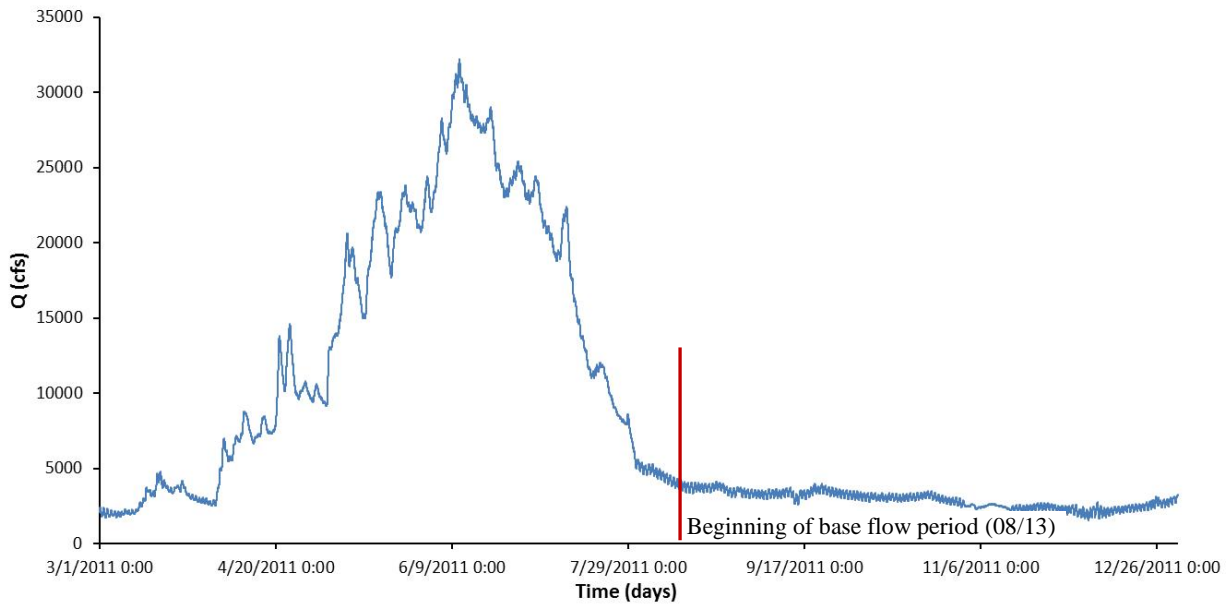


FIGURE A3-3 Jensen Gage Station Hydrograph in 2011 (Beginning of the base-flow period is shown for reference, but is based on the analysis provided in Figure A3-4.)

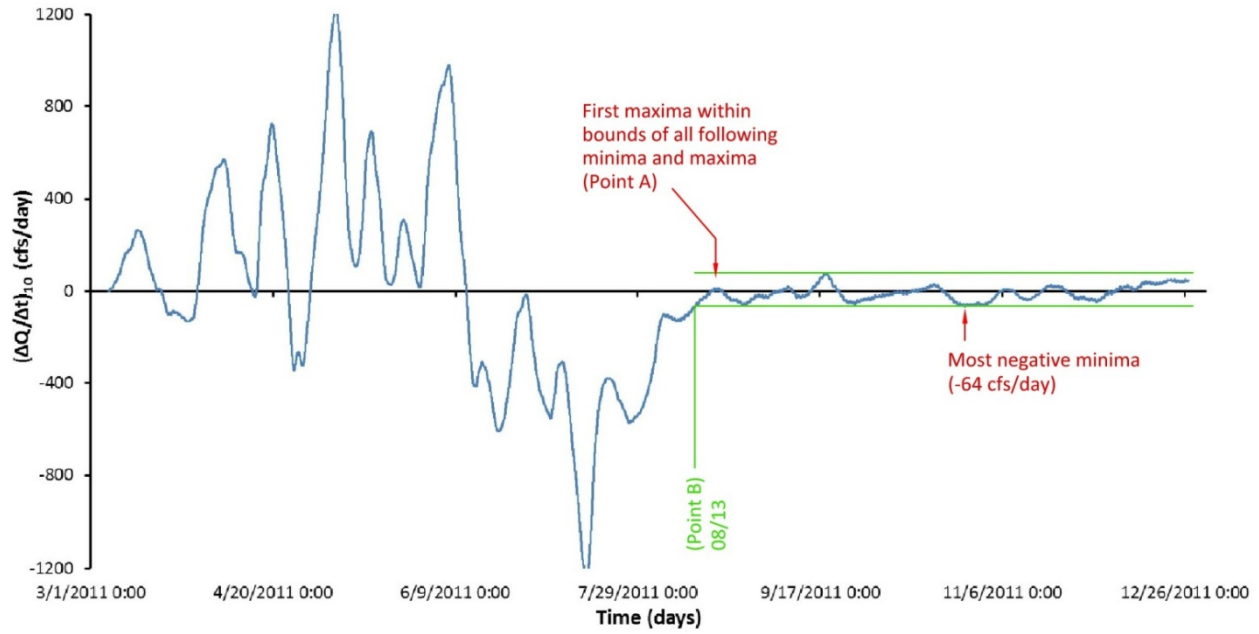


FIGURE A3-4 Plot of $(\Delta Q/\Delta t)_{10}$ Versus t Illustrating the Method for Base-Flow Period Delineation in 2011 (2011 base flow defined in this way starts on August 13, 2011.)

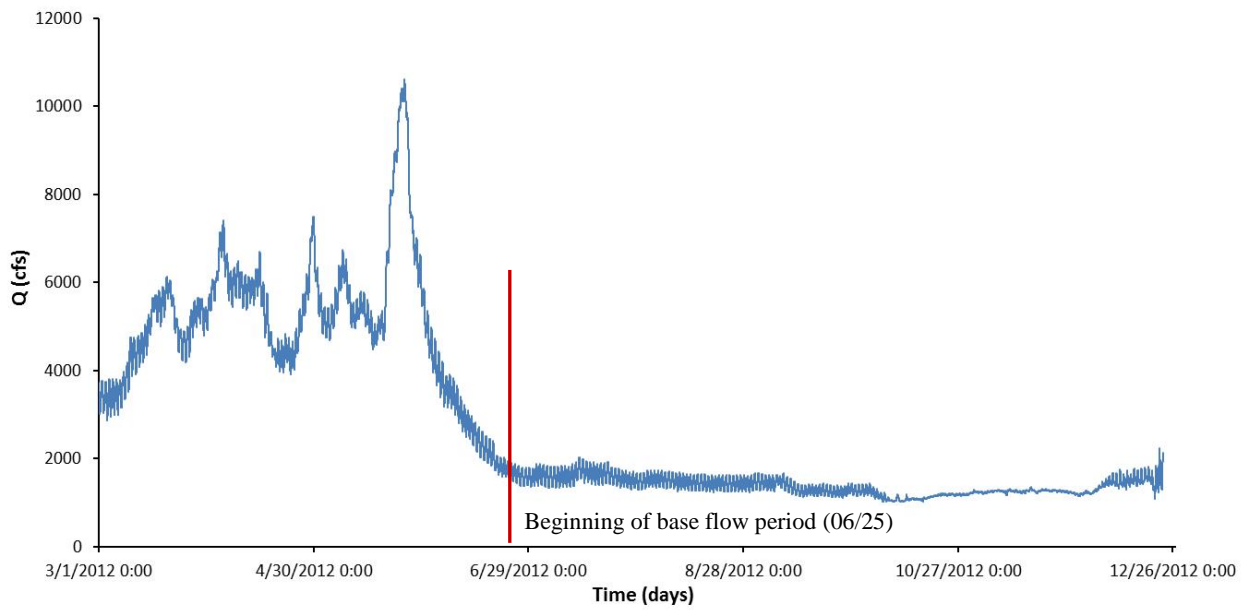


FIGURE A3-5 Jensen Gage Station Hydrograph in 2012 (Beginning of the base-flow period is shown for reference, but is based on the analysis provided in Figure A3-6.)

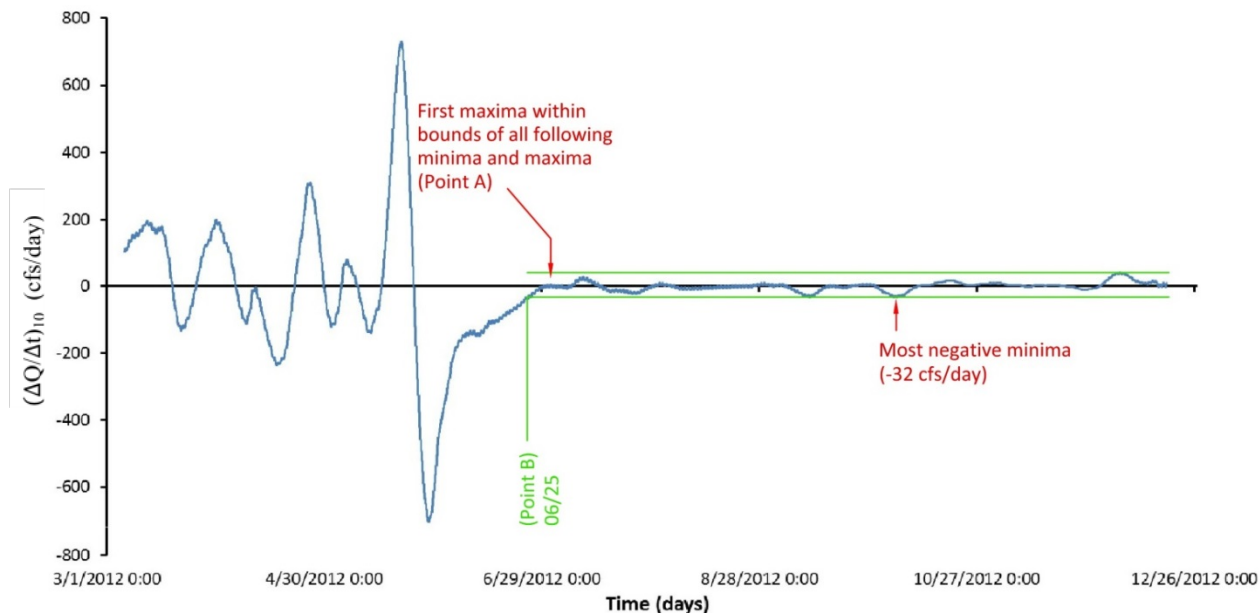


FIGURE A3-6 Plot of $(\Delta Q/\Delta t)_{10}$ Versus t Illustrating the Method for Base-Flow Period Delineation in 2012 (2012 base flow defined in this way starts on June 25, 2012.)

Table A3-1 shows the results of the base-flow delineation analysis for the years of the backwater surveys (2003–2013). Base flows began as early as June 25 in 2012 and as late as August 13 in the high-flow year of 2011. The base-flow period began in mid- to late July in most years.

TABLE A3-1 Start of the Base-Flow Period and Maximum Slope from 2003 to 2013

Year	Start Date of Base-Flow Period	$(\Delta Q/\Delta t)_{10, \text{bfmax}}$ (cfs/day)
2003	07/18/2003	-31
2004	07/31/2004	-72
2005	07/23/2005	-43
2006	07/04/2006	-46
2007	07/11/2007	-43
2008	07/28/2008	-40
2009	07/25/2009	-47
2010	07/19/2010	-58
2011	08/13/2011	-64
2012	06/25/2012	-32
2013	07/06/2013	-35

A3.3 REFERENCE

Chow, V.T, D.R. Maidment, and L.W. Mays, 1988, *Applied Hydrology*, McGraw-Hill, Inc., New York, New York.

This page is intentionally left blank.

APPENDIX 4

**BACKWATER SURVEY LOCATIONS, RELATIONSHIPS
OF CHARACTERISTICS TO FLOW, AND CHANGES IN CHARACTERISTICS
DURING THE BASE-FLOW PERIOD**

This page is intentionally left blank.

APPENDIX 4**BACKWATER SURVEY LOCATIONS, RELATIONSHIPS
OF CHARACTERISTICS TO FLOW, AND CHANGES IN CHARACTERISTICS
DURING THE BASE-FLOW PERIOD**

Surveys of selected backwaters were made annually from 2003 to 2013 (2007 was the only year surveys were not conducted during this time period). This appendix provides information on (1) the location of surveyed backwaters in each year; (2) the relationships to flow of surface area, volume, maximum depth, and mean depth in each year; and (3) modeled changes in these characteristics over the base-flow period of each year. The information is provided in a series of figures for each year. See Appendix 5 for summary statistics of these variables, as well as the start date of the base-flow period and the hydrologic classification in each year.

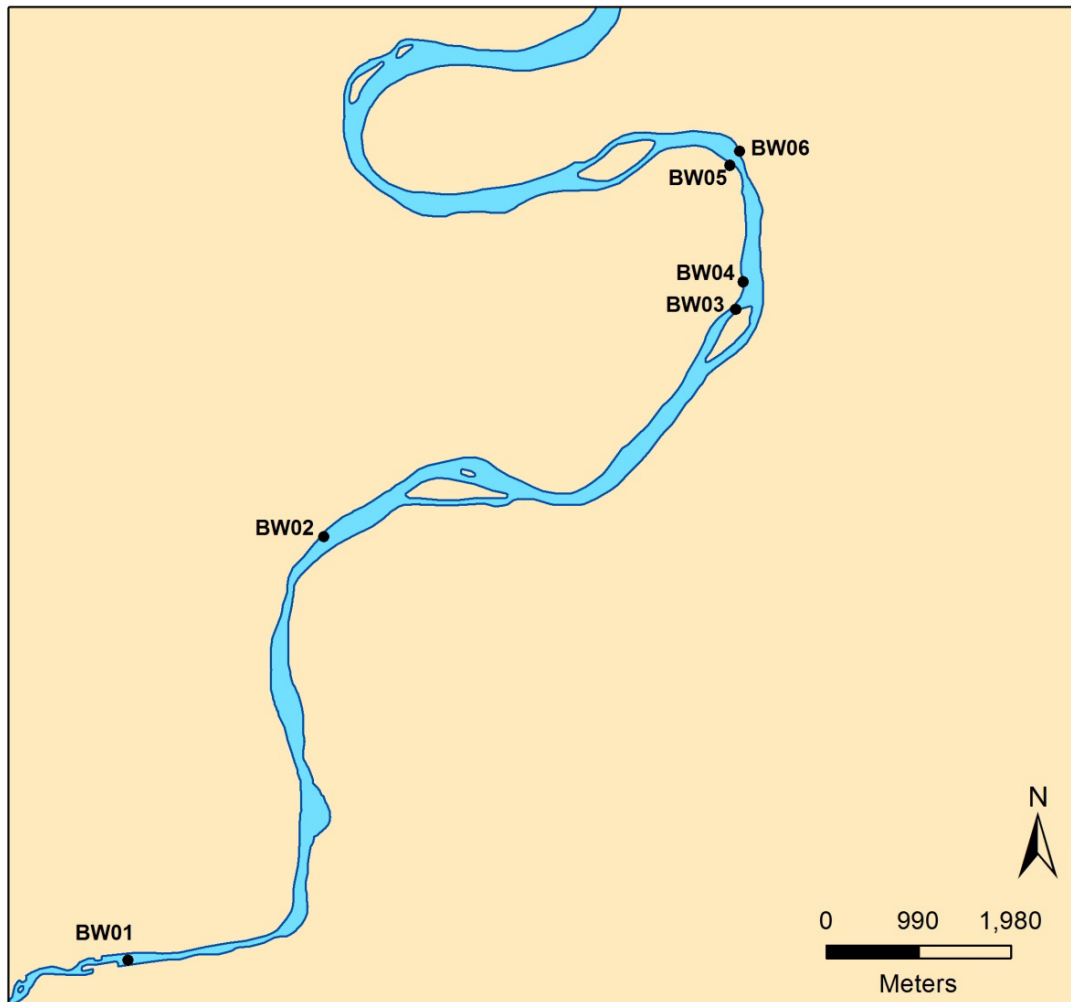


FIGURE A4-1 Green River Backwater Areas BW01, BW02, BW03, BW04, BW05, and BW06 Surveyed and Modeled in 2003

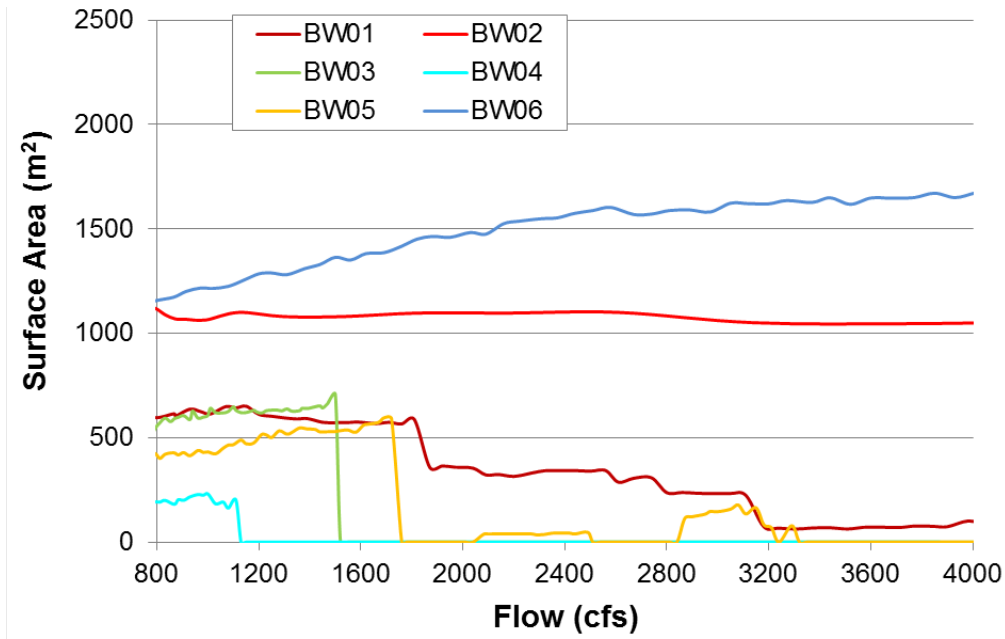


FIGURE A4-2 Surface Area (m²) of the Six Backwater Areas Surveyed in 2003 Modeled across Base Flows (800–4,000 cfs)

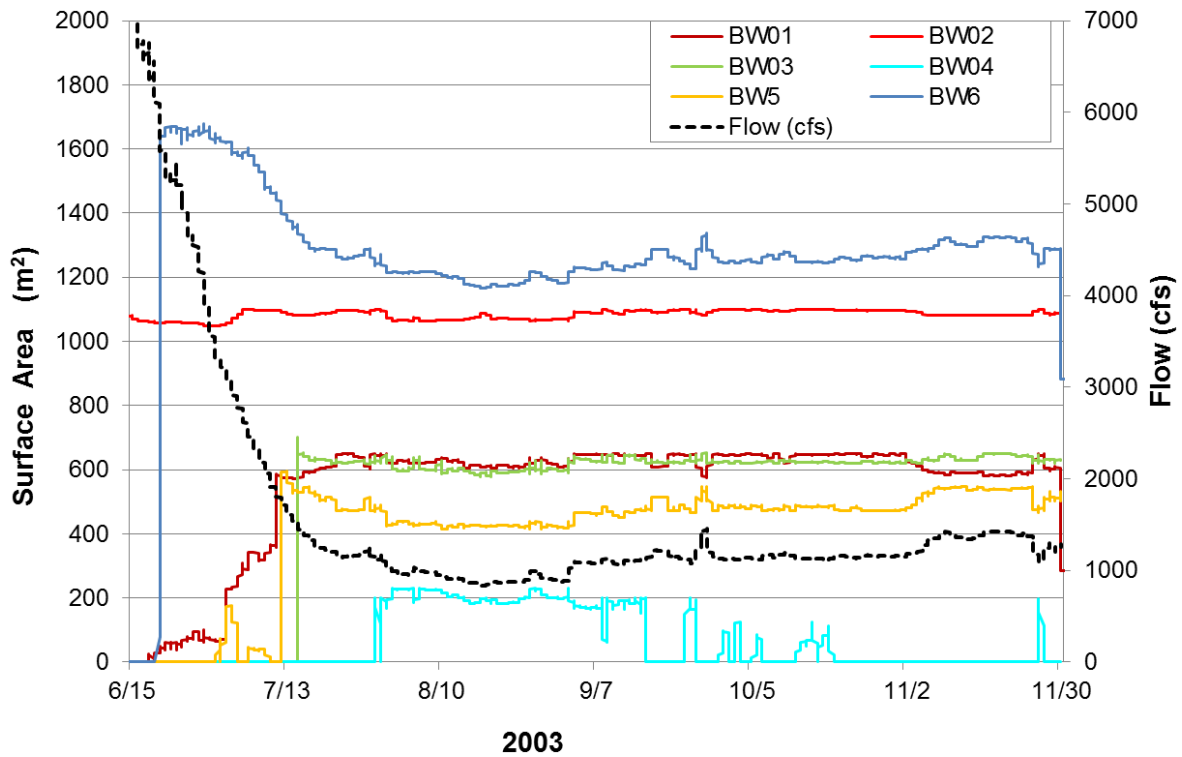


FIGURE A4-3 Surface Area (m²) of Each of the Six Backwater Areas Modeled during 2003 (June 15–November 30)

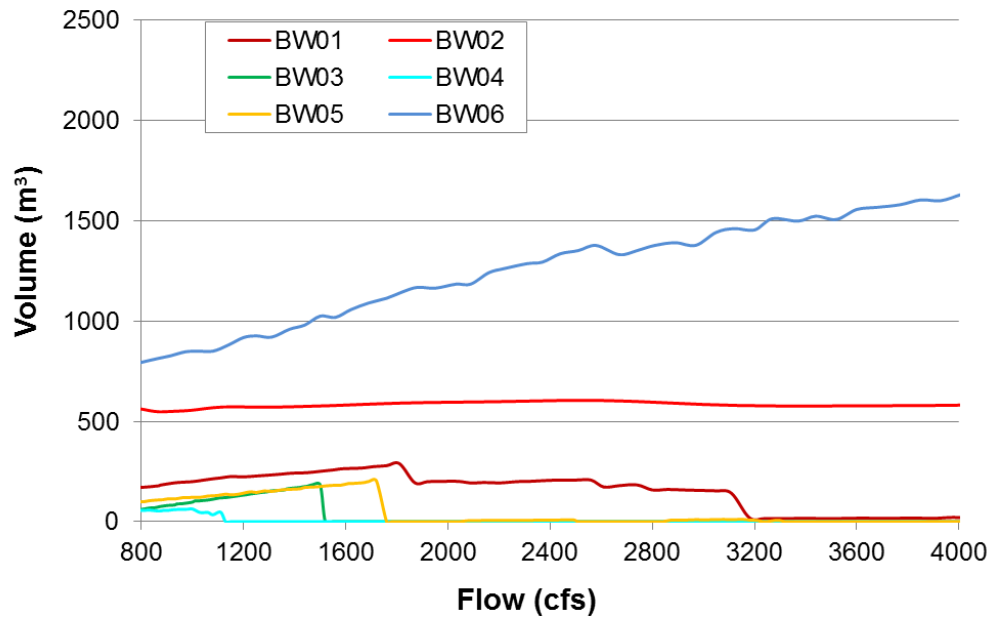


FIGURE A4-4 Volume (m³) of the Six Backwater Areas Surveyed in 2003 Modeled across Base Flows (800–4,000 cfs)

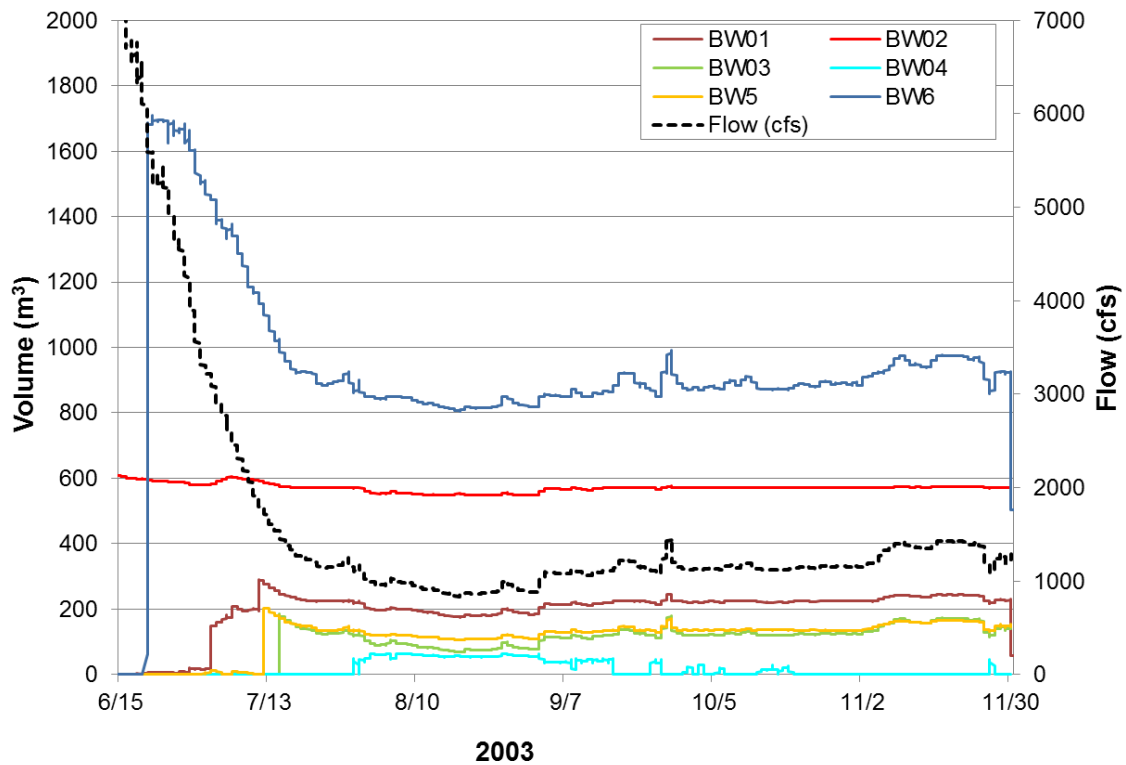


FIGURE A4-5 Surface Area (m²) of Each of the Six Backwater Areas Modeled during 2003 (June 15–November 30)

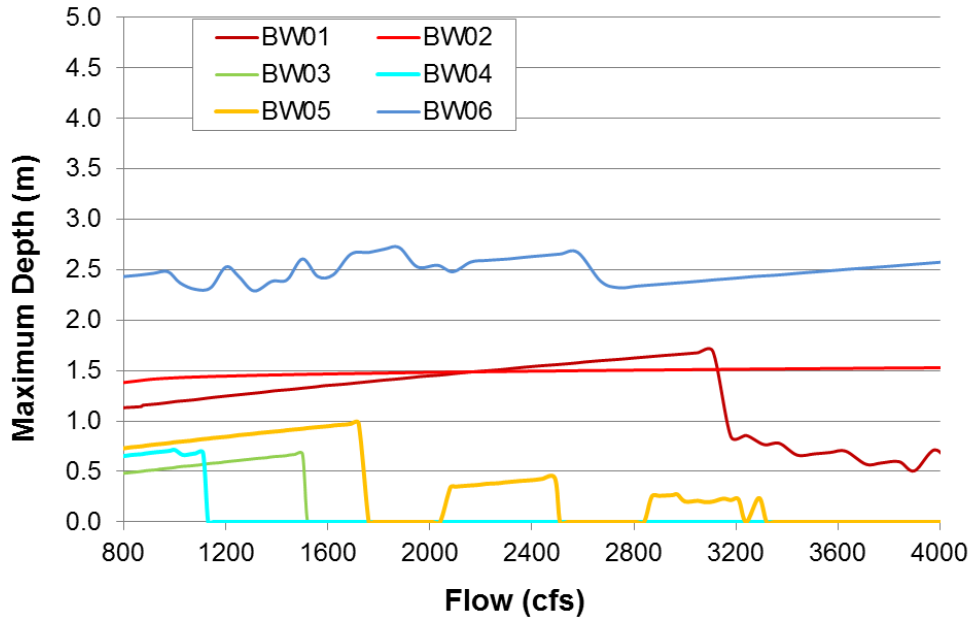


FIGURE A4-6 Maximum Depth (m) of the Six Backwater Areas Surveyed in 2003 Modeled across Base Flows (800–4,000 cfs)

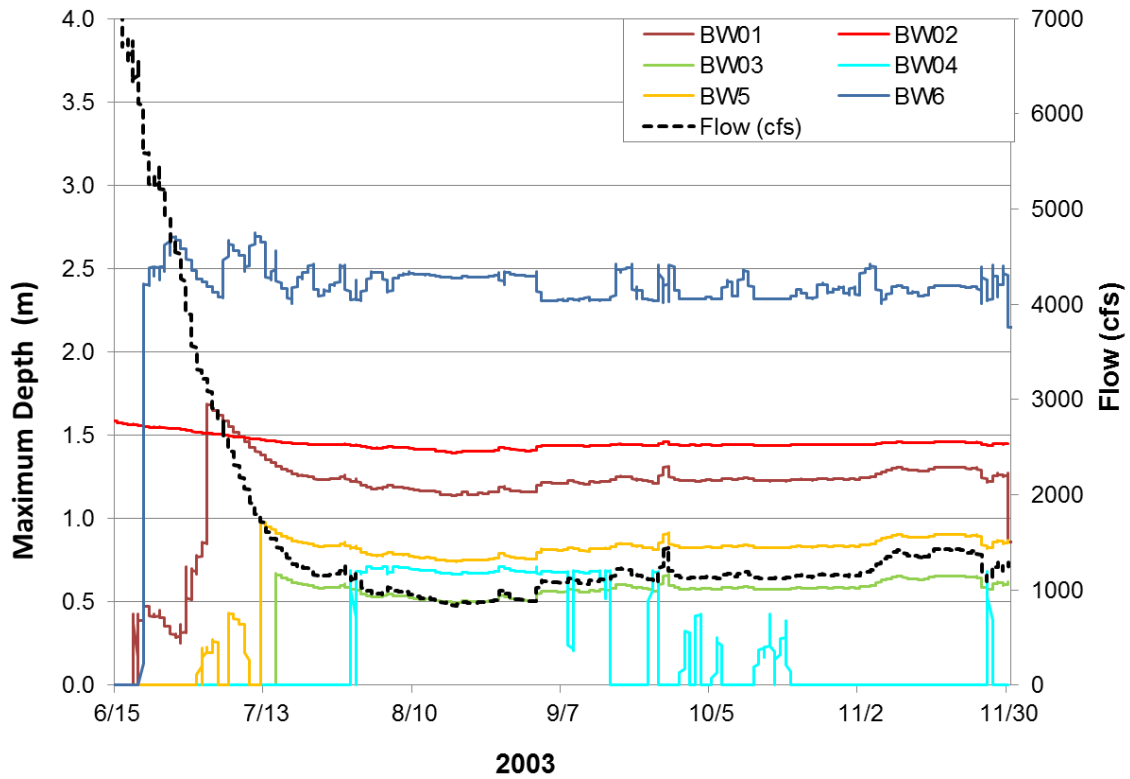


FIGURE A4-7 Maximum Depth (m) of Each of the Six Backwater Areas Modeled during 2003 (June 15–November 30)

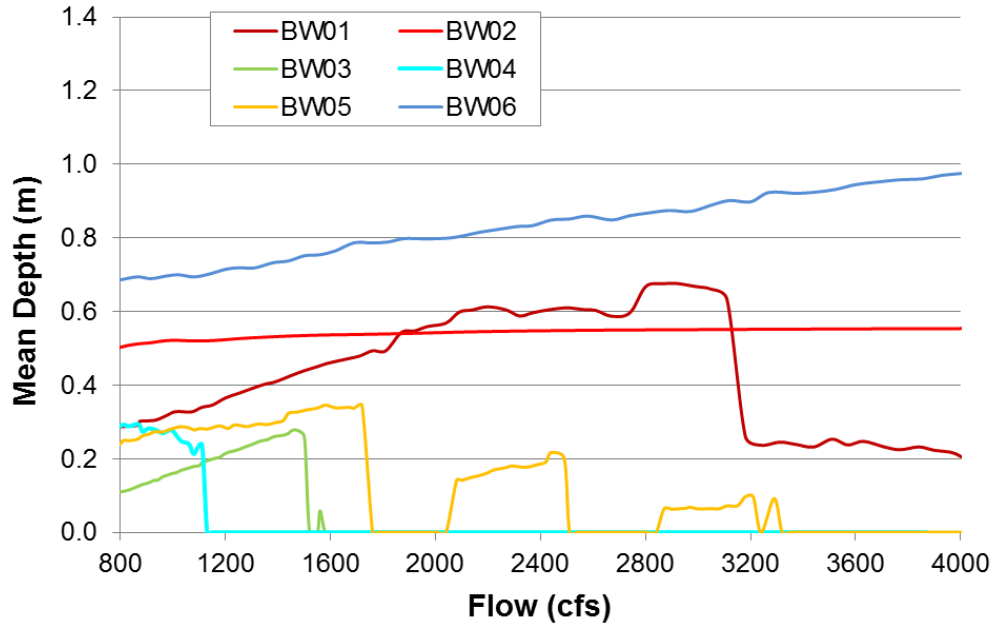


FIGURE A4-8 Mean Depth (m) of the Six Backwater Areas Surveyed in 2003 Modeled across Base Flows (800–4,000 cfs)

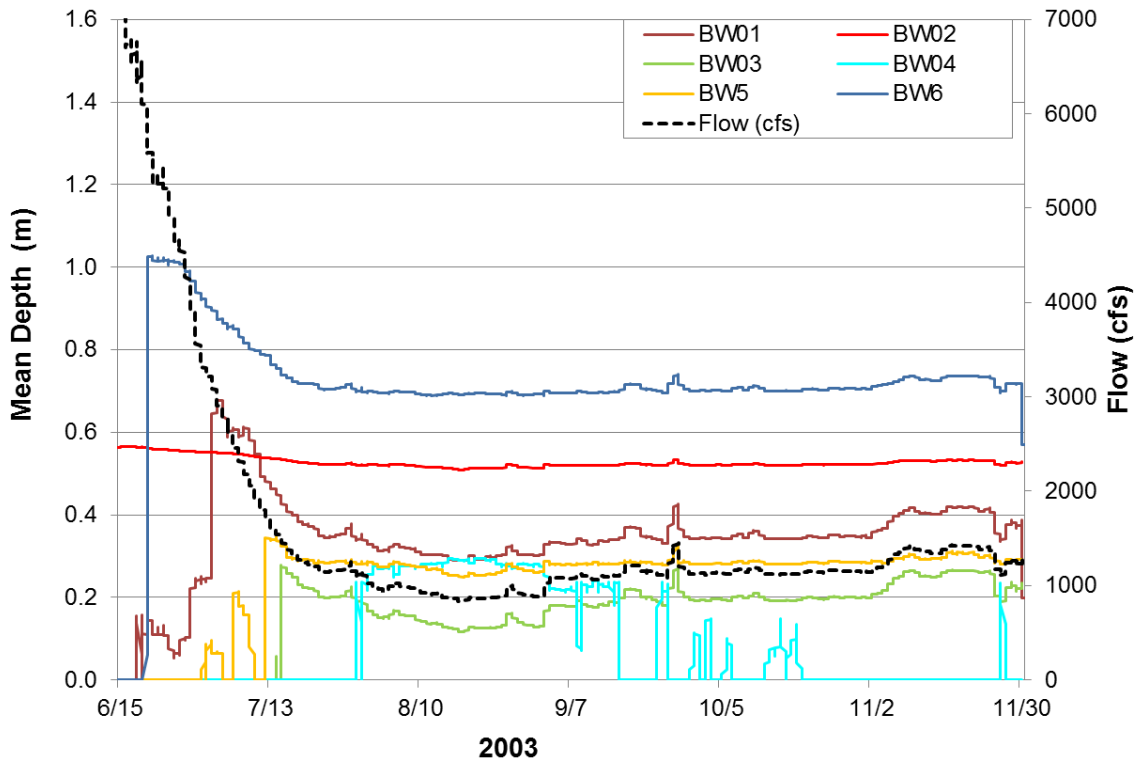


FIGURE A4-9 Mean Depth (m) of Each of the Six Backwater Areas Modeled during 2003 (June 15–November 30)

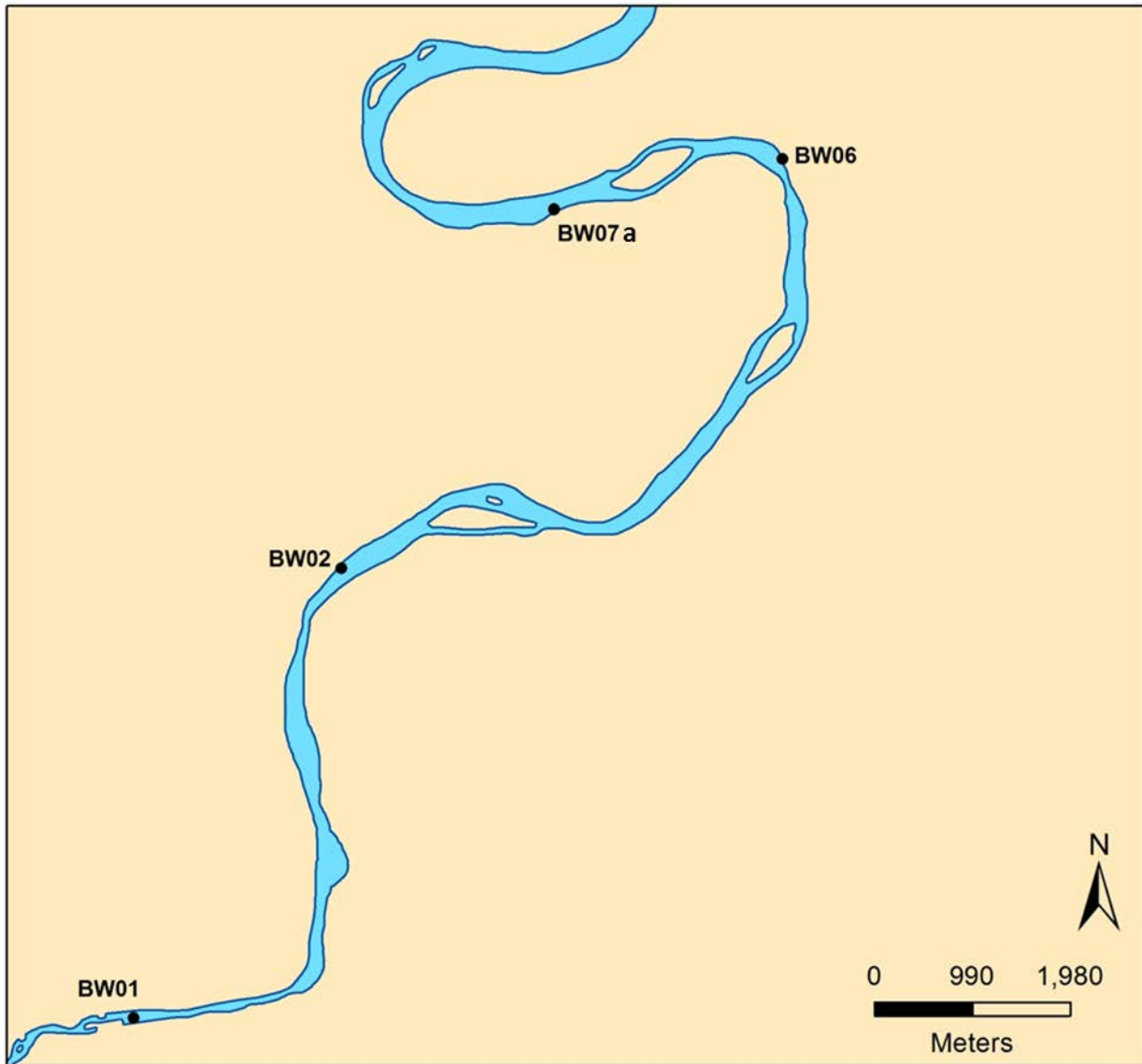


FIGURE A4-10 Green River Backwater Areas BW01, BW02, BW6, and BW07a Surveyed and Modeled in 2004

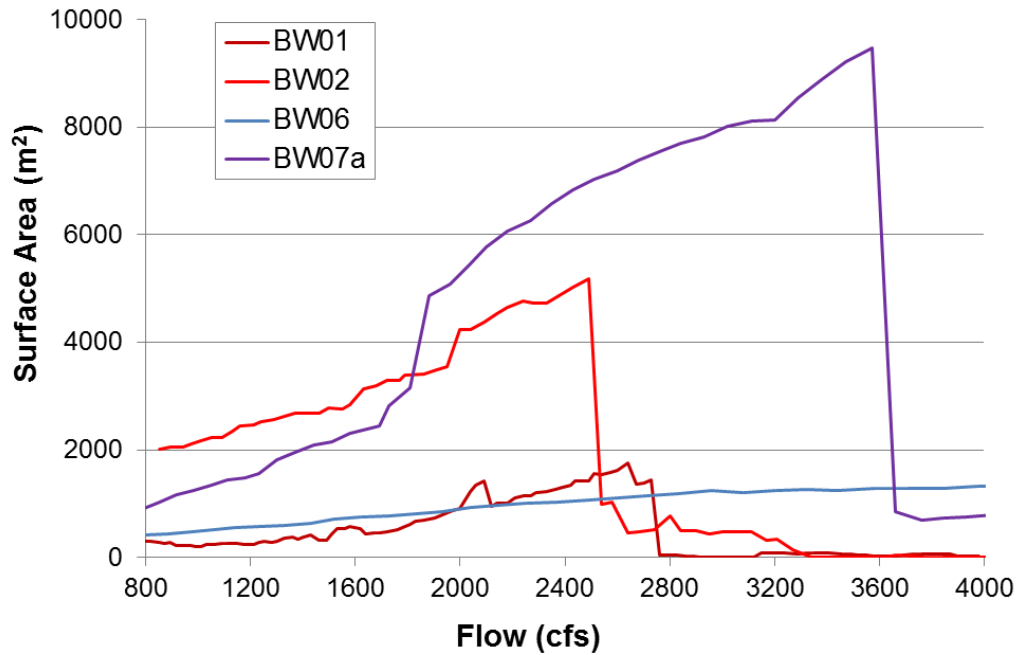


FIGURE A4-11 Surface Area (m²) of the Six Backwater Areas Surveyed in 2004 Modeled across Base Flows (800–4,000 cfs)

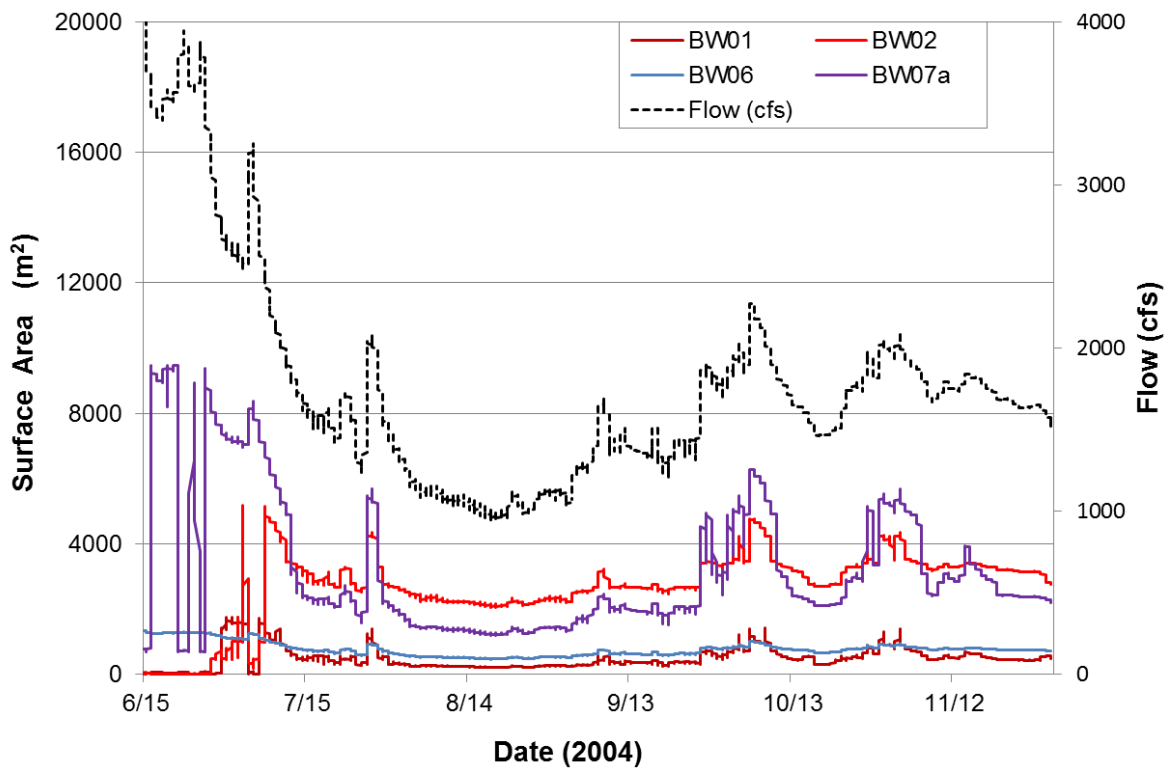


FIGURE A4-12 Surface Area (m²) of Each of the Six Backwater Areas Modeled during 2004 (June 15–November 30)

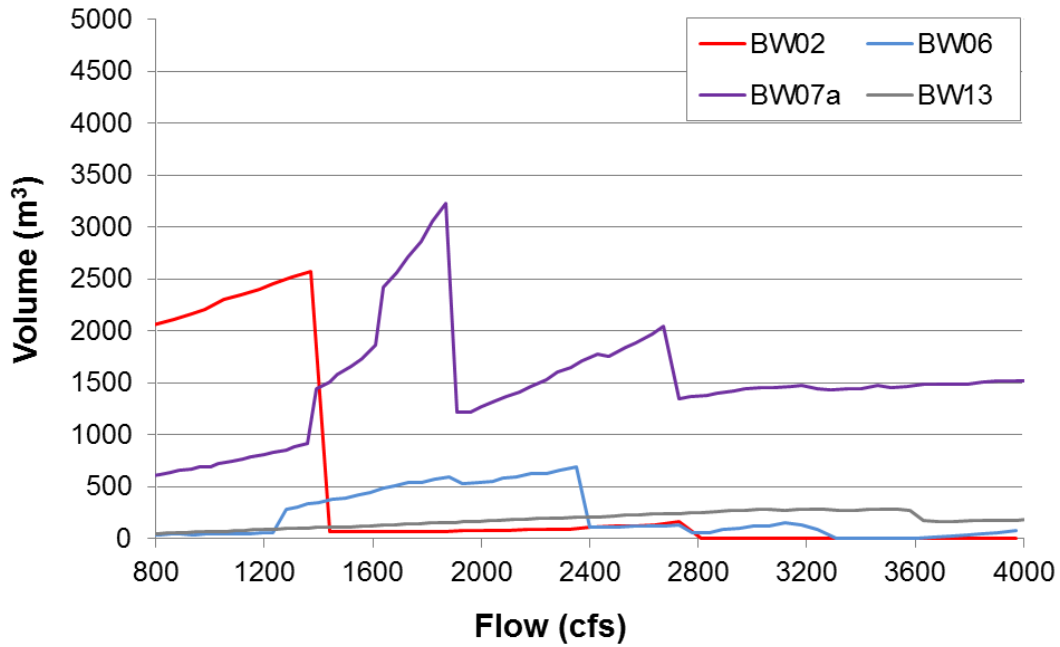


FIGURE A4-13 Volume (m^3) of the Six Backwater Areas Surveyed in 2004 Modeled across Base Flows (800–4,000 cfs)

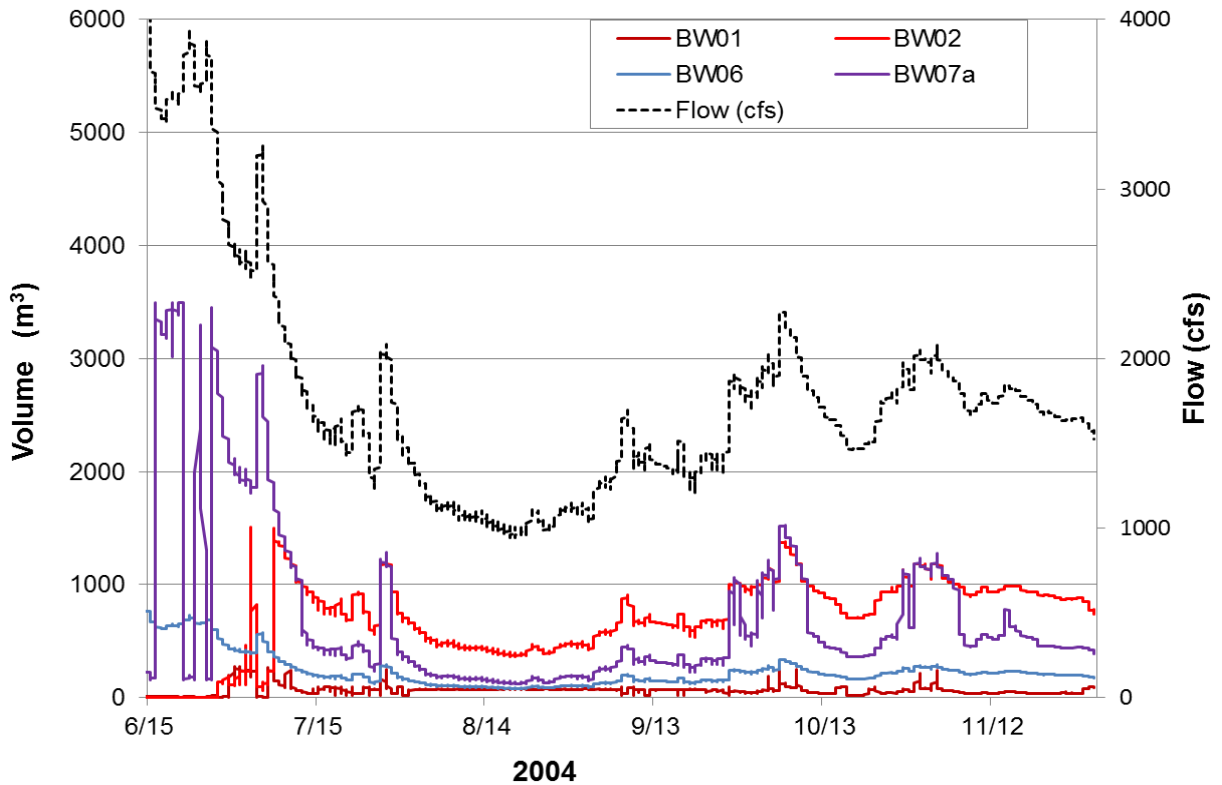


FIGURE A4-14 Volume (m^3) of Each of the Six Backwater Areas Modeled during 2004 (June 15–November 30)

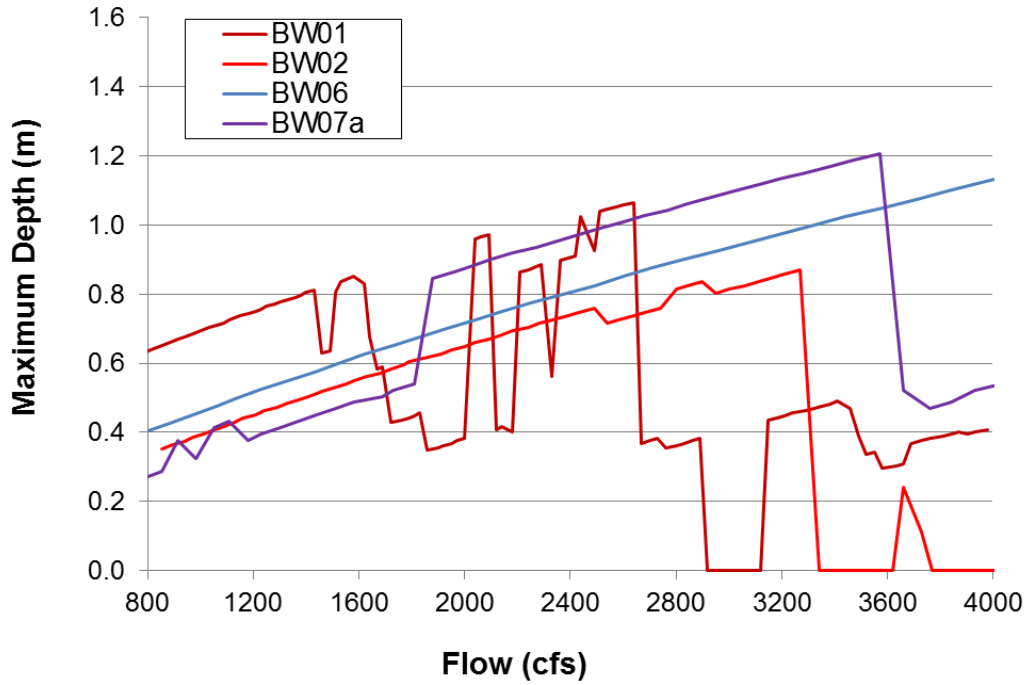


FIGURE A4-15 Maximum Depth (m) of the Six Backwater Areas Surveyed in 2004 Modeled across Base Flows (800–4,000 cfs)

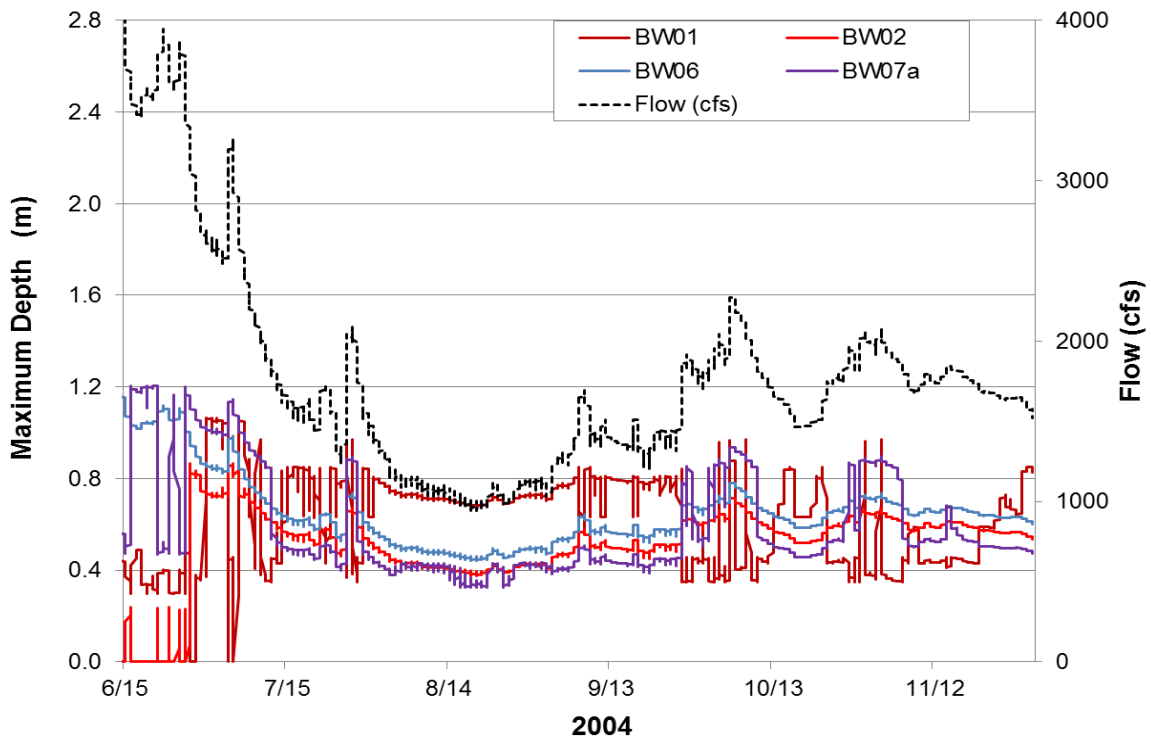


FIGURE A4-16 Maximum Depth (m) of Each of the Six Backwater Areas Modeled during 2004 (June 15–November 30)

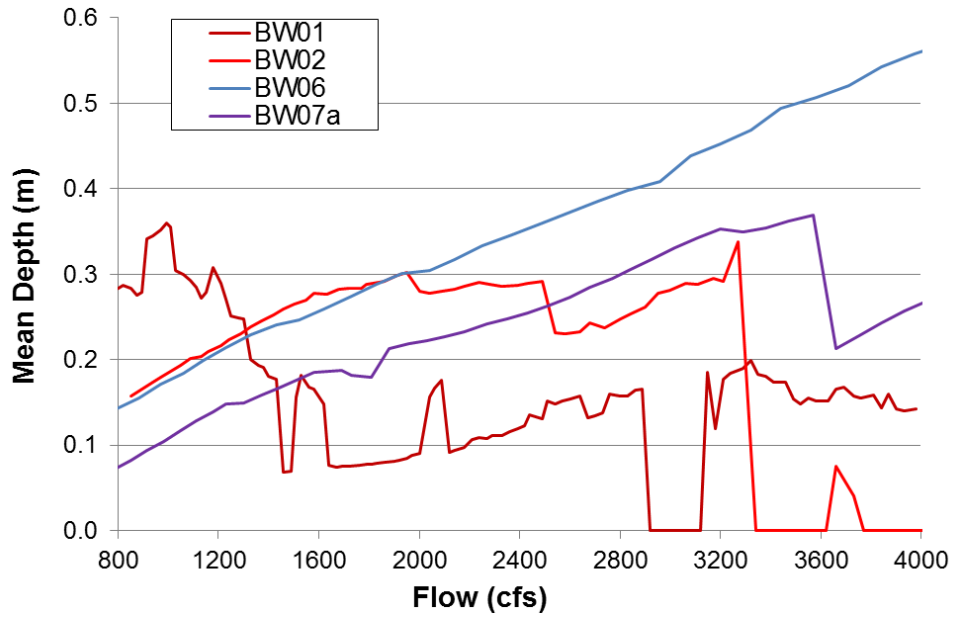


FIGURE A4-17 Mean Depth (m) of the Six Backwater Areas Surveyed in 2004 Modeled across Base Flows (800–4,000 cfs)

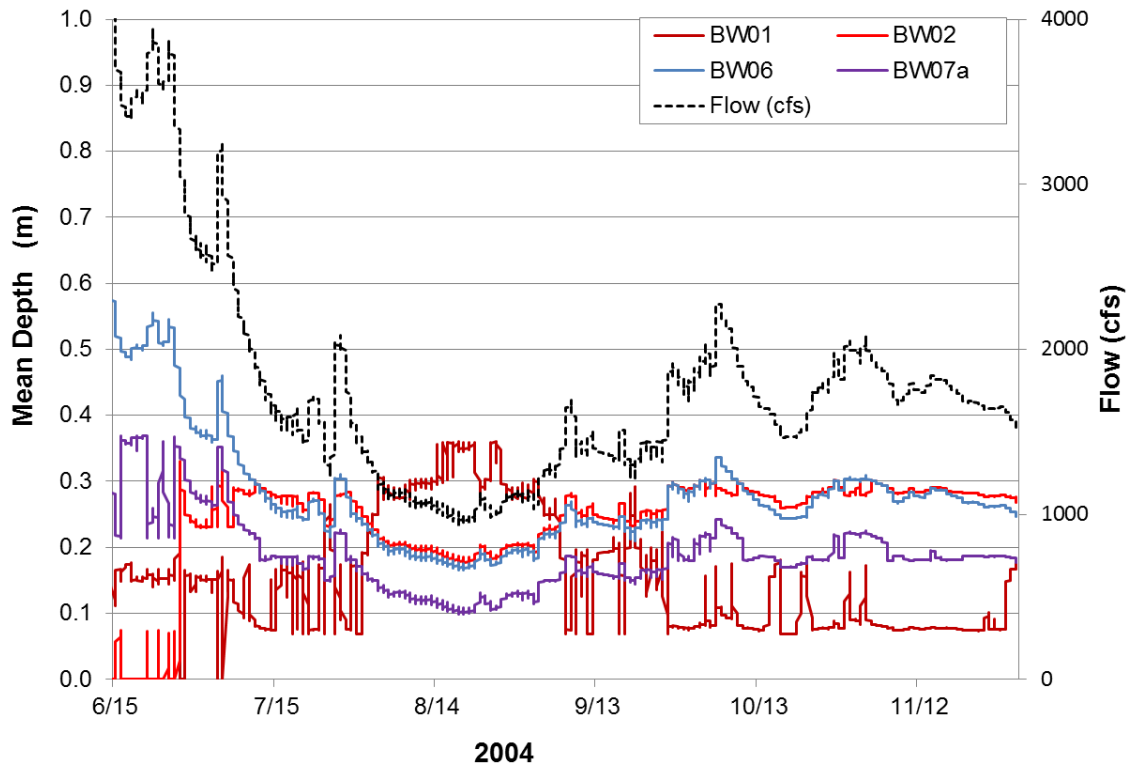


FIGURE A4-18 Mean Depth (m) of Each of the Six Backwater Areas Modeled during 2004 (June 15–November 30)

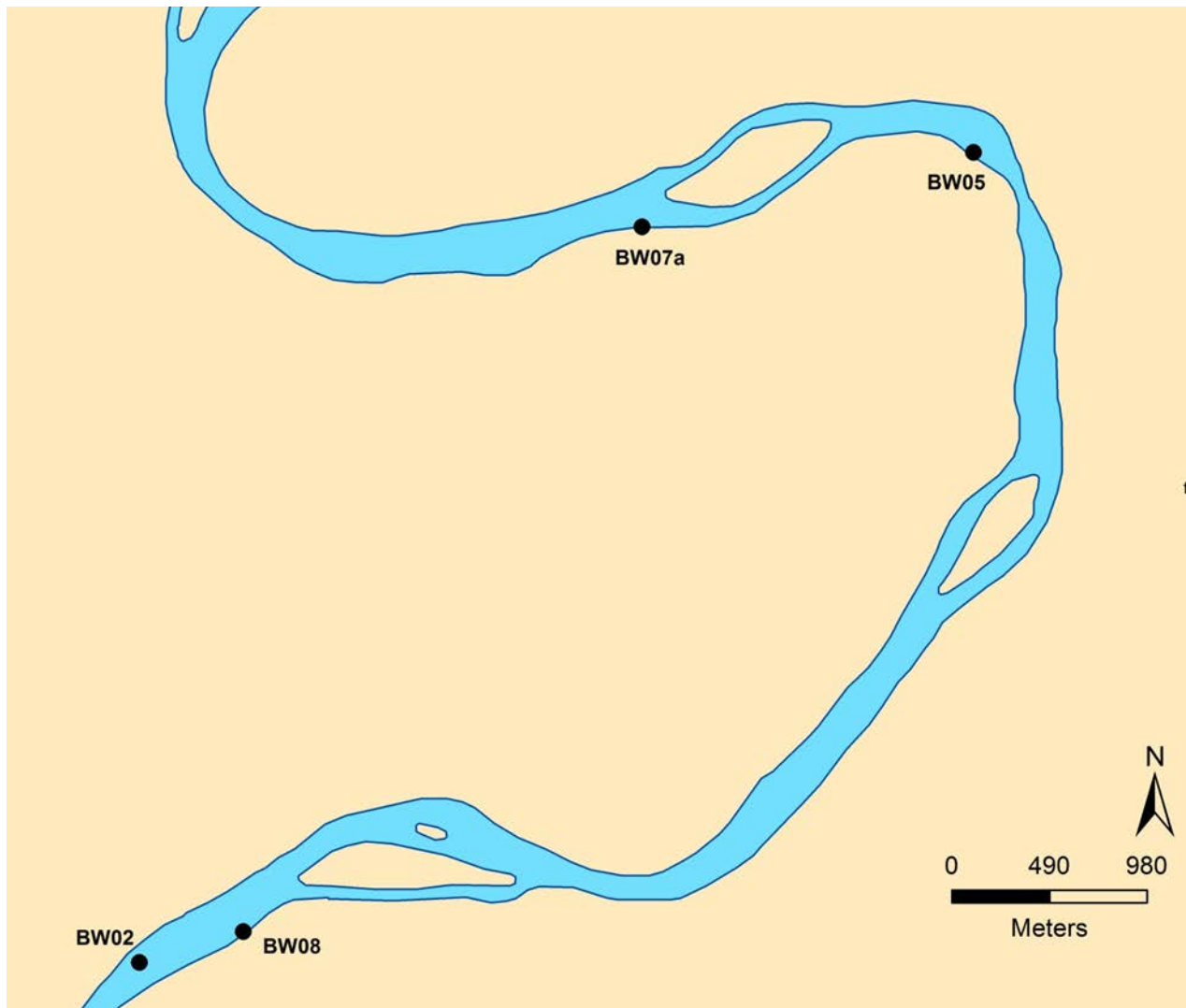


FIGURE A4-19 Green River Backwater Areas BW02, BW05, BW07a, and BW08 Surveyed and Modeled in 2005

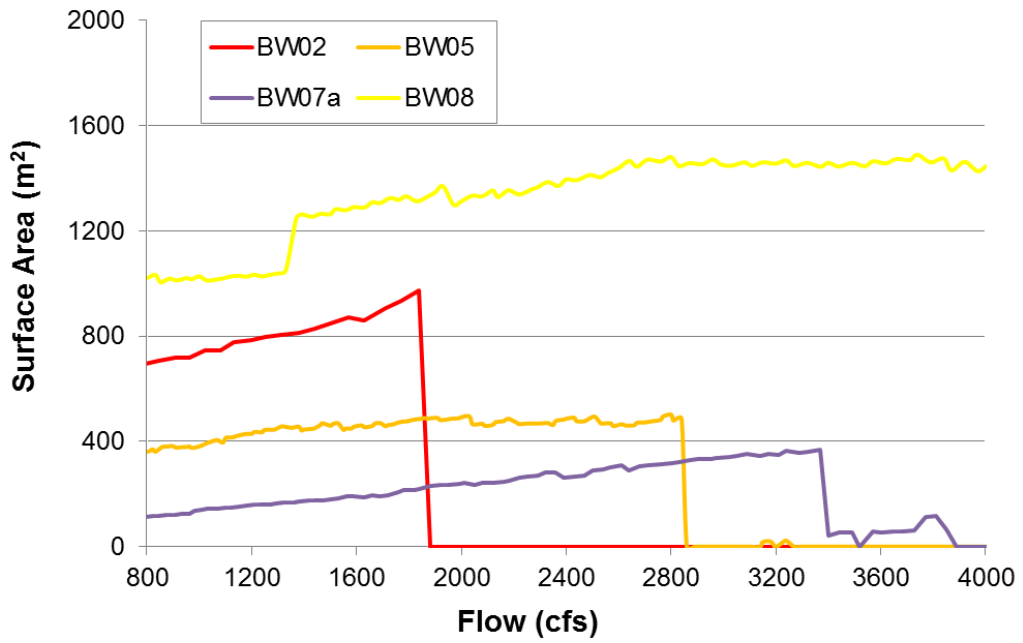


FIGURE A4-20 Surface Area (m^2) of the Four Backwater Areas Surveyed in 2005 Modeled across Base Flows (800–4,000 cfs)

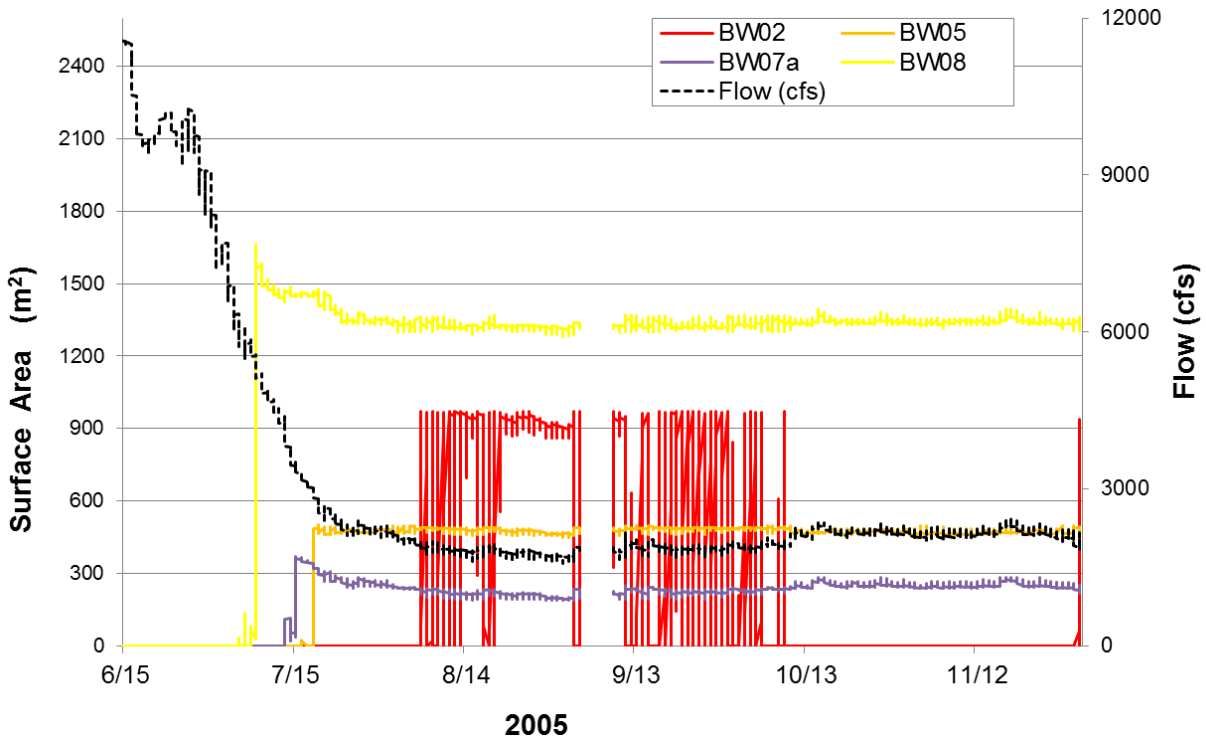


FIGURE A4-21 Surface Area (m^2) of Each of the Four Backwater Areas Modeled during 2005 (June 15–November 30)

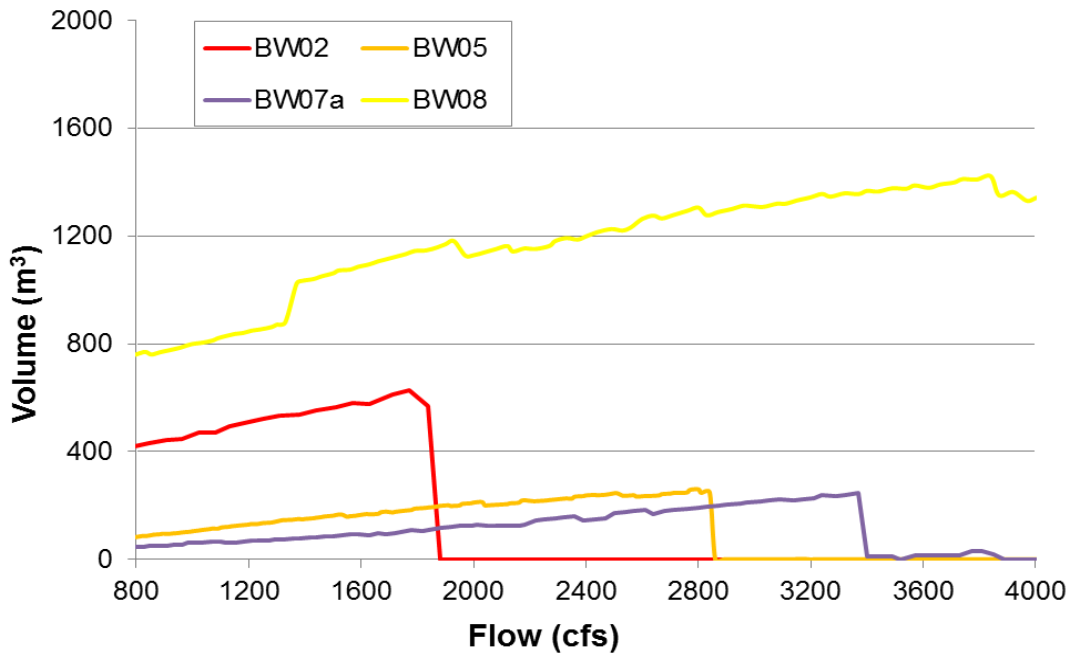


FIGURE A4-22 Volume (m³) of the Four Backwater Areas Surveyed in 2005 Modeled across Base Flows (800–4,000 cfs)

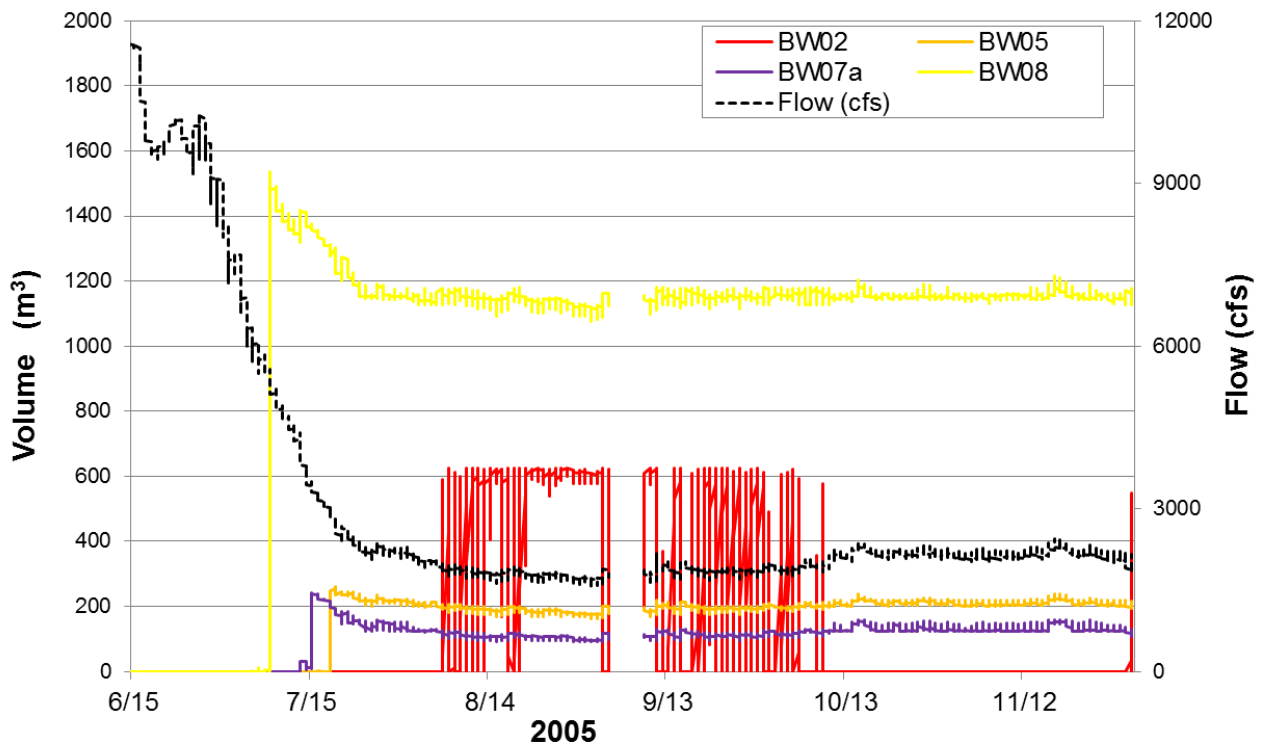


FIGURE A4-23 Volume (m³) of Each of the Four Backwater Areas Modeled during 2005 (June 15–November 30)

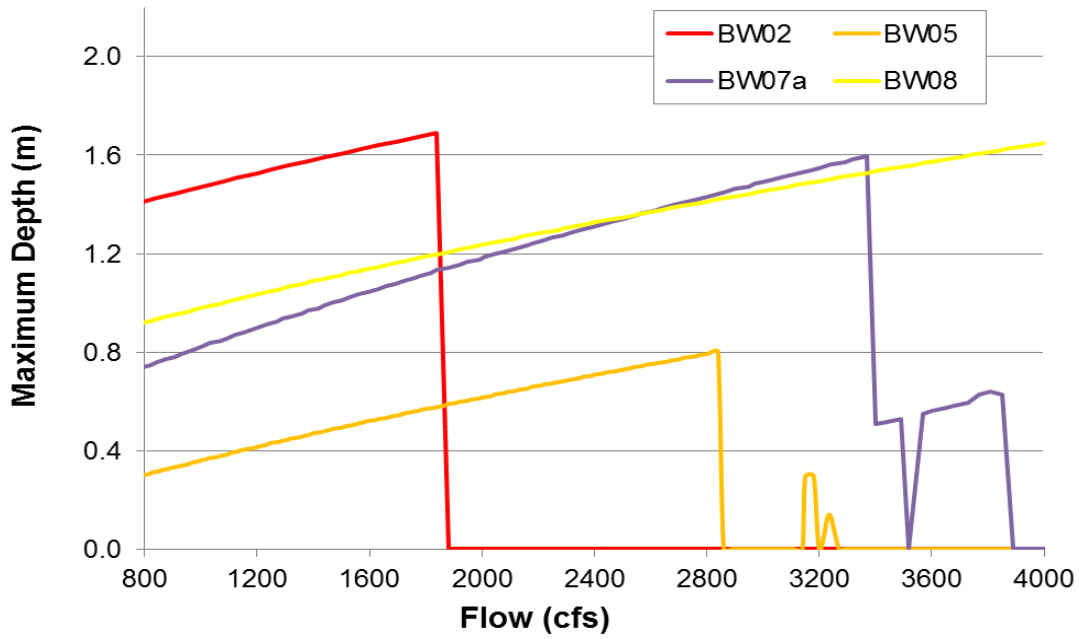


FIGURE A4-24 Maximum Depth (m) of the Four Backwater Areas Surveyed in 2005 Modeled across Base Flows (800–4,000 cfs)

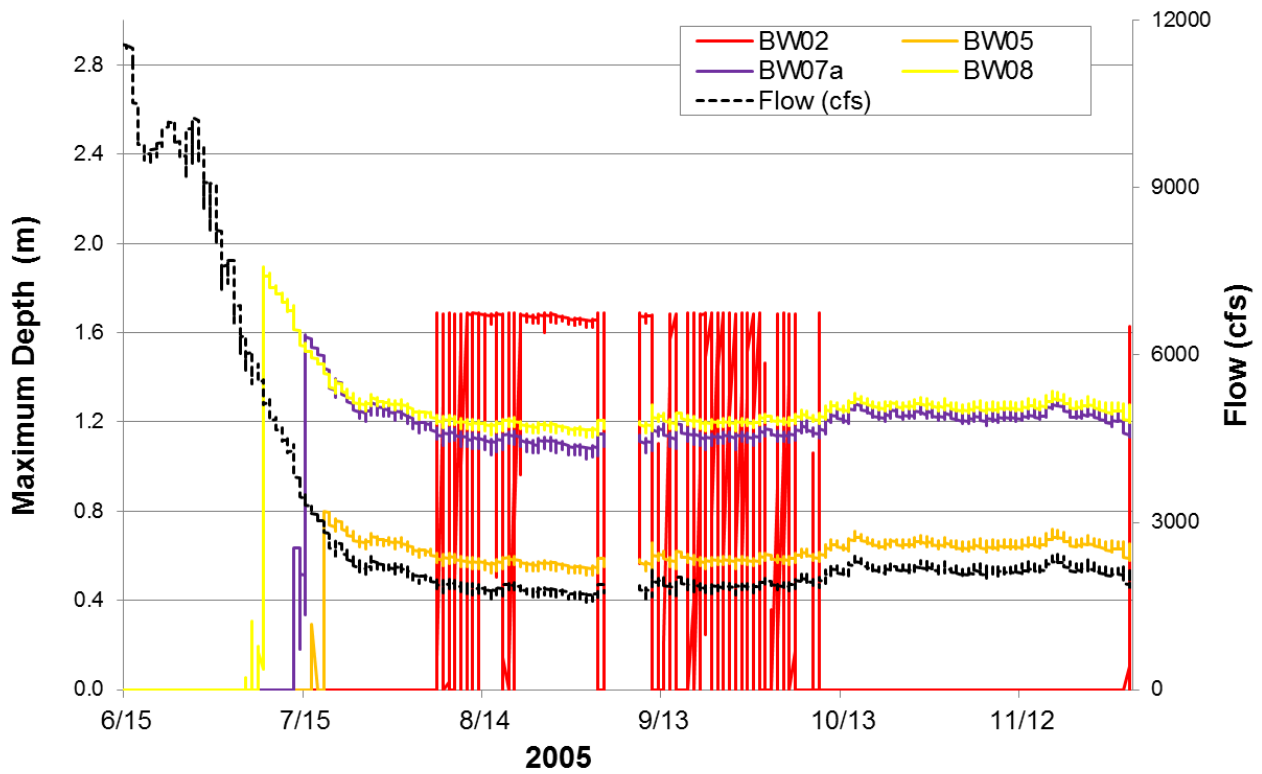


FIGURE A4-25 Maximum Depth (m) of Each of the Four Backwater Areas Modeled during 2005 (June 15–November 30)

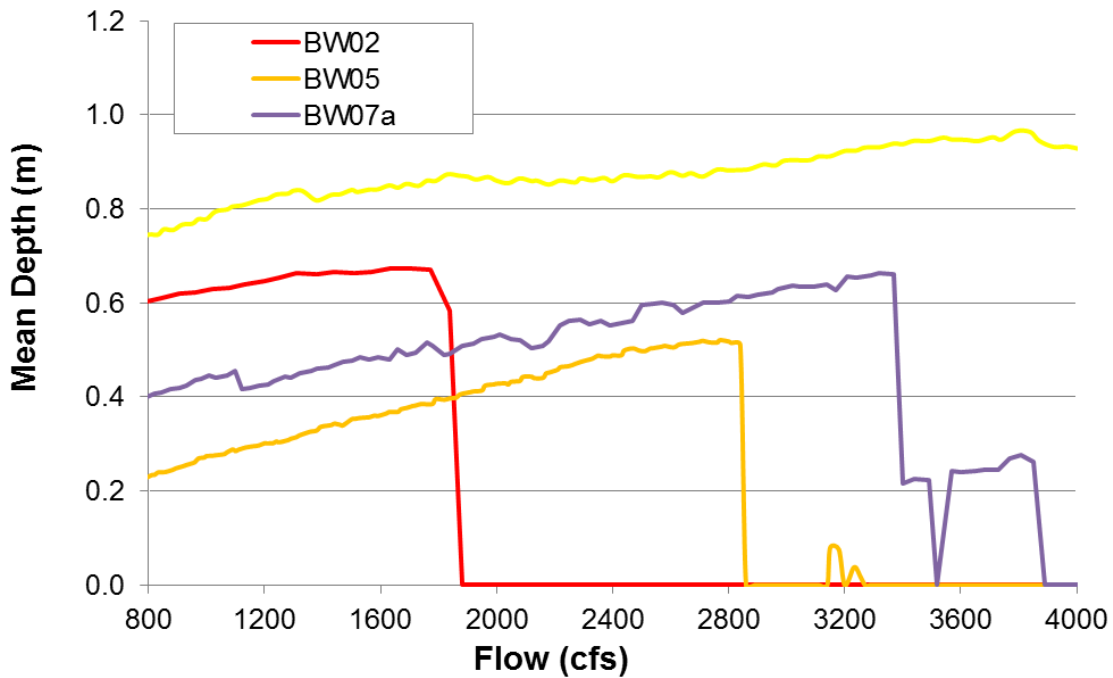


FIGURE A4-26 Mean Depth (m) of the Four Backwater Areas Surveyed in 2005 Modeled across Base Flows (800–4,000 cfs)

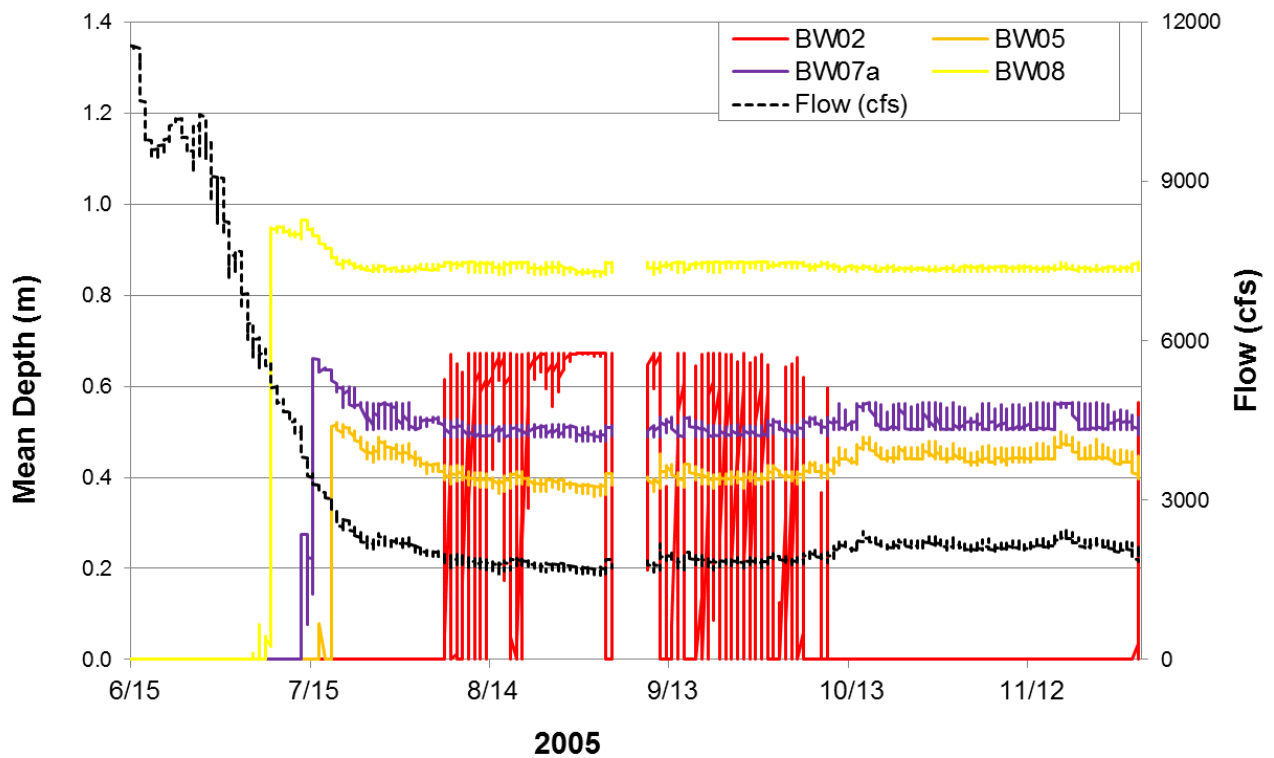


FIGURE A4-27 Mean Depth (m) of Each of the Four Backwater Areas Modeled during 2005 (June 15–November 30)

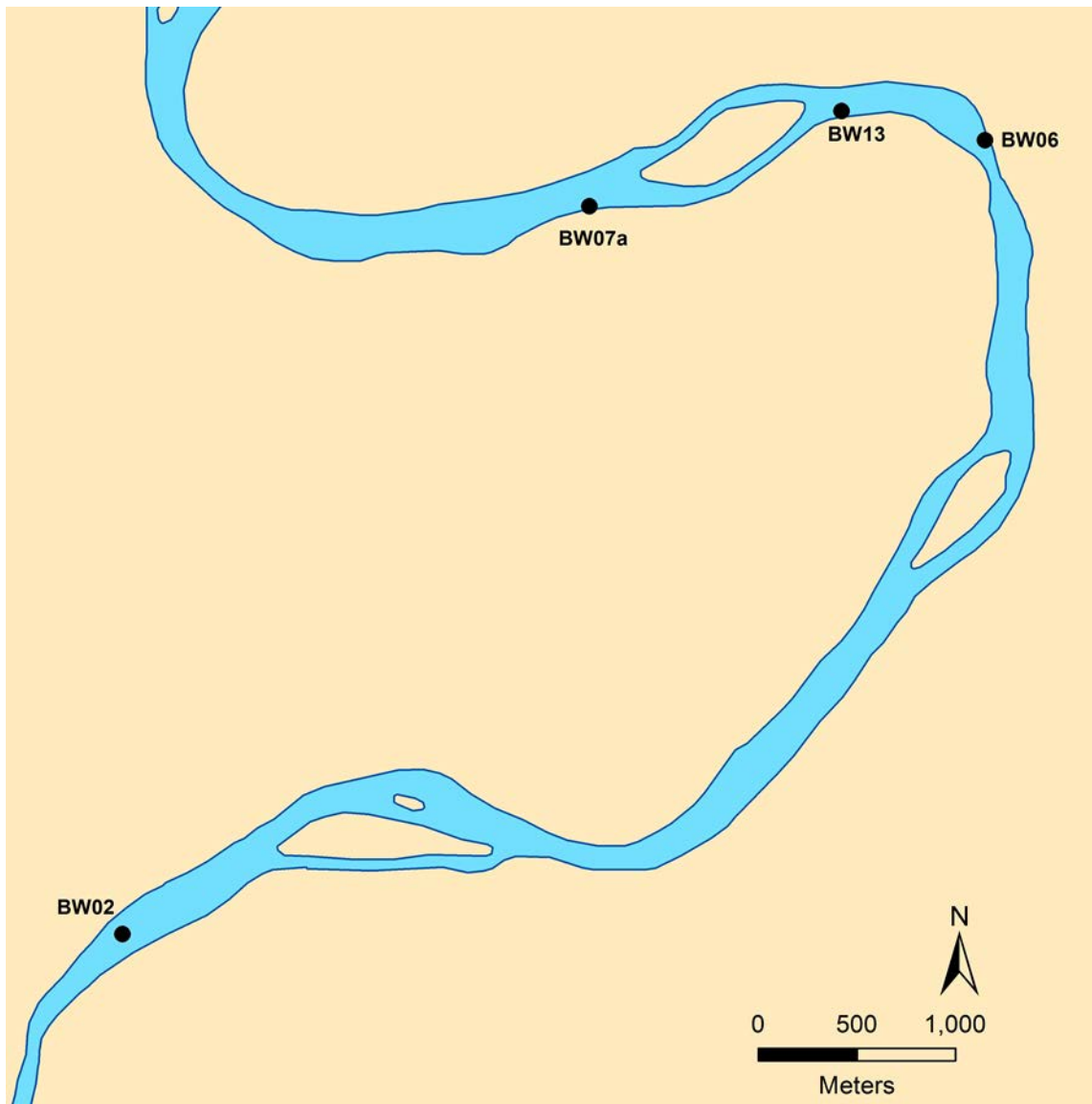


FIGURE A4-28 Green River Backwater Areas BW02, BW06, BW07a, and BW13 Surveyed and Modeled in 2006

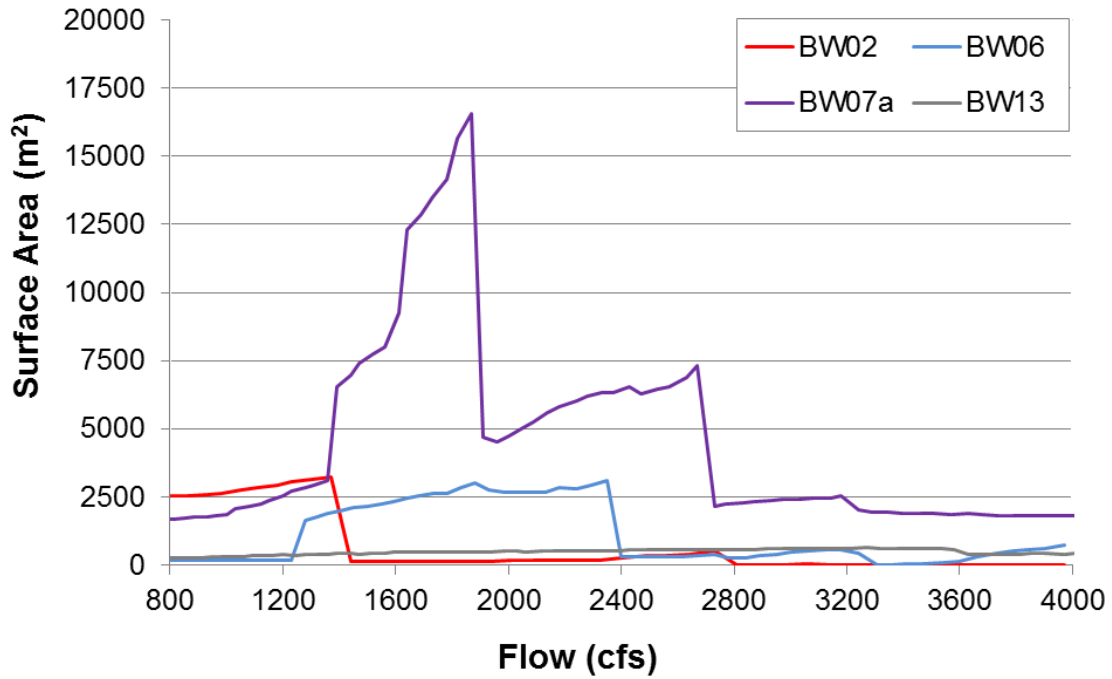


FIGURE A4-29 Surface Area (m²) of the Four Backwater Areas Surveyed in 2006 Modeled across Base Flows (800–4,000 cfs)

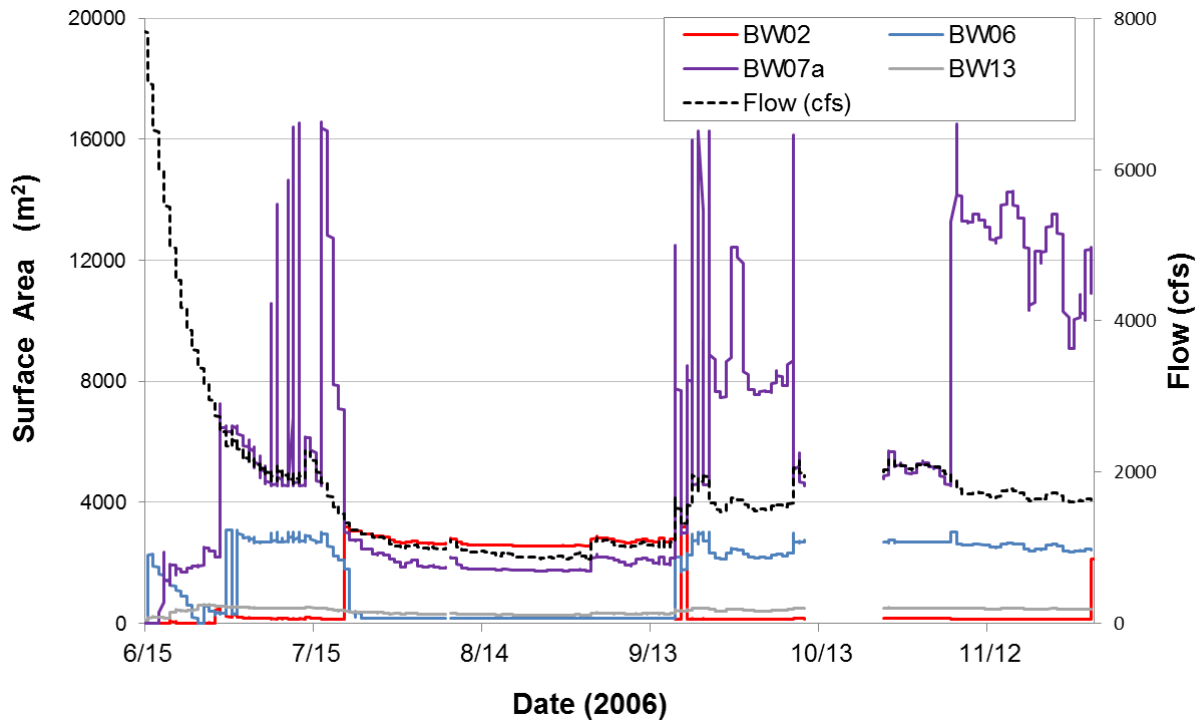


FIGURE A4-30 Surface Area (m²) of Each of the Four Backwater Areas Modeled during 2006 (June 15–November 30)

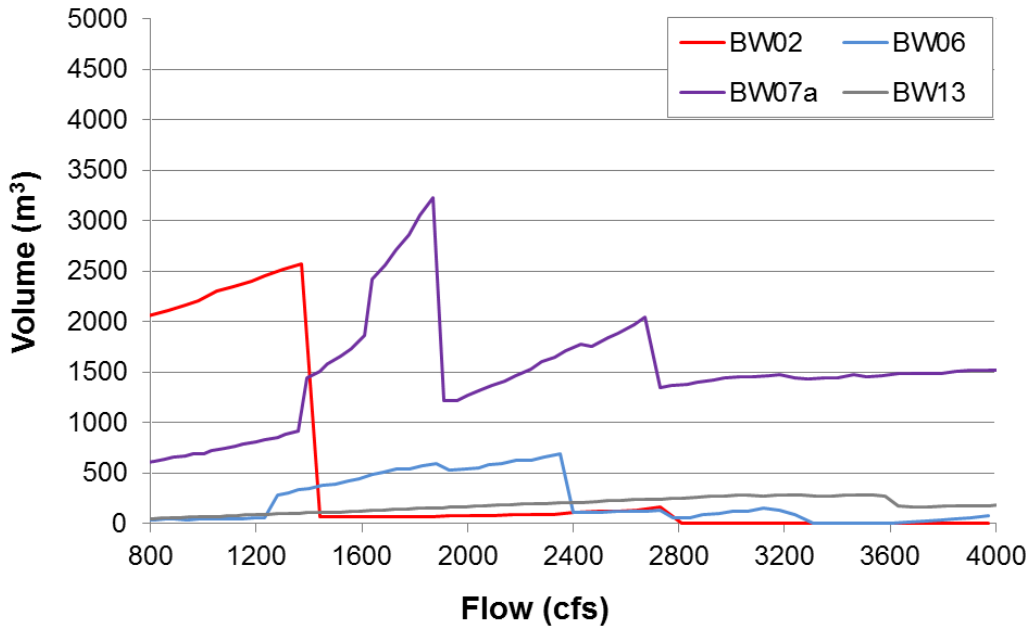


FIGURE A4-31 Volume (m^3) of the Four Backwater Areas Surveyed in 2006 Modeled across Base Flows (800–4,000 cfs)

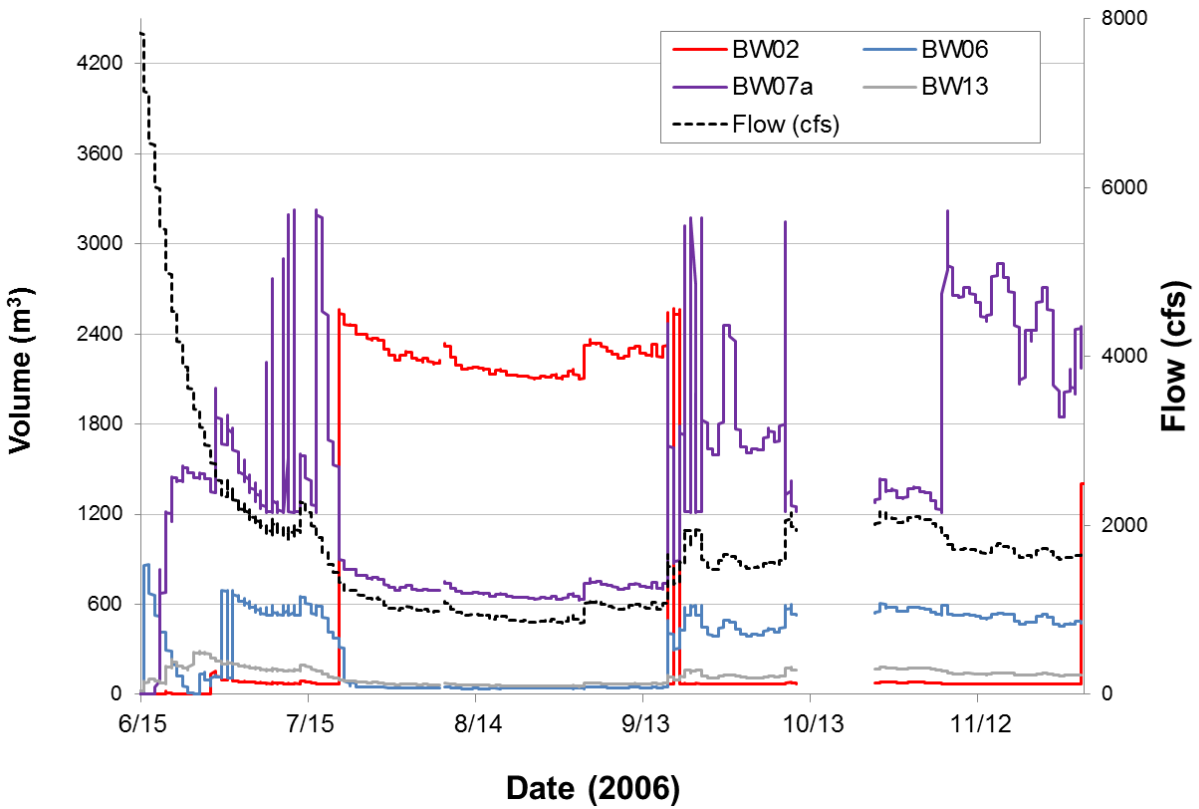


FIGURE A4-32 Volume (m^3) of Each of the Four Backwater Areas Modeled during 2006 (June 15–November 30)

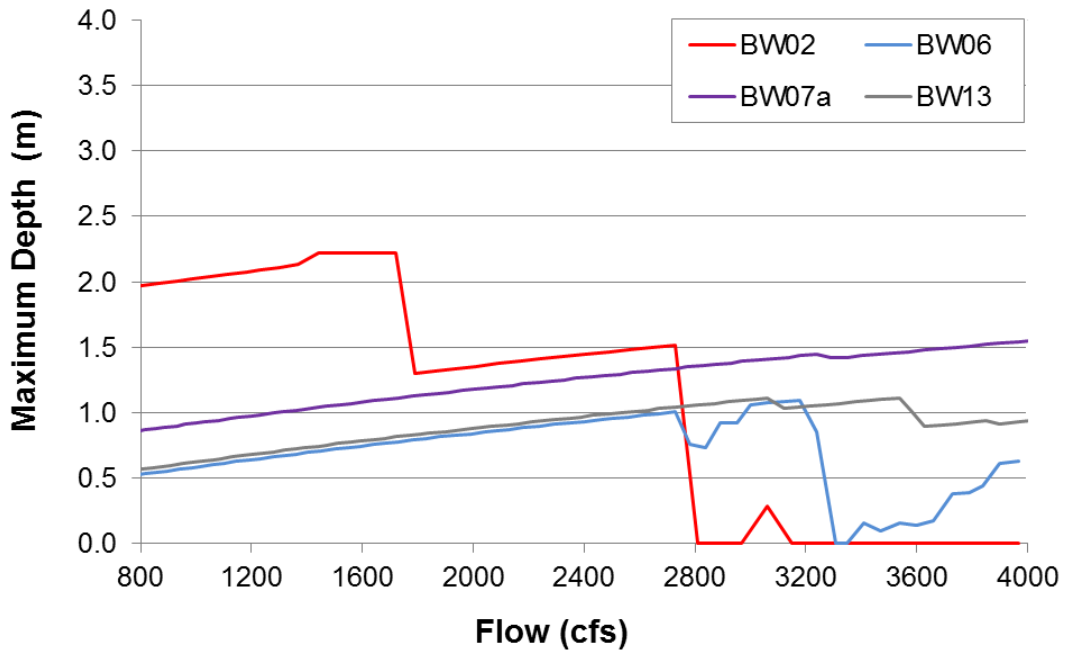


FIGURE A4-33 Maximum Depth (m) of the Four Backwater Areas Surveyed in 2006 Modeled across Base Flows (800–4,000 cfs)

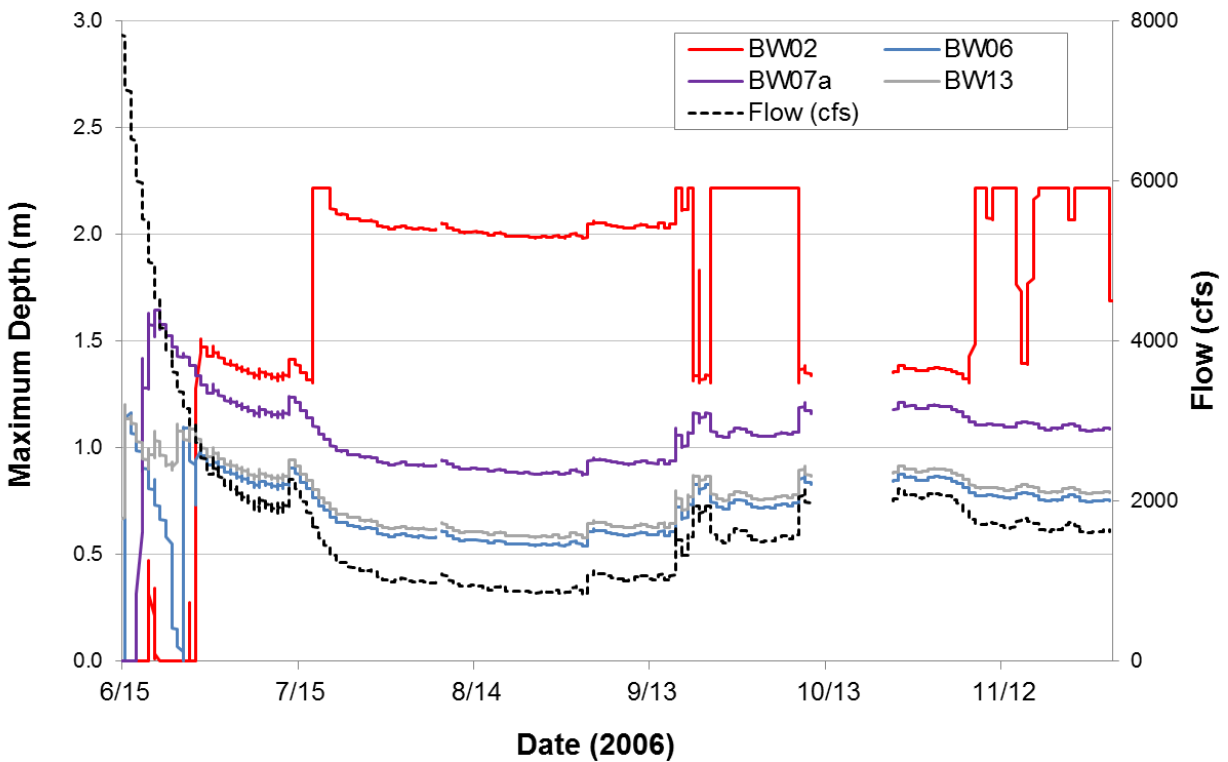


FIGURE A4-34 Maximum Depth (m) of Each of the Four Backwater Areas Modeled during 2006 (June 15–November 30)

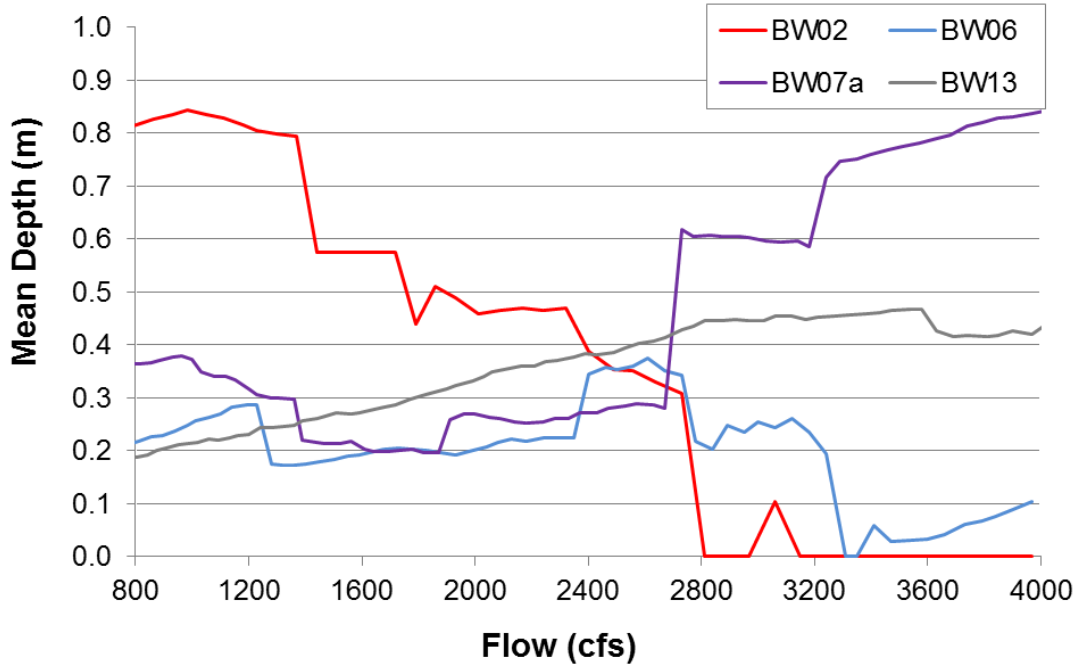


FIGURE A4-35 Mean Depth (m) of the Four Backwater Areas Surveyed in 2006 Modeled across Base Flows (800–4,000 cfs)

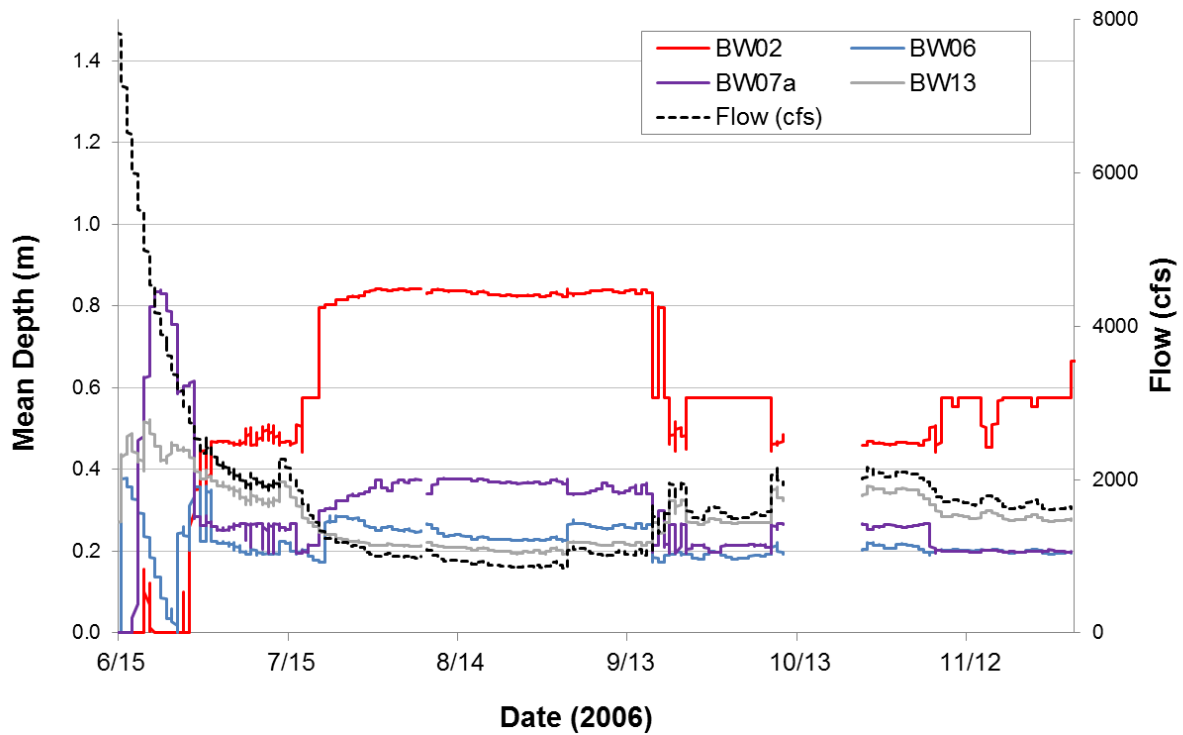


FIGURE A4-36 Mean Depth (m) of Each of the Four Backwater Areas Modeled during 2006 (June 15–November 30)

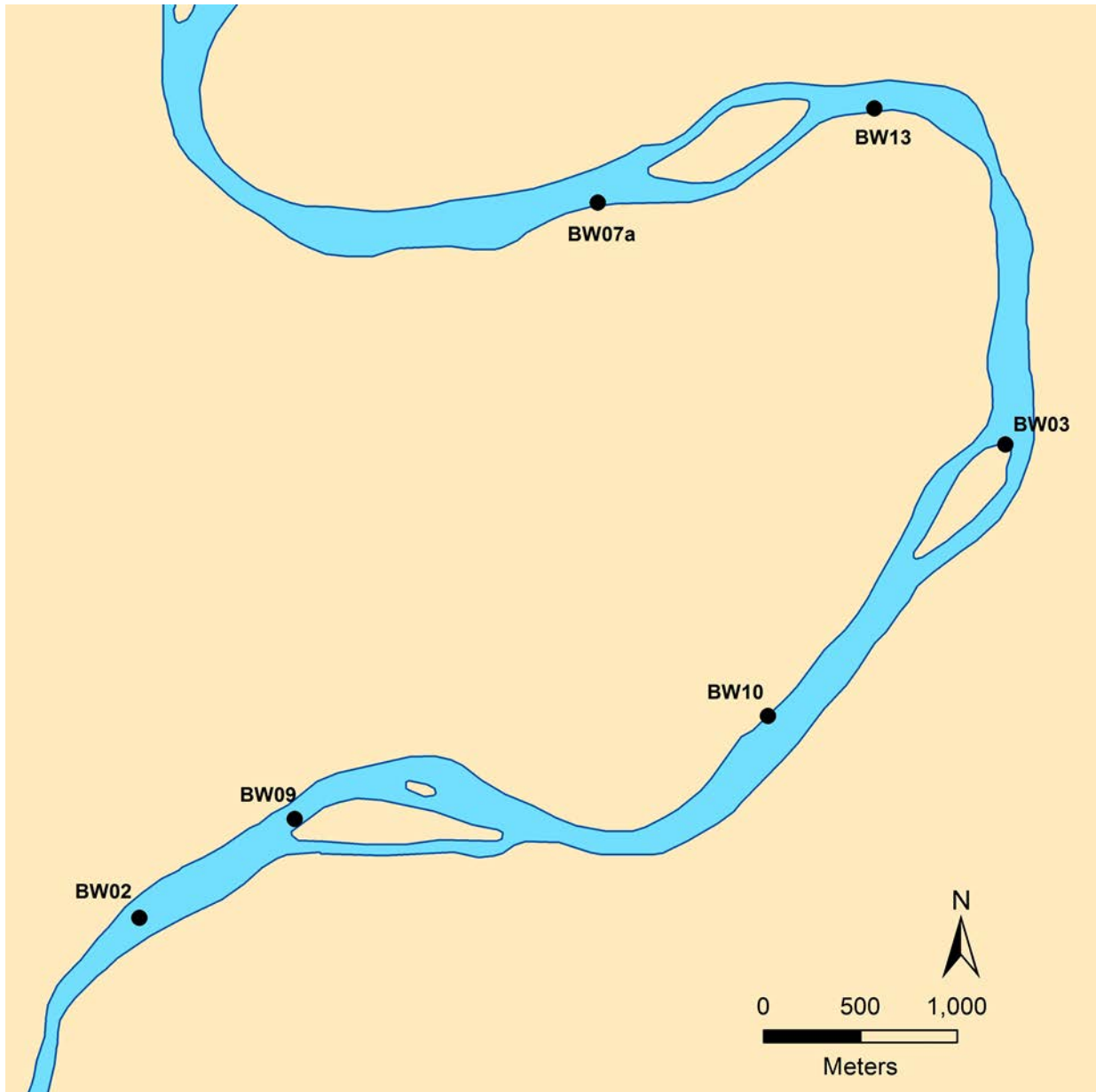


FIGURE A4-37 Green River Backwater Areas BW02, BW03, BW07a, BW13, BW09, and BW10 Surveyed and Modeled in 2008

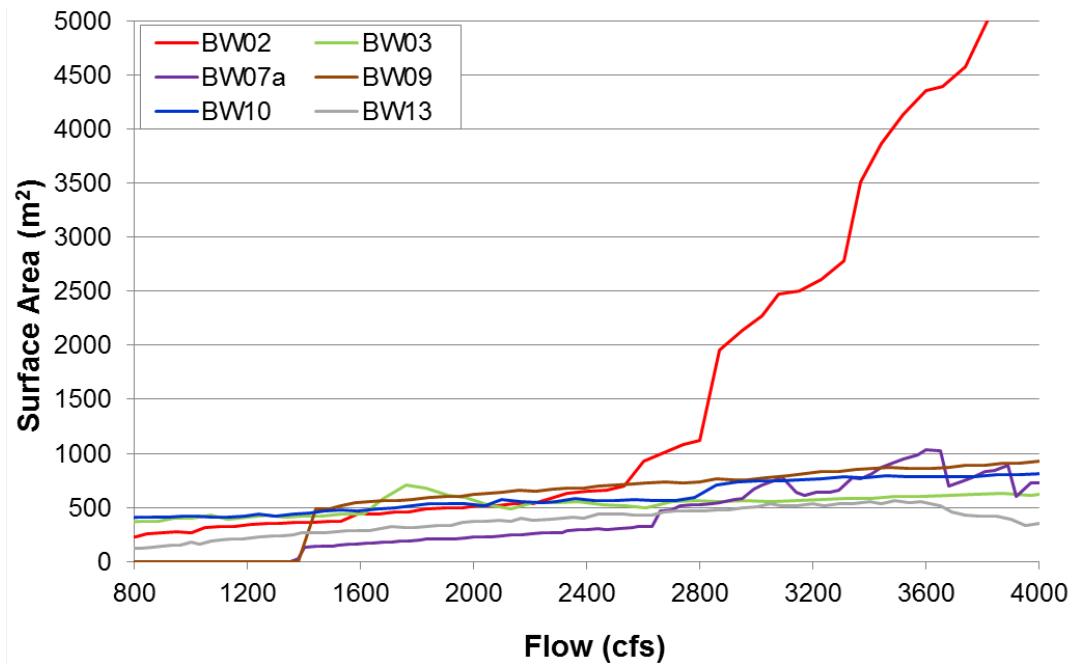


FIGURE A4-38 Surface Area (m²) of the Six Backwater Areas Surveyed in 2008 Modeled across Base Flows (800–4,000 cfs)

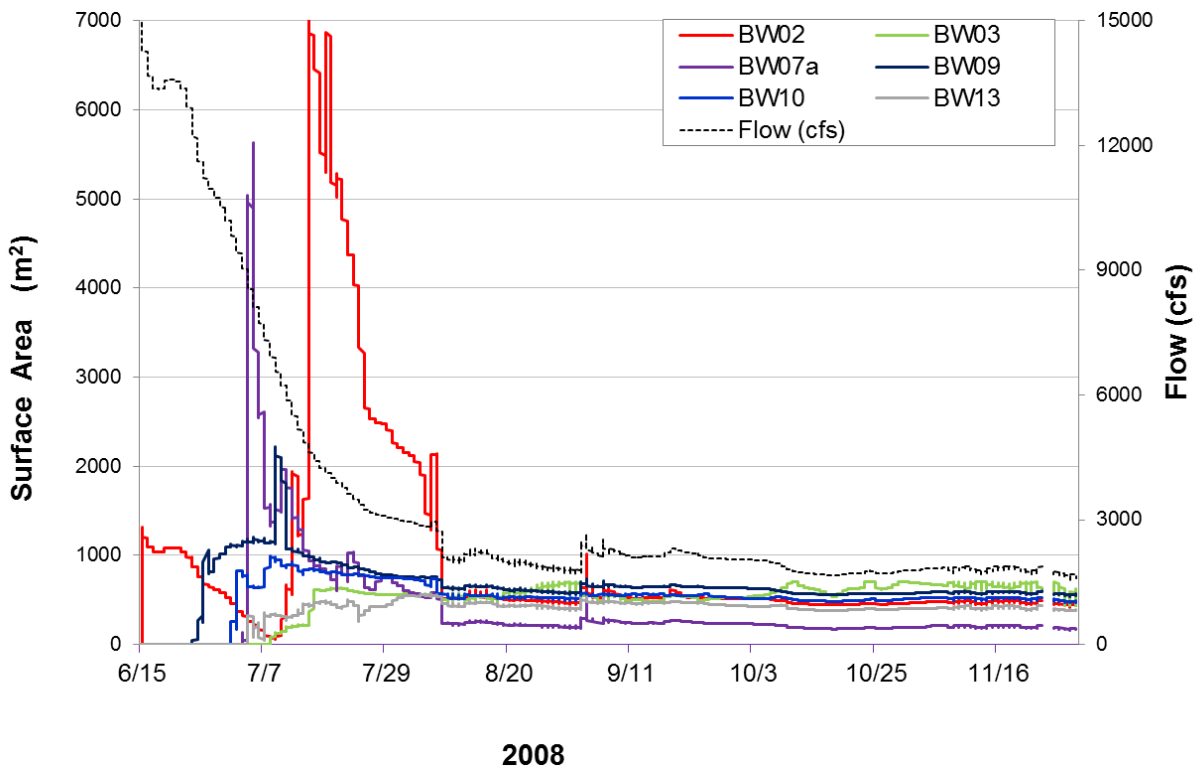


FIGURE A4-39 Surface Area (m²) of Each of the Six Backwater Areas Modeled during 2008 (June 15–November 30)

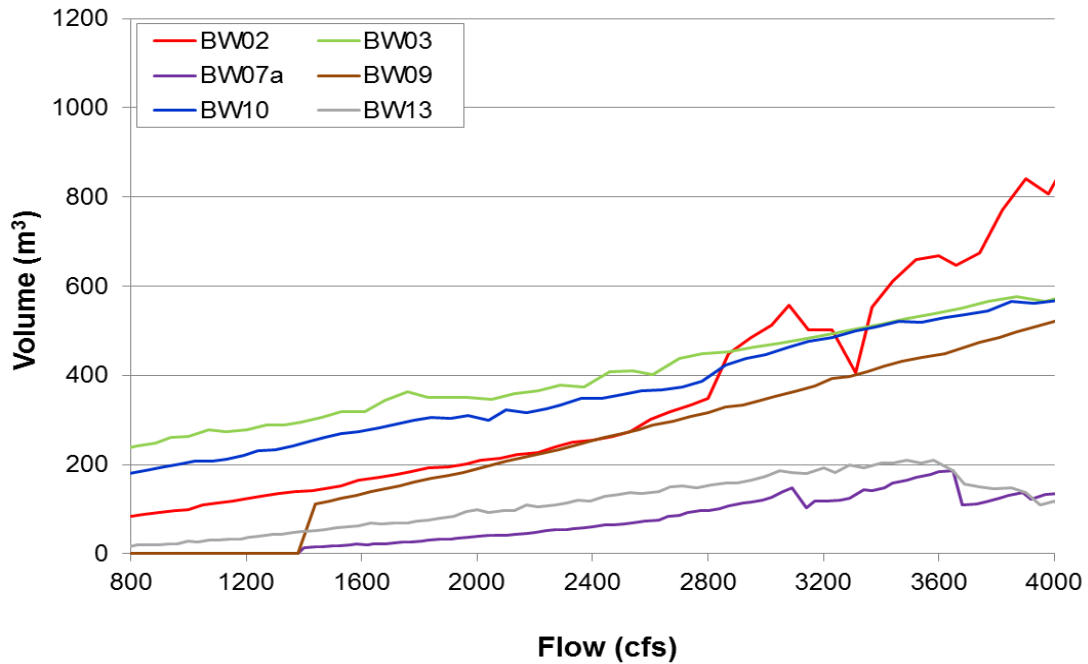


FIGURE A4-40 Volume (m³) of the Six Backwater Areas Surveyed in 2008 Modeled across Base Flows (800–4,000 cfs)

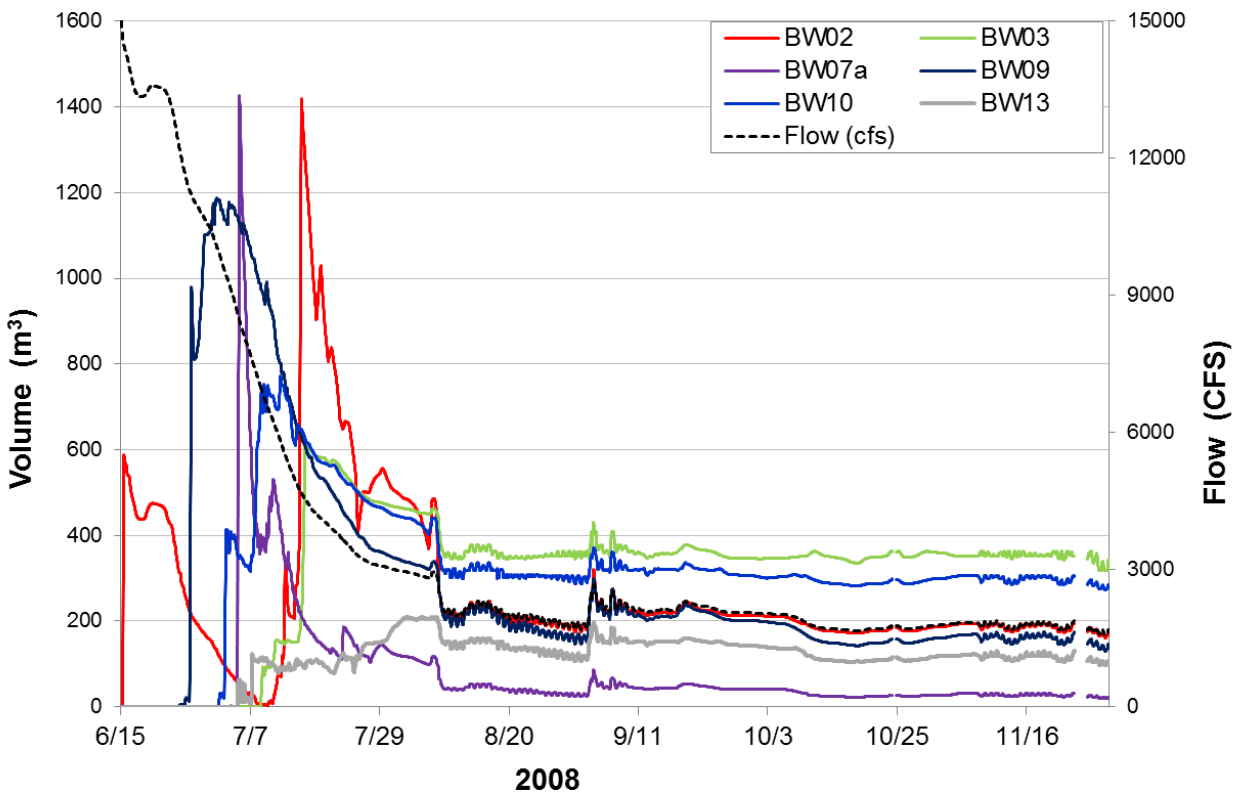


FIGURE A4-41 Volume (m³) of Each of the Six Backwater Areas Modeled during 2008 (June 15–November 30)

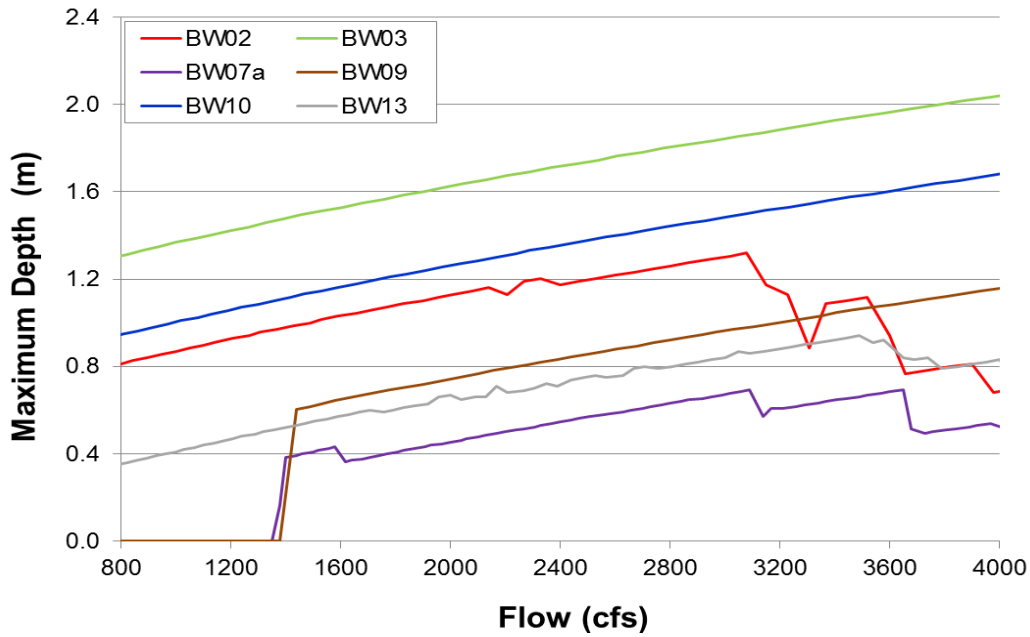


FIGURE A4-42 Maximum Depth (m) of the Six Backwater Areas Surveyed in 2008 Modeled across Base Flows (800–4,000 cfs)

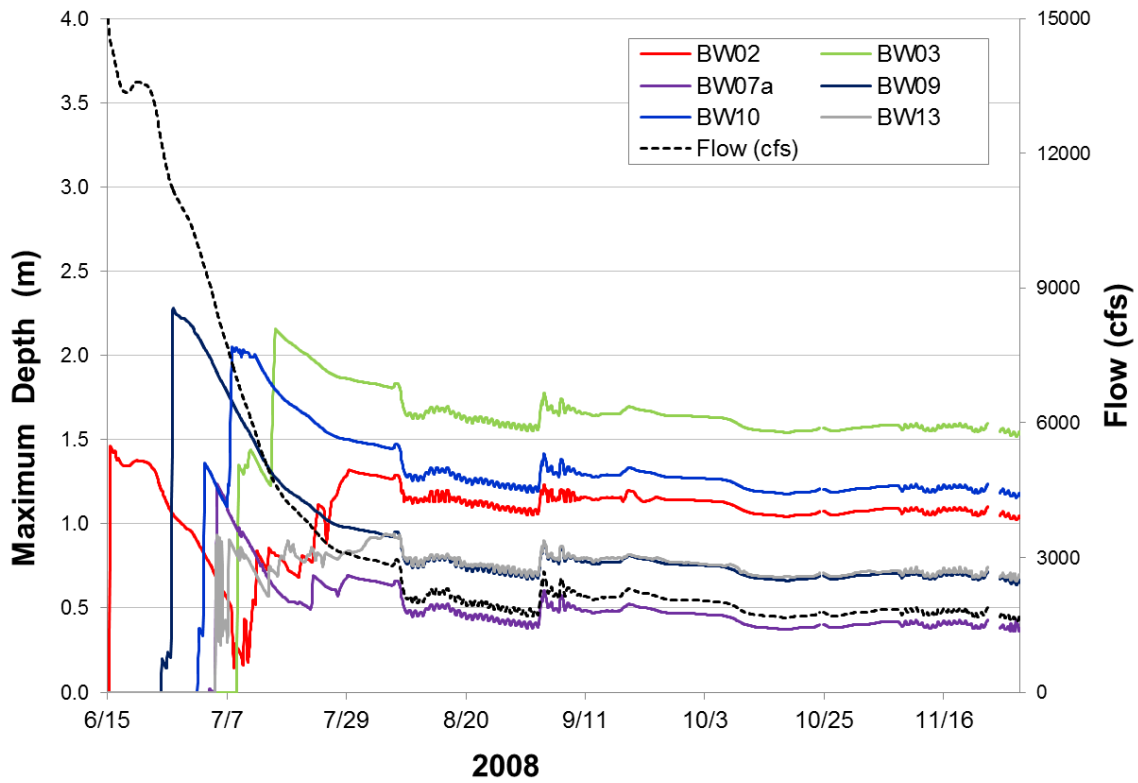


FIGURE A4-43 Maximum Depth (m) of Each of the Six Backwater Areas Modeled during 2008 (June 15–November 30)

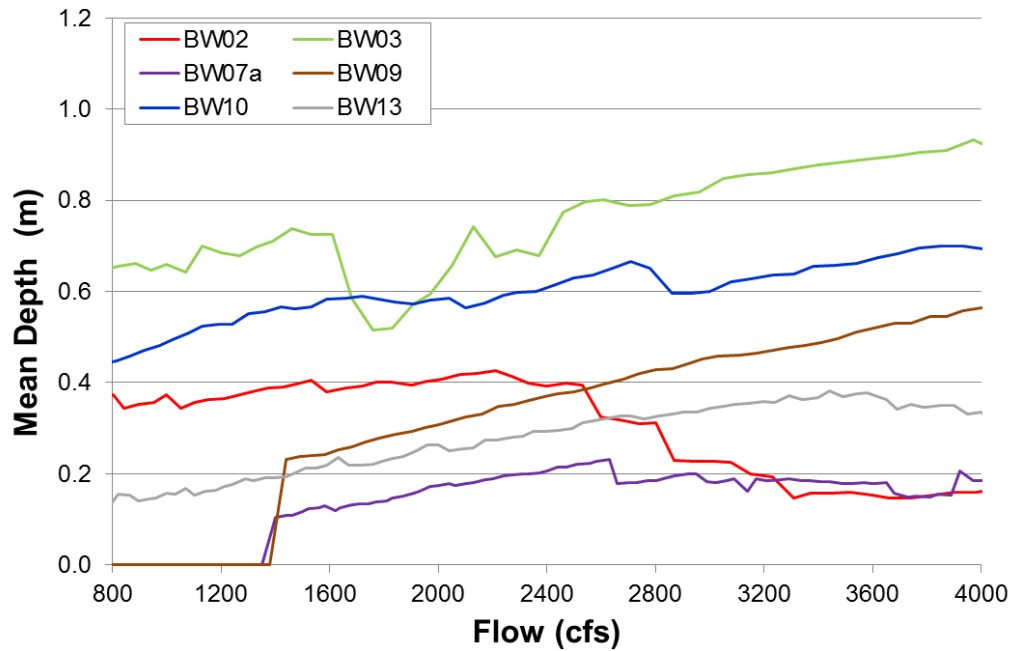


FIGURE A4-44 Mean Depth (m) of the Six Backwater Areas Surveyed in 2008 Modeled across Base Flows (800–4,000 cfs)

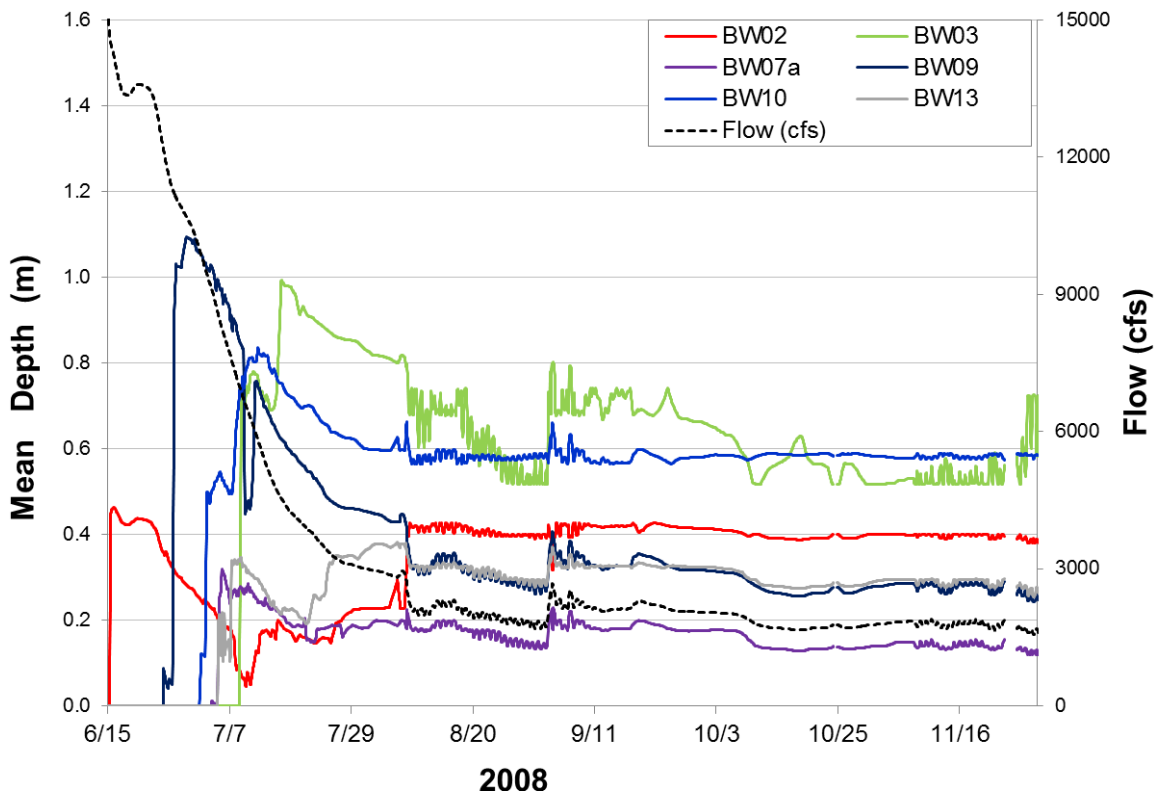


FIGURE A4-45 Mean Depth (m) of Each of the Six Backwater Areas Modeled during 2008 (June 15–November 30)

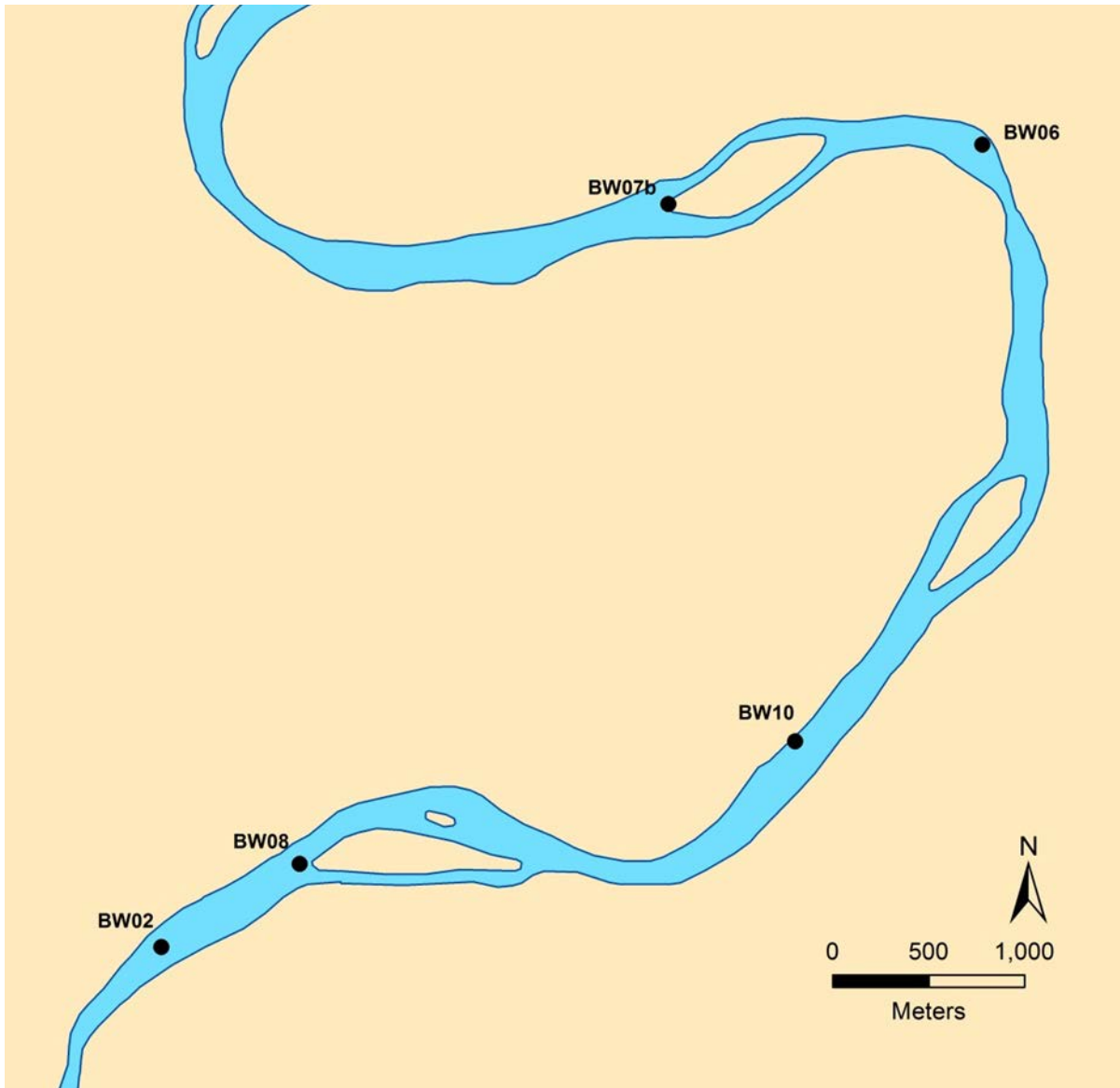


FIGURE A4-46 Green River Backwater Areas BW02, BW06, BW07b, BW08, and BW10 Surveyed and Modeled in 2009

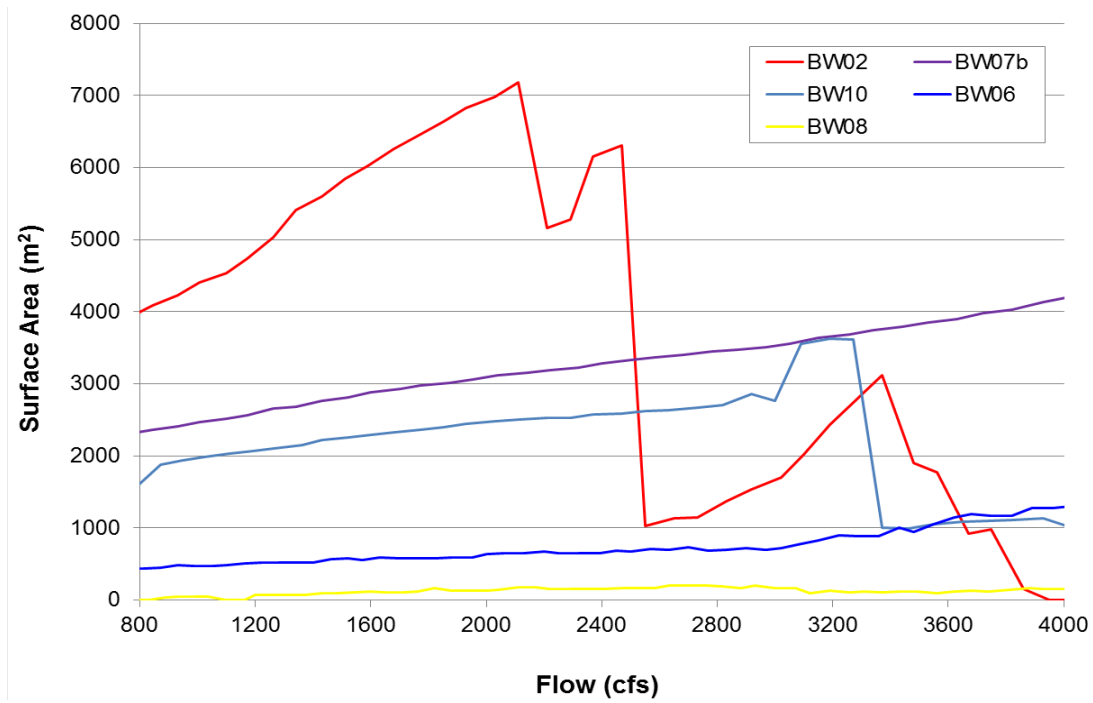


FIGURE A4-47 Surface Area (m²) of the Five Backwater Areas Surveyed in 2009 Modeled across Base Flows (800–4,000 cfs)

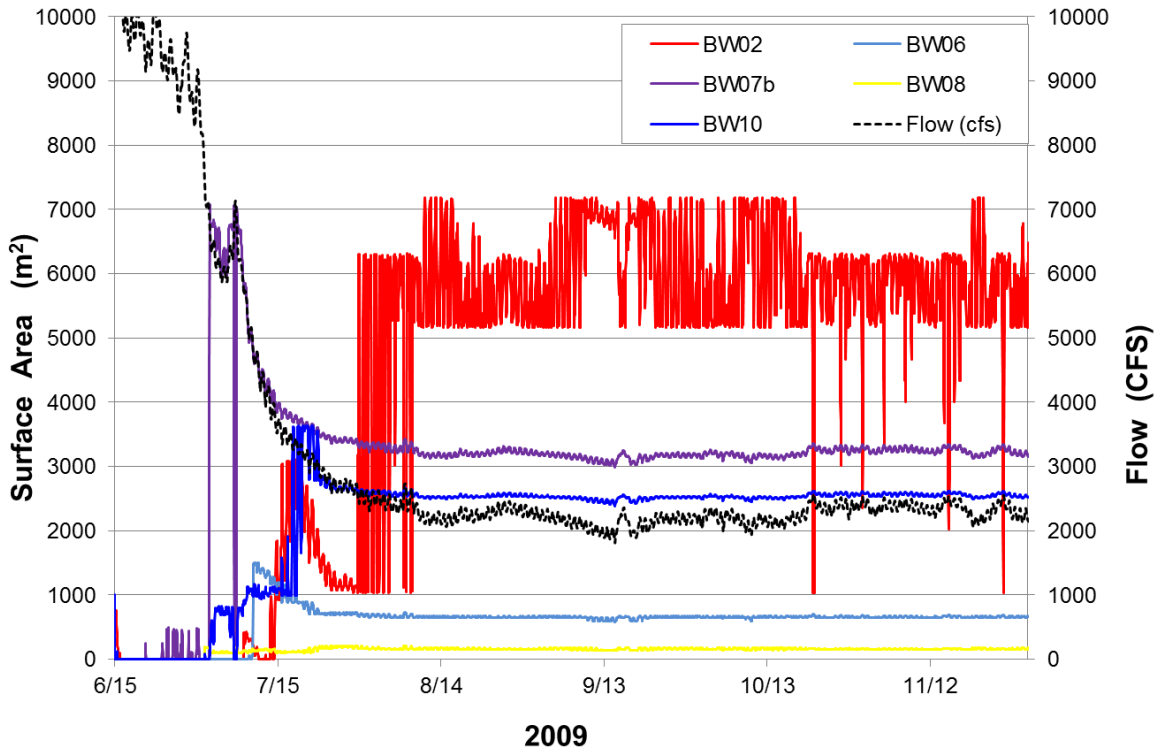


FIGURE A4-48 Surface Area (m²) of Each of the Five Backwater Areas Modeled during 2009 (June 15–November 30)

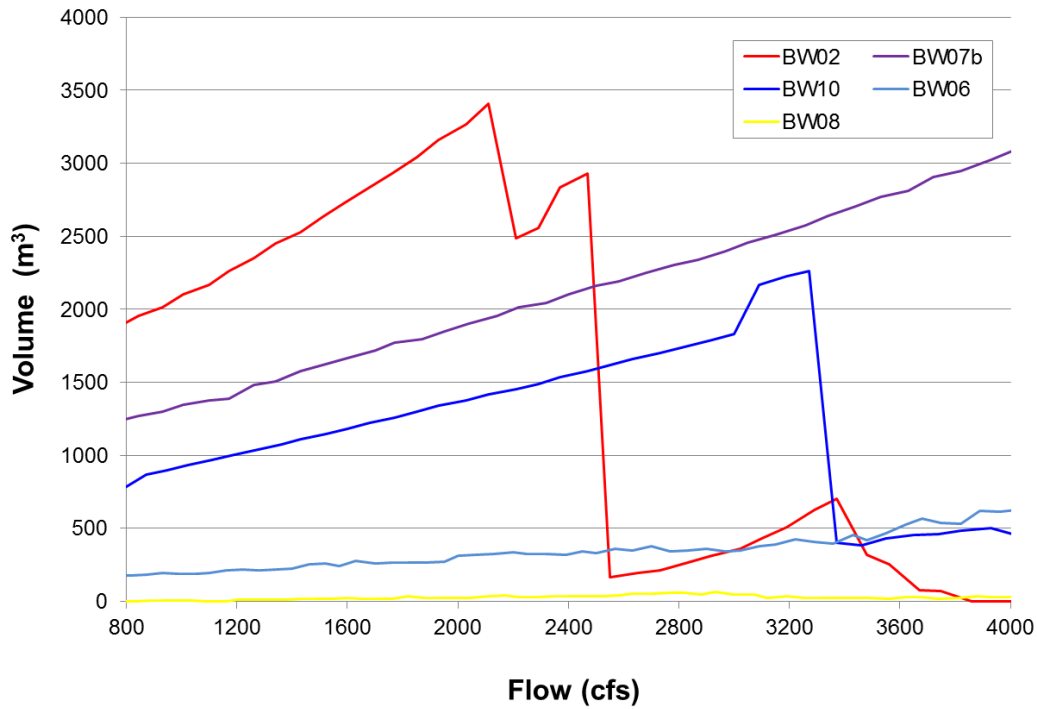


FIGURE A4-49 Volume (m³) of the Five Backwater Areas Surveyed in 2009 Modeled across Base Flows (800–4,000 cfs)

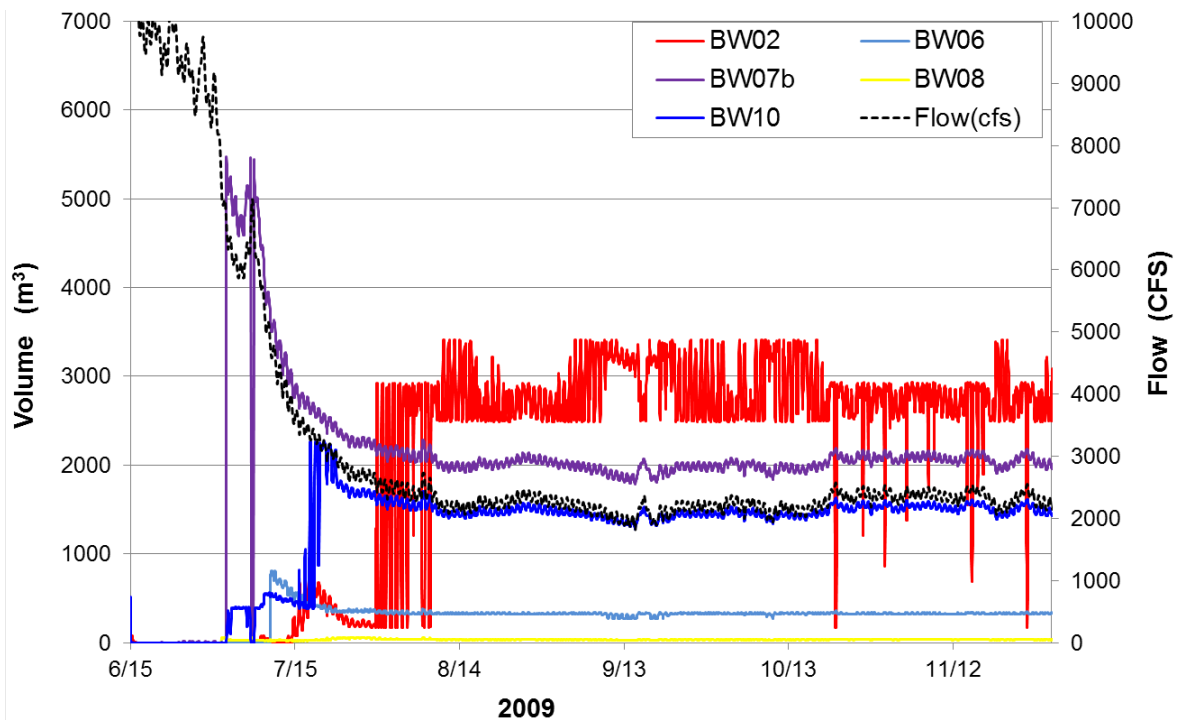


FIGURE A4-50 Volume (m³) of Each of the Five Backwater Areas Modeled during 2009 (June 15–November 30)

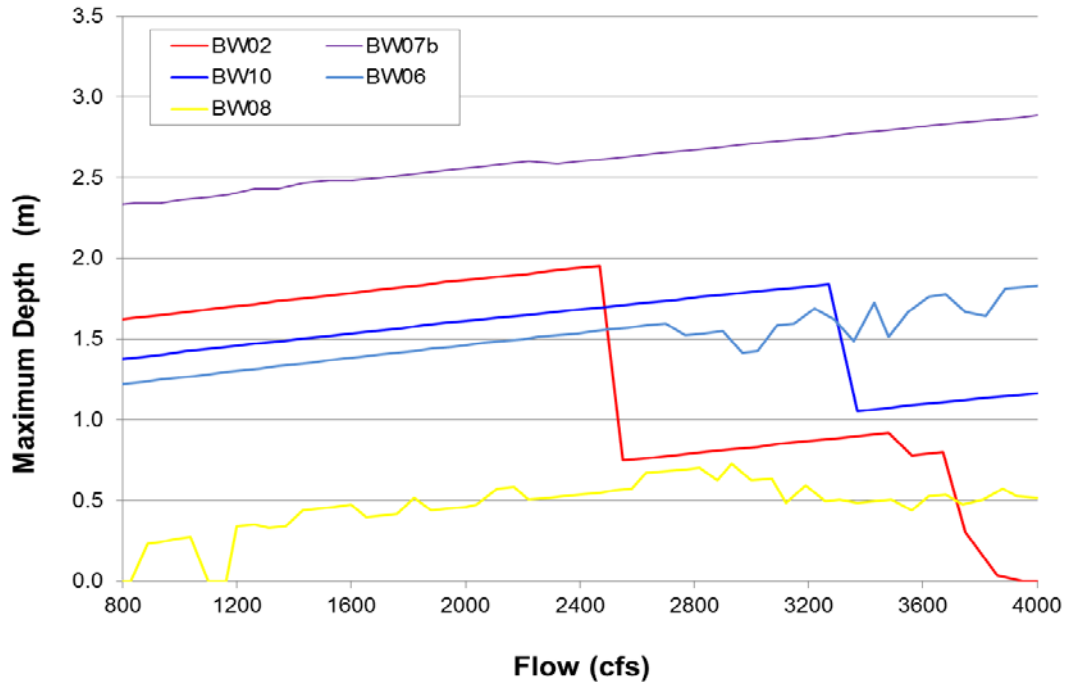


FIGURE A4-51 Maximum Depth (m) of the Five Backwater Areas Surveyed in 2009 Modeled across Base Flows (800–4,000 cfs)

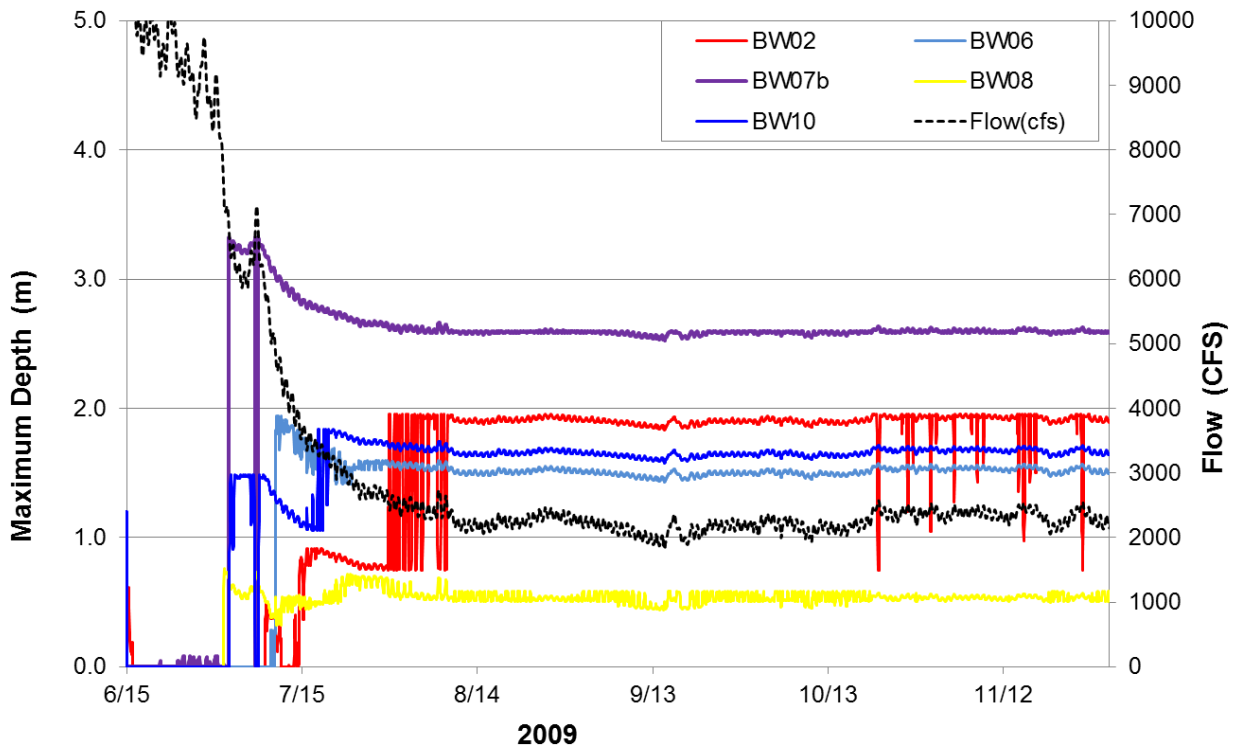


FIGURE A4-52 Maximum Depth (m) of Each of the Five Backwater Areas Modeled during 2009 (June 15–November 30)

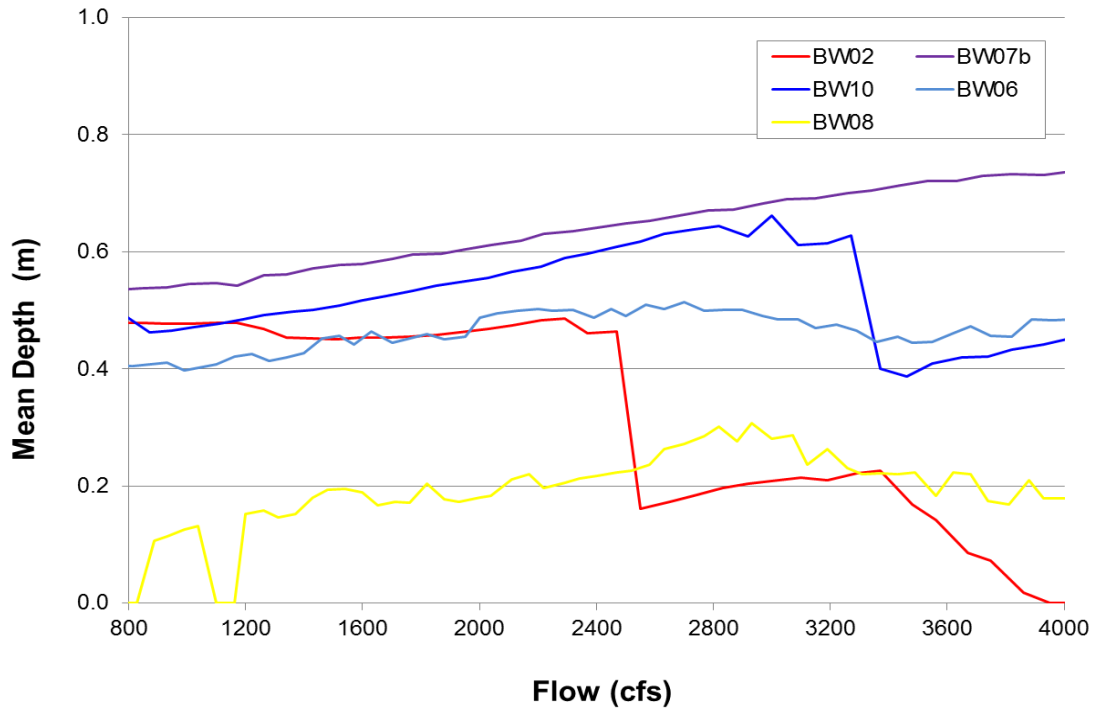


FIGURE A4-53 Mean Depth (m) of the Five Backwater Areas Surveyed in 2009 Modeled across Base Flows (800–4,000 cfs)

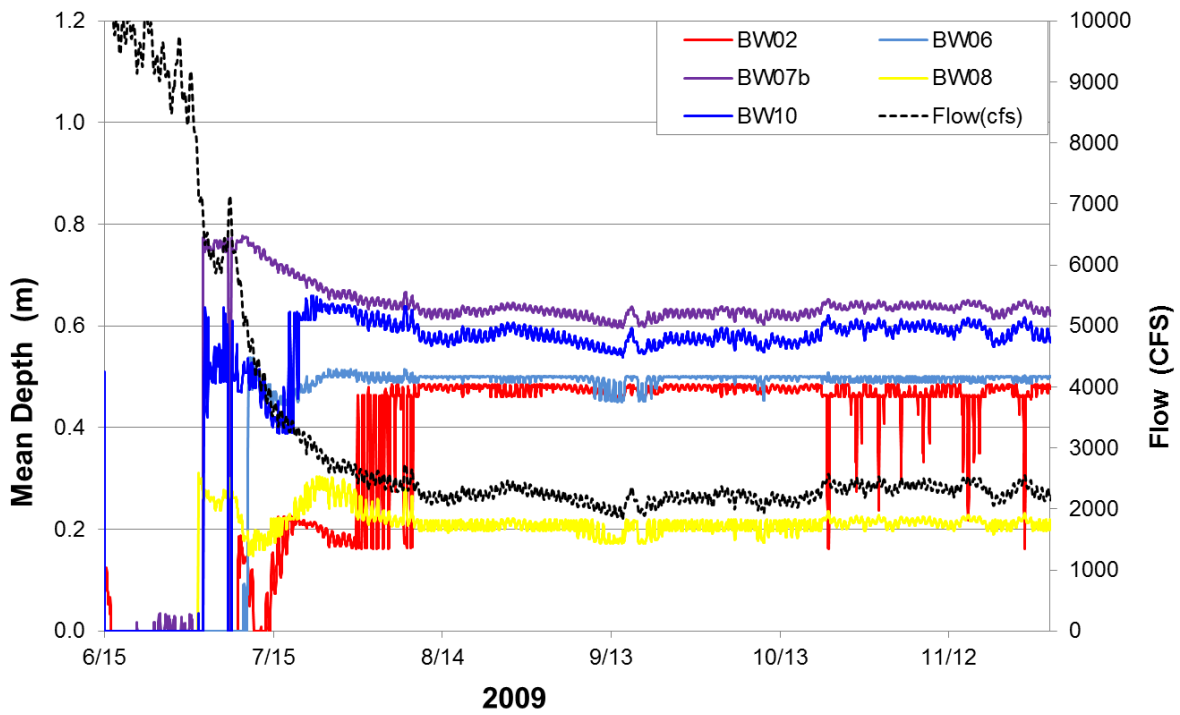


FIGURE A4-54 Mean Depth (m) of Each of the Five Backwater Areas Modeled during 2009 (June 15–November 30)

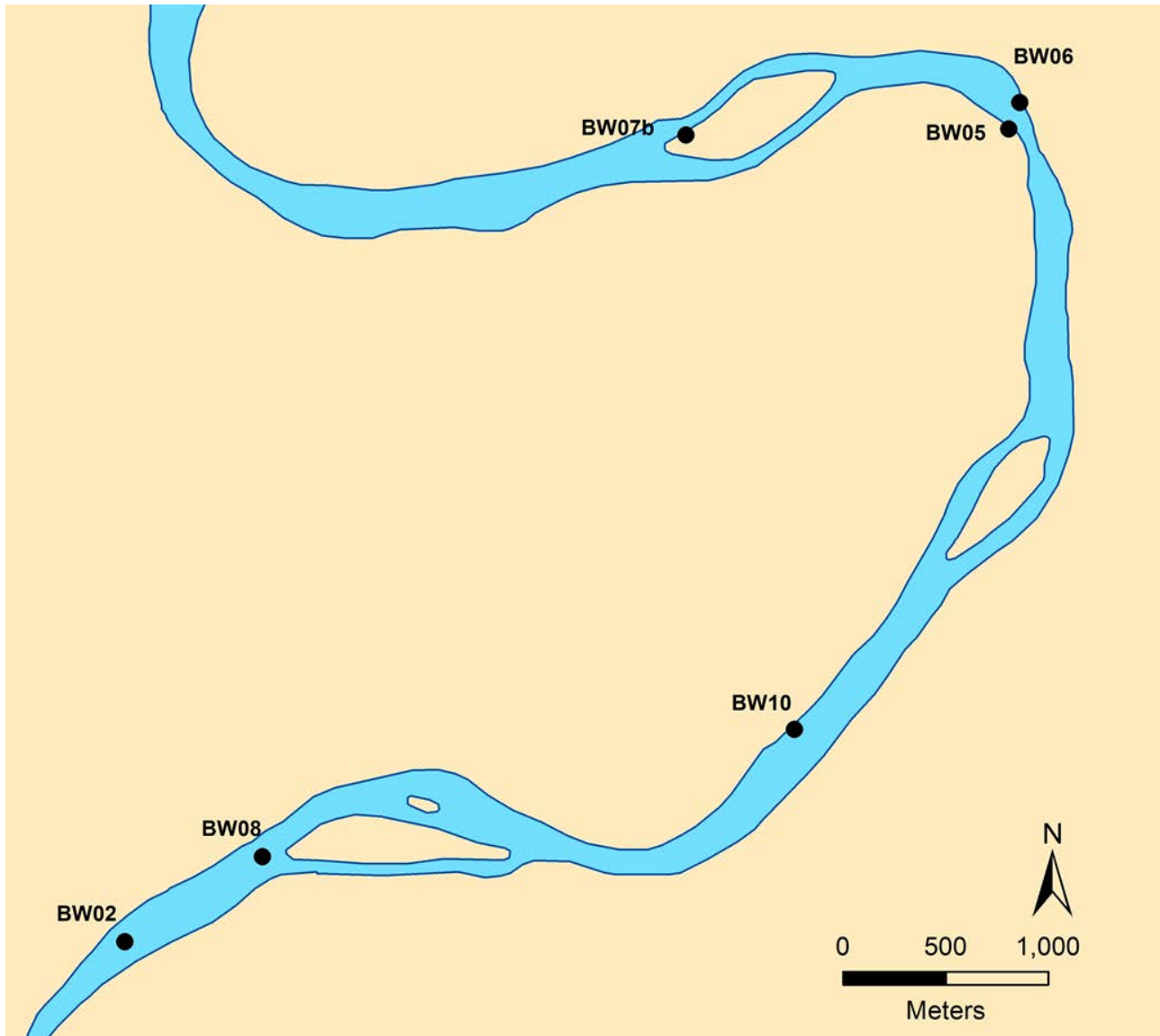


FIGURE A4-55 Green River Backwater Areas BW02, BW05, BW06, BW07b, BW08, and BW10 Surveyed and Modeled in 2010

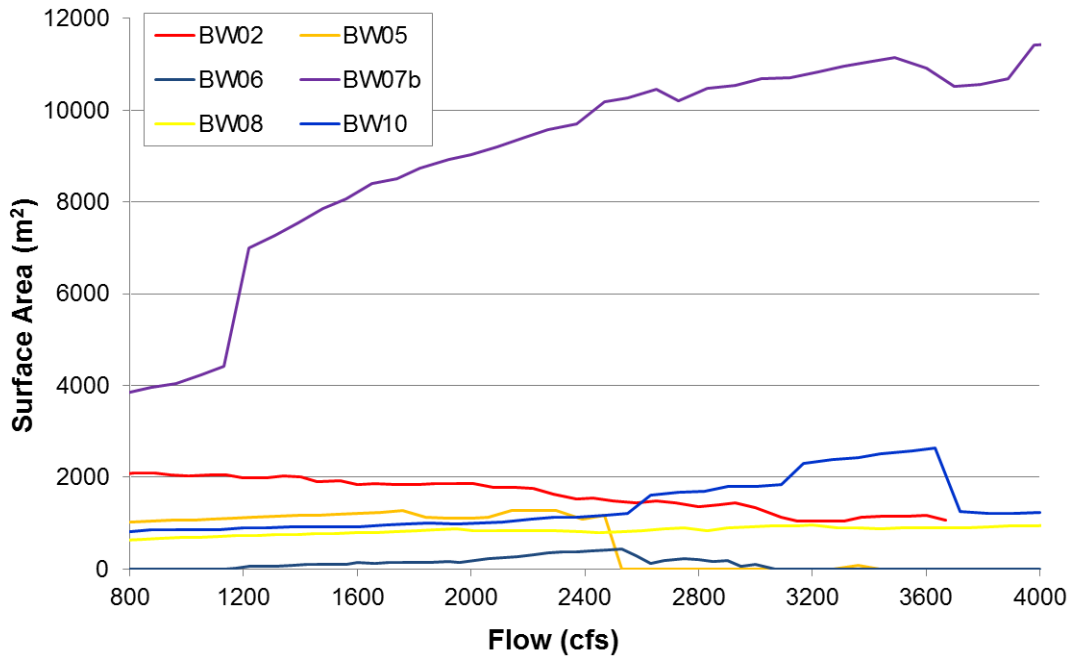


FIGURE A4-56 Surface Area (m²) of the Six Backwater Areas Surveyed in 2010 Modeled across Base Flows (800–4,000 cfs)

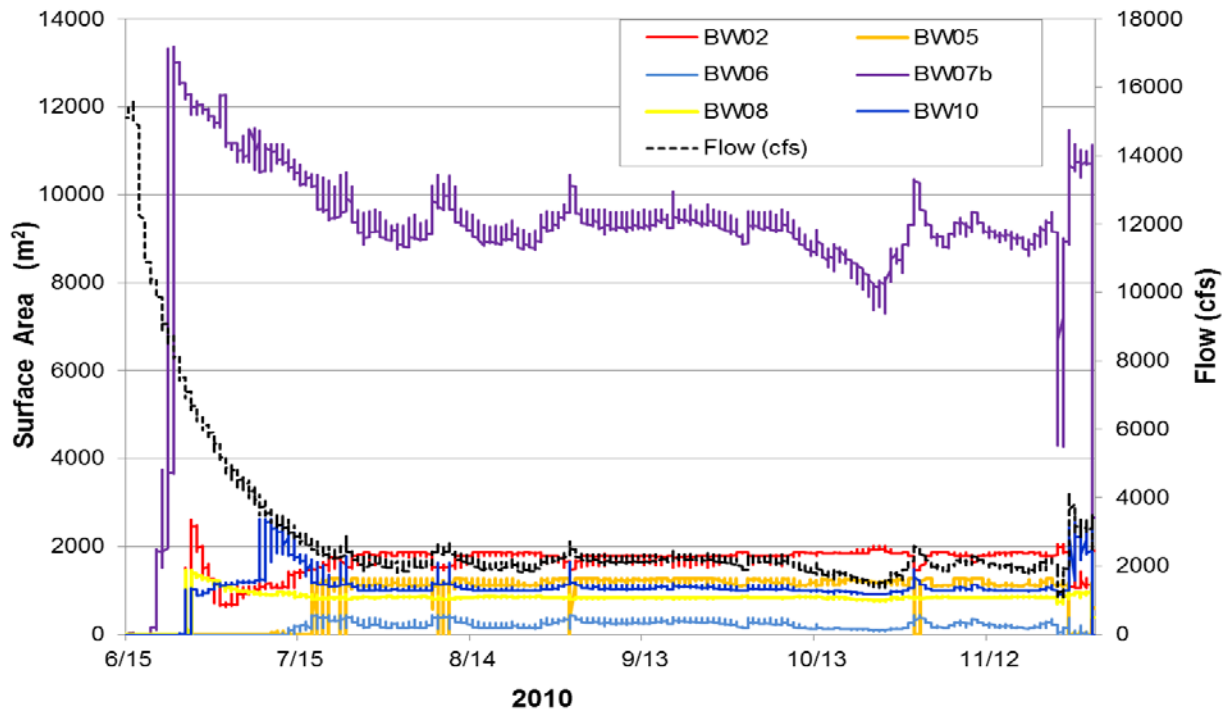


FIGURE A4-57 Surface Area (m²) of Each of the Six Backwater Areas Modeled during 2010 (June 15–November 30)

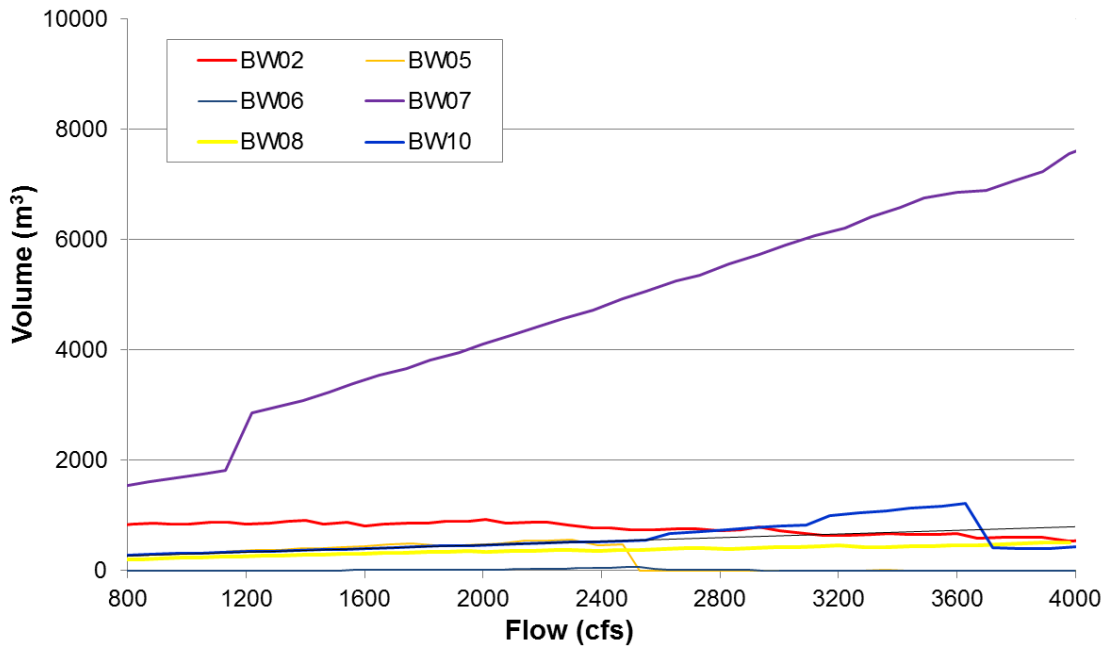


FIGURE A4-58 Volume (m^3) of the Six Backwater Areas Surveyed in 2010 Modeled across Base Flows (800–4,000 cfs)

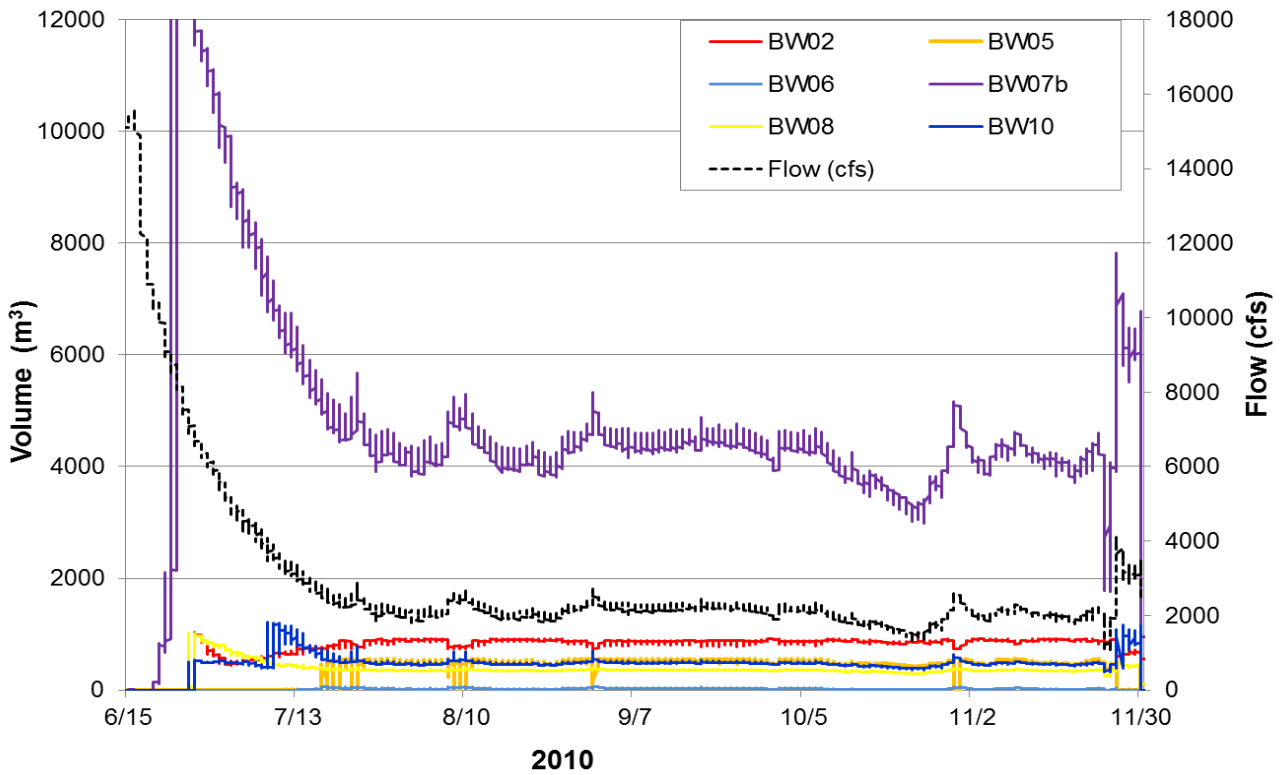


FIGURE A4-59 Volume (m^3) of Each of the Six Backwater Areas Modeled during 2010 (June 15–November 30)

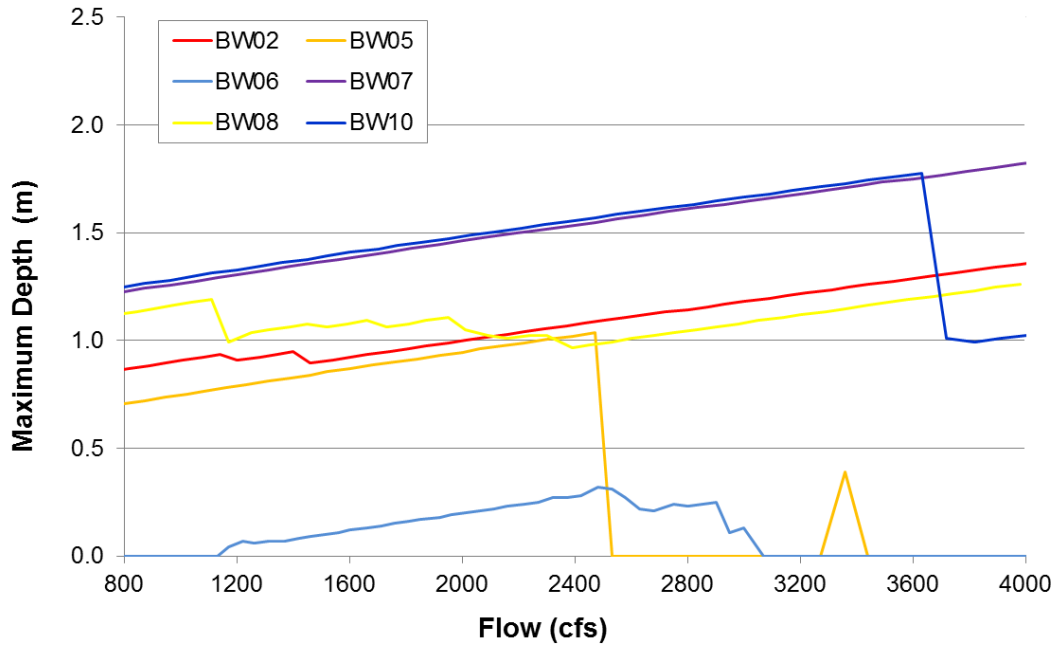


FIGURE A4-60 Maximum Depth (m) of the Six Backwater Areas Surveyed in 2010 Modeled across Base Flows (800–4,000 cfs)

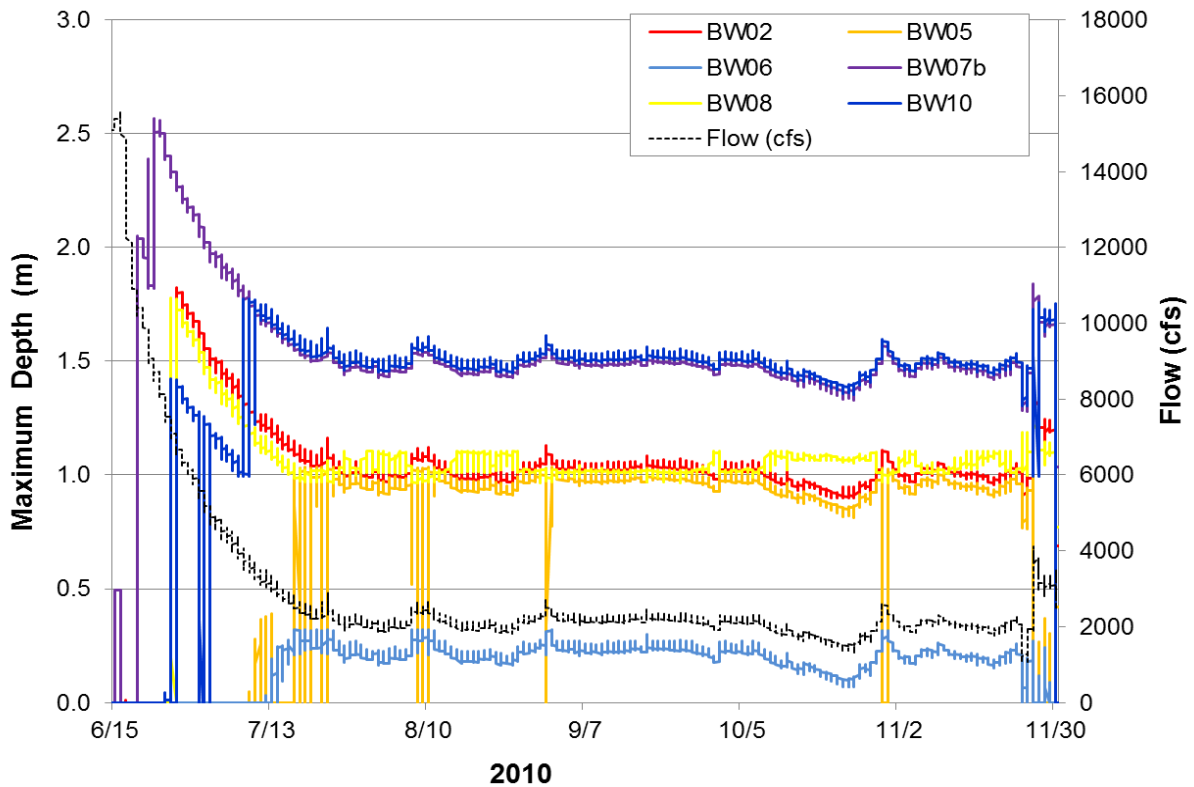


FIGURE A4-61 Maximum Depth (m) of Each of the Six Backwater Areas Modeled during 2010 (June 15–November 30)

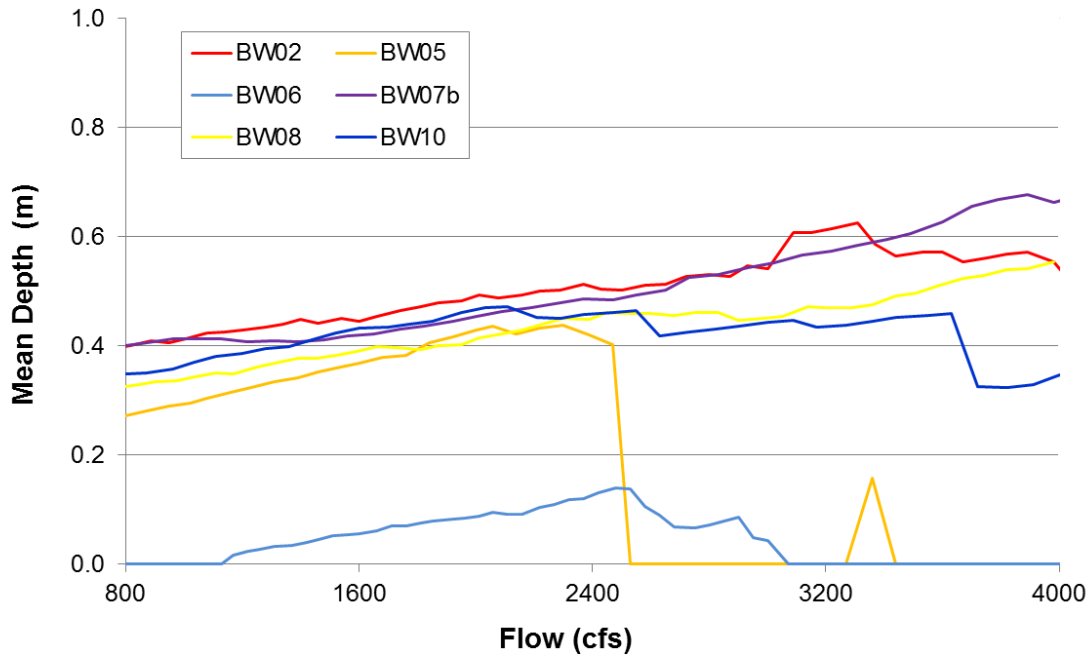


FIGURE A4-62 Mean Depth (m) of the Six Backwater Areas Surveyed in 2010 Modeled across Base Flows (800–4,000 cfs)

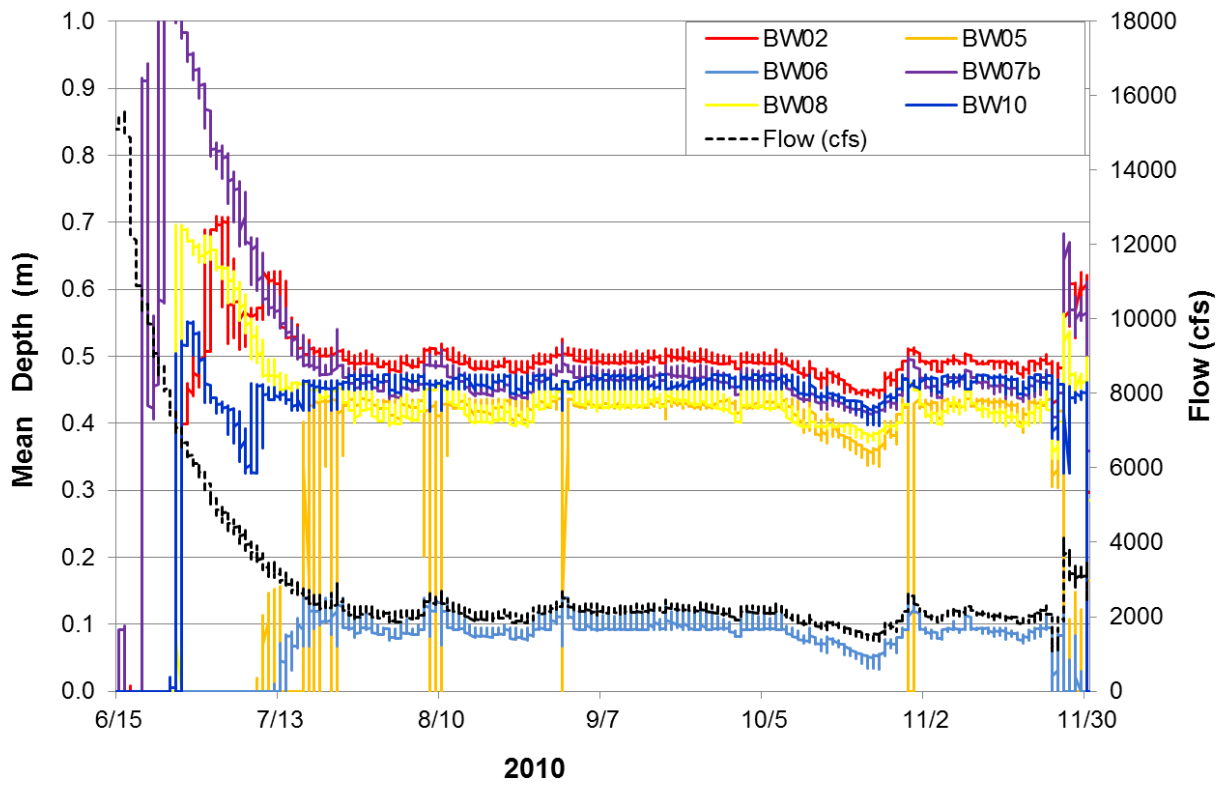


FIGURE A4-63 Mean Depth (m) of Each of the Six Backwater Areas Modeled during 2010 (June 15–November 30)

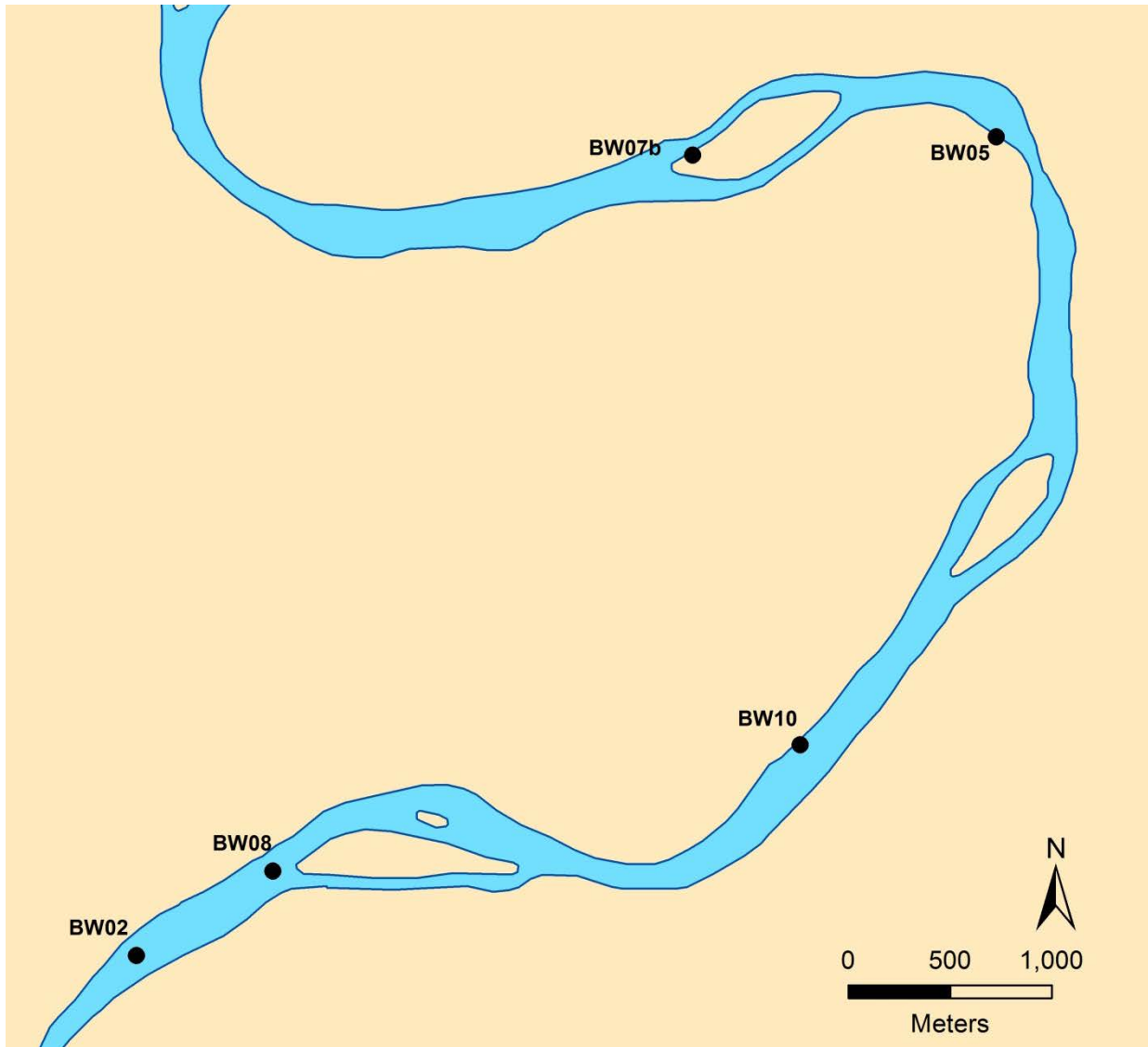


FIGURE A4-64 Green River Backwater Areas BW02, BW05, BW07b, BW08, and BW10 Surveyed and Modeled in 2011

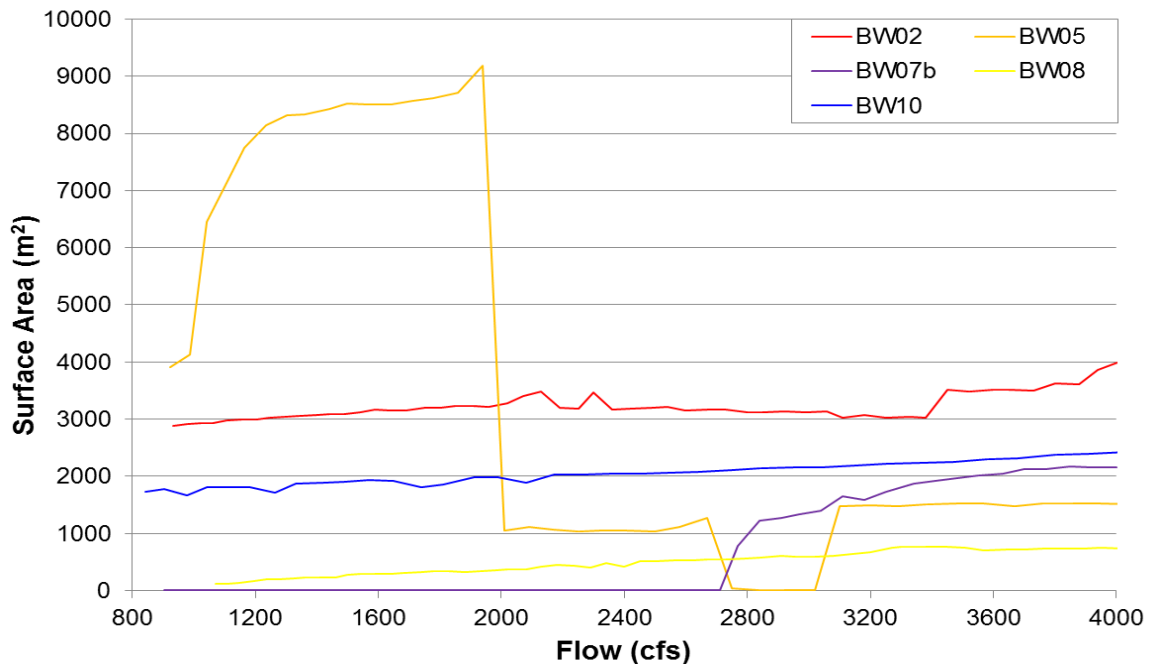


FIGURE A4-65 Surface Area (m²) of the Five Backwater Areas Surveyed in 2011 Modeled across Base Flows (800–4,000 cfs)

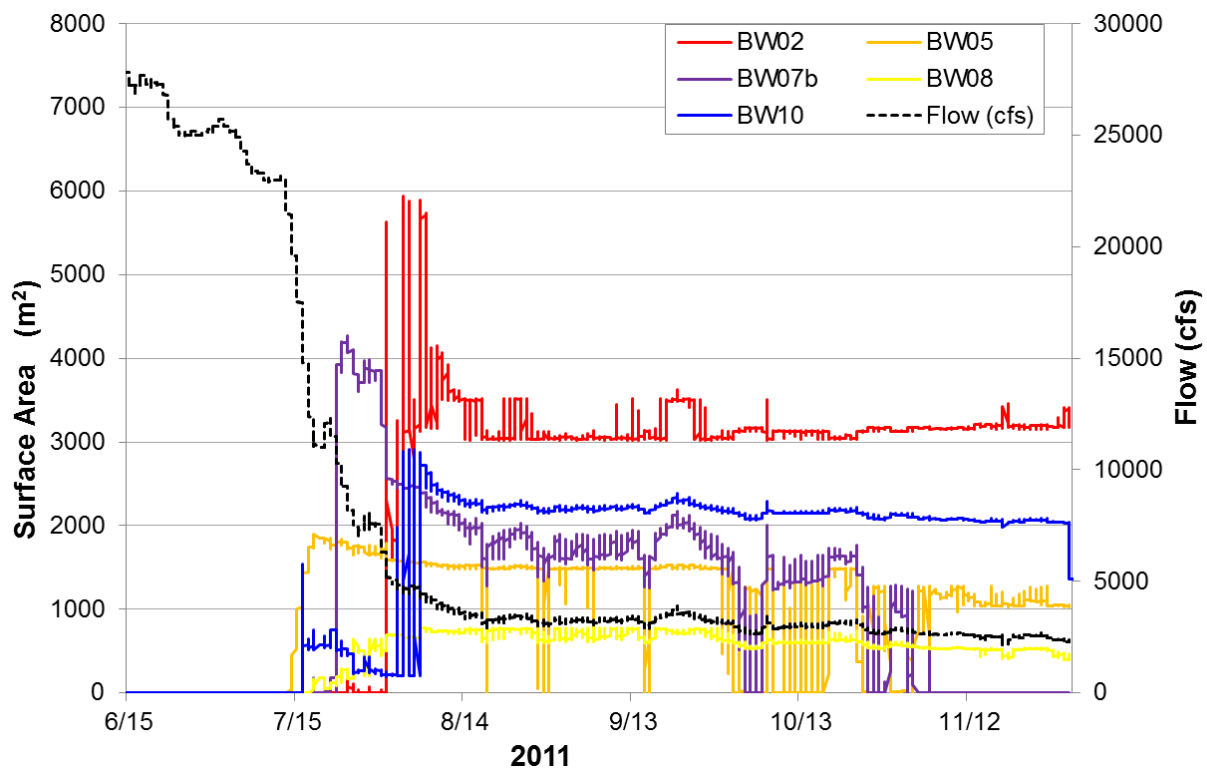


FIGURE A4-66 Surface Area (m²) of Each of the Five Backwater Areas Modeled during 2011 (June 15–November 30)

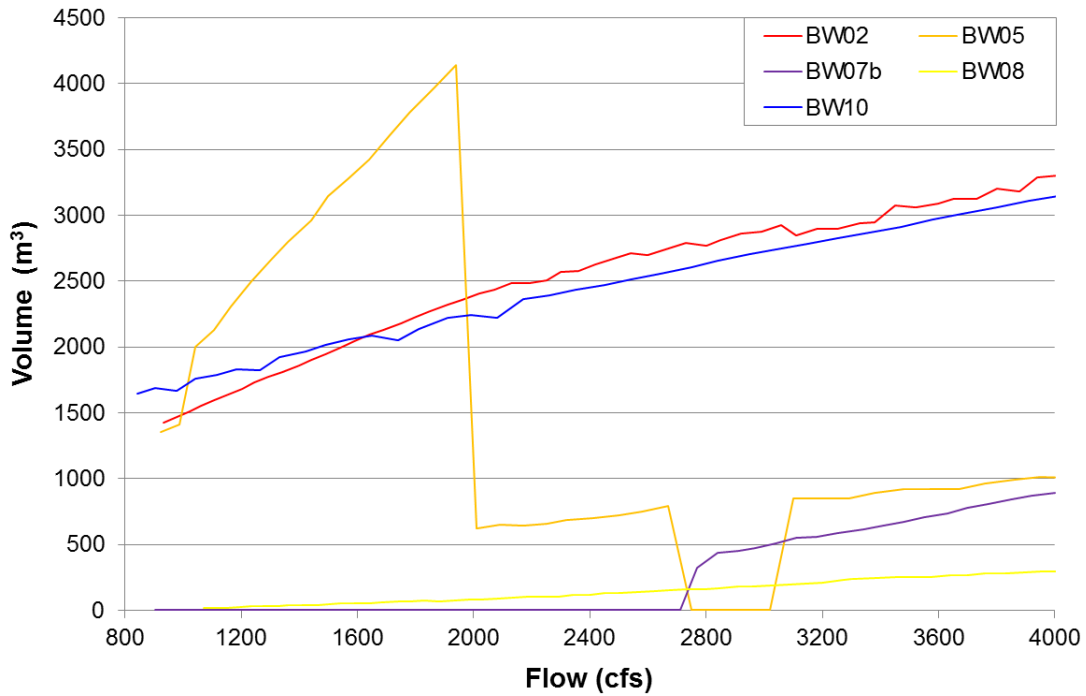


FIGURE A4-67 Volume (m³) of the Five Backwater Areas Surveyed in 2011 Modeled across Base Flows (800–4,000 cfs)

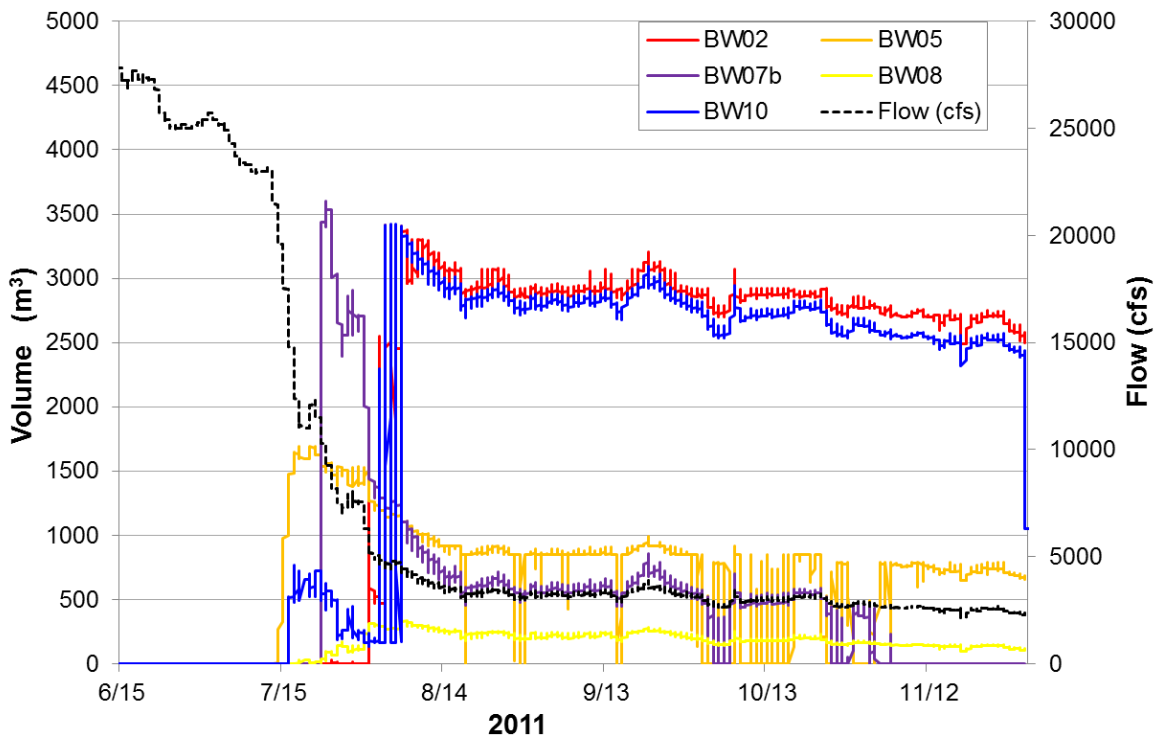


FIGURE A4-68 Volume (m³) of Each of the Five Backwater Areas Modeled during 2011 (June 15–November 30)

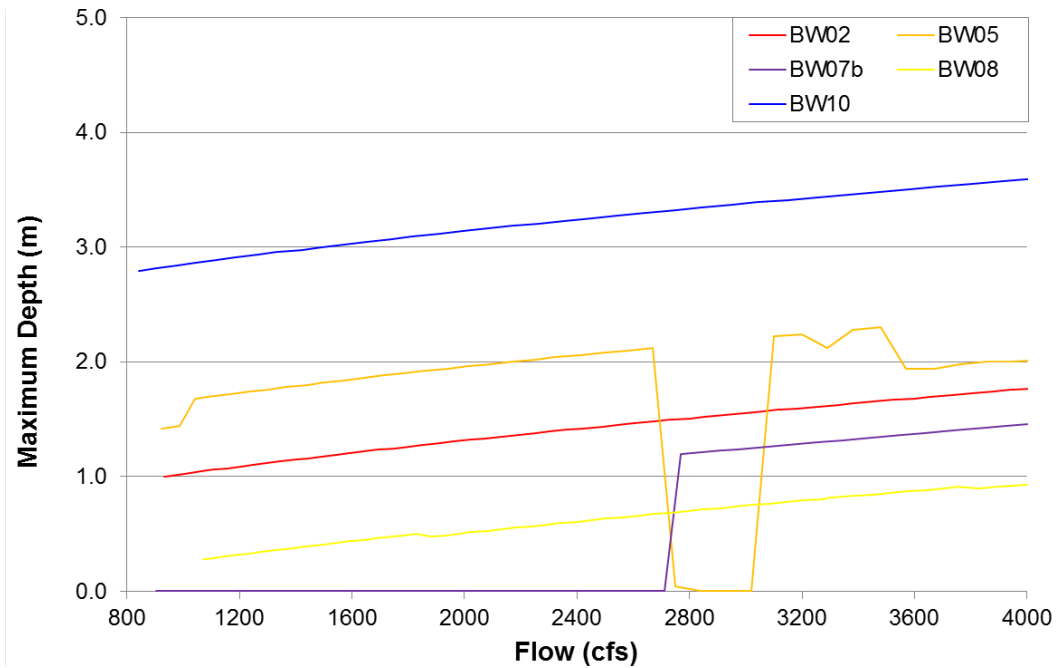


FIGURE A4-69 Maximum Depth (m) of the Five Backwater Areas Surveyed in 2011 Modeled across Base Flows (800–4,000 cfs)

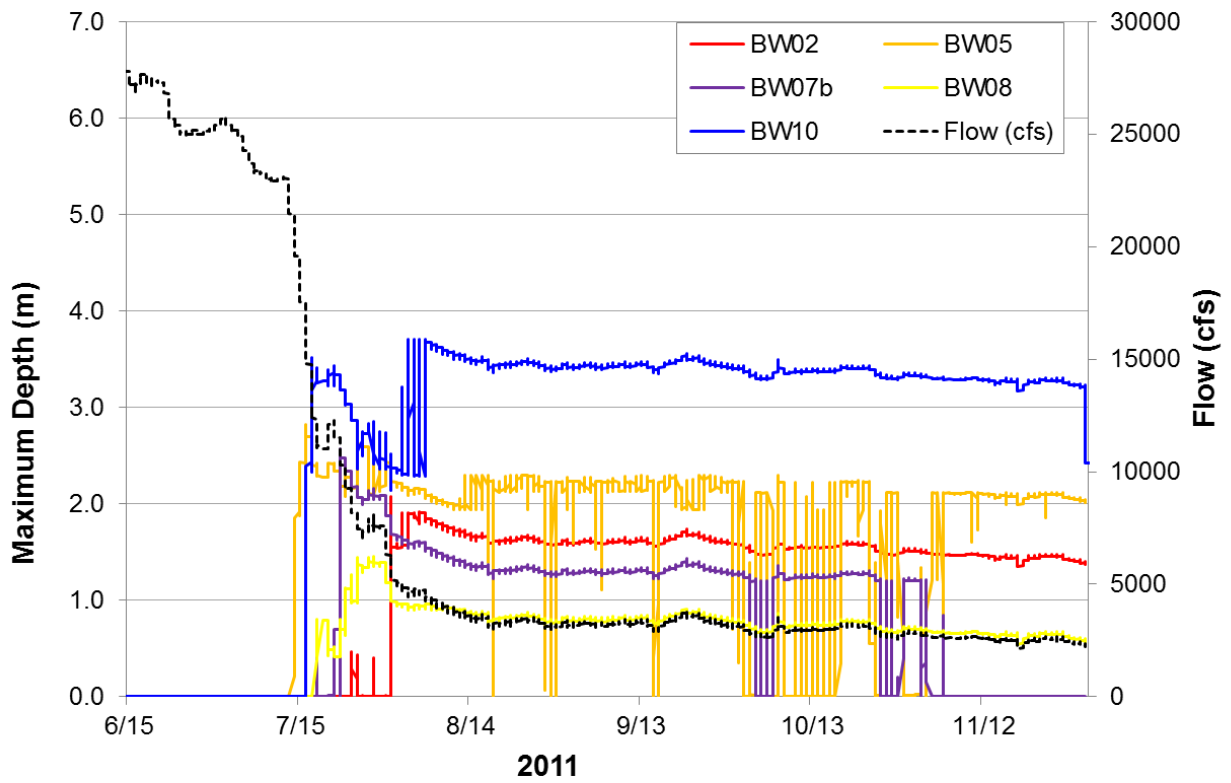


FIGURE A4-70 Maximum Depth (m) of Each of the Five Backwater Areas Modeled during 2011 (June 15–November 30)

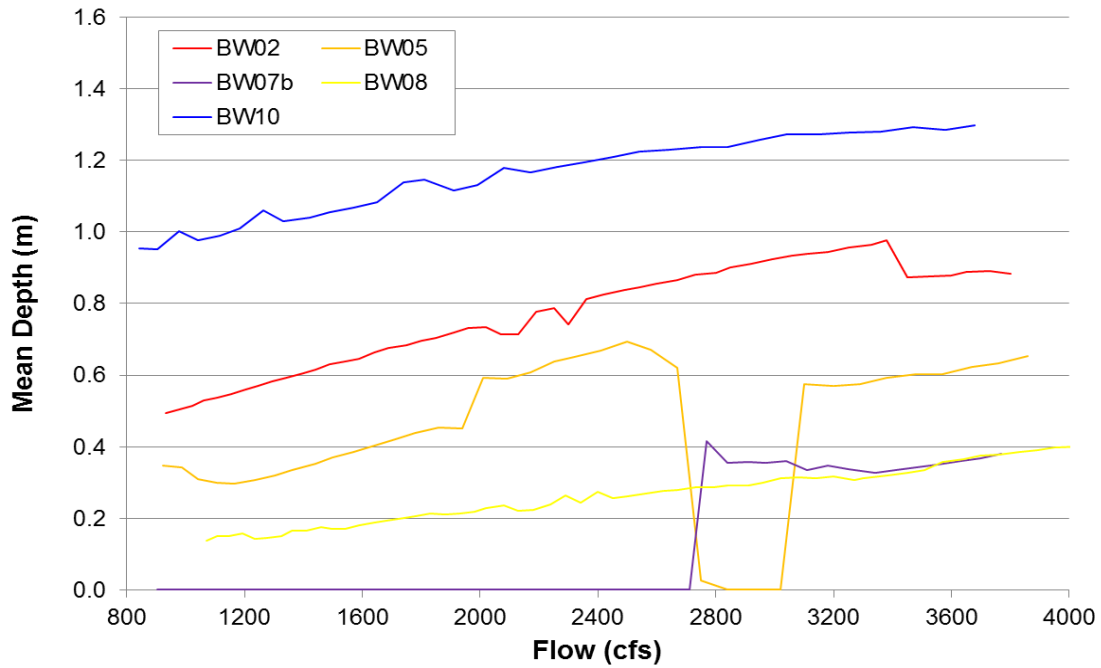


FIGURE A4-71 Mean Depth (m) of the Five Backwater Areas Surveyed in 2011 Modeled across Base Flows (800–4,000 cfs)

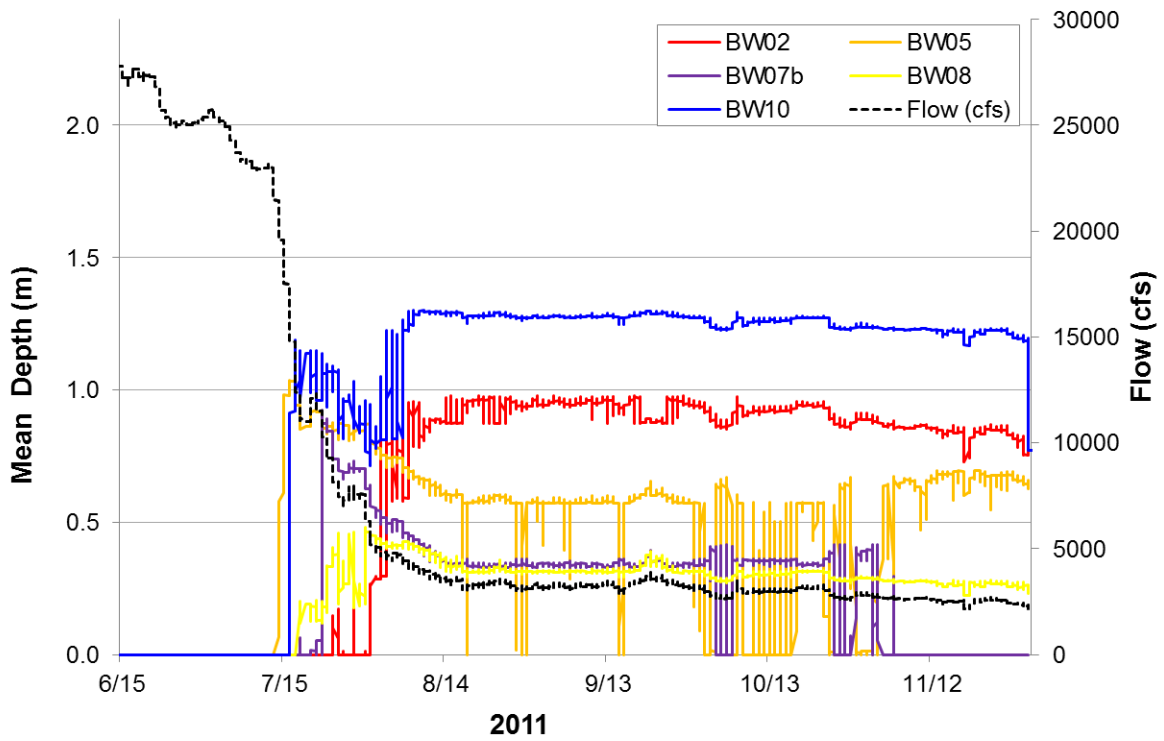


FIGURE A4-72 Mean Depth (m) of Each of the Five Backwater Areas Modeled during 2011 (June 15–November 30)

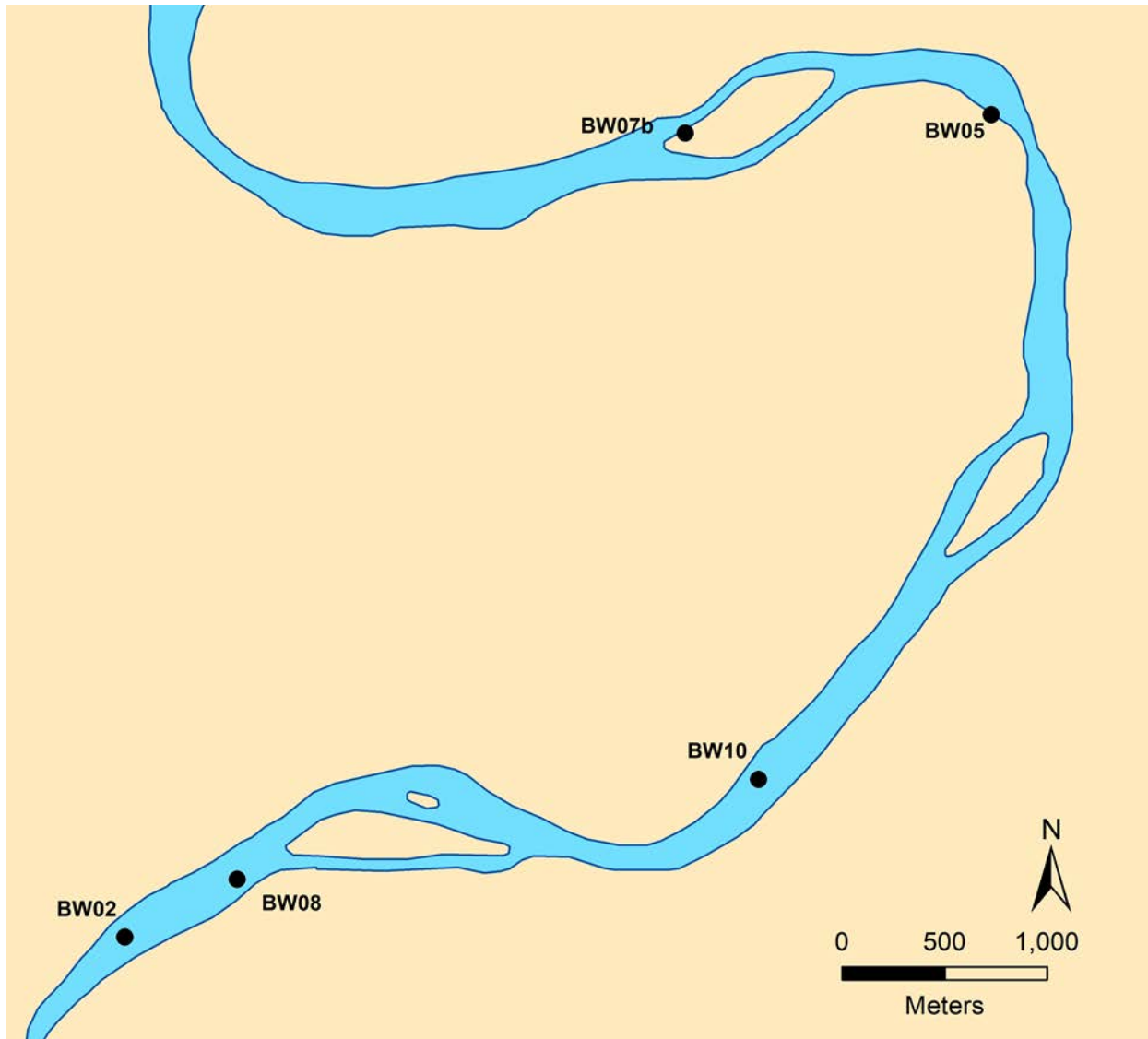


FIGURE A4-73 Green River Backwater Areas BW02, BW05, BW07b, BW08, and BW10 Surveyed in 2012

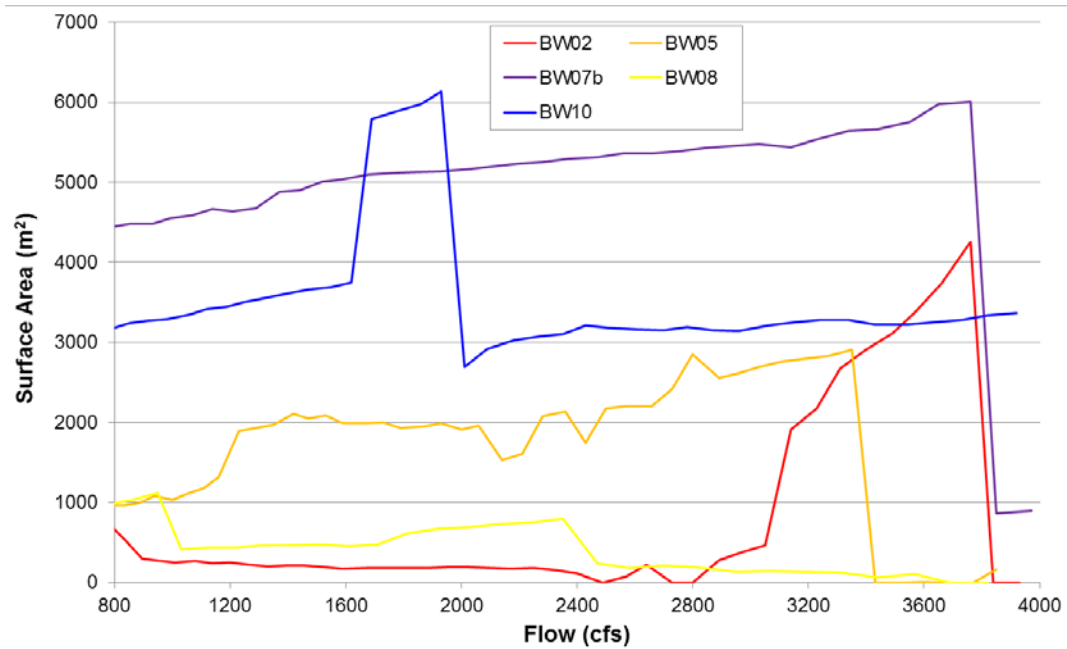


FIGURE A4-74 Surface Area (m²) of the Five Backwater Areas Surveyed in 2012 Modeled across Base Flows (800–4,000 cfs)

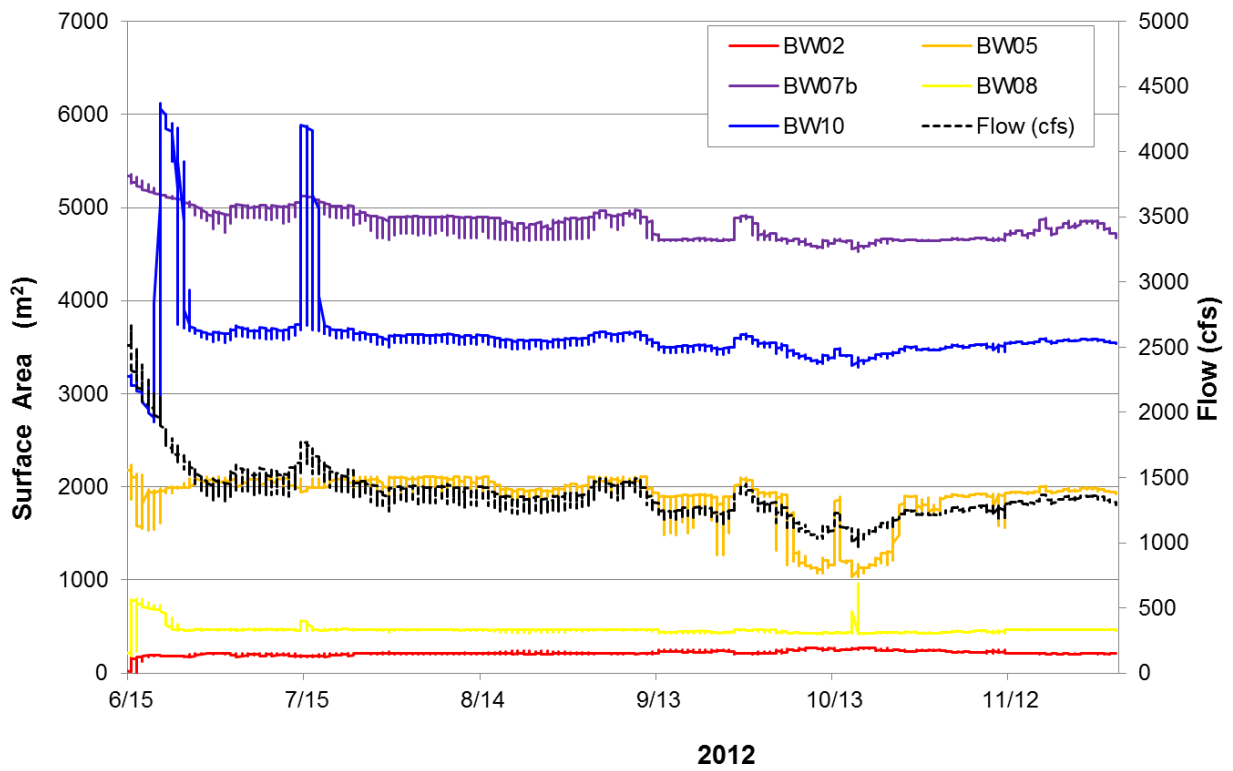


FIGURE A4-75 Surface Area (m²) of Each of the Five Backwater Areas Modeled during 2012 (June 15–November 30)

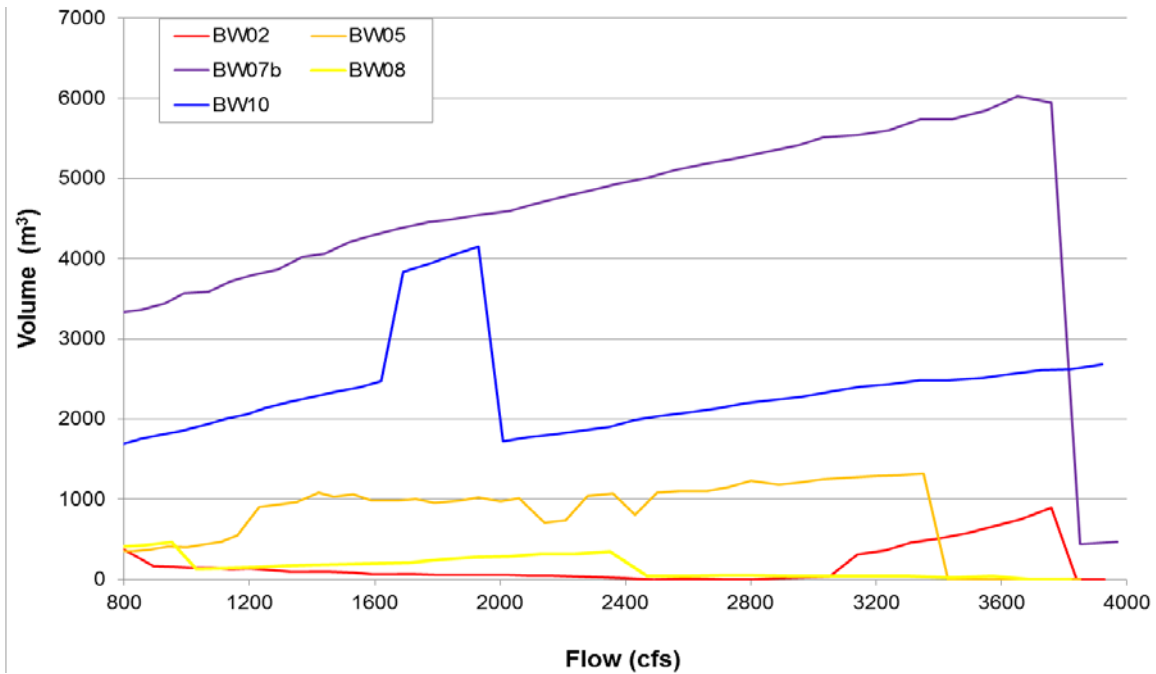


FIGURE A4-76 Volume (m³) of the Five Backwater Areas Surveyed in 2012 Modeled across Base Flows (800–4,000 cfs)

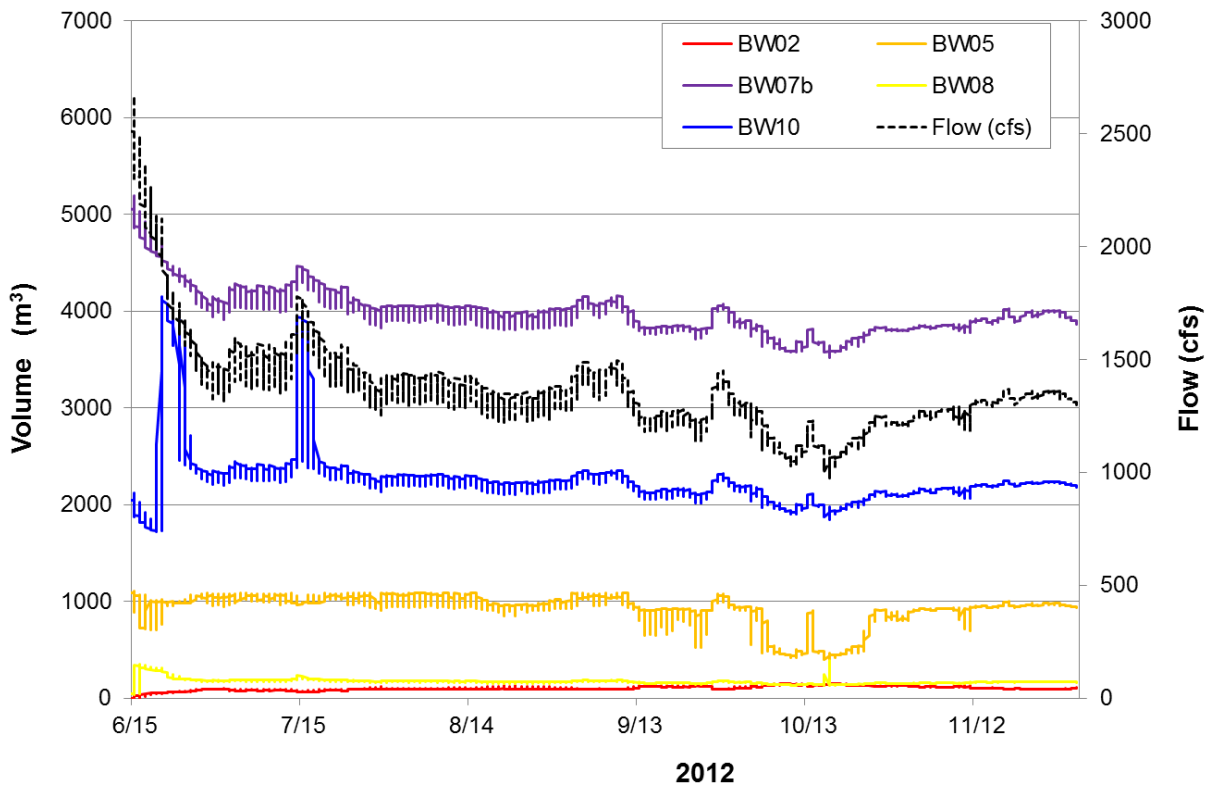


FIGURE A4-77 Volume (m³) of Each of the Five Backwater Areas Modeled during 2012 (June 15–November 30)

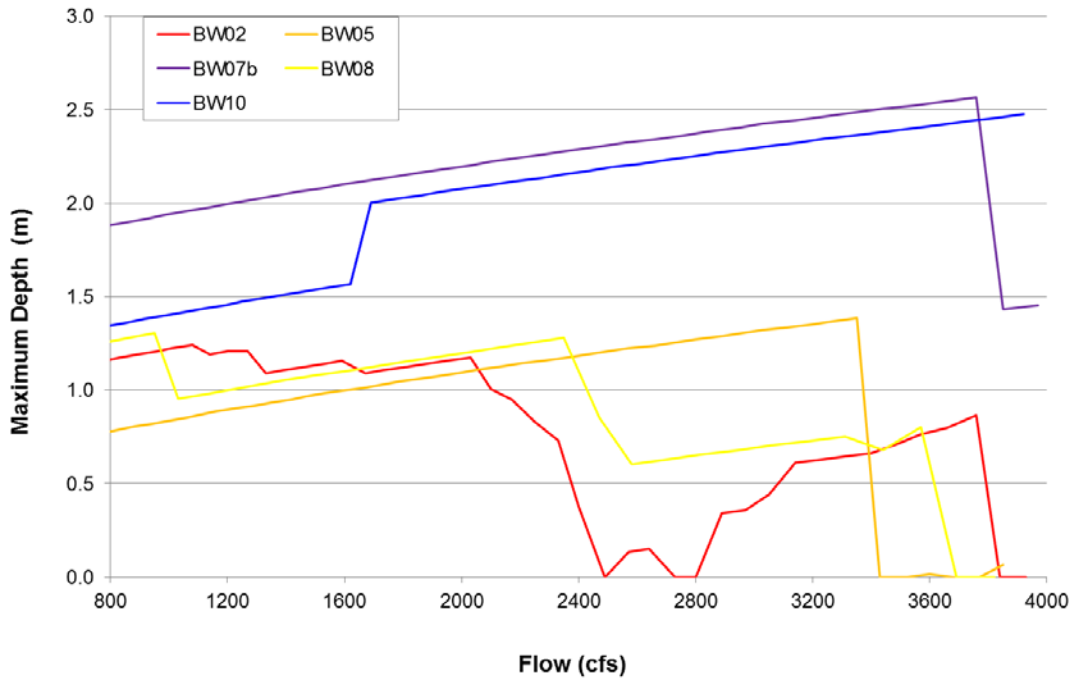


FIGURE A4-78 Maximum Depth (m) of the Five Backwater Areas Surveyed in 2012 Modeled across Base Flows (800–4,000 cfs)

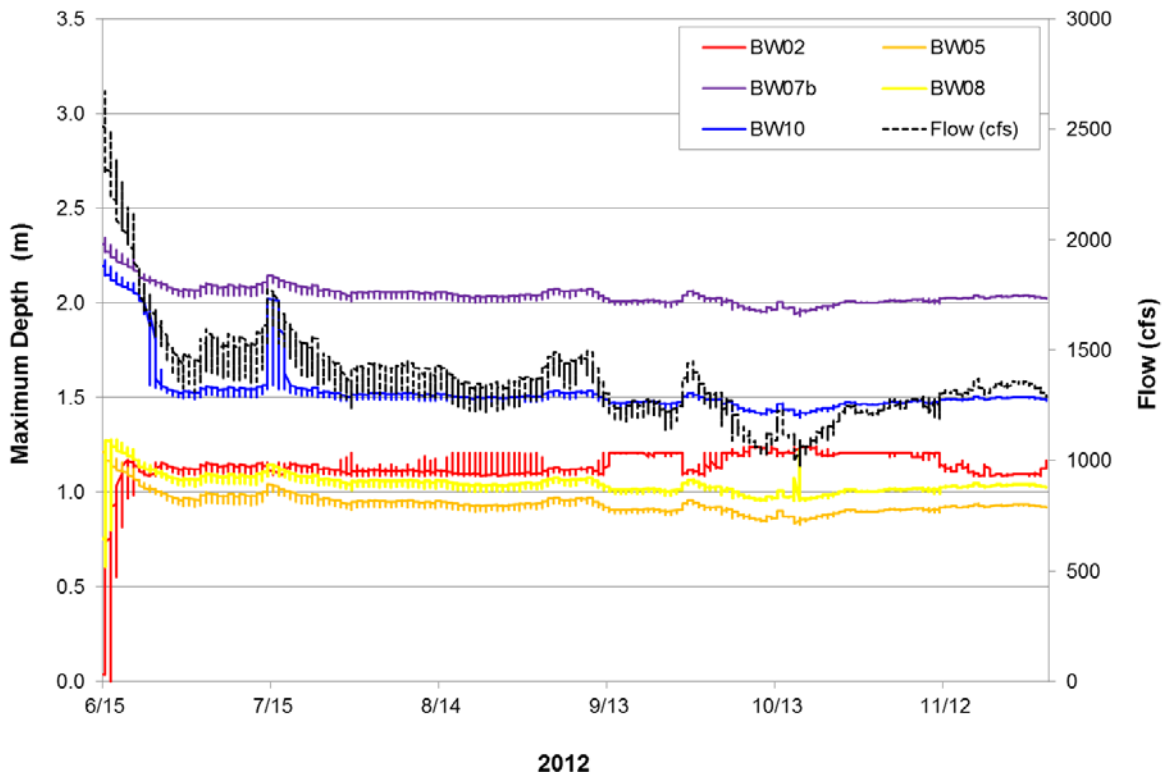


FIGURE A4-79 Maximum Depth (m) of Each of the Five Backwater Areas Modeled during 2012 (June 15–November 30)

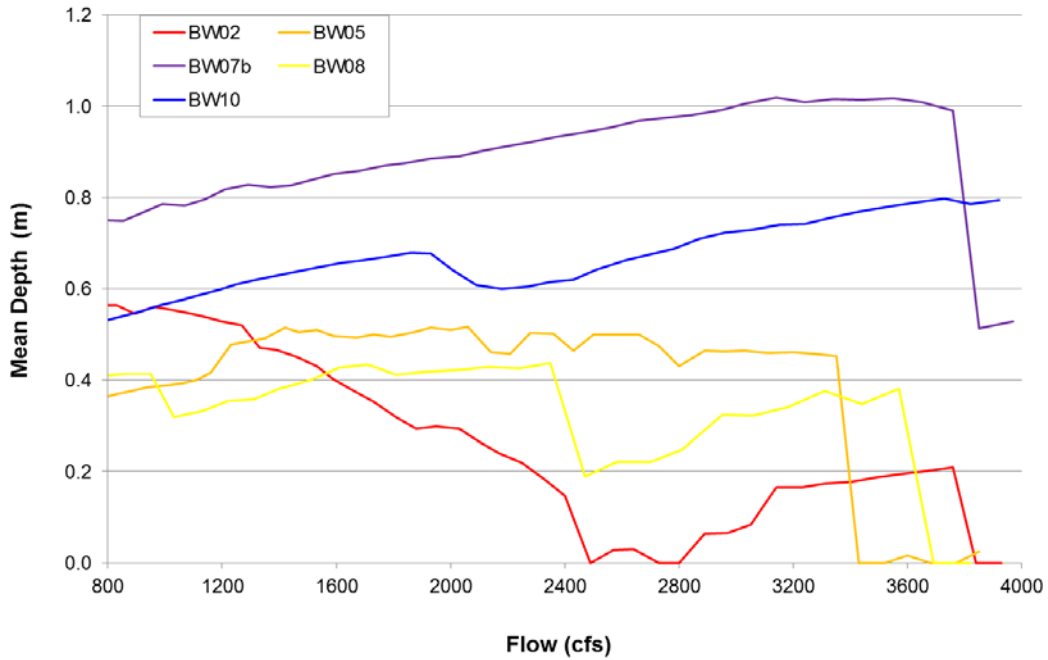


FIGURE A4-80 Mean Depth (m) of the Five Backwater Areas Surveyed in 2012 Modeled across Base Flows (800–4,000 cfs)

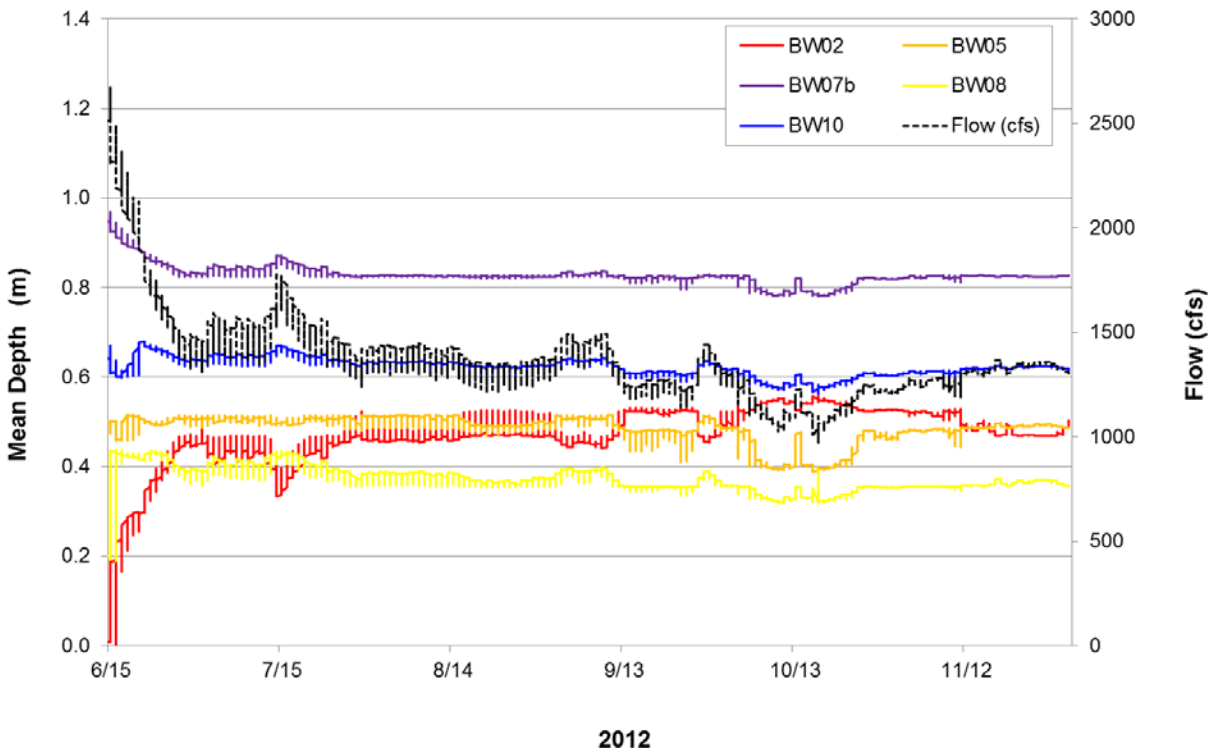


FIGURE A4-81 Mean Depth (m) of Each of the Five Backwater Areas Modeled during 2012 (June 15–November 30)

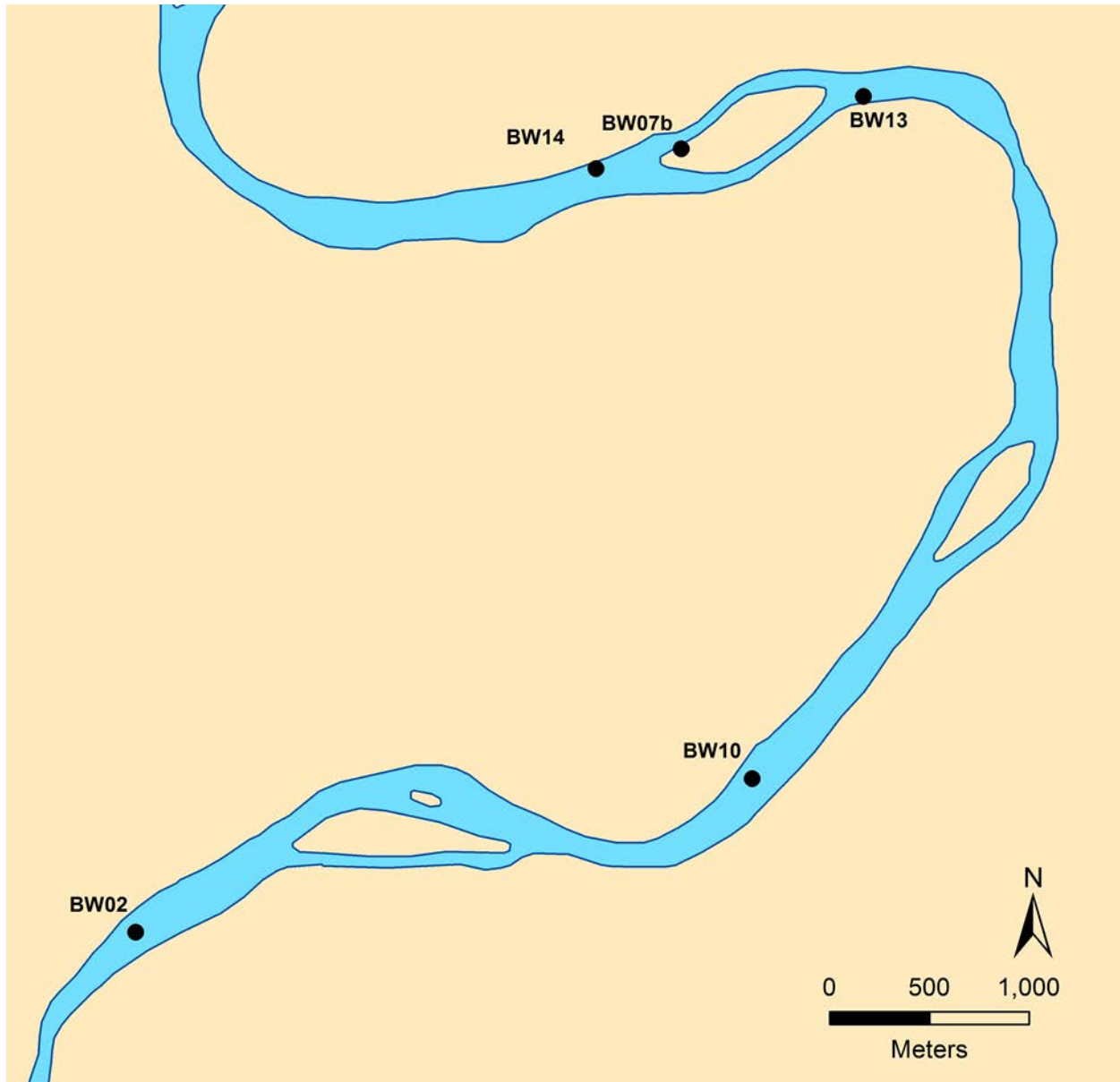


FIGURE A4-82 Green River Backwater Areas BW02, BW07b, BW10, BW13, and BW14 Surveyed in 2013

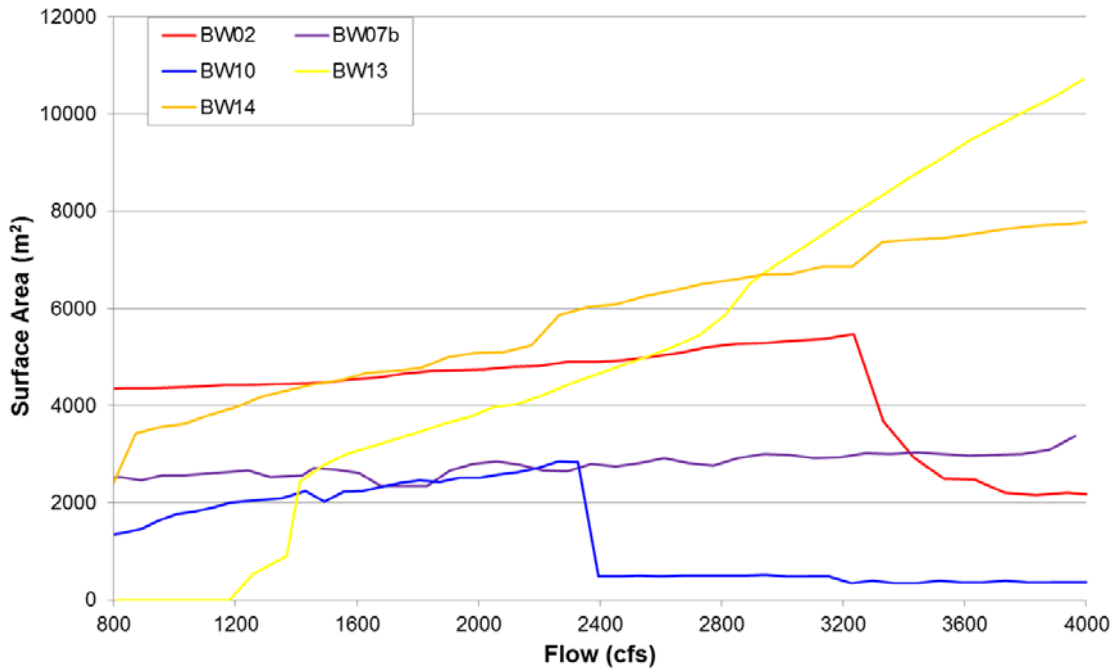


FIGURE A4-83 Surface Area (m²) of the Five Backwater Areas Surveyed in 2013 Modeled across Base Flows (800–4,000 cfs)

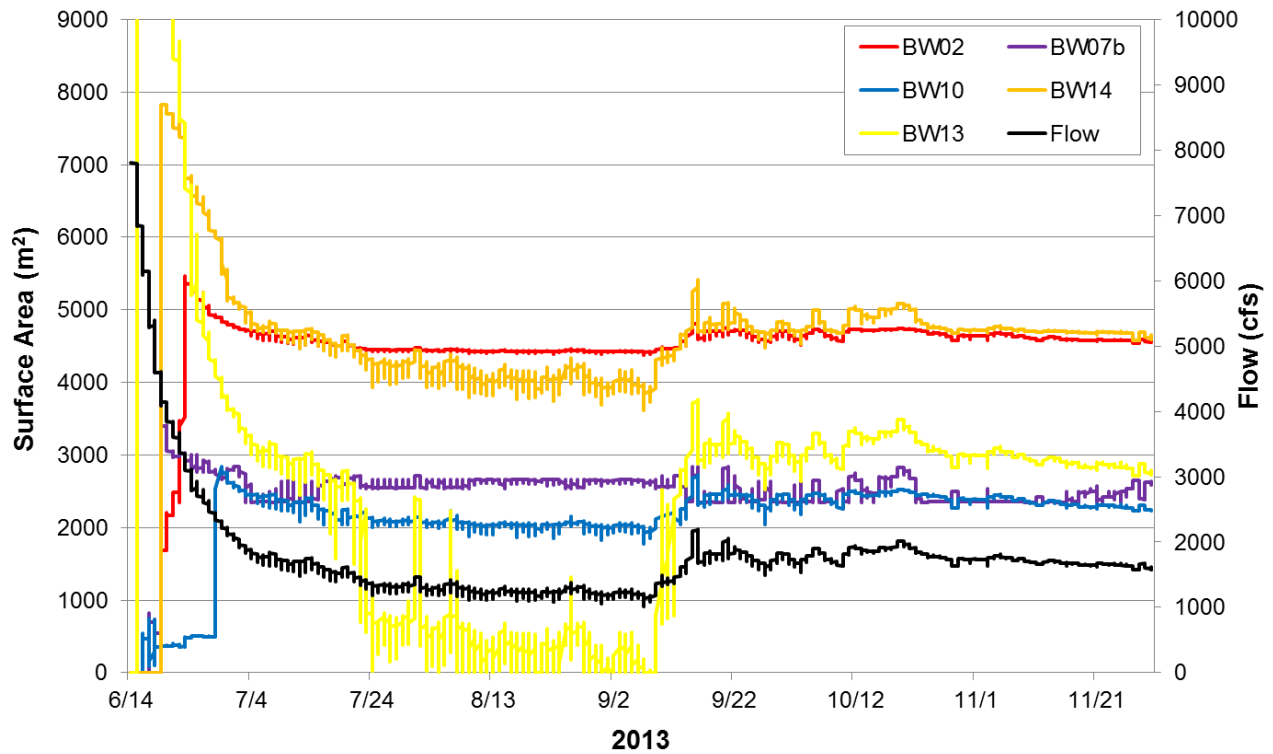


FIGURE A34-84 Surface Area (m²) of Each of the Five Backwater Areas Modeled during 2013 (June 15–November 30)

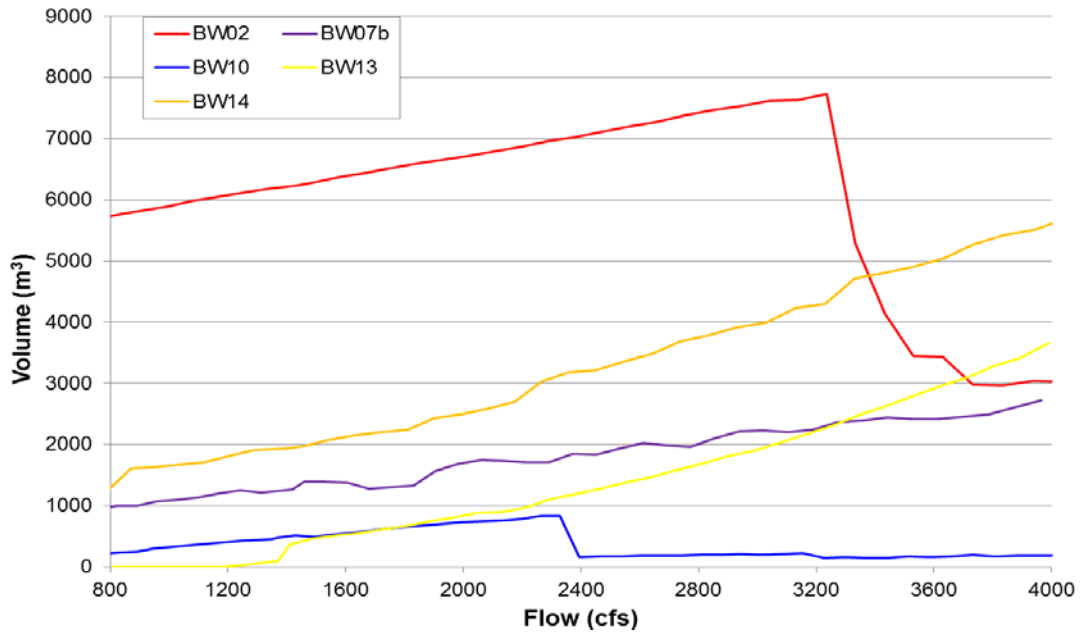


FIGURE A4-85 Volume (m³) of the Five Backwater Areas Surveyed in 2013 Modeled across Base Flows (800–4,000 cfs)

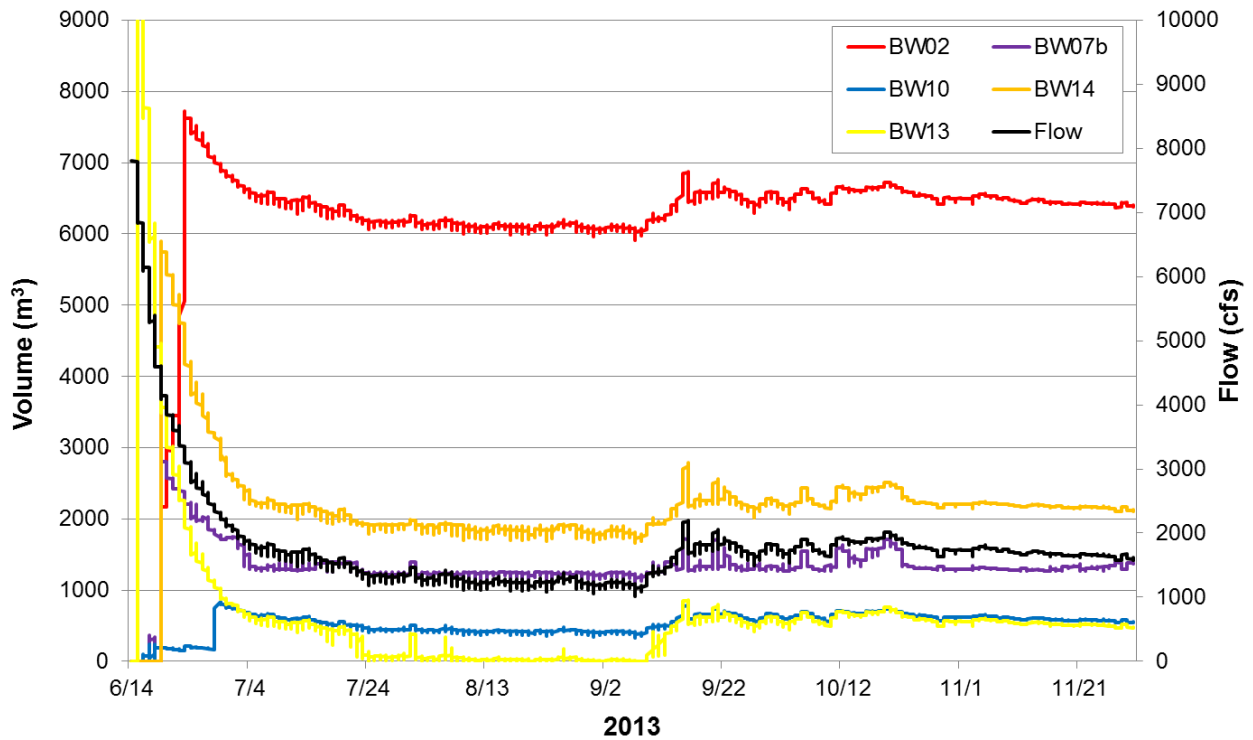


FIGURE A4-86 Volume (m³) of Each of the Five Backwater Areas Modeled during 2013 (June 15–November 30)

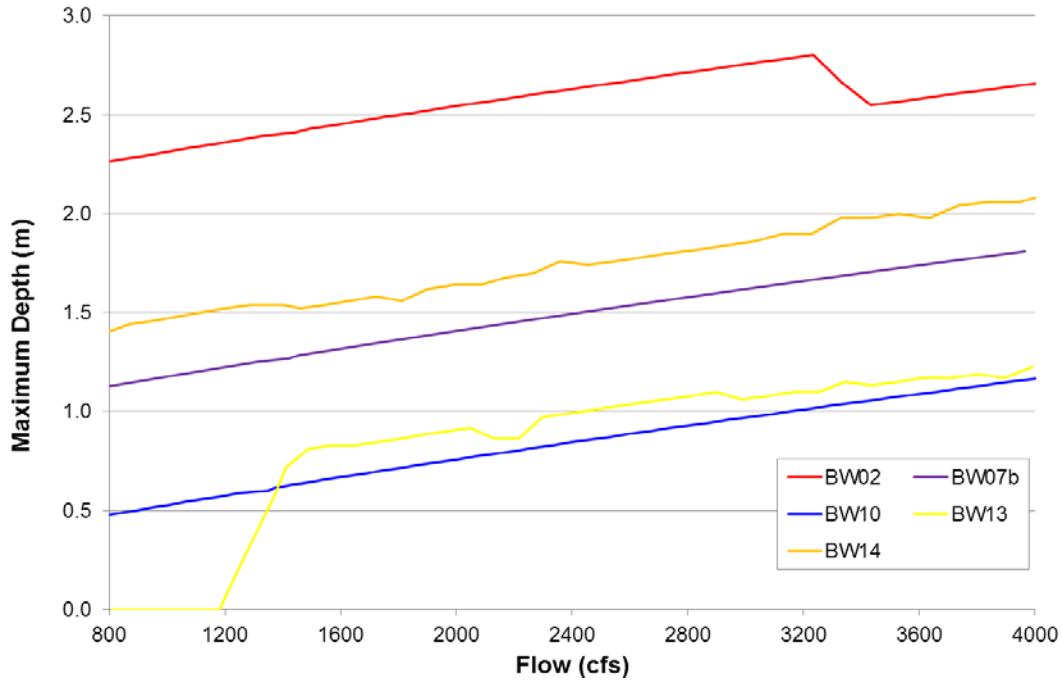


FIGURE A4-87 Maximum Depth (m) of the Five Backwater Areas Surveyed in 2013 Modeled across Base Flows (800–4,000 cfs)

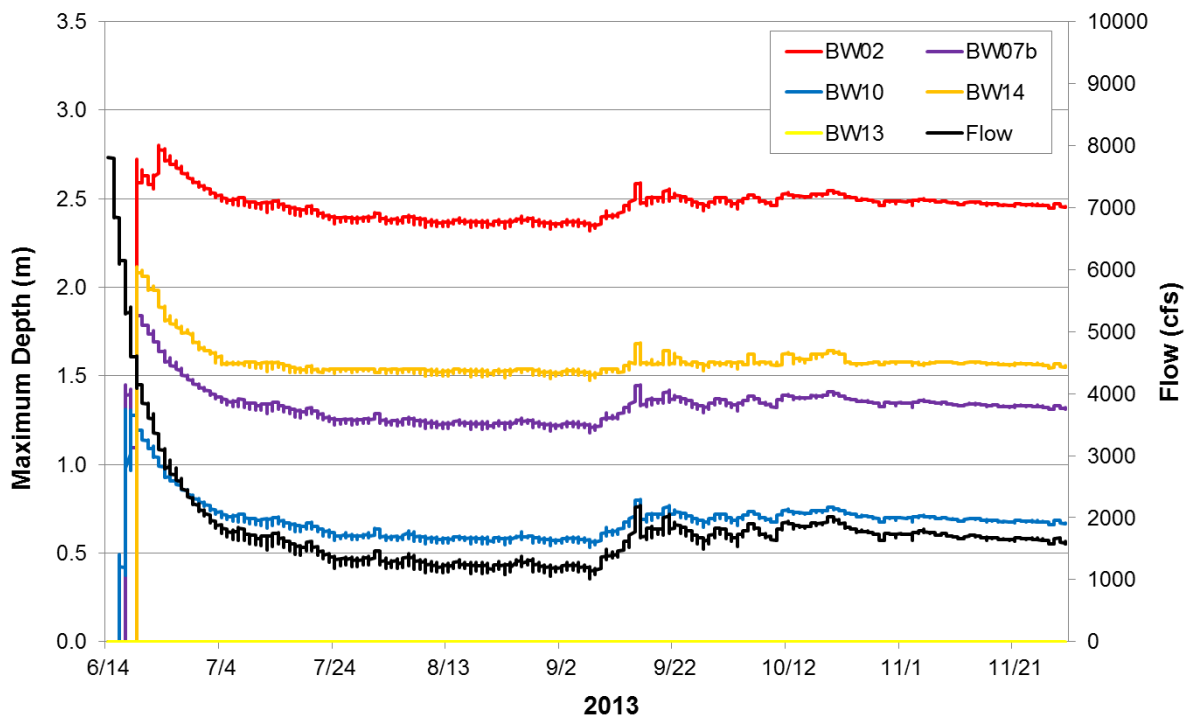


FIGURE A4-88 Maximum Depth (m) of Each of the Five Backwater Areas Modeled during 2013 (June 15–November 30)

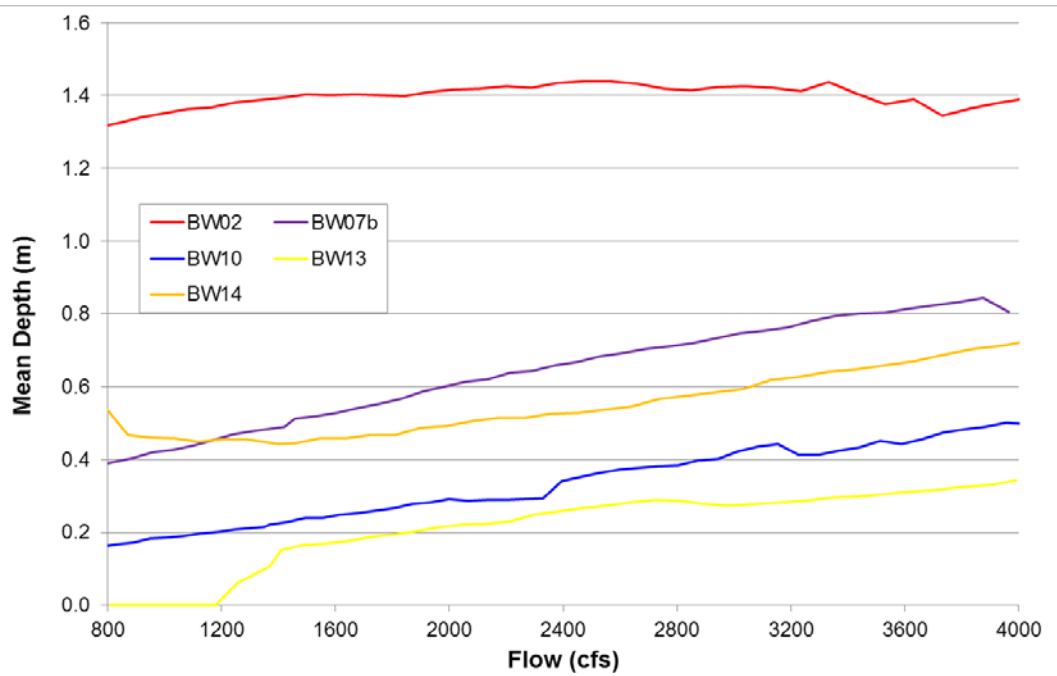


FIGURE A4-89 Mean Depth (m) of the Five Backwater Areas Surveyed in 2013 Modeled across Base Flows (800–4,000 cfs)

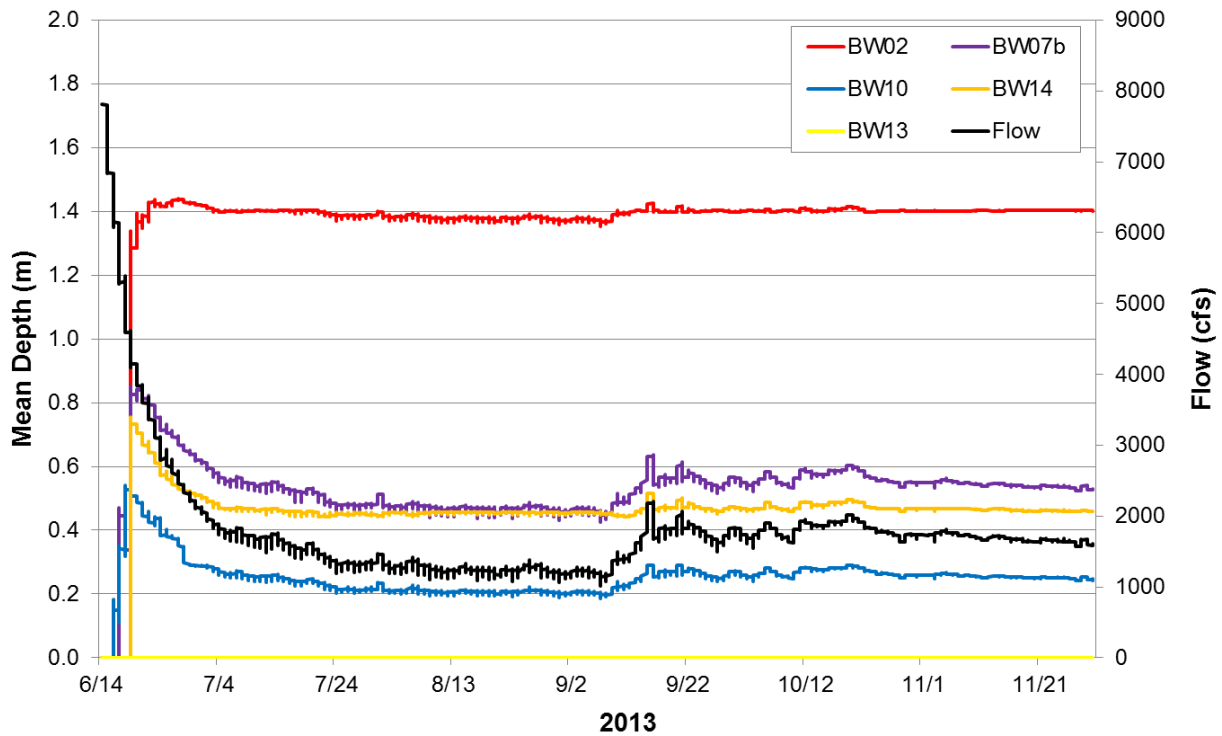


FIGURE A4-90 Mean Depth (m) of Each of the Five Backwater Areas Modeled during 2013 (June 15–November 30)

APPENDIX 5

**CHARACTERISTICS OF THE BASE-FLOW PERIOD
AND SURVEYED BACKWATERS FROM 2003 TO 2013**

This page is intentionally left blank.

APPENDIX 5**CHARACTERISTICS OF THE BASE-FLOW PERIOD
AND SURVEYED BACKWATERS FROM 2003 TO 2013**

Surveys of selected backwaters were made annually from 2003 to 2013 (2007 was the only year surveys were not conducted during this time period). This appendix provides summary information for each year including (1) the start of the base-flow period (as determined from methods described in Appendix 3); (2) flows during the base-flow period; (3) hydrologic classification; and (4) mean, standard deviation, and range of backwater volume, surface area, mean depth, and maximum depth of each backwater. The information is provided in a series of tables for each backwater variable. See Appendix 4 for the location of backwaters, relationship of backwater variables to flow, and changes in the values of backwater variables during the base-flow period of each year.

TABLE A5-1 (Cont.)

Year	2009		2010		2011		2012		2013	
Start of base-flow period ^a	July 25		July 19		August 13		June 25		July 6	
Mean \pm SD flow at Ouray ^b (cfs)	2,277 \pm 154		2,128 \pm 235		3,011 \pm 355		1,317 \pm 119		1,552 (249)	
Hydrologic condition	Average (above median)		Moderately dry		Wet		Dry		Dry	
Backwater	Mean \pm SD Volume (m ³)	Range in Volume (m ³)	Mean \pm SD Volume (m ³)	Range in Volume (m ³)	Mean \pm SD Volume (m ³)	Range in Volume (m ³)	Mean \pm SD Volume (m ³)	Range in Volume (m ³)	Mean \pm SD Volume (m ³)	Range in Volume (m ³)
BW01	NA	NA								
BW02	2,627 \pm 728	165–3,406	855 \pm 55	539–921	2,853 \pm 129	2,487–3,202	108 \pm 18	61–150	6,354 \pm 200	5,914–6,869
BW03	NA	NA								
BW04	NA	NA								
BW05	NA	NA	470 \pm 129	0–560	658 \pm 318	0–996	906 \pm 171	401–1,086	NA	NA
BW06	327 \pm 14	266–378	24 \pm 14	0–62	NA	NA	NA	NA	NA	NA
BW07a	NA	NA								
BW07b	2,032 \pm 92	1,782–2,323	4,327 \pm 572	1,769–7,830	396 \pm 269	0–854	3,927 \pm 161	3,525–4,463	1,310 \pm 105	1,089–1,744
BW08	34 \pm 5.7	23–57	355 \pm 26	244–543	192 \pm 43	95–287	167 \pm 16	134–389	NA	NA
BW09	NA	NA								
BW10	1,492 \pm 81	1,278–1,748	493 \pm 89	321–1,165	2,721 \pm 153	2,320–3,094	2,212 \pm 183	1,865–3,952	543 \pm 101	329–790
BW13	NA	NA	NA	NA	NA	NA	NA	NA	415 \pm 283	0–963
BW14	NA	NA	NA	NA	NA	NA	NA	NA	2,082 \pm 202	1,657–2,791

^a Dates represent the beginning of the base-flow period. November 30 was used as the end of the base-flow period. See Appendix 3 for a description of how the beginning of the base-flow period was determined.

^b Mean flow at Ouray during the base-flow period.

^c NA = Backwater did not exist or was not surveyed during survey year

TABLE A5-2 (Cont.)

Year	2009		2010		2011		2012		2013	
Start of base-flow period ^a	July 25		July 19		August 13		June 25		July 6	
Mean \pm SD flow at Ouray ^b (cfs)	2,277 \pm 154		2,077 \pm 235		3,011 \pm 355		1,317 \pm 119		1,552 \pm 249	
Hydrologic condition	Average (above median)		Moderately dry		Wet		Dry		Dry	
	Mean \pm SD Area (m ²)	Range in Area (m ²)	Mean \pm SD Area (m ²)	Range in Area (m ²)	Mean \pm SD Area (m ²)	Range in Area (m ²)	Mean \pm SD Area (m ²)	Range in Area (m ²)	Mean \pm SD Area (m ²)	Range in Area (m ²)
BW01	NA	NA								
BW02	5,629 \pm 1,342	1,190–7,187	1,742 \pm 161	977–2,056	3,156 \pm 136	3,019–3,629	220 \pm 20	175–273	4,557 \pm 108	4,372–4,816
BW03	NA	NA								
BW04	NA	NA								
BW05	NA	NA	1,120 \pm 299	0–1,281	1,090 \pm 534	0–1,523	1,867 \pm 264	1,032–2,108	NA	NA
BW06	658 \pm 19	582–735	239 \pm 97	0–444	NA	NA	NA	NA	NA	NA
BW07a	NA	NA								
BW07b	3,216 \pm 78	2,990–3,463	9,257 \pm 639	4,279–11,474	1,148 \pm 787	0–2,172	4,773 \pm 131	4,522–5,121	2,522 \pm 136	2,351–2,845
BW08	161 \pm 14	131–202	833 \pm 27	705–967	630 \pm 97	395–771	455 \pm 21	421–962	NA	NA
BW09	NA	NA								
BW10	2,541 \pm 124	2,379–2,725	1,084 \pm 204	853–2,561	2,162 \pm 76	1,984–2,390	3,593 \pm 208	3,341–5,903	2,242 \pm 176	1,769–2,724
BW13	NA	NA	NA	NA	NA	NA	NA	NA	2,306 \pm 1,383	0–4,189
BW14	NA	NA	NA	NA	NA	NA	NA	NA	4,504 \pm 347	3,613–5,421

^a Dates represent the beginning of the base-flow period. November 30 was used as the end of the base-flow period. See Appendix 3 for a description of how the beginning of the base-flow period was determined.

^b Mean flow at Ouray during the base-flow period.

^c NA = Backwater did not exist or was not surveyed during survey year

TABLE A5-3 (Cont.)

Year	2009		2010		2011		2012		2013	
Start of base-flow period ^a	July 25		July 19		August 13		June 25		July 6	
Mean \pm SD Flow at Ouray ^b (cfs)	2,277 \pm 154		2,077 \pm 235		3,011 \pm 355		1,317 \pm 119		1,552 \pm 249	
Hydrologic condition	Average (above median)		Moderately dry		Wet		Dry		Dry	
Backwater	Mean \pm SD Mean Depth (m)	Range in Mean Depth (m)	Mean \pm SD Mean Depth (m)	Range in Mean Depth (m)	Mean \pm SD Mean Depth (m)	Range in Mean Depth (m)	Mean \pm SD Mean Depth (m)	Range in Mean Depth (m)	Mean \pm SD Mean Depth (m)	Range in Mean Depth (m)
BW01	NA	NA								
BW02	0.5 \pm 0.07	0.2–0.5	0.5 \pm 0.02	0.4–0.6	0.9 \pm 0.05	0.7–1.0	0.5 \pm 0.04	0.3–0.6	1.4 \pm 0.01	1.3–1.4
BW03	NA	NA								
BW04	NA	NA								
BW05	NA	NA	0.4 \pm 0.1	0.0–0.4	0.5 \pm 0.2	0–0.7	0.5 \pm 0.03	0.4–0.5	NA	NA
BW06	0.5 \pm 0.009	0.4–0.5	0.1 \pm 0.02	0.0–0.1	NA	NA	NA	NA	NA	NA
BW07a	NA	NA								
BW07b	0.6 \pm 0.01	0.6–0.7	0.5 \pm 0.03	0.4–0.7	0.2 \pm 0.16	0–0.4	0.8 \pm 0.01	0.8–0.9	0.5 \pm 0.04	0.42–0.63
BW08	0.2 \pm 0.02	0.2–0.3	0.4 \pm 0.02	0.3–0.6	0.3 \pm 0.03	0.2–0.4	0.4 \pm 0.02	0.3–0.4	NA	NA
BW09	NA	NA								
BW10	0.6 \pm 0.008	0.5–0.6	0.5 \pm 0.02	0.3–0.5	1.3 \pm 0.03	1.2–1.3	0.6 \pm 0.02	0.6–0.7	0.2 \pm 0.03	0.19–0.29
BW13	NA	NA	NA	NA	NA	NA	NA	NA	0.1 \pm 0.07	0–0.23
BW14	NA	NA	NA	NA	NA	NA	NA	NA	0.46 \pm 0.11	0.44–0.51

^a Dates represent the beginning of the base-flow period. November 30 was used as the end of the base-flow period. See Appendix 3 for a description of how the beginning of the base-flow period was determined.

^b Mean flow at Ouray during the base-flow period.

^c NA = Backwater did not exist or was not surveyed during survey year

TABLE A5-4 (Cont.)

Year	2009		2010		2011		2012		2013	
Start of base-flow period ^a	July 25		July 19		August 13		June 25		July 6	
Mean \pm SD Flow at Ouray ^b (cfs)	2,277 \pm 154		2,077 \pm 235		3,011 \pm 355		1,317 \pm 119		1,552 \pm 249	
Hydrologic condition	Average (above median)		Moderately dry		Wet		Dry		Dry	
Backwater	Mean \pm SD Maximum Depth (m)	Range in Maximum Depth (m)	Mean \pm SD Maximum Depth (m)	Range in Maximum Depth (m)	Mean \pm SD Maximum Depth (m)	Range in Maximum Depth (m)	Mean \pm SD Maximum Depth (m)	Range in Maximum Depth (m)	Mean \pm SD Maximum Depth (m)	Range in Maximum Depth (m)
BW01	NA	NA								
BW02	1.8 \pm 0.3	0.8–2.0	1.0 \pm 0.6	0.9–1.4	1.6 \pm 0.08	1.4–1.7	1.2 \pm 0.05	1.1–1.2	2.4 \pm 0.06	2.3–2.6
BW03	NA	NA								
BW04	NA	NA								
BW05	NA	NA	0.9 \pm 0.2	0–1.0	1.7 \pm 0.8	0–2.3	0.9 \pm 0.03	0.8–1.0	NA	NA
BW06	1.5 \pm 0.03	1.4–1.6	0.2 \pm 0.6	0–0.3	NA	NA	NA	NA	NA	NA
BW07a	NA	NA								
BW07b	2.6 \pm 0.02	2.5–2.7	1.5 \pm 0.06	1.3–1.8	0.9 \pm 0.6	0–1.4	2.0 \pm 0.03	1.9–2.1	1.3 \pm 0.06	1.2–1.4
BW08	0.5 \pm 0.04	0.4–0.7	1.0 \pm 0.04	1.0–1.3	0.8 \pm 0.08	0.5–0.9	1.0 \pm 0.03	1.0–1.2	NA	NA
BW09	NA	NA								
BW10	1.7 \pm 0.03	1.6–1.8	1.5 \pm 0.07	1.0–1.8	3.4 \pm 0.08	3.2–3.6	1.5 \pm 0.05	1.4–2.0	0.7 \pm 0.58	0.53–0.80
BW13	NA	NA	NA	NA	NA	NA	NA	NA	0.6 \pm 0.32	0–0.92
BW14	NA	NA	NA	NA	NA	NA	NA	NA	1.6 \pm 0.03	1.5–1.7

^a Dates represent the beginning of the base-flow period. November 30 was used as the end of the base-flow period. See Appendix 3 for a description of how the beginning of the base-flow period was determined.

^b Mean flow at Ouray during the base-flow period.

^c NA = Backwater did not exist or was not surveyed during survey year

This page is intentionally left blank.

APPENDIX 6

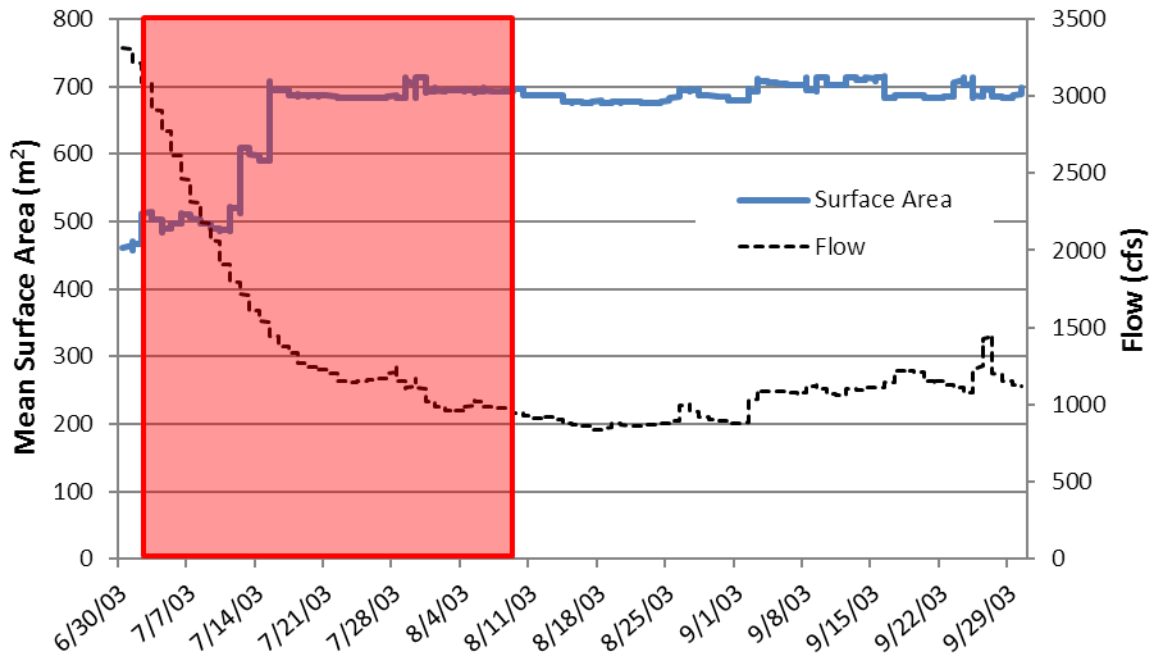
**CHARACTERISTICS OF SURVEYED BACKWATERS
DURING THE COLORADO PIKEMINNOW LARVAL DRIFT PERIOD (2003–2012)**

This page is intentionally left blank.

APPENDIX 6**CHARACTERISTICS OF SURVEYED BACKWATERS
DURING THE COLORADO PIKEMINNOW LARVAL DRIFT PERIOD (2003–2012)**

Surveys of selected backwaters were made annually from 2003 to 2013 (2007 was the only year surveys were not conducted during this period). This appendix provides information for each year on mean surface area and average mean depth of surveyed backwaters during the Colorado pikeminnow larval drift period. The larval drift period was defined as extending from when larvae were first detected in drift samples to the last detection as presented in Bestgen and Hill (2016). Larval drift data were available for 2003 to 2012.

a)



b)

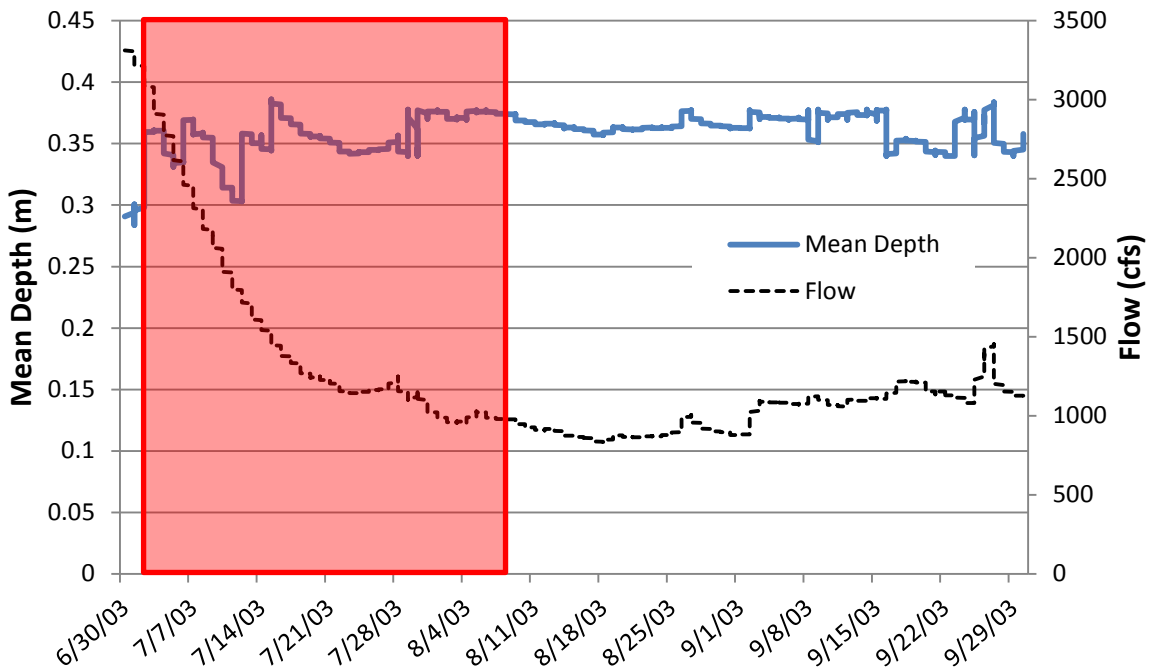


FIGURE A6-1 Backwater Mean Surface Area (a) and Mean Depth (b) during the 2003 Colorado Pikeminnow Larval Drift Period (red box). The larval drift period was defined as extending from when larvae were first detected in drift samples to the last detection (Bestgen and Hill 2016).

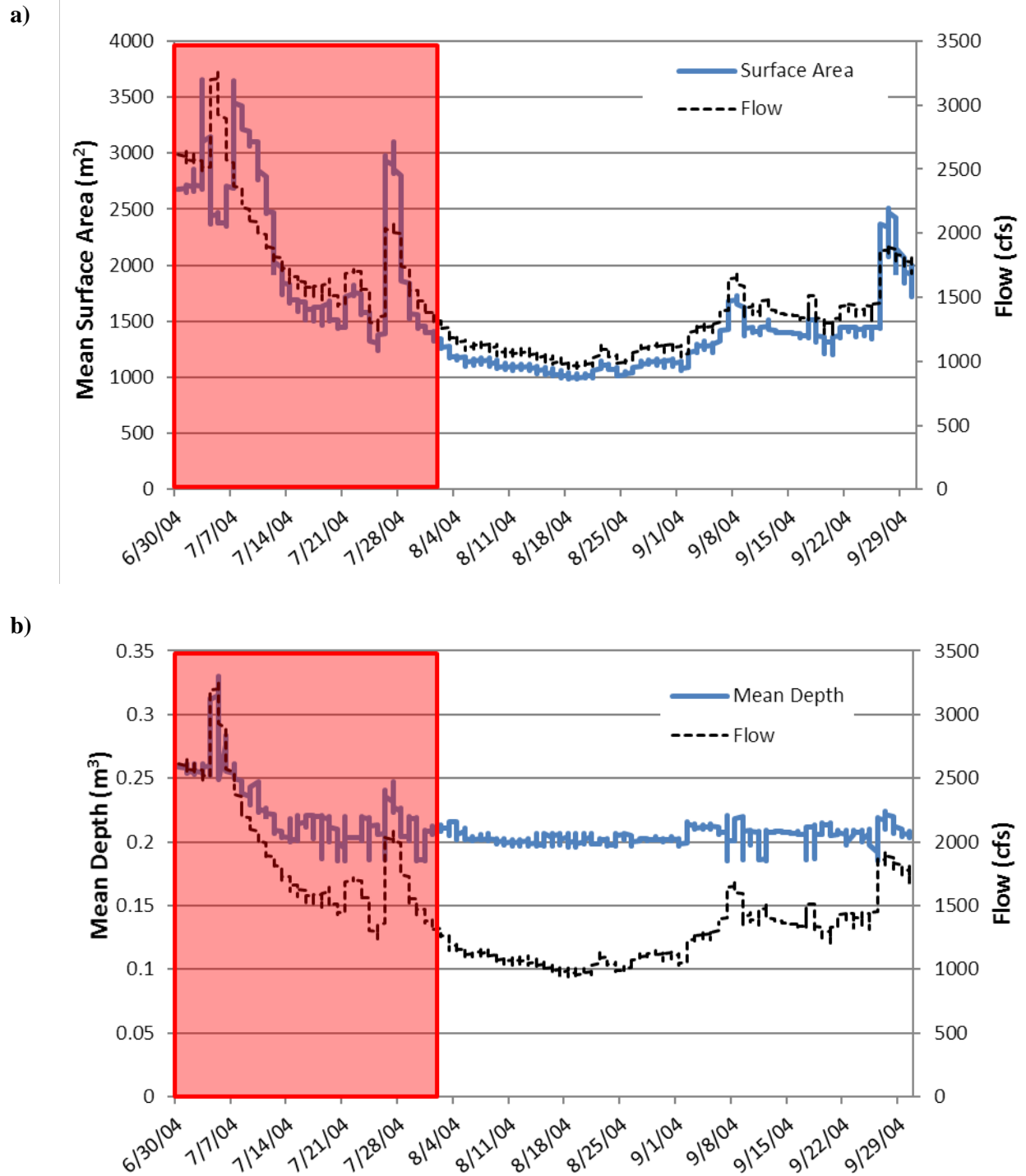
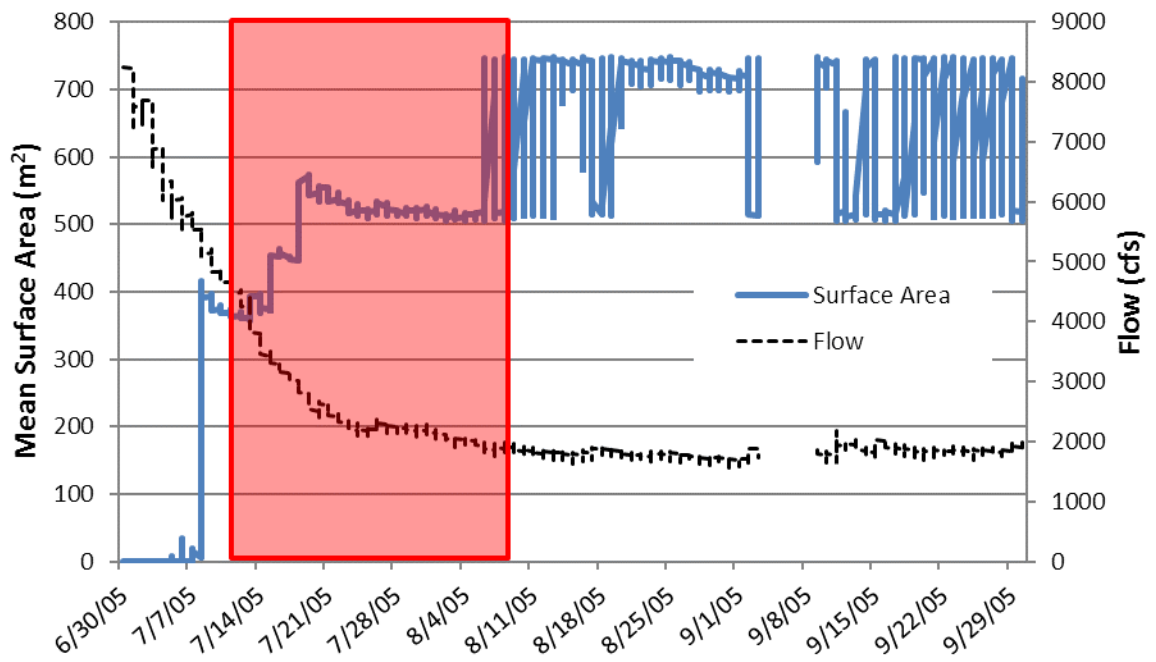


FIGURE A6-2 Backwater Mean Surface Area (a) and Mean Depth (b) during the 2004 Colorado Pikeminnow Larval Drift Period (red box). The larval drift period was defined as extending from when larvae were first detected in drift samples to the last detection (Bestgen and Hill 2016).

a)



b)

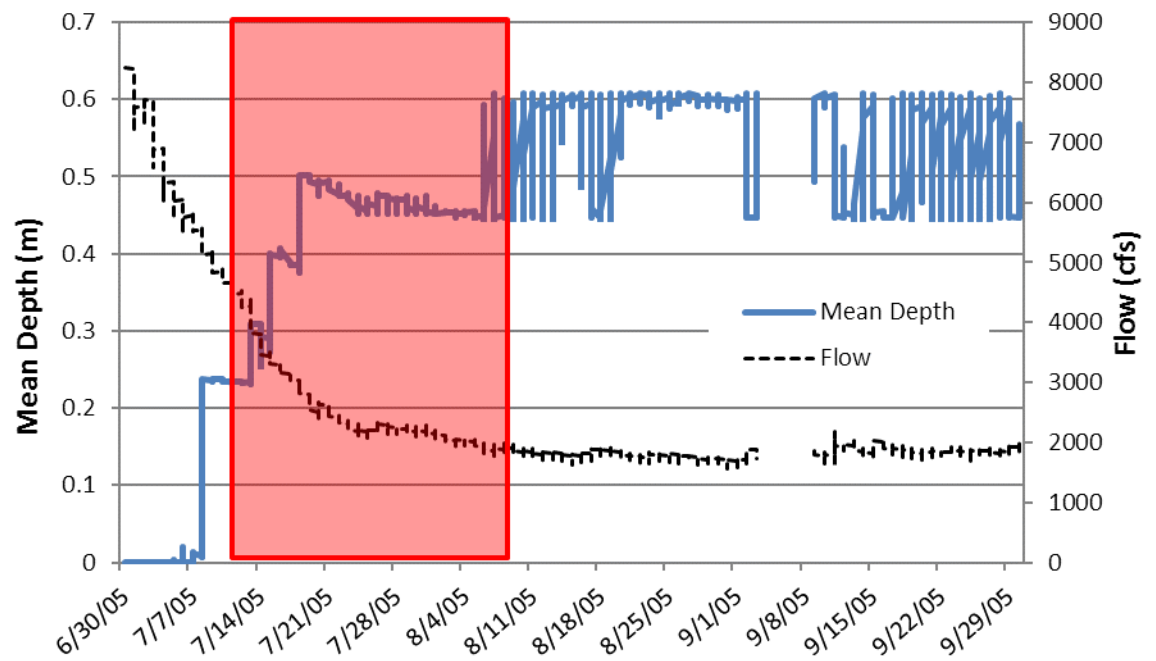


FIGURE A6-3 Backwater Mean Surface Area (a) and Mean Depth (b) during the 2005 Colorado Pikeminnow Larval Drift Period (red box). The larval drift period was defined as extending from when larvae were first detected in drift samples to the last detection (Bestgen and Hill 2016).

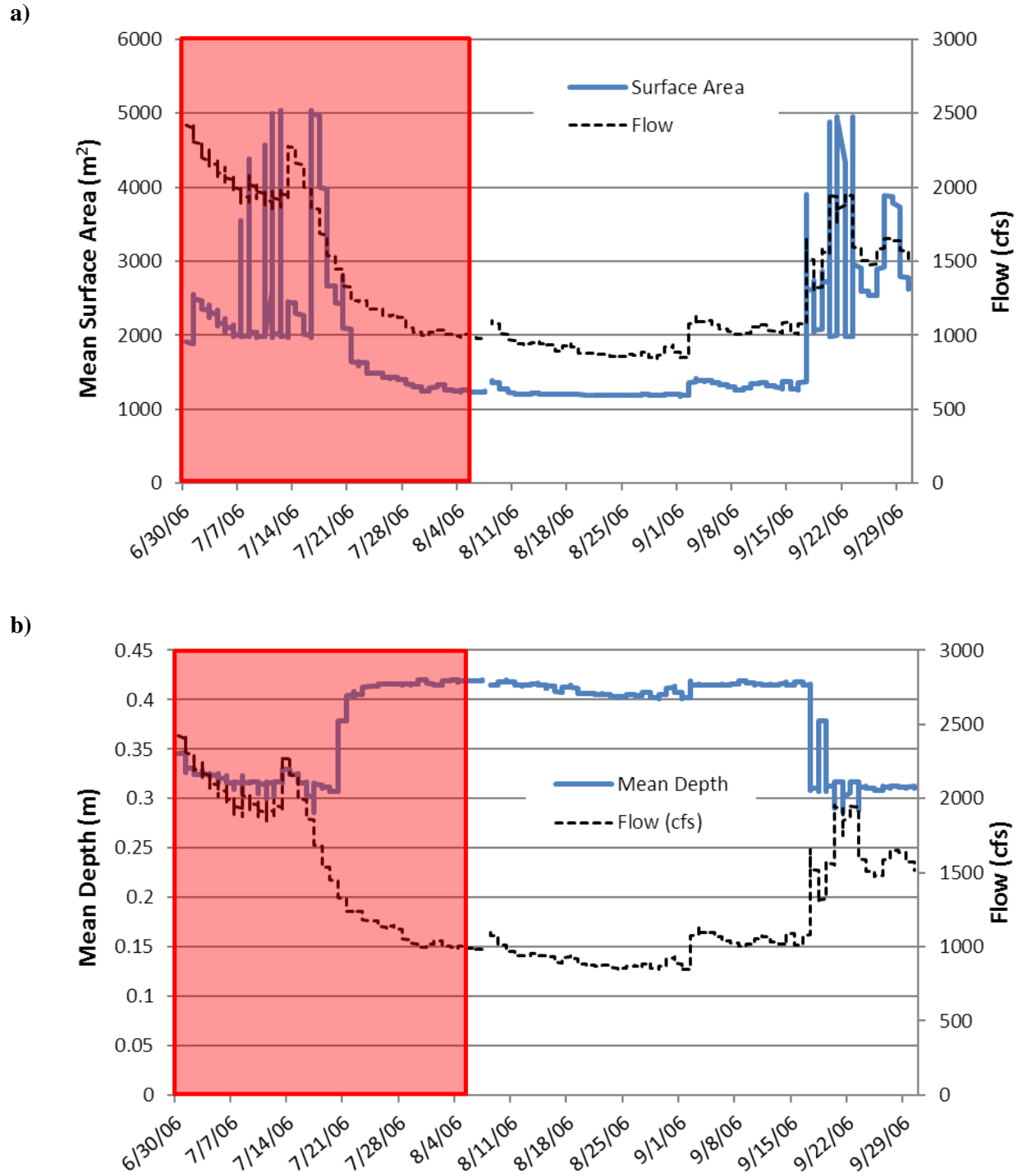
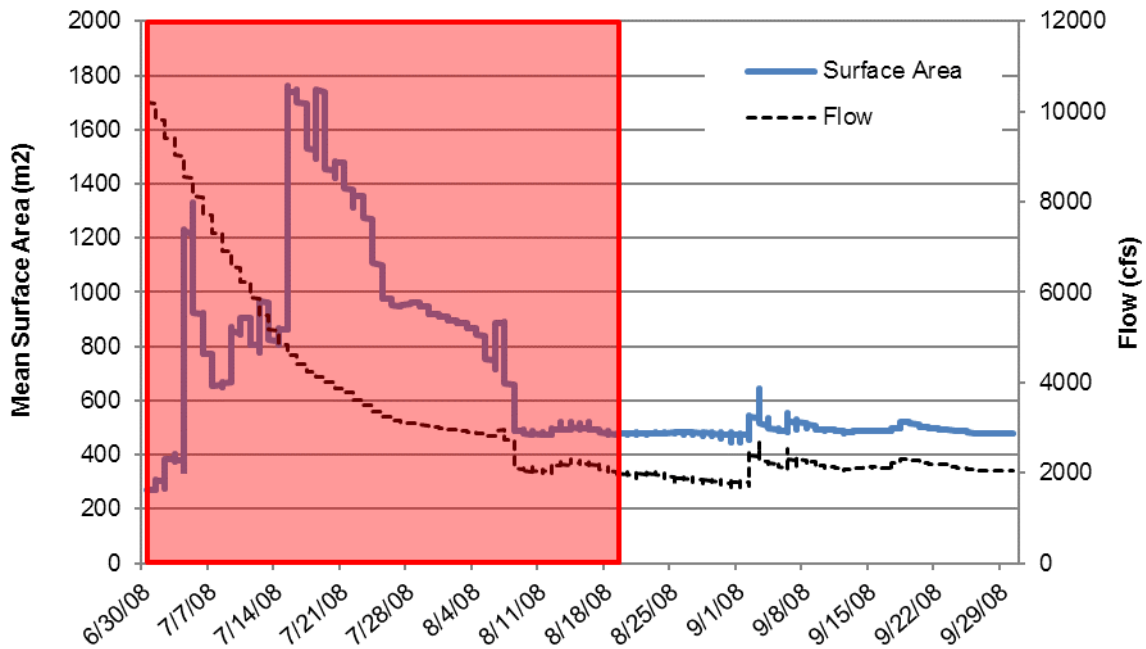


FIGURE A6-4 Backwater Mean Surface Area (a) and Mean Depth (b) during the 2006 Colorado Pikeminnow Larval Drift Period (red box). The larval drift period was defined as extending from when larvae were first detected in drift samples to the last detection (Bestgen and Hill 2016).

a)



b)

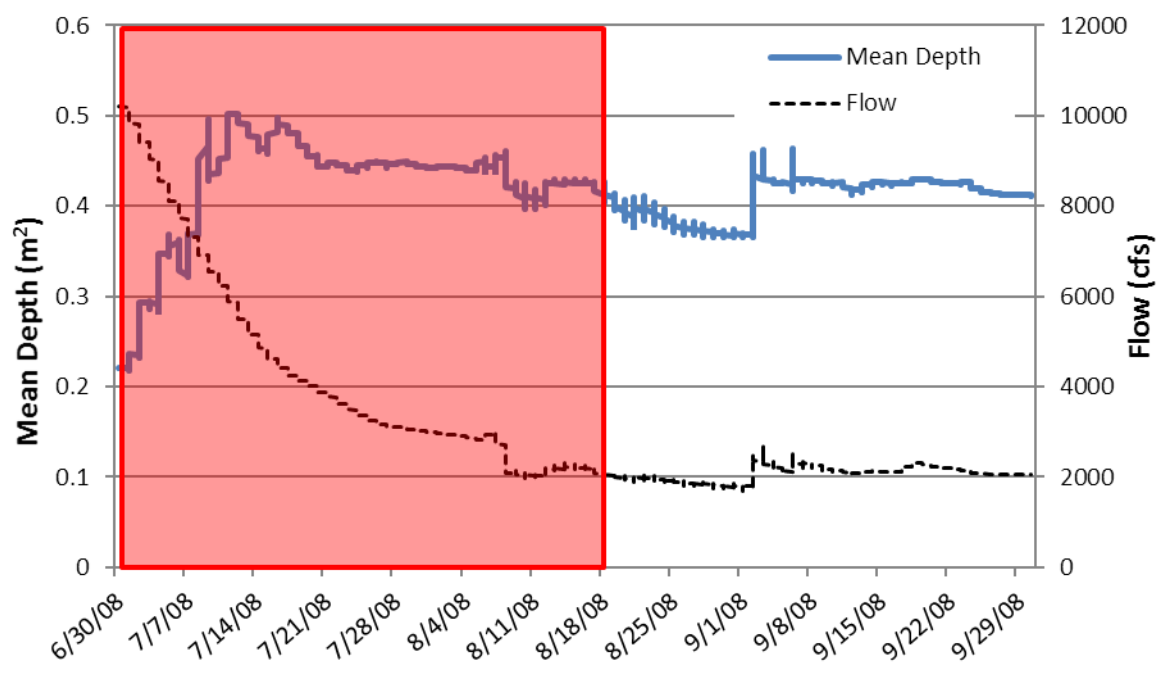


FIGURE A6-5 Backwater Mean Surface Area (a) and Mean Depth (b) during the 2008 Colorado Pikeminnow Larval Drift Period (red box). The larval drift period was defined as extending from when larvae were first detected in drift samples to the last detection (Bestgen and Hill 2016).

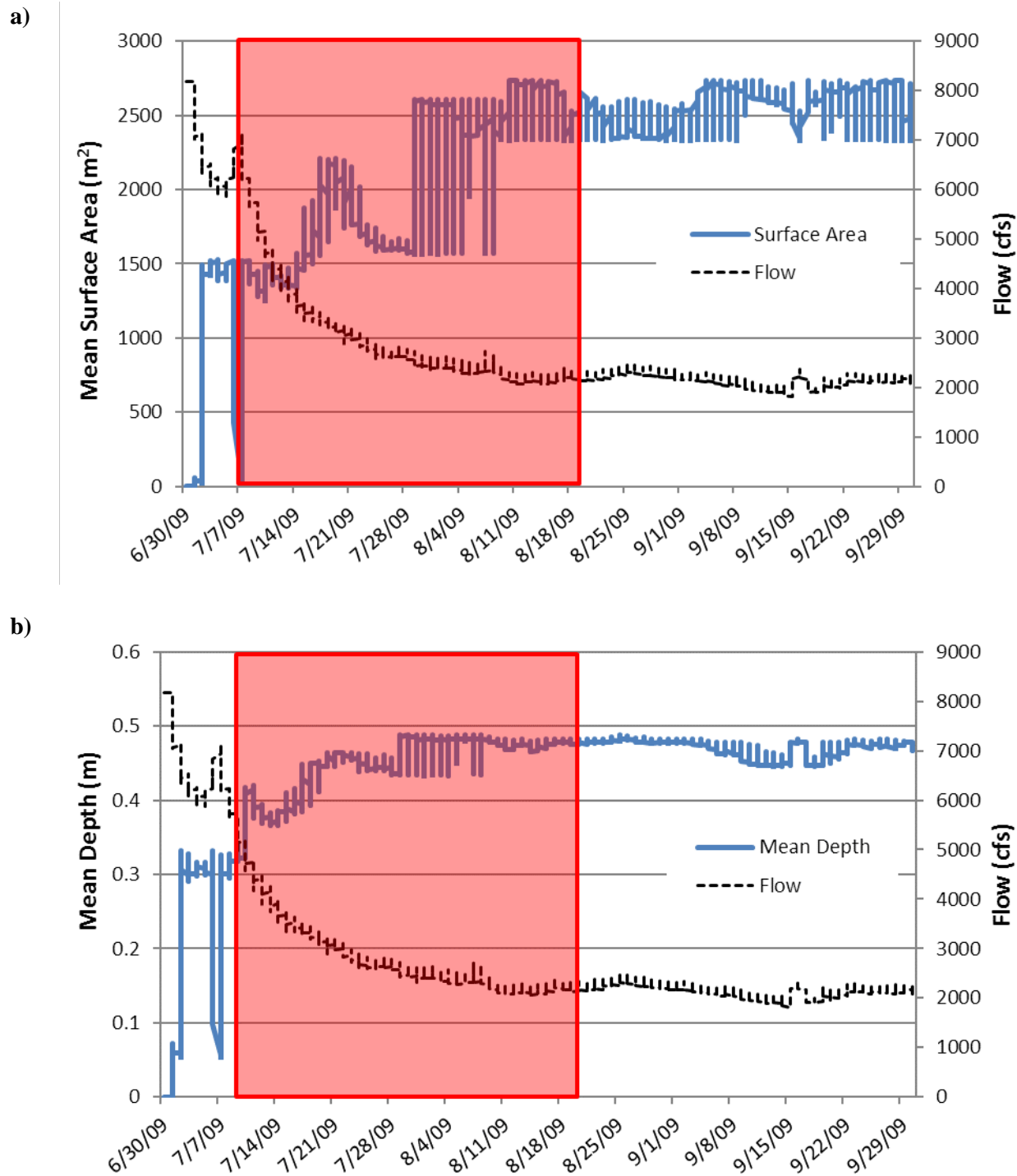


FIGURE A6-6 Backwater Mean Surface Area (a) and Mean Depth (b) during the 2009 Colorado Pikeminnow Larval Drift Period (red box). The larval drift period was defined as extending from when larvae were first detected in drift samples to the last detection (Bestgen and Hill 2016).

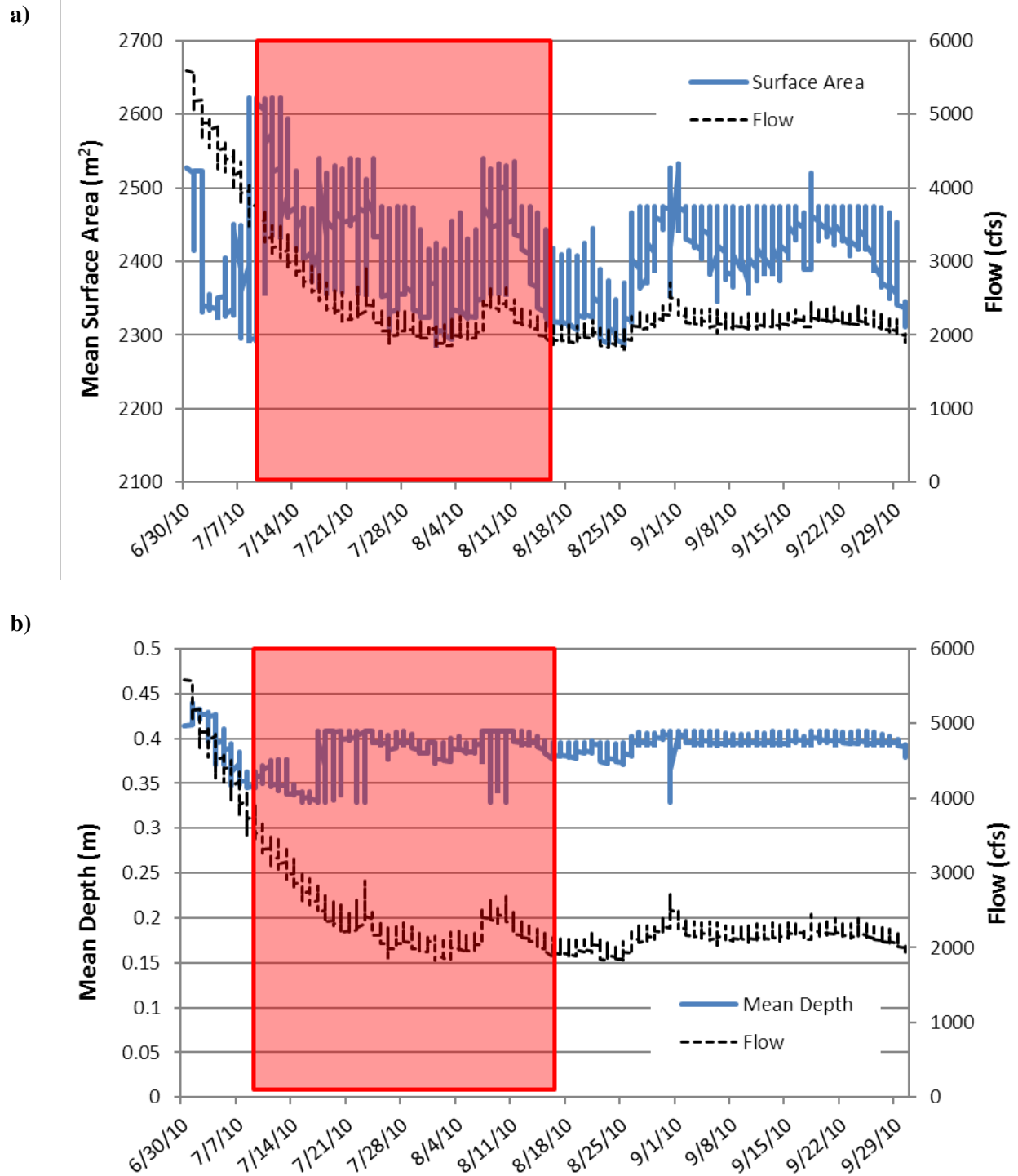


FIGURE A6-7 Backwater Mean Surface Area (a) and Mean Depth (b) during the 2010 Colorado Pikeminnow Larval Drift Period (red box). The larval drift period was defined as extending from when larvae were first detected in drift samples to the last detection (Bestgen and Hill 2016).

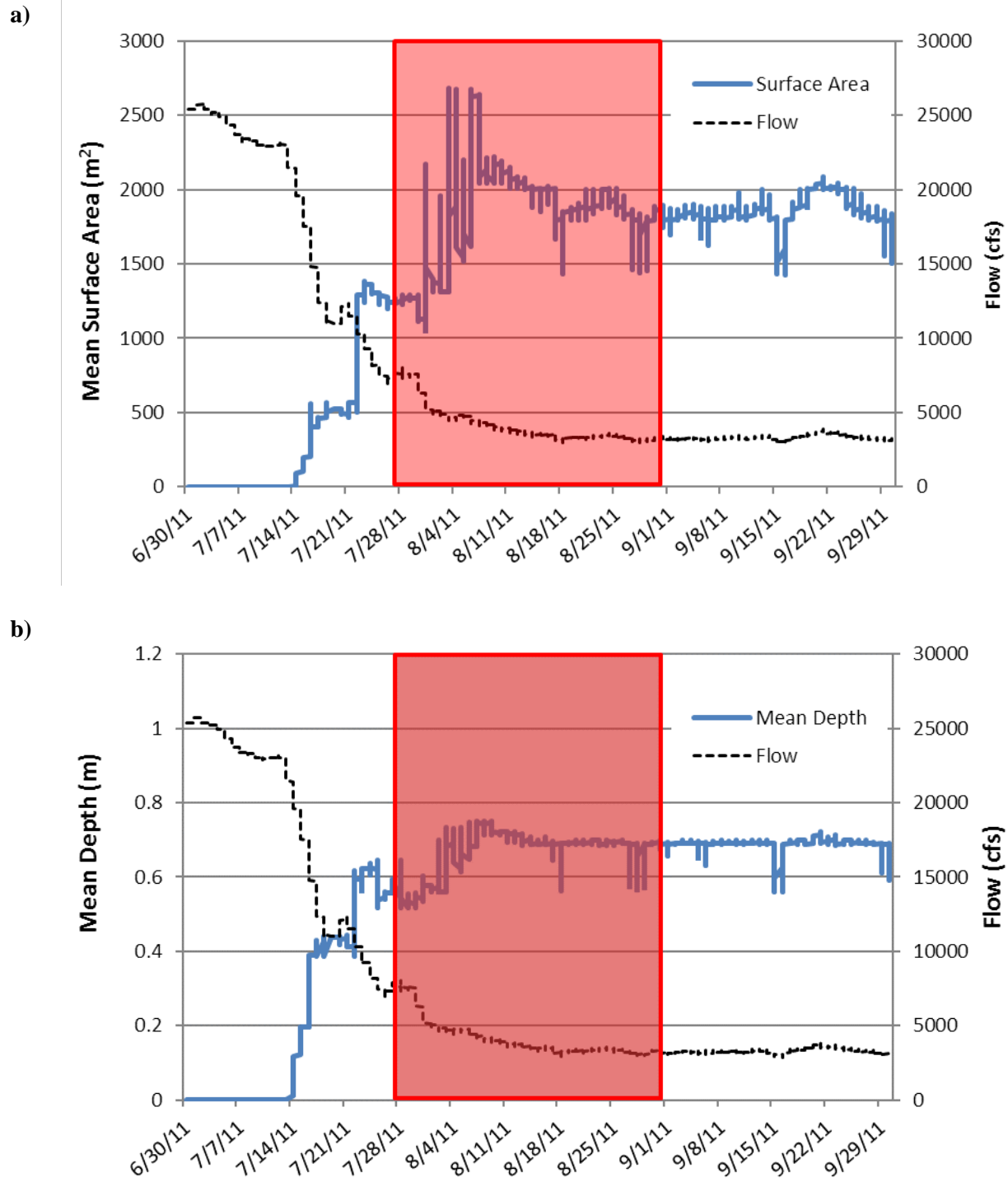


FIGURE A6-8 Backwater Mean Surface Area (a) and Mean Depth (b) during the 2011 Colorado Pikeminnow Larval Drift Period (red box). The larval drift period was defined as extending from when larvae were first detected in drift samples to the last detection (Bestgen and Hill 2016).

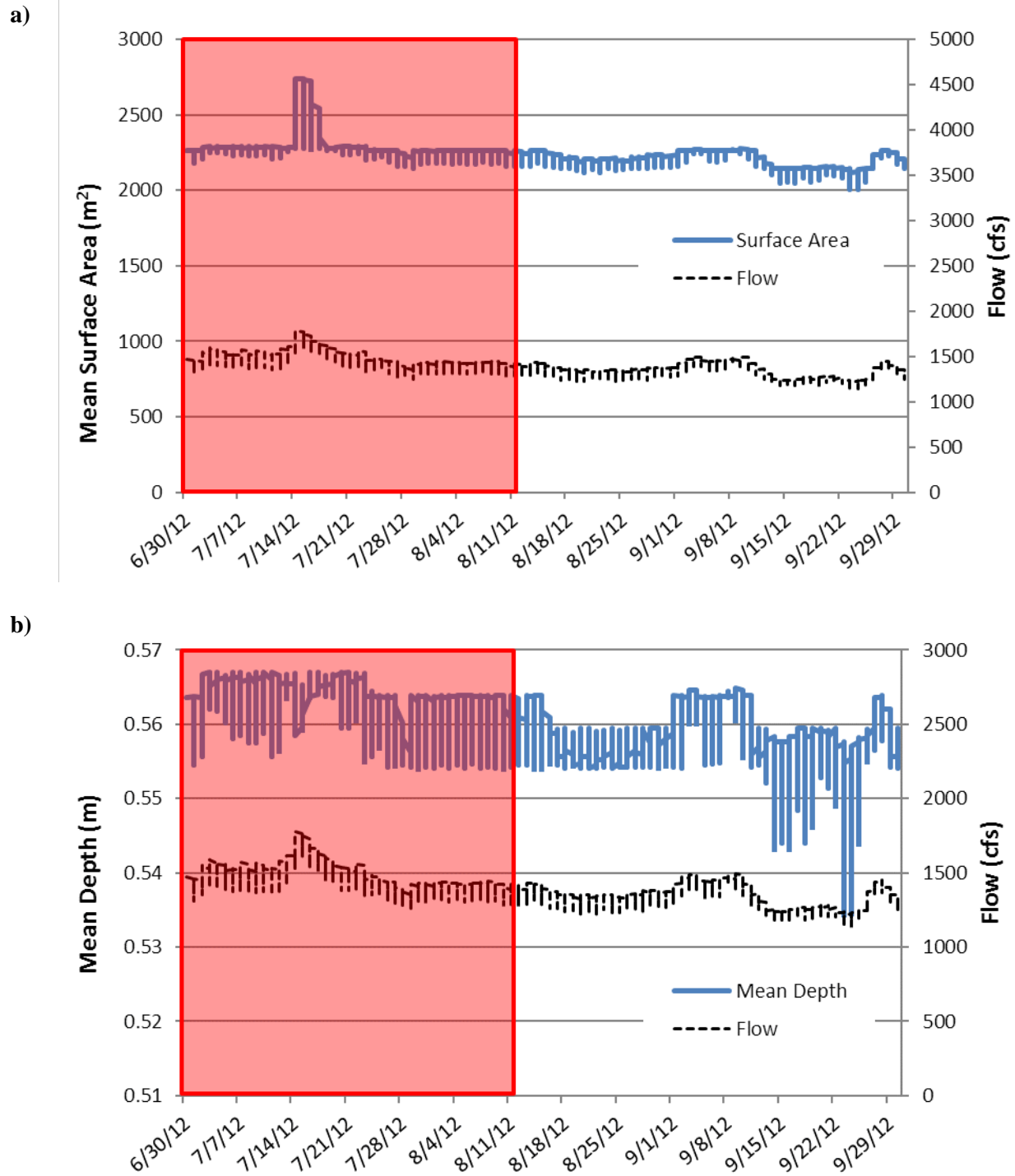


FIGURE A6-9 Backwater Mean Surface Area (a) and Mean Depth (b) during the 2012 Colorado Pikeminnow Larval Drift Period (red box). The larval drift period was defined as extending from when larvae were first detected in drift samples to the last detection (Bestgen and Hill 2016).

A6.1 REFERENCE

Bestgen, K.R., and A.A. Hill, 2016, *Reproduction, Abundance, and Recruitment Dynamics of Young Colorado Pikeminnow in the Green and Yampa Rivers, Utah and Colorado, 1979-2012*. Final report to the Upper Colorado River Endangered Fish Recovery Program, Project FW BW-Synth. Larval Fish Laboratory, Department of Fish, Wildlife, and Conservation Biology, Colorado State University, Fort Collins, Contribution 183.



Environmental Science Division

Argonne National Laboratory
9700 South Cass Avenue, Bldg. 240
Argonne, IL 60439-4847

www.anl.gov



Argonne National Laboratory is a U.S. Department of Energy
laboratory managed by UChicago Argonne, LLC